Surveillance Satellite Attitude Control Design Using RCS and Momentum Wheels

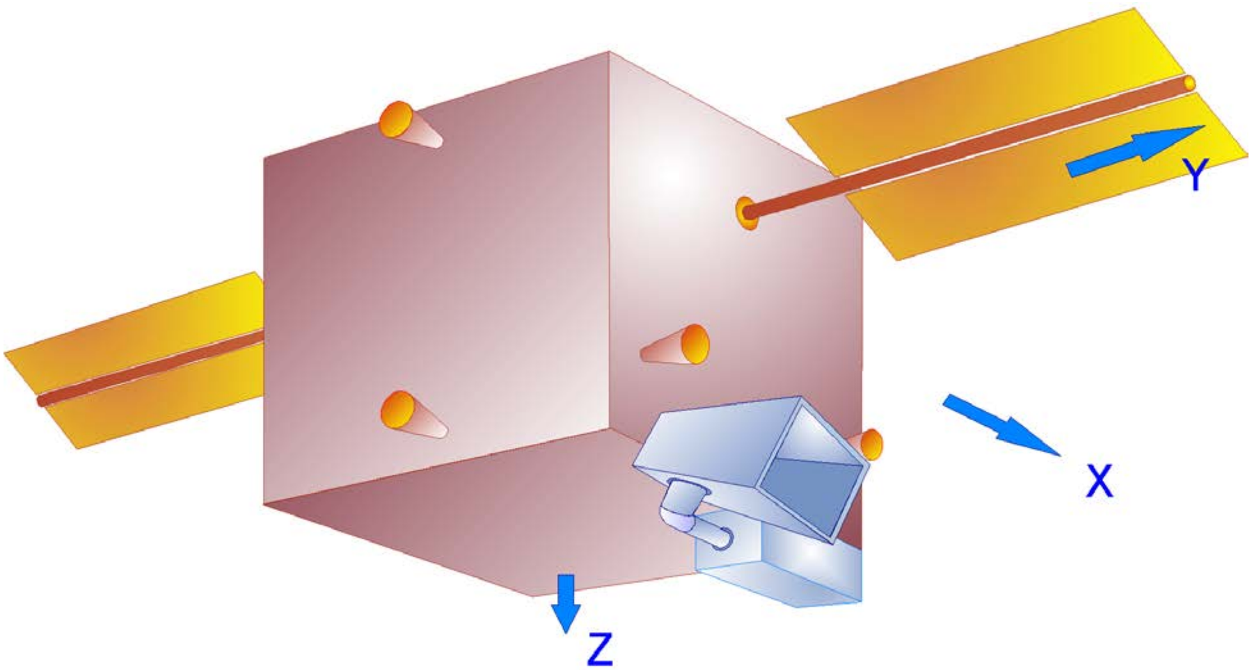

Figure (1) Surveillance Spacecraft with Reaction Wheels and a Rotating Telescope

The spacecraft in this example is a typical satellite with a pair of solar arrays and an attached optical instrument that is capable to rotate in two directions (azimuth and elevation). It has 3 attitude control wheels which are mounted as shown in figure (1.1). Two of the wheels are reaction wheels, RW#2 & RW#3. Their spin axes are tilted 20° from horizontal, and they provide control torques only in pitch and yaw directions. Wheel #1 is a momentum wheel. It spins at constant rate and is not actively used for control but it provides a constant momentum of -40 (ft-lb-sec) in the pitch direction for passive roll/ yaw stabilization. The momentum bias has a stiffening effect in the out-of-plane directions, but it creates a nutation resonance that couples the roll and yaw axes. The lateral RW control law takes advantage of this dynamic coupling and dampens the nutation resonance. By stabilizing the roll axis it also has a stabilizing effect in yaw due to the gyroscopic coupling. For attitude measurements the spacecraft uses horizon sensors which provide accurate pitch and roll attitude with respect to the local vertical local horizontal (LVLH) axes. The attitude control requirement in pitch and roll is 1.5 (deg). Yaw control is allowed to be more relaxed during RW control, up to 7 (deg) of attitude error. Yaw attitude data are not required for attitude control purposes. There is, however, a slow and less accurate derived yaw estimate which is used to correct yaw drifts during momentum de-saturations. External disturbance torques cause the RW momentum to build up, and the excess momentum stored in the two reaction wheels is taken out by firing the reaction control jets. During desaturation the RCS jets control also the spacecraft attitude.

The analysis of this spacecraft focuses on a variety of typical satellite control design issues, (a) the design of a reaction wheel control for a momentum biased spacecraft, (b) the design of an RCS momentum desaturation system, (c) the design of a telescope gimbal positioning system, (d) there are flexibility stabilization issues, and (e) sensitivity evaluation to typical spacecraft disturbances. The ACS design and control analysis is presented systematically by separating it in six sections. The complexity of the models and analysis increases from section to section. In Section 1 we derive the RW control laws for the momentum biased satellite which maintains an LVLH attitude. In Section 2 we develop a rigid-body simulation model in Matlab for the orbiting spacecraft in LVLH attitude. The model has both, the reaction wheel and the RCS loops closed, and it uses a logic to switch between the two modes of operation. We simulate a pitch attitude maneuver using the RW controls followed by momentum desaturation using the jets. In Section 3 we use the Flixan flex modeling program to develop state-space models for the flexible spacecraft structure from a Finite Element Model (FEM) including rigid-body modes implemented as structure modes. We develop a simple Simulink model to simulate the flex system using closed-loop RCS control and gimbal control, and analyze sensitivity to spacecraft disturbance. In Section 4 we combine the non-linear rigid body model of Section 2 in parallel with the flex structure model of Section 3, and analyze stability and performance of the combined system. We also design filters to attenuate the structural flexibility. In Section 5 we introduce the dynamics of the gimbaling telescope which rotates in two directions (elevation, and azimuth) with respect to the spacecraft bus. A non-linear 3-body dynamic model is used to simulate the relative motion of the 3 bodies (spacecraft, telescope, and telescope yoke). The Solar Arrays are not gimbaling but they are assumed to be rigidly attached to the spacecraft. Translational dofs are also included in the simulation. The 3-body model is also combined with a flex model and the previous analysis is repeated using the more complex vehicle dynamics. A simple position control system for the telescope gimbals is designed, and the stability and performance of the two telescope gimbal loops (elevation & azimuth) are also checked. In Section 6 we develop a different state-space model for the spacecraft using the Flixan Flight Vehicle Modeling Program. This is a linear model relative to the LVLH attitude. It includes the RWs, the two telescope gimbals, RCS jets, Gravity-Gradient, LVLH dynamics, plus flexibility. We also use this model to evaluate stability and Line-of-Sight (LOS) sensitivity to internal spacecraft disturbances.

1. Spacecraft Attitude Control system

The surveillance satellite is in circular orbit around the earth and it is maintaining a local vertical, local horizontal (LVLH) attitude. The orbital rate is ω_o=0.00113 (rad/sec) so the spacecraft has a steady negative pitch rate equal to ($-\omega_o$). There are three wheels mounted on the spacecraft for attitude control and stabilization. Wheel #1 in the middle is a Momentum Wheel (MW). Its spin axis is horizontal and it is rotating in negative pitch direction about the spacecraft -y axis. Its speed is maintained at a constant rate -500 (deg/sec) by a motor speed controller which provides -40 (ft-lb-sec) momentum bias to the spacecraft, that is, in addition to the momentum due to negative spacecraft rotation at orbital rate. Wheel #1 is not actively used for attitude control but it provides passive roll/yaw stabilization. The other two are reaction wheels (RW#2 and RW#3). They are tilted ±20° with respect to the spacecraft y axis and provide active pitch and yaw control. There is no reaction wheel momentum component in the x direction for controlling roll directly, but the spacecraft is stabilized gyroscopically in the out of plane directions by the pitch momentum biasing which couples rotations in roll and yaw axes.

The purpose of the attitude control system is to maintain the spacecraft attitude as nearly as possible to the LVLH attitude. It allows up to 1.5º error in pitch and roll and up to 7º error in yaw. The spacecraft is excited by environmental disturbances in pitch and yaw, both cyclic, and steady-state (secular) that induce attitude errors. The disturbances are aerodynamic and gravity gradient torques. Secular disturbances cause the RW momentum to increase requiring frequent desaturation when the momentum approaches saturation levels. There are 7 jets of 0.05 (lbf) thrust each for attitude control and RW desaturation. There are 3 jets thrusting in the velocity (+x) direction used for pitch control and orbit re-boost. There are also 4 jets pointing in the ±y direction for roll and yaw control. In addition to attitude control the RCS jets are mainly used to desaturate the reaction wheel momentum which is only in pitch and yaw since there is no RW component in the x direction. The attitude control system (ACS) operates in two modes: the RW mode, and the RCS mode. In the RW mode the RWs are used to control attitude until the RW momentum exceeds a certain amount from the desired bias level, and when it happens, jets are fired to desaturate the wheels. In actuality it switches to RCS attitude control mode while the wheels are torqued in the direction that reduces the RW (#2 and #3) momentum. The duration of the RCS mode is much shorter because there is more torque availability. Telescope operations occur only during RW control periods because the jets generate a lot more jitter on the image quality. During RCS control RW #1 is continuously commanded to maintain the -40 (ft-lb-sec) bias momentum.

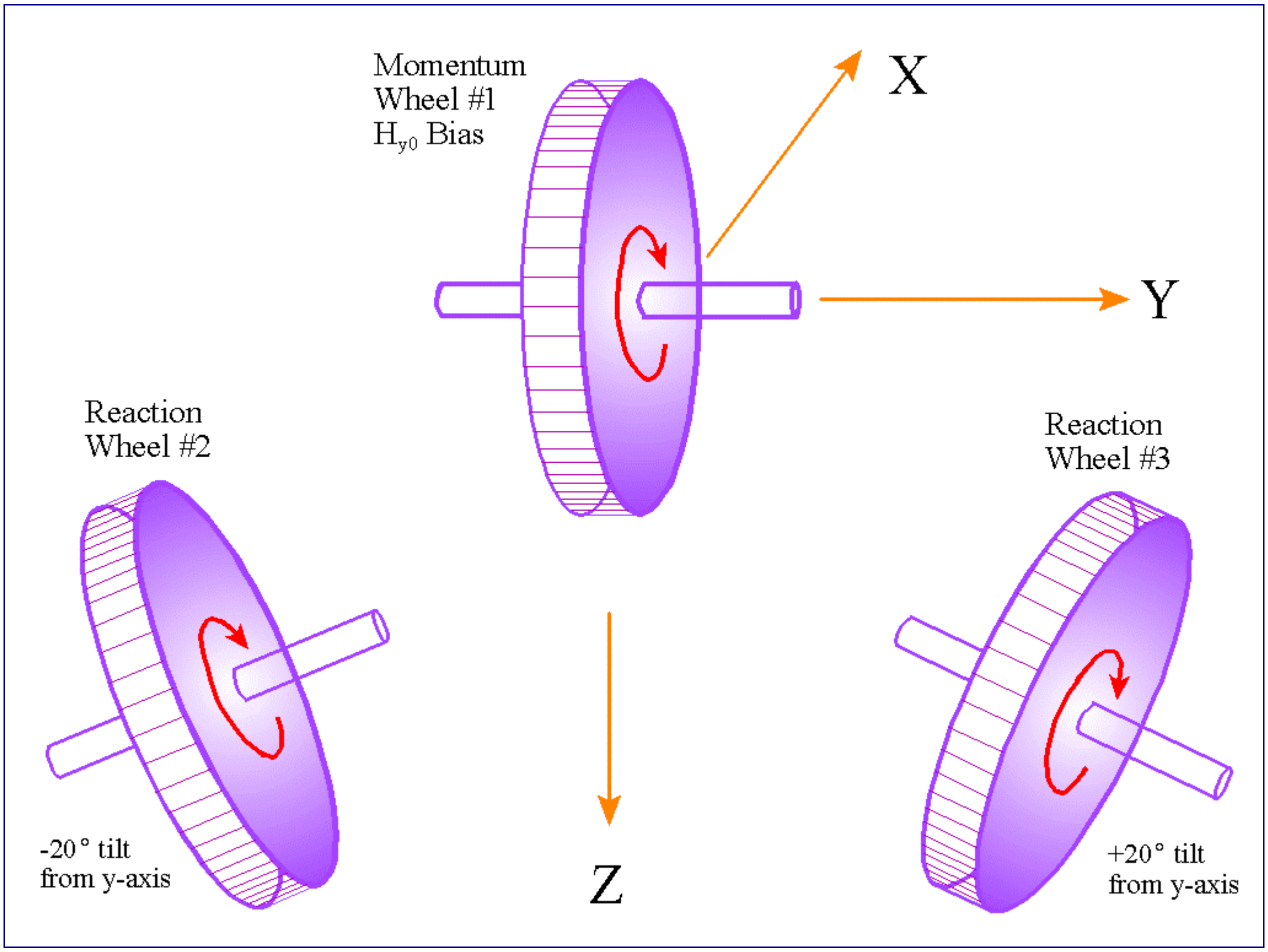

Figure 1.1 Momentum and Reaction Wheel Configuration

1.1 Attitude Control Design

The attitude control system is designed based on the attitude equations of motion of a spacecraft in the LVLH attitude. The linearized equations of motion about the spacecraft principle axis are:

$$I_X \ddot{\phi} + \omega_0 H'_{WY} \phi + H'''_{WY} \dot{\psi} - \omega_0 H_{WZ} + \dot{H}_{WX} = T_{dX} + T_{cX}$$

$$I_Y \ddot{\theta} + 3\omega_0^2 (I_X - I_Z)\theta + \dot{H}_{WY} = T_{dY} + T_{cY}$$

$$I_Z \ddot{\psi} + \omega_0 H''_{WY} \psi + H_{WY}''' \dot{\phi} + \omega_0 H_{WX} + \dot{H}_{WZ} = T_{dZ} + T_{cZ}$$

$$where:$$

$$H'_{WY} = 4\omega_0 (I_Y - I_Z) + H_B$$

$$H''_{WY} = \omega_0 (I_Y - I_X) + H_B$$

$$H'''_{WY} = \omega_0 (I_Y - I_X - I_Z) + H_B$$

(ϕ,θ,ψ)	are the attitude angles in the LVLH frame about (x, y, z) respectively
(ω_0)	is the spacecraft orbital rate (rad/sec)
(H_B)	is the bias momentum in the pitch axis (positive along $-y_b$)
(T_d)	are the environmental disturbance torques
(T_c)	are the reaction wheel control torques

The pitch equation is decoupled from the roll/ yaw (out-of-plane) dynamics allowing the three axis control problem to be reduced to two separate, a pitch axis and a lateral axis problems. The control system attempts to minimize the attitude perturbations caused by the environmental torques. The gains are designed directly from the equations of motion.

Pitch Control

The pitch axis is a standard reaction wheel attitude PID controller designed to provide a bandwidth of 0.02 (rad/sec), and 0.8 damping zeta. The rate of change of pitch wheel momentum is commanded as a shaped function of the measured pitch attitude in order to remove the pitch attitude errors and to dampen the pitch motion.

Roll/ Yaw Control Law

Out of plane control in this spacecraft is achieved gyroscopically by virtue of the pitch momentum bias. From the roll and yaw equations, assuming only pitch momentum bias and ignoring the slow orbital rate, we can obtain an open-loop solution for the roll and yaw rates which are coupled by the nutation frequency (ω_n). Passive damping is used to attenuate the nutation oscillations amplitude after being excited by jet firing (not shown).

$$\dot{\phi} = A\cos(\omega_n t) \; where: \omega_n = \frac{H_B}{\sqrt{I_X I_Z}}$$

$$\dot{\psi} = A\sqrt{\frac{I_X}{I_Z}} \sin(\omega_n t)$$

By taking advantage of the gyroscopic coupling between roll and yaw, the yaw momentum is commanded as a function of the measured roll attitude error. After combining the yaw and roll equations together and ignoring the small orbital rate we obtain

$$I_X \ddot{\phi} + \frac{H_B^2}{I_Z}\phi - \frac{H_B}{I_Z} H_{WZ} = T_{dX} + T_{cX} - \frac{H_B}{I_Z}\int \left(T_{dX} + T_{cX}\right) dt$$

Controlled damping of the roll and yaw nutational motion can be accomplished by commanding the yaw momentum H_{WZ} as a function of roll rate. In addition, to reduce the roll attitude offsets in response to external disturbances, the yaw momentum is also commanded as a function of the integral of roll attitude. Finally, since the roll rate is not measured directly but it is derived by lead shaping of the measured roll attitude, a roll attitude error term will also be present in the control law for commanding yaw momentum as a function of roll attitude, that is

$$H_{WZC} = -\left\lfloor K_1 \dot{\phi} + K_2 \phi + K_3 \int \phi \, dt \right\rfloor$$

After substitution the characteristic equation can be simplified to a third order in the following form

$$\left[I_X \lambda^2 + \frac{K_1 H_B}{I_Z}\lambda + \frac{H_B}{I_Z}\left(K_2 + H_B\right) \right] \left(\lambda + \frac{K_3}{K_2 + H_B} \right) \approx 0$$

The complex pair of roots can be characterized by a natural frequency and damping ratio

$$\omega_c = \sqrt{\frac{H_B\left(K_2 + H_B\right)}{I_X \, I_Z}} \quad ; \quad \varsigma = \frac{K_1}{2}\sqrt{\frac{H_B}{I_X \, I_Z\left(K_2 + H_B\right)}}$$

The objective in gain selection is to achieve the desired nutation damping by the proper choice of K_1 gain. The nutation frequency increases with K_2. The integrator root should be more than 1/10 the real part of the complex root pair. A good choice of gains is

$$K_1 = \frac{0.1\zeta^2 \, I_X \, I_Z}{H_B} + \sqrt{\frac{0.01\zeta^4 \, I_X^2 I_Z^2}{H_B^2} + 4\zeta^2 \, I_X \, I_Z}$$

$$K_2 = 0.05 K_1$$

$$K_3 \le 0.1\zeta \left(K_2 + H_B\right)\sqrt{\frac{H_B}{I_X \, I_Z}}$$

2. Rigid Body Simulation Model

In this section we will develop a non-linear simulation model of the orbiting spacecraft relative to the local vertical local horizontal (LVLH) frame. We start by describing the non-linear rigid-body equations, the vehicle dynamics and control system files, the Simulink model that implement these models, and we present some simulation results. The Simulink files for this example are in "…*\Examples\Surveillance Satellite React-Wheels\Rigid-Body Sim*".

2.1 Non-Linear Dynamic Equations

The linearized equations of motion in Section (1) were used for the derivation of attitude control gains. The attitude control system attempts to keep the spacecraft at constant attitude with respect to the LVLH. The LVLH frame rotates at orbital rate. Its x axis is towards the spacecraft velocity vector, the z axis is pointing towards the center of the earth, and the y axis is perpendicular to the x-z plane towards the right solar array. The following equations describe the non-linear dynamic motion of a spacecraft with Reaction Wheels with respect to the LVLH frame.

$$\begin{aligned} I\,\dot{\underline{\omega}} &= -\left(\underline{\omega}\times I\,\underline{\omega}\right)+3\omega_o^2\left(\underline{c}\times I\,\underline{c}\right)+\underline{T}_{RCS}+\underline{T}_d-\underline{T}_{RW} \\ \dot{\underline{H}}_{RW} &= \underline{T}_{RW}-\left(\underline{\omega}\times\underline{H}_{RW}\right) \end{aligned} \qquad (2.1)$$

If we assume that the reaction wheel torque T_{RW} consists of the control torque plus a term that cancels out the gyroscopic torque ($\omega\times H_{RW}$)

$$T_{RW} = T_{WC} + \left(\omega\times H_{RW}\right)_{estim} \qquad (2.2)$$

Then the equations simplify in the following form

$$\begin{aligned} I\,\dot{\underline{\omega}} &= -\left(\underline{\omega}\times\underline{H}_{sys}\right)+3\omega_o^2\left(\underline{c}\times I\,\underline{c}\right)+\underline{T}_{RCS}+\underline{T}_d-\underline{T}_{WC} \\ \dot{\underline{H}}_{RW} &= +\underline{T}_{WC} \\ \underline{H}_{sys} &= I\,\underline{\omega}+\underline{H}_{RW} \end{aligned} \qquad (2.3)$$

Where:

T_{WC} is only the control part of the RW torque, excluding the gyroscopic torque
H_{RW} is the reaction wheel momentum, and
H_{sys} is the system momentum

$$I = \begin{bmatrix} I_{XX} & I_{XY} & I_{XZ} \\ I_{XY} & I_{YY} & I_{YZ} \\ I_{XZ} & I_{YZ} & I_{ZZ} \end{bmatrix}; \quad c = \begin{bmatrix} -\sin\theta\cos\psi \\ \cos\phi\sin\theta\sin\psi + \sin\phi\cos\theta \\ -\sin\phi\sin\theta\sin\psi + \cos\phi\cos\theta \end{bmatrix}$$

$$\begin{pmatrix} \dot{\phi} \\ \dot{\theta} \\ \dot{\psi} \end{pmatrix}_{LVLH} = \omega_{LVLH} = C_B^L \underline{\omega} + \begin{pmatrix} 0 \\ \omega_o \\ 0 \end{pmatrix} \qquad (2.4)$$

$$where: C_B^L = \frac{1}{\cos\psi} \begin{bmatrix} \cos\psi & -\cos\phi\sin\psi & \sin\phi\sin\psi \\ 0 & \cos\phi & -\sin\phi \\ 0 & \sin\phi\cos\psi & \cos\phi\cos\psi \end{bmatrix}$$

Where: $\underline{\omega}$ is the spacecraft body rate and ω_o is its circular orbit rate (0.0011 rad/sec). In the top equation, the first two non-liner terms on the RHS of the moment equation are the gyroscopic and gravity gradient torques respectively. T_{RCS}, T_{WC} and T_D are the RCS torques, the reaction wheel control torques, and the disturbance torques respectively applied in the body axes. The state-vector is initialized in the LVLH attitude, which has an initial pitch rate equal to ($-\omega_o$). The attitude kinematics equation calculates the Euler angles (ϕ, θ, ψ) with respect to the LVLH frame by integrating the transformed body rates. The bottom equation in equations (2.1) calculates the rate of change in the reaction wheel momentum in body axis as a function of the RW torque T_{RW}. The spacecraft attitude control system is designed by taking into consideration the constant pitch bias in the system momentum. The 3 wheels are initialized at H_{RW}= (-40, 0, 0)’ (ft-lb-sec).

The Matlab simulation model is in folder *"…\Examples\Surveillance Satellite React-Wheels\Rigid-Body Sim"*. The Simulink model is "*NonLinear_Sim.mdl*", shown below in figure (2.1). The non-linear equations (2.1) are coded in Matlab function "*NonLin-Vehi-Dynamics.m*" which is implemented in the subsystem block "*Spacecraft Non-Linear Dynamics*" in the following Simulink model, Figure (2.1). There is a pitch attitude command on the left side. The roll and yaw commands are zero.

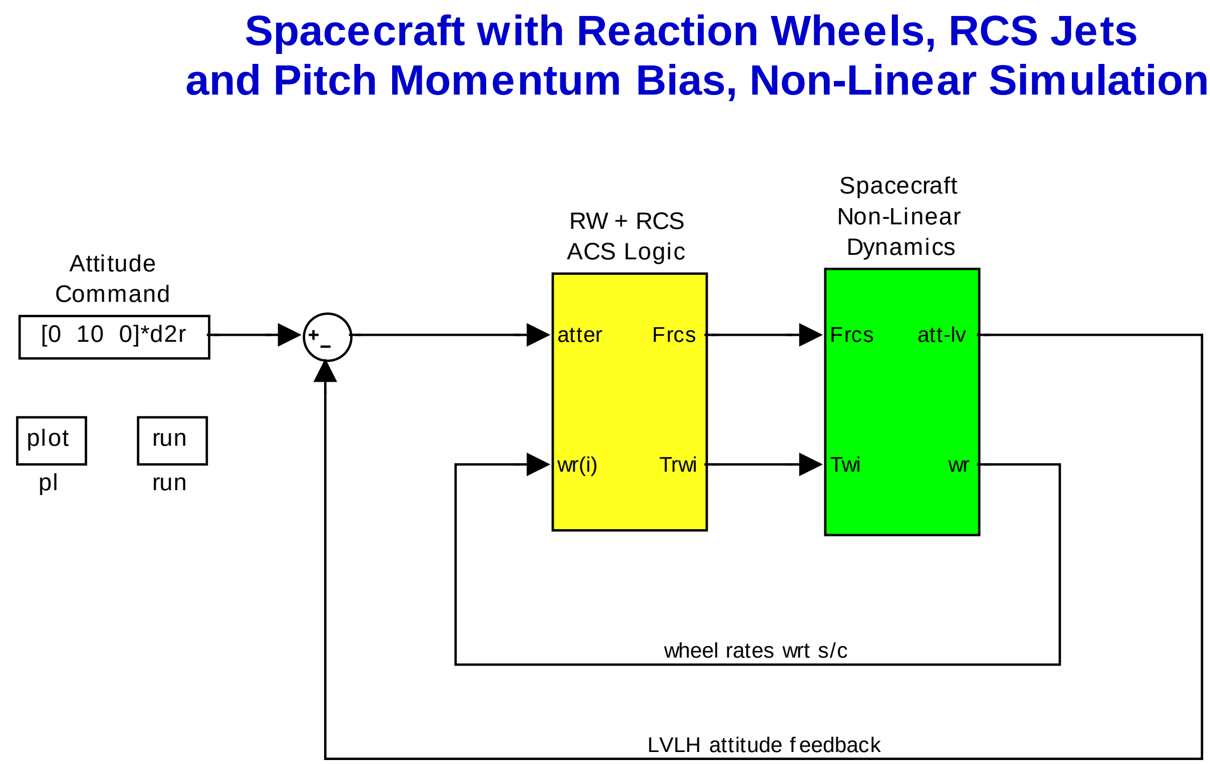

Figure 2.1 Rigid-Body Simulation Model in file "NonLinear_Sim.mdl"

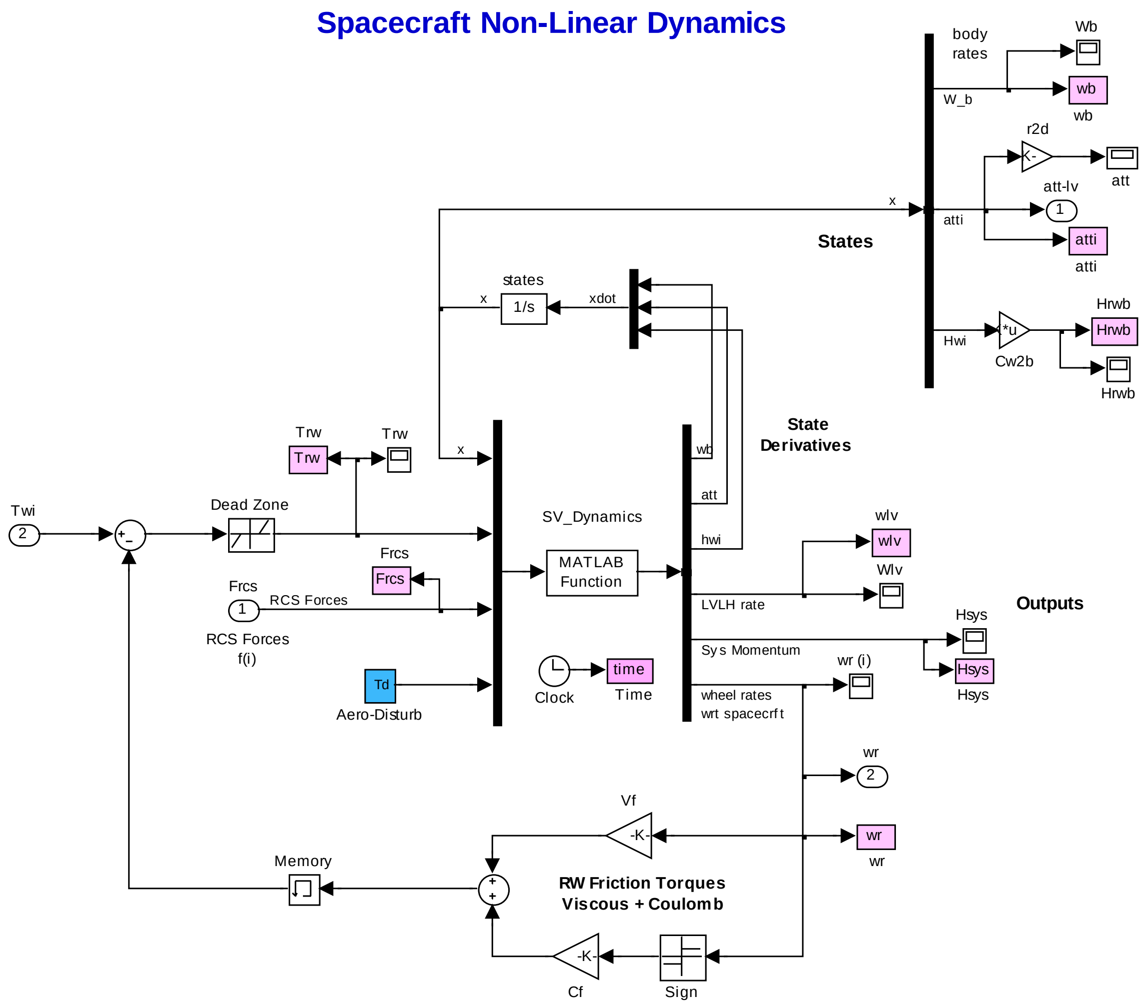

Figure 2.2 Spacecraft dynamics block using Matlab function "NonLin_Vehi_Dynamics.m"

Figure (2.2) shows the spacecraft dynamics block. The spacecraft model inputs are: 3 reaction-wheel control torques (T_{RW}), the first one being zero. There are also 7 RCS jet forces, and external aero disturbance torques (T_d) in pitch and yaw. The gravity-gradient torques are calculated inside the Matlab vehicle dynamics function "*NonLin-Vehi-Dynamics.m*" as a function of the LVLH Euler angles. There is a mechanical feedback loop that calculates the RW friction torque as a function of the wheel speeds. The friction consists of viscous plus coulomb friction torques. The motor torque for each wheel must exceed the Coulomb friction before the wheels begin accelerating. The state vector consists of spacecraft body rates, LVLH attitude, and momentum for the 3 reaction wheels. There are additional outputs used in the simulation, such as: rates with respect to the LVLH, combined spacecraft and RW system momentum, individual wheel rates relative to spacecraft, and the reaction wheel momentum resolved in body axes. The equations of motion block calculates also the transformation matrix CB2L used to transform the vehicle attitude and rate from body to LVLH coordinates. It calculates the derivative of the state-vector (9 states) which is updated by an integrator loop around the Matlab function. The vehicle parameters and integrators are initialized by the Matlab script "run.m" prior to simulation.

The spacecraft is excited by an external aerodynamic disturbance torque (T_d) in pitch and yaw, which consists of secular and cyclic components. The cyclic components are mainly due to the rotation of the solar arrays at orbital rate (ω_o) and the variation in density between the bright and dark sides of the earth. There is also disturbance torques occurring at twice the orbital rate ($2\omega_o$) because the satellite has less aero drag when the arrays are horizontal and more drag when they are vertical. There are secular disturbances in both pitch and yaw due to lack of symmetry (the satellite center of pressure is above the CG, and there is also an optical instrument on its right side). This requires a biased RW control torque which eventually approaches to the RW momentum saturation levels and a regular momentum desaturation is needed using RCS jets.

2.2 Reaction Wheels

A simplified RW model is shown in figure (2.3). The torque applied to the spacecraft is equal to the torque generated by the RW motor minus the friction torque. The friction torque consists of viscous friction which is proportional to the wheel rate plus Coulomb friction which is at constant magnitude. The wheel does not accelerate until the applied torque exceeds the Coulomb friction which is represented by a small dead-zone. This model is implemented in the Simulink file “RW.mdl”. The momentum wheel device is almost identical to the reaction wheels. It has the same moment of inertia as the RW. It does not accelerate but its speed is maintained at constant rate 4770 (rpm). It does not produce any torque about the spin direction but only gyroscopic torques in the orthogonal directions due to (ωxH) coupling with the vehicle rate.

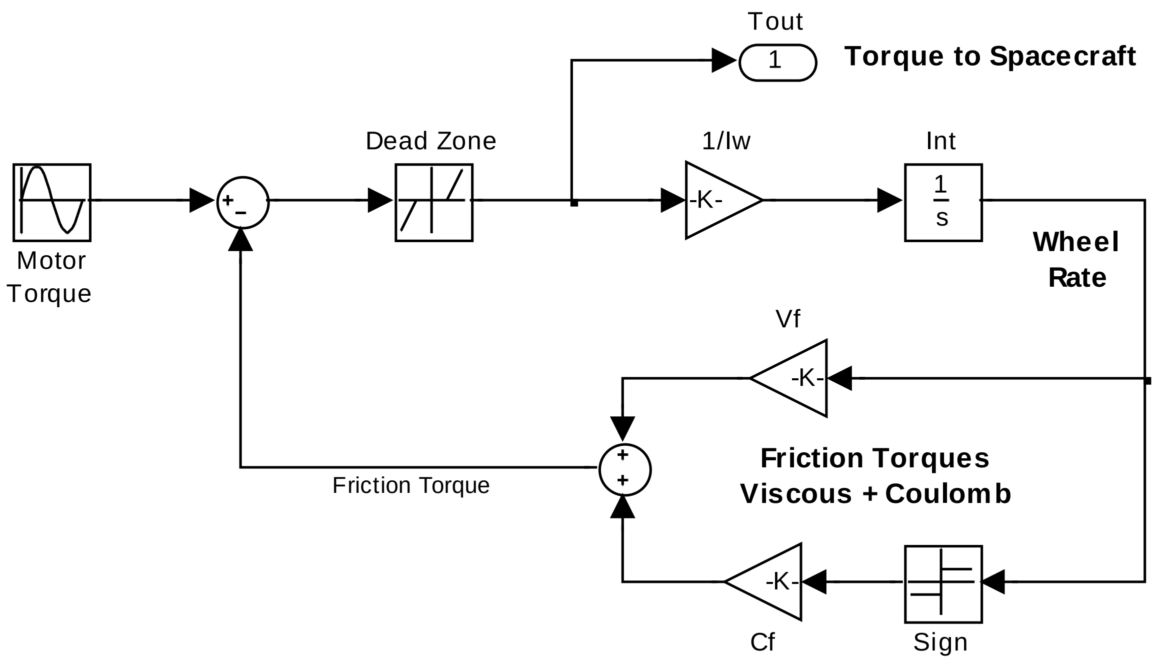

Figure 2.3 Reaction Wheel Model

2.3 Attitude Control System

The RCS attitude control system uses a phase-plane with jet selection logic. It is implemented in Matlab function "*Phase-Plane.m*". The phase-plane logic inputs are attitude and rate errors. Since only attitude measurements are available and not rates, the rates are estimated from the attitude errors. The phase-plane calculates the required direction of rotation eigenvector and calls the jet-selection logic (function "*Jet_Select_dot.m*") to determine which jets to fire. The jet-select logic fires one or two jets in order to rotate the spacecraft about an axis that is as close as possible to the commanded direction. The selection of jets is determined by calculating the dot-product contribution of each thruster in the commanded direction. Then, one or two jets are selected that provide maximum acceleration in that direction. The inputs to this block are rate errors (rad/sec) and attitude errors (rad). The outputs are 7 jet thrusts and the direction of rotation unit vector.

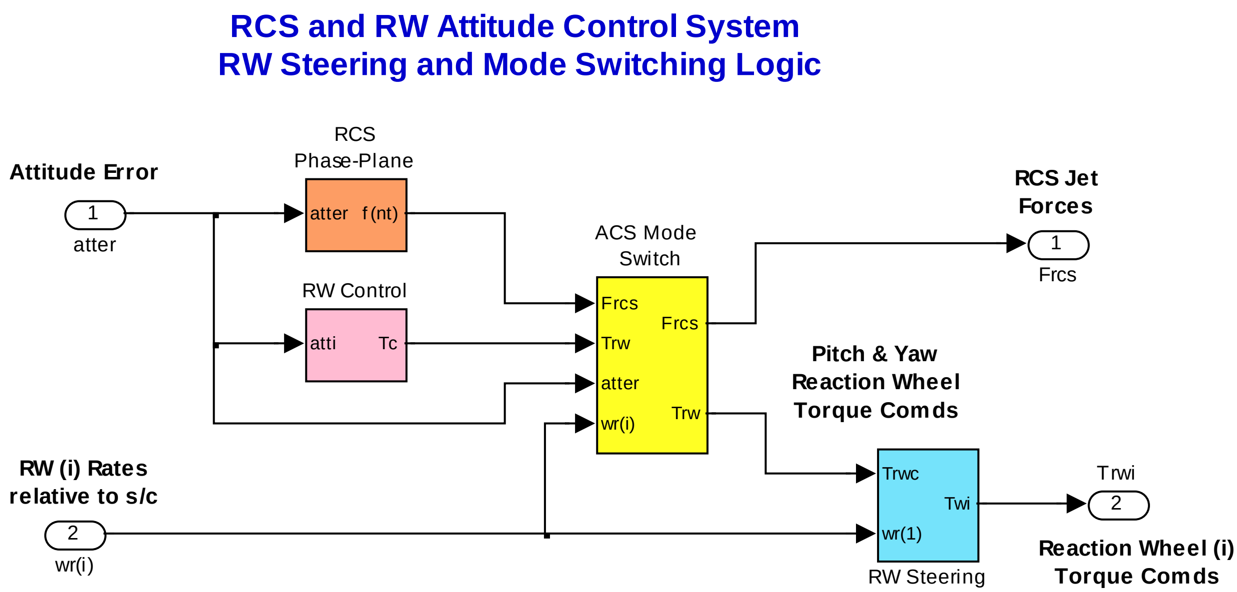

Figure 2.4 Combined Reaction Wheel plus RCS Attitude Control System

2.3.1 Reaction Wheel Control Law

The reaction wheel control law was derived in Section (1). The inputs are roll and pitch errors and the outputs are pitch and yaw torque commands to the RW. Roll is controlled gyroscopically by yaw RW commands by taking advantage of the pitch momentum bias. The coupling between roll and yaw also provides some degree of yaw stabilization.

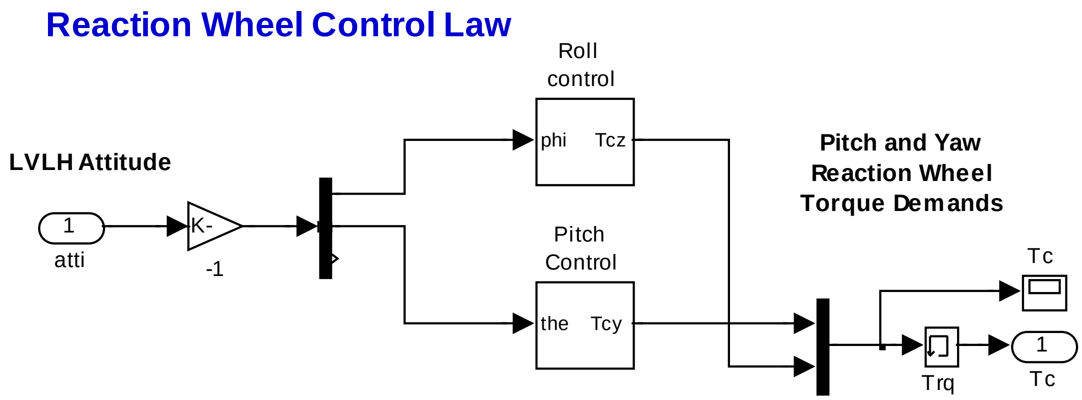

Figure 2.5 Reaction Wheel Control Law

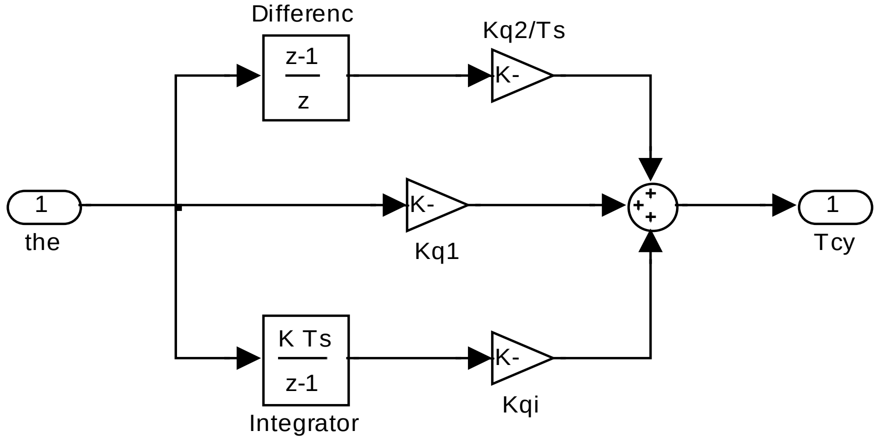

Figure 2.5.1 Pitch Reaction Wheel PID Control Law

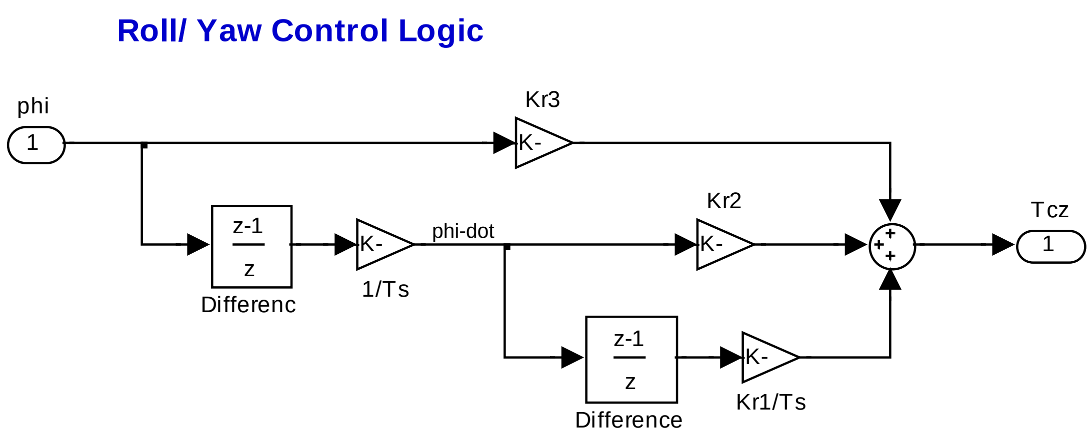

Figure 2.5.2 Lateral Reaction Wheel Control Law

2.3.2 Reaction Wheel Steering Logic

The RW steering logic performs two functions. The first function is to transform the pitch and yaw torque commands from the RW attitude control system into RW#2 and RW#3 torque commands. As we described earlier the average momentum in RW#2 and RW#3 is zero and they are used to provide pitch and yaw control torque to the spacecraft. There is an electric motor that accelerates or decelerates the wheels about their spin axis that produces a torque. The max torque magnitude that each RW produces is approx. 0.05 (ft-lb). There is a limiter in the steering logic that saturates the commanded wheel torques magnitude, so that their torques does not exceed the max torque capability. During torque limiting, the maneuver maintains the commanded eigenaxis direction. The logic in the steering subsystem also regulates the speed of wheel #1 by providing the necessary torque for wheel #1 to overcome friction and to maintain constant rate -500 (rad/sec) relative to the spacecraft. Wheel #1 provides momentum biasing to the spacecraft in the pitch direction for passive roll/ yaw stabilization. The total pitch momentum of the spacecraft system consists of wheel plus spacecraft momentum and they are both in the negative direction.

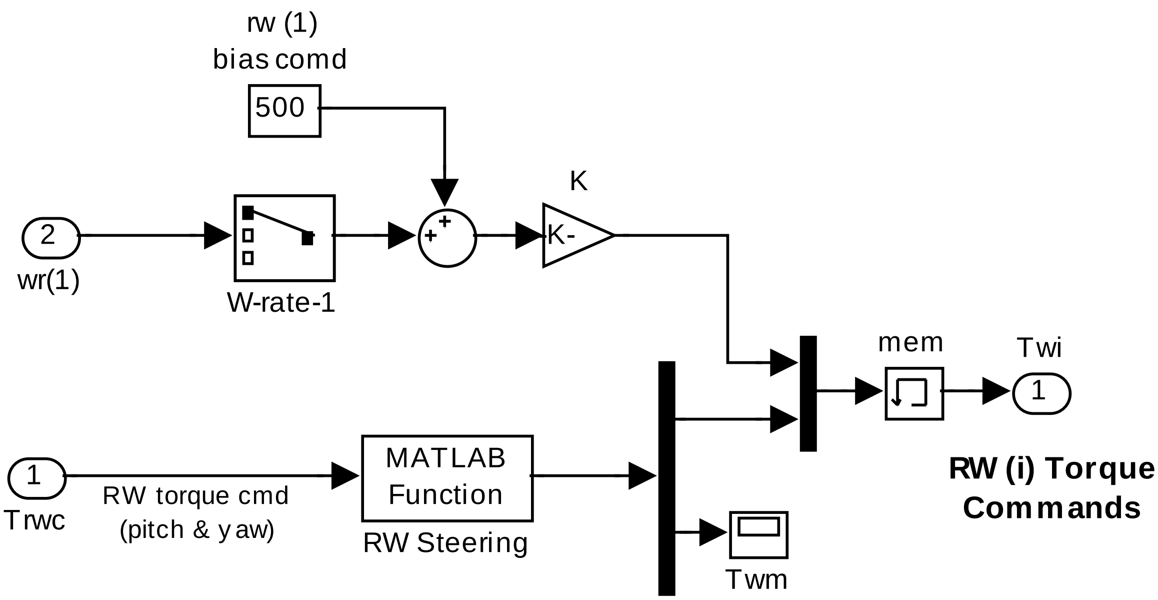

Figure 2.6 Reaction Wheel Steering and Wheel #1 Speed Control

```
function out = RW_Steering(Tc)
global J JI Iw Jw Cw2b Cb2w Tmax d2r
% Converts the Torque Commands from s/c Body to Wheel torques
% Tc     =  Torque Command (ft-lb)

Twc=zeros(3,1);
Twc= Cb2w*Tc;                           % Wheel(2,3) Torque command
Twm= sqrt(Twc'*Twc);                    % Magnitude of torque commd
if Twm>Tmax; Twc= Tmax*Twc/Twm; end     % Limit Torque Command
out= [Twc; Twm];                        % Torque Commands for wheels 2 & 3, Torq magn
```

2.3.3 RCS Phase-Plane/ Jet Selection Attitude Control System

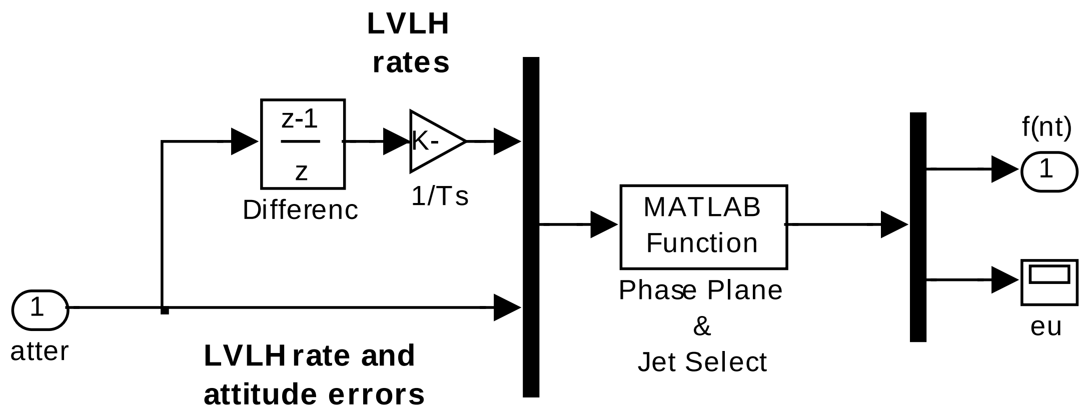

Figure 2.7 Phase-Plane and RCS Jet Selection Logic

Figure (2.7) shows the jets reaction control subsystem (orange block in figure 2.4) which is a phase-plane logic operating on the attitude and rate errors. The rate error is obtained by differentiating the attitude error in the z-domain. The phase-plane logic determines the ideal direction of rotation unit vector and calls the jet selection logic to fire either one or two jets that will torque the vehicle as close as possible to the desired direction. The jets are selected by means of a dot-product jet selection logic. The phase-plane logic is implemented in Matlab functions "*Phase-Plane.m*" and "*Jet_Select_dot.m*".

2.3.4 ACS Mode Switching Logic for Momentum Desaturation

The ACS mode switching block (yellow block in figure 2.4) is shown in Figure (2.8). It is used to switch between the RW and RCS attitude control modes of operation. When the combined magnitude of RW#2 and RW#3 momentum is below a certain level (10 ft-lb-sec) the spacecraft remains in the RW mode and it does not fire any jets. Pitch and roll attitudes are controlled more accurately than yaw. Yaw errors drift to larger magnitudes due to greater yaw aero disturbances but they are maintained within 6 (deg) due to the stiffening effect of momentum biasing. The surveillance system can tolerate a reasonable amount of attitude error because the telescope is gimbaling. When the RW momentum exceeds the threshold the logic switches to RCS attitude control in order to maintain LVLH attitude. The yaw attitude error is reduced by the RCS to within the RCS dead-band, and the two reaction wheels are torqued in the direction that reduces RW momentum. The RW torque during desaturation is maintained below max torque and its direction is applied against the accumulated momentum direction in order to bring it to zero in both directions in unison. The jet forces overpower any RW desaturation torques. When the RW momentum magnitude drops below (1 ft-lb-sec) it switches back to RW control. This logic is implemented in Matlab function "*Mode-Switch.m*". In Section (6) we replaced it with a Matlab/ State-flow switching logic.

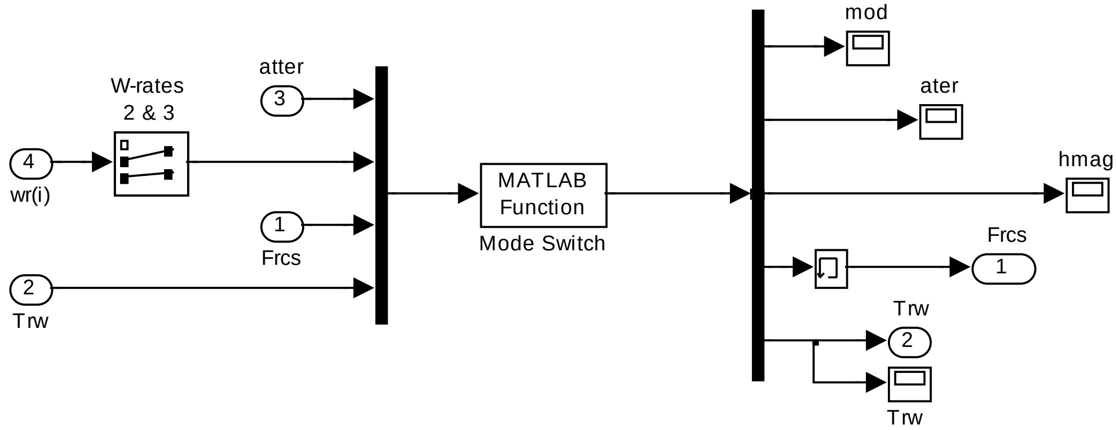

Figure 2.8 Reaction Wheel/ RCS Mode Switching Logic

2.3 Simulation Results

The following simulation results are obtained using the rigid body Simulink model of equations (2.1). The simulation starts using reaction wheel control. It is commanded to maneuver to 10 (deg) in pitch attitude and it achieves that attitude in a short time. After a while the aero and gravity-gradient torques cause the RW momentum to increase. When the RW momentum exceeds the desaturation threshold the logic switches to RCS control and fires the jets to control and maintain the LVLH attitude while at the same time it torques the reaction wheels #2 and #3 to de-saturate the accumulated momentum. The desaturation periods are short in comparison to the RW control periods and they occur approximately every two hours. During RW control the spacecraft maintains good pitch and roll control within 1.5 (deg) of attitude error. The yaw drift can go as high as 6 (deg) and it is corrected every time the logic switches to the RCS jet control mode.

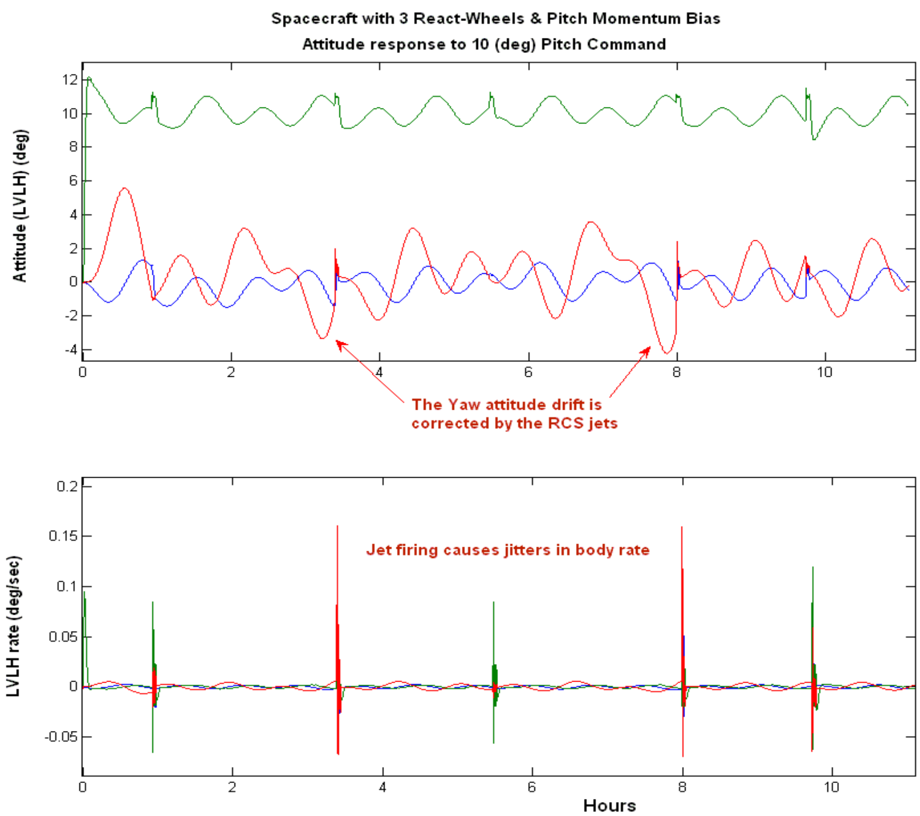
Spacecraft with 3 React-Wheels & Pitch Momentum Bias
Attitude response to 10 (deg) Pitch Command
Attitude (LVLH) (deg)
The Yaw attitude drift is
corrected by the RCS jets
LVLH rate (deg/sec)
Jet firing causes jitters in body rate
Hours

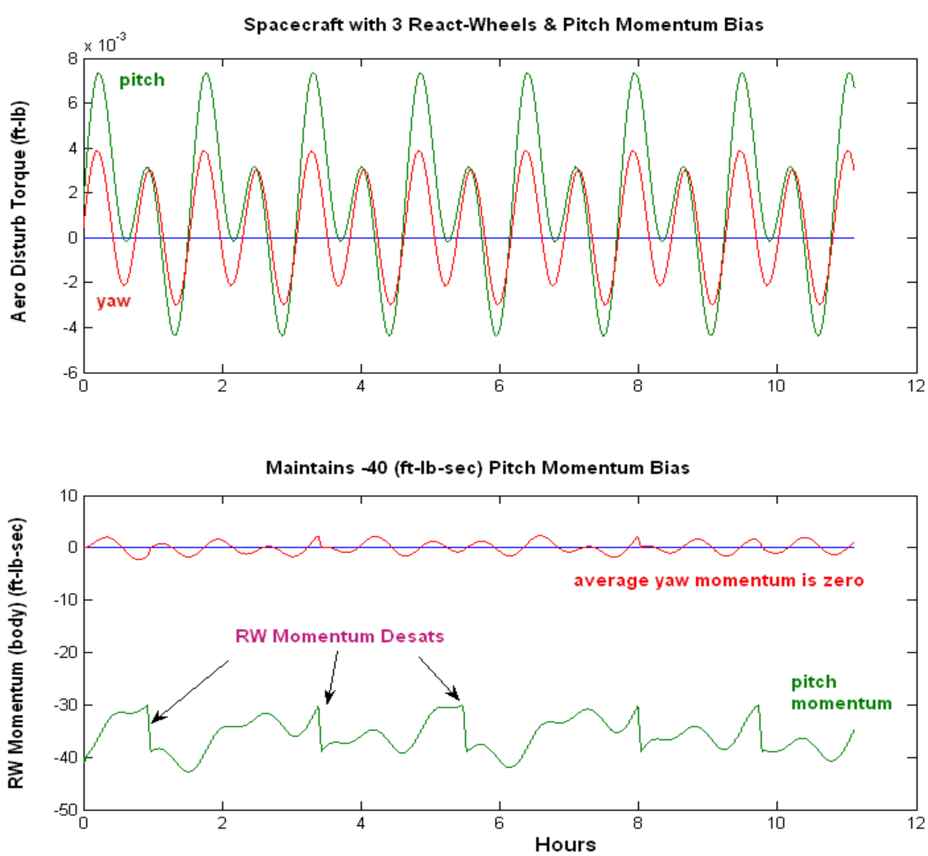
Spacecraft with 3 React-Wheels & Pitch Momentum Bias
Aero Disturb Torque (ft-lb)
x 10^-3
pitch
yaw
Maintains -40 (ft-lb-sec) Pitch Momentum Bias
RW Momentum (body) (ft-lb-sec)
average yaw momentum is zero
RW Momentum Desats
pitch
momentum
Hours

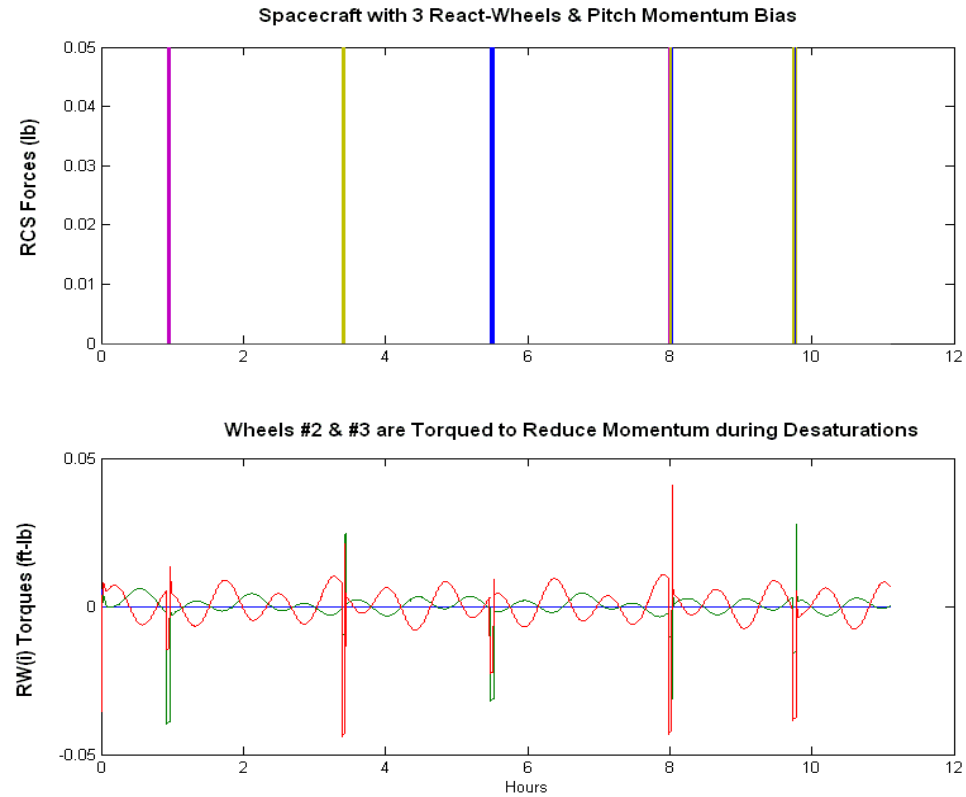

Spacecraft with 3 React-Wheels & Pitch Momentum Bias
RCS Forces (lb)
0.05
0.04
0.03
0.02
0.01
0
0 2 4 6 8 10 12
Wheels #2 & #3 are Torqued to Reduce Momentum during Desaturations
RW(i) Torques (ft-lb)
0.05
0
-0.05
0 2 4 6 8 10 12
Hours

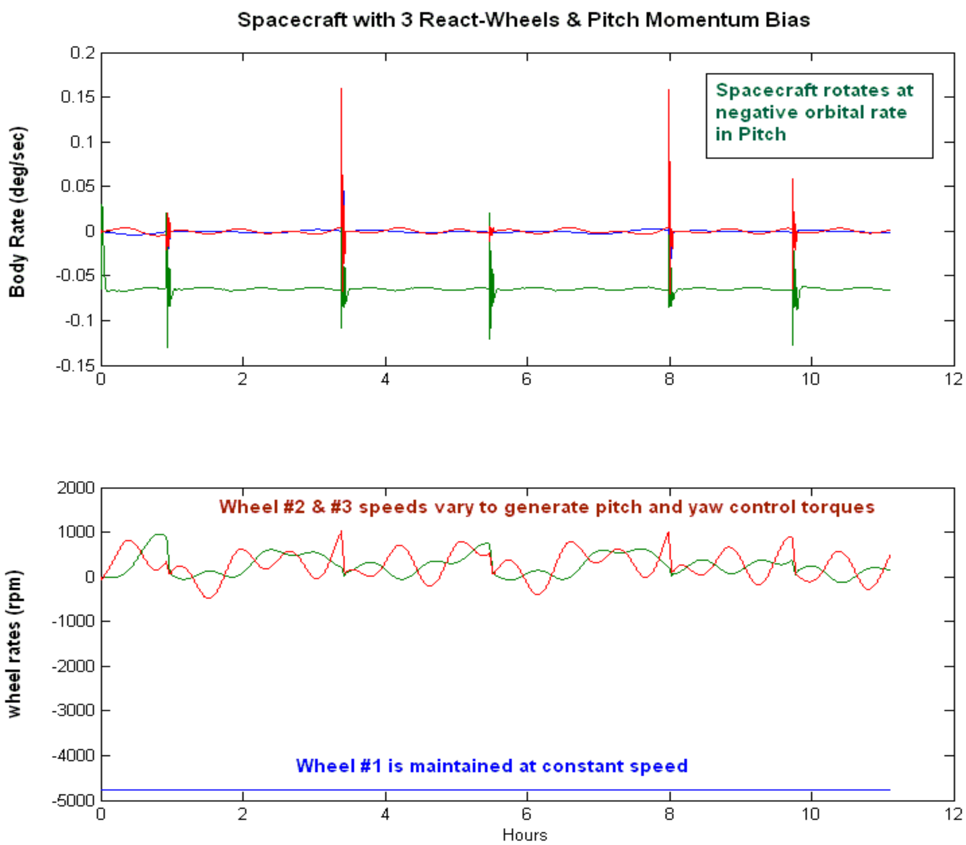

Spacecraft with 3 React-Wheels & Pitch Momentum Bias
Body Rate (deg/sec)
0.2
0.15
0.1
0.05
0
-0.05
-0.1
-0.15
Spacecraft rotates at negative orbital rate in Pitch
0 2 4 6 8 10 12
wheel rates (rpm)
2000
1000
0
-1000
-2000
-3000
-4000
-5000
Wheel #2 & #3 speeds vary to generate pitch and yaw control torques
Wheel #1 is maintained at constant speed
0 2 4 6 8 10 12
Hours

3 Flexible Spacecraft Modeling Using Modal Data

This section describes the creation of flexible spacecraft state-space systems which are entirely derived from a finite elements structural model (FEM) of the spacecraft by means of mode shapes and frequencies. The dynamic model is obtained by using the Flixan Flex Spacecraft Modeling program, and consists of 67 modes from which the first six are rigid-body modes at zero frequency that define the rigid-body behavior of the spacecraft and the rotating appendages, and the remaining 61 modes are structural flexibility modes associated with resonant frequencies. Not all the flex modes generated by the FEM program are included in the analysis model.

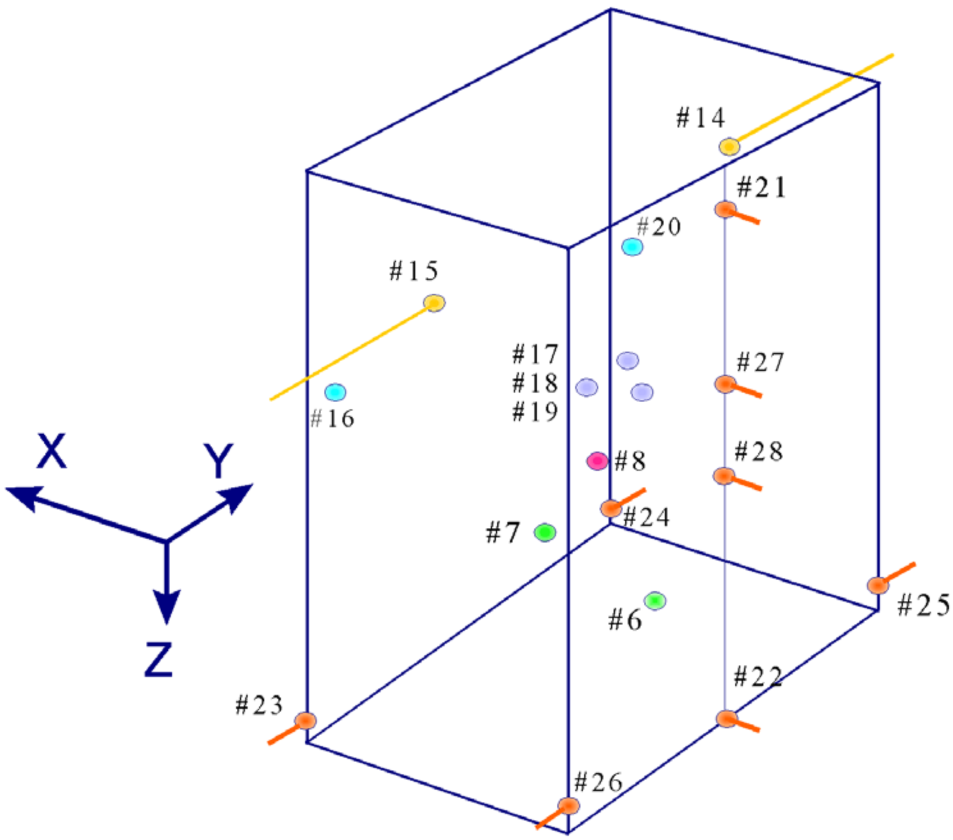

Figure 3.1 Some Important Node Locations on the Spacecraft Bus

The modal data is obtained from a finite elements modeling program which produces a huge number of mode shapes at multitude of structural locations (nodes). The original FEM data is reduced to a smaller modal data file "*Surveillance-Sat.Mod*" that contains only the first 100 modes at 28 possibly useful nodes. Out of the 100 modes we selected 67 (6 rigid and 61 flex) modes to be included in the state-space model. The 28 nodes which are included in the modal data file are listed in a file "*Surveillance-Sat.Nod*" with a short description, node numbers, FEM id numbers, and location coordinates. The nodes map is shown in Table (3.1). Figure (3.1) shows the locations of some of the nodes on the spacecraft bus. By means of a mode selection process we discard the mode resonances which do not participate much between certain excitation and measurements points or other sensitive locations on the spacecraft, and we retain a smaller set of 67 modes. The mode selection process displays the nodes file in menus for selecting structural locations.

Table (3.1) The Nodes Map

NODE IDENTIFICATION TABLE FOR SURVELLANCE SATELLITE WITH SOLAR ARRAYS AND TELESCOPE

Node Description	Node No	FEM ID	Location X,Y,Z (feet)		
Moving Mirror	1	2101			
Fixed Mirror	2	2102			
Focal Plane	3	2103			
Moving Antenna	4	2104			
Fixed Antenna	5	2105			
Inertial Attitude Sensors	6	31001	-0.747	0.114	25.572
Accelerometers	7	31002	0.338	0.648	25.57
Cryo Cooler Pump	8	40101			
Second Mirror	9	40102			
Sensitive Instrument 2	10	40103			
Sensitive Instrument 3	11	40104			
Sensitive Instrument 4	12	40105			
Sensitive Instrument 5	13	40106			
Right Solar Array Attachm	14	62131	-0.37	1.832	17.075
Left Solar Array Attachm	15	62231	-0.37	-1.832	17.075
Left Horizon Sensor	16	10001	1.0	-1.446	21.604
Reaction Wheel #1 CG	17	58041	-0.792	0.049	21.594
Reaction Wheel #2 CG	18	58042	0.354	-0.71	21.594
Reaction Wheel #3 CG	19	58043	0.438	0.661	21.594
Right Horizon Sensor	20	10002	0.907	1.57	21.142
RCS Jet #1 (+X)	21	98001	-2.362	0.0	18.075
RCS Jet #2 (+X)	22	98002	-2.362	0.0	24.675
RCS Jet #3 (+Y)	23	98003	1.271	-1.433	24.802
RCS Jet #4 (-Y)	24	98004	1.271	1.433	24.802
RCS Jet #5 (-Y)	25	98005	-1.787	0.708	24.675
RCS Jet #6 (+Y)	26	98006	-1.787	-0.708	24.675
RCS Jet #7 (+X)	27	98007	-2.362	0.0	21.45
RCS Jet #8 (+X)	28	98008	-2.34	0.0	21.783

The flex spacecraft configuration and its modal properties are defined by a set of data in an input file "*Surveillance-Sat.Inp*". Parameters such as input forces, torques, measurements and other sensors, locations and directions are defined in that file. The model preparation is an interactive process during which the modal strengths of all modes are calculated and a selected set of modal data is extracted and it is included at the bottom of the input data file. The title of the spacecraft data set is "*Flex Spacecraft with Gimbaling Telescope and Reaction Wheels (67-modes)*". The Flex Spacecraft modeling program reads this set of input data and creates the state-space model in file: "*Surveillance-Sat.Qdr*".

3.1 Gimbaling Appendages

The rotating appendages add some further dynamic complexity to the model. The surveillance spacecraft in this example has four gimbaling bodies that can be made to rotate with respect to the spacecraft by applying torques at the corresponding hinges. There is an optical sensor that gimbals in two orthogonal directions, and two solar arrays that rotate about the y axis. The mode shapes and frequencies are initially created in the FEM by assuming that all gimbals are locked and do not rotate. The relative motion between the spacecraft and the rotating appendages is captured in the equations by means of the inertial coupling coefficients, or otherwise known as H-parameters. The H-parameters is a matrix of data also created by the finite element modeling program, extracted from the mass matrix. They provide dynamic coupling between the flex equations and the rotational equations of the gimbaling bodies, as shown in equations (3.1). They are included in a separate file "*Surveillance-Sat.Hpr*". This file starts with the vehicle title, the number of modes (100), which should correspond to the number of modes in the modal data file "*Surveillance-Sat.Mod*", and also the number of gimbaling body degrees-of-freedom (dof) (4). The H-parameters matrix has 100 rows of and 4 columns corresponding to the four hinges (Telescope rotations in elevation and azimuth, left solar array, and right solar array rotations respectively). If the original modal data in file "*Surveillance-Sat.Mod*" had to be rescaled during mode selection (fortunately they did not have to be modified this example), the units in the H-parameters file should match the rescaled modal data, not the original file. At the bottom of the H-parameters file, the (4x4) moments of inertia matrix of the four appendages is also included in the corresponding order. Each element in the H-parameters matrix couples a bending mode excitation with the rotational acceleration of an appendage. It determines also the relative rotation at a hinge due to both: rigid-body motion and flexibility. The flex spacecraft modeling program reads the H-parameters file and introduces the additional dofs and equations to unlock the gimbals.

The flex spacecraft dynamics can be expressed by three sets of equations (3.1). The first set of equations describes how the structure modes (η) are excited by the external forces and torques (F and T). Rotational accelerations at the hinges ($\ddot{\alpha}$) also excite flexibility via the H-coefficients. The second set of equations relates rotation accelerations at the hinges ($\ddot{\alpha}$) as a function of the control torques (T_α) at the joints, which control the rotation angles of the appendages. Structure flexibility also adds a flex mode component via the H-coefficients. The third set of equations represents the measurements, both, for translation and rotation sensors. The interaction between the modes and the rotating appendages is determined by the inertial coupling coefficients matrix (H). This linear, multi-body model is very useful for servo control design and stability analysis purposes, and also for evaluating sensitivity and attitude control system performance with respect to commands and disturbances (jitter analysis, payload pointing, etc). It is not intended for large angle slewing.

$$
\begin{aligned}
& M_G\left(\underline{\ddot{\eta}} + 2\zeta\,\Omega\underline{\dot{\eta}} + \Omega^2\underline{\eta}\right) + H\underline{\ddot{\alpha}} = \Phi^T \begin{bmatrix} F \\ T \end{bmatrix} \\
& I_\alpha \underline{\ddot{\alpha}} + H^T \underline{\ddot{\eta}} = \underline{T}_\alpha
\end{aligned}
\qquad (3.1)
$$

Where:

η is the modal displacements vector of dimension (n) where (n) is the number of modes

M_G is a (n x n) diagonal matrix whose elements are the modal masses

Ω is a (n x n) diagonal matrix whose elements are the mode frequencies in (rad/sec)

ς is the modal damping coefficient of each mode, typically (ς=0.005)

$\underline{\alpha}$ is a vector of dimension (m) representing the rotation angles of the payloads with respect to the spacecraft, where (m) is the number of gimbaling bodies

H is the Inertial Coupling Coefficients matrix of dimension (n x m). It couples the motion of the gimbaling bodies with modal displacements vector q

Φ^T is the mode shapes matrix of size (n x 6) containing the modal data at the points where control forces, moments, and disturbances are applied to the s/c structure.

$\underline{F}$ is a vector of the externally applied forces along x, y, and z

$\underline{T}$ is a vector of the externally applied torques about axes x, y, and z

I_α is an (m x m) moments of inertia matrix of the (m) gimbaling bodies about their axis of rotation in (ft-lf-sec^2)

$\underline{T}\alpha$ is a vector of size (m) representing the control torques in (ft-lb) at the payload gimbals.

The moments of inertia matrix ($I_{\underline{\alpha}}$) and the coupling coefficients matrix (H) are extracted from the mass matrix of the finite elements model. The measured displacement or rotation vector $\underline{X}_s$ at a sensor point (s) on the structure is a linear combination from all the modes, that is, rigid body modes plus flexible modes.

$$\underline{X}_s = \Phi_s \underline{\eta}$$

Where:

$\underline{X}_s$ is a sensor measurement vector of dimension (6) representing three translations and three rotations at point (s)

Φ_s is a (6 x n) modal matrix containing the mode shapes and slopes for (n) modes at the sensor location (s)

During model preparation the flex spacecraft modeling program interacts with the user who defines the spacecraft configuration and saves the spacecraft parameters in file “*Surveillance-Sat.Inp*”. Immediately after data preparation the program processes the spacecraft data and generates the state-space model in the systems file “*Surveillance-Sat.Qdr*”. In the absence of an H-parameters file the program ignores the gimbals. It assumes that the bodies are rigidly attached to the spacecraft and the state model will not include inputs for the gimbal torques and gimbal rotation outputs, like in our Space Station example, where we did not include an (.Hpr) file. The H-parameters file “*Surveillance-Sat.Hpr*” should match the modal data file “*Surveillance-Sat.Mod*”. The H matrix should have 100 rows that correspond to the 100 modes in the modal data file, and 4 columns for the 4 hinges. When fewer than the max number of modes is selected (as we do in this case) the program will read only the H-parameters for the selected modes and ignore the data for the modes which are not selected. When the model preparation is complete the program saves the spacecraft data and the selected modal data in file “*Surveillance_Sat.Inp*” to be processed by the flex spacecraft modeling program. Since in this example we are using an

H-parameters file, the last statement in the input data set includes the following line that references the H-parameters filename “*Surveillance-Sat.Hpr*”.

```
Inertial Coupling Coefficients (H-Parameters) File Name for the 4 gimbaling
bodies :  Surveillance-Sat.Hpr
```

If the above line is not included but the spacecraft data set ends with the selected modal data the program will assume that the spacecraft has a locked hinge structure without rotating bodies, and the state model will not include additional states, inputs, and outputs associated with the gimbaling bodies. Note, that the modal data created by the FEM must have all the gimbals locked. The presence of H-parameters unlocks the gimbals by introducing additional state variables in the model.

3.2 The Creation of the Flex Spacecraft State-Space Model

We will now present step by step instructions on how to prepare the flex spacecraft input data including the process of selecting a set of dominant resonances. It is an interactive process and the purpose here is to define the locations and directions of input forces and torques. That is, inputs such as RCS jets, reaction wheel torques, and disturbances. We must also define the locations and directions of sensors, such as, attitude control measurements, accelerometer sensors, and other sensitive locations on the structure. After defining the configuration inputs and outputs the next step is to compare and select some of the most dominant modes. The spacecraft modeling program makes frequent use of the nodes map file “*Surveillance-Sat.Nod*”. This file defines the locations of the nodes included in the modal data file “*Surveillance-Sat.Mod*”, and it is used by menus that select actuator and sensor locations. The excitation locations are defined by the node number and their direction is defined by a unit vector. The sensors are also defined by the node number, the direction of measurement (roll, pitch, yaw) or along (x, y, z), and type of measurement (position, rate, acceleration).

To run the flex spacecraft modeling program you must first select the project directory that contains the Flixan files, "*C:\Flixan\Examples\Surveillance Satellite React-Wheels*".

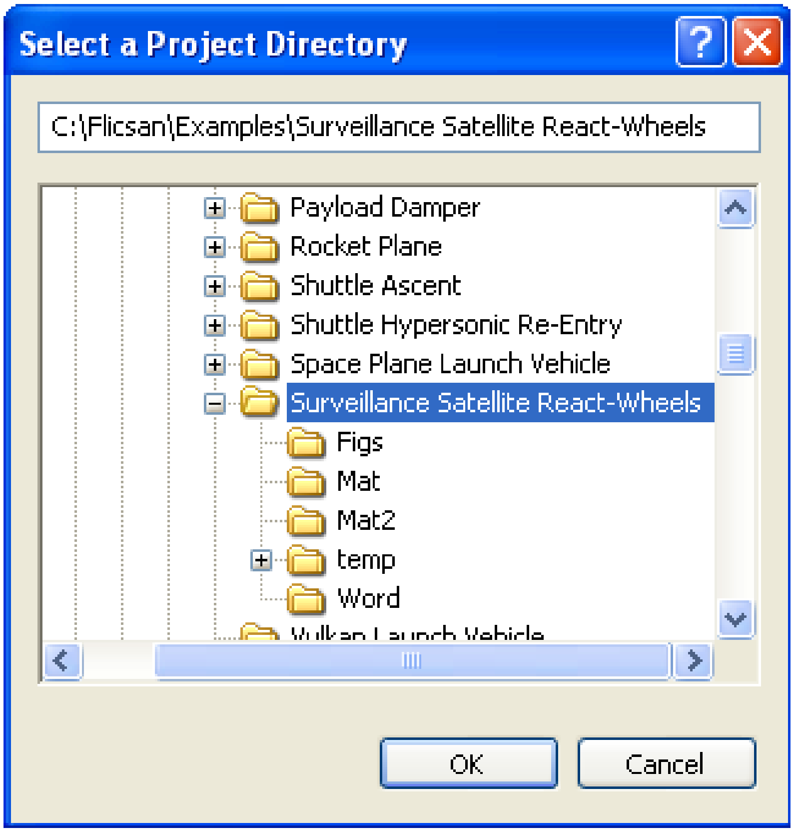

From "*Analysis Tools*", go to "*Flight Vehicle Modeling Options*" and select "*Flex Spacecraft (Using Modal Data)*". This will activate the Flex Spacecraft Modeling Program.

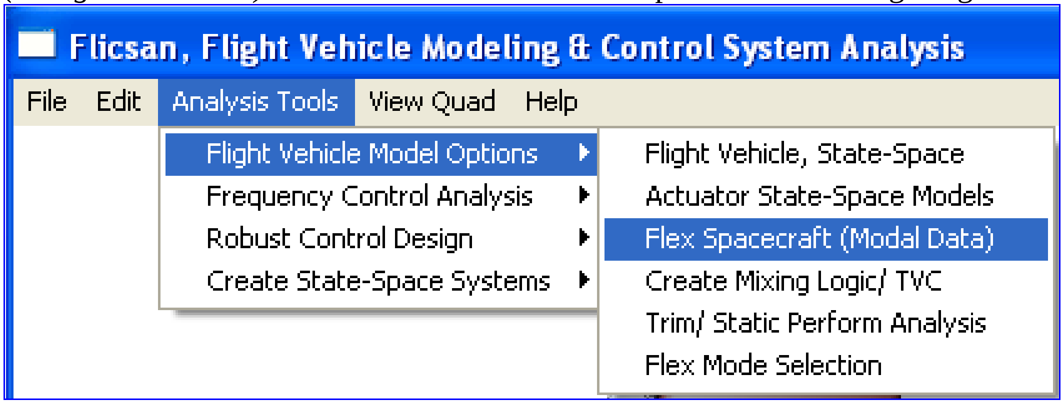

The next step is to select the input data file (.Inp) that will contain the flex spacecraft data that will be entered by the user, and also the systems file (.Qdr) that will contain the flex spacecraft state-space models. In these files we will create several sets of data and state-space systems, with and without the rigid body modes.

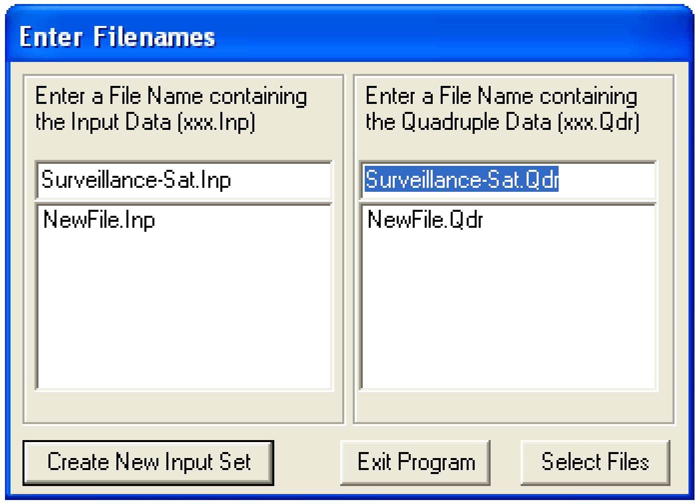

In the following dialog the user enters the new spacecraft title and the number of inputs and outputs which define the spacecraft structure configuration. In this case there are 8 input RCS forces, 6 torque excitation inputs, (3 reaction wheel control torques and 3 disturbance torques). We also define 2 translational acceleration measurements, and 13 rotational measurements (control measurements plus other sensitivity measurements). In the 3 menus on the right we select file names. The modal data file "*Surveillance-Sat.Mod*", the nodes file "*Surveillance-Sat.Nod*", and the H-parameters file "*Surveillance-Sat.Hpr*" (which is required only when there are gimbaling bodies). We may also enter a short paragraph that describes the flex spacecraft model in the yellow field at the bottom of the dialog. This paragraph will appear as comment lines in the data files, below the title.

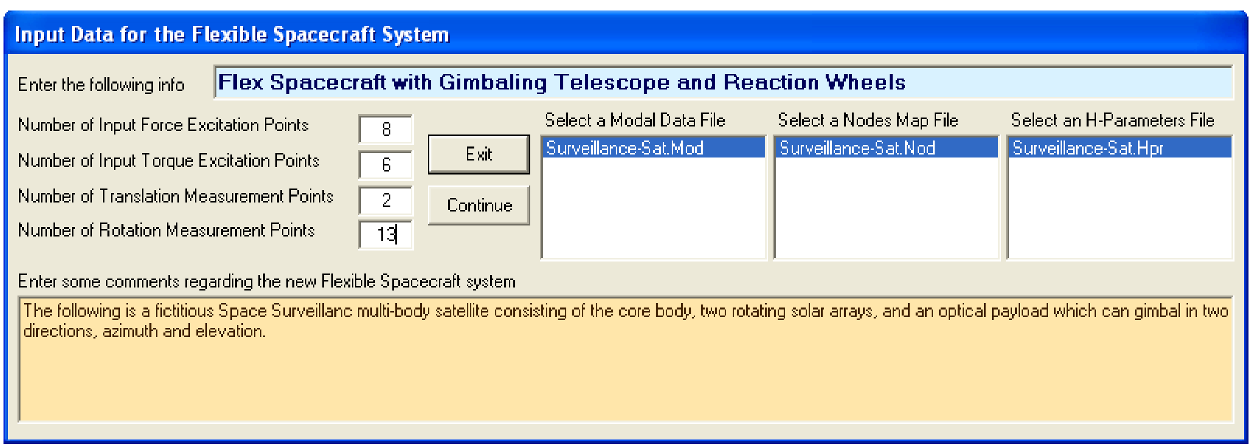

The next step is to evaluate the strength of the flex modes which are in file "*Surveillance-Sat.Mod*" and to select some of the strongest modes to be included in the flex model. We must define some excitation points and some sensor points (structure nodes) to be used strictly for mode selection. These nodes do not have to be the same locations as the ones defined as actuators and sensors in the data but they could be any nodes used only for mode strength comparison.

In the following dialog we will select from the full range of modes (1 to 100). The mode strength will be calculated between two force excitation points, 6 torque excitation points, and 6 rotational measurement points. There will be no translational measurements used in the mode selection process. We click "OK", and in the following menu we choose not to modify or scale the modal data because the units and x, y, z directions are acceptable and do not need to be rescaled.

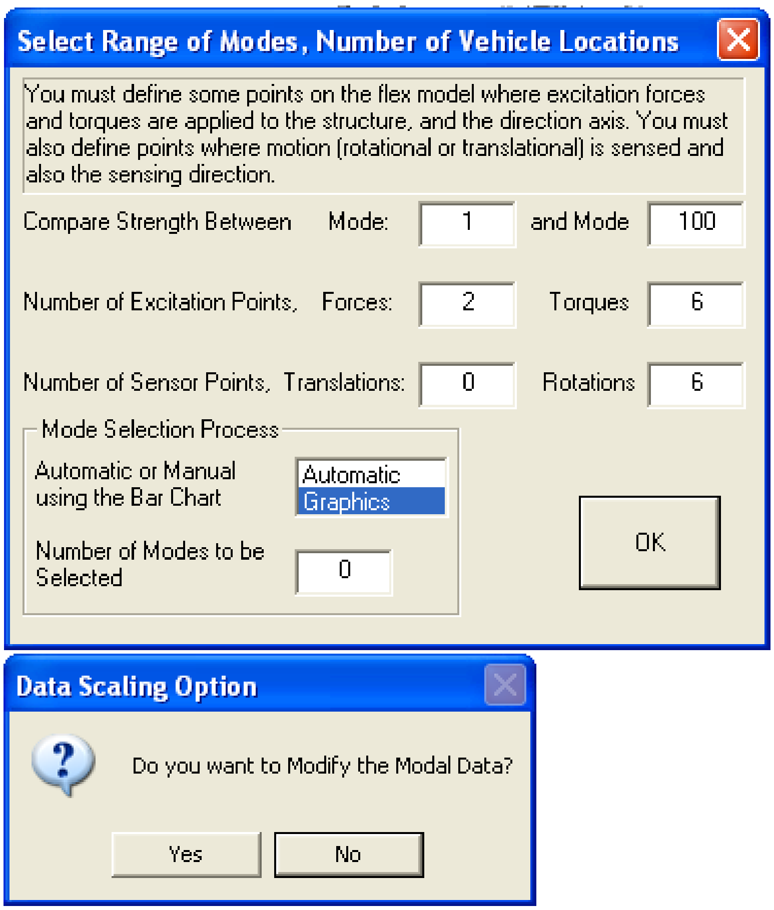

The following dialog/ menus in amber background are used for selecting structural locations only for mode selection purposes. The menu below consists of the nodes table and we use it to select nodes where to apply the first one of the two excitation forces specified earlier. In this case, node #21 was selected to apply a force in the +X direction. Node #26 was selected next (not shown) to apply the second force in the +Y direction. This is only for mode comparison and mode selection purposes.

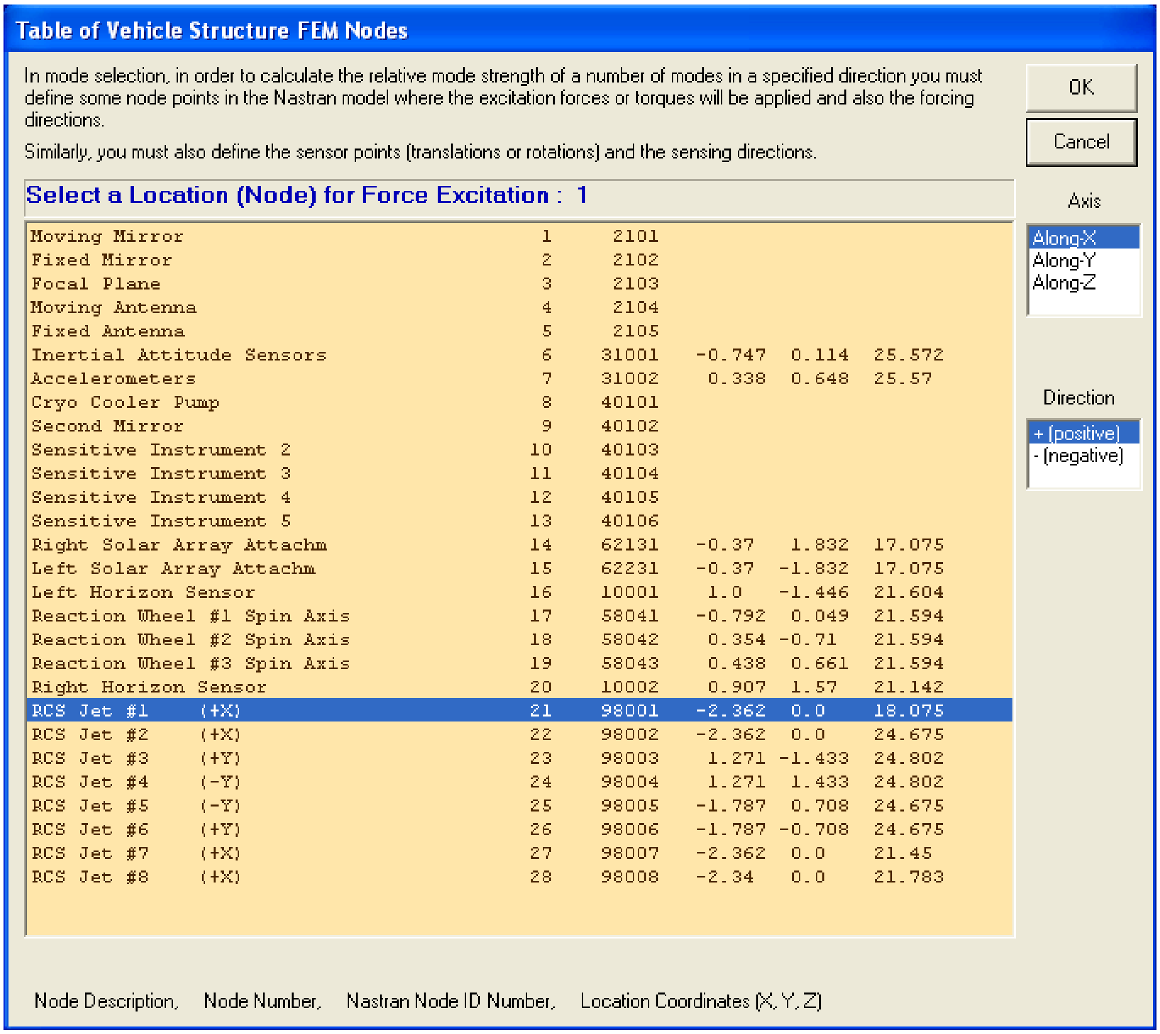

Moving Mirror	1	2101			
Fixed Mirror	2	2102			
Focal Plane	3	2103			
Moving Antenna	4	2104			
Fixed Antenna	5	2105			
Inertial Attitude Sensors	6	31001	-0.747	0.114	25.572
Accelerometers	7	31002	0.338	0.648	25.57
Cryo Cooler Pump	8	40101			
Second Mirror	9	40102			
Sensitive Instrument 2	10	40103			
Sensitive Instrument 3	11	40104			
Sensitive Instrument 4	12	40105			
Sensitive Instrument 5	13	40106			
Right Solar Array Attachm	14	62131	-0.37	1.832	17.075
Left Solar Array Attachm	15	62231	-0.37	-1.832	17.075
Left Horizon Sensor	16	10001	1.0	-1.446	21.604
Reaction Wheel #1 Spin Axis	17	58041	-0.792	0.049	21.594
Reaction Wheel #2 Spin Axis	18	58042	0.354	-0.71	21.594
Reaction Wheel #3 Spin Axis	19	58043	0.438	0.661	21.594
Right Horizon Sensor	20	10002	0.907	1.57	21.142
RCS Jet #1 (+X)	21	98001	-2.362	0.0	18.075
RCS Jet #2 (+X)	22	98002	-2.362	0.0	24.675
RCS Jet #3 (+Y)	23	98003	1.271	-1.433	24.802
RCS Jet #4 (-Y)	24	98004	1.271	1.433	24.802
RCS Jet #5 (-Y)	25	98005	-1.787	0.708	24.675
RCS Jet #6 (+Y)	26	98006	-1.787	-0.708	24.675
RCS Jet #7 (+X)	27	98007	-2.362	0.0	21.45
RCS Jet #8 (+X)	28	98008	-2.34	0.0	21.783

Similarly we define some points to apply torques (1, 2, 3), out of the total six torques defined for mode selection purposes. We select the reaction wheel nodes #17, #18, #19 to apply torques in +roll, +pitch, and +yaw directions respectively.

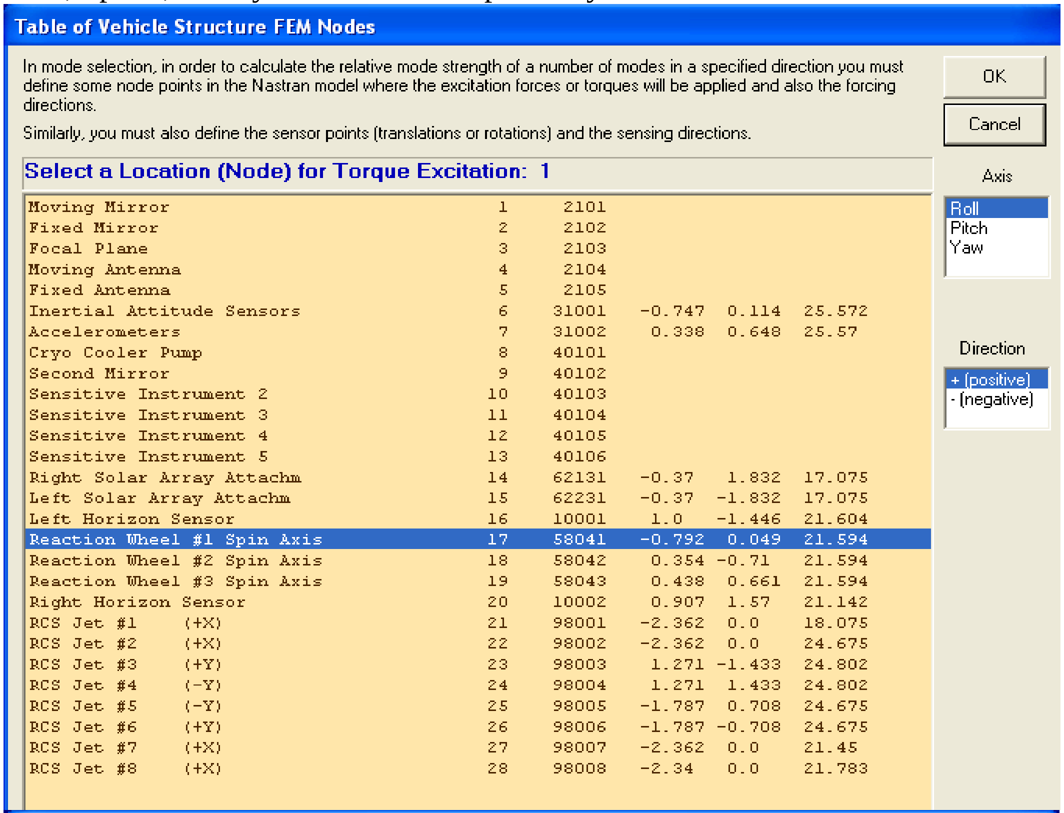

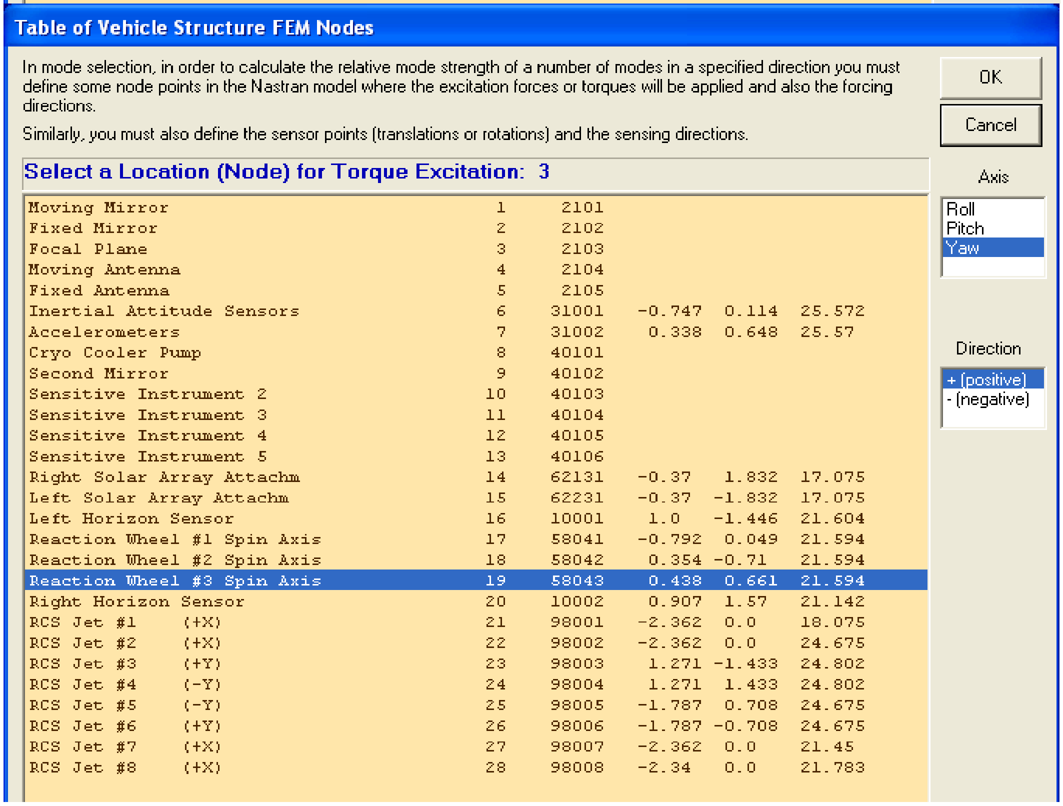

The next three torques (4, 5, 6) represent disturbances coming from a noisy cryo-cooler pump inside the spacecraft which is located at node #8. All 3 excitation torques are applied at the same node, in +roll, +pitch, and +yaw directions respectively, only for mode selection. Two of the torque definitions are shown below.

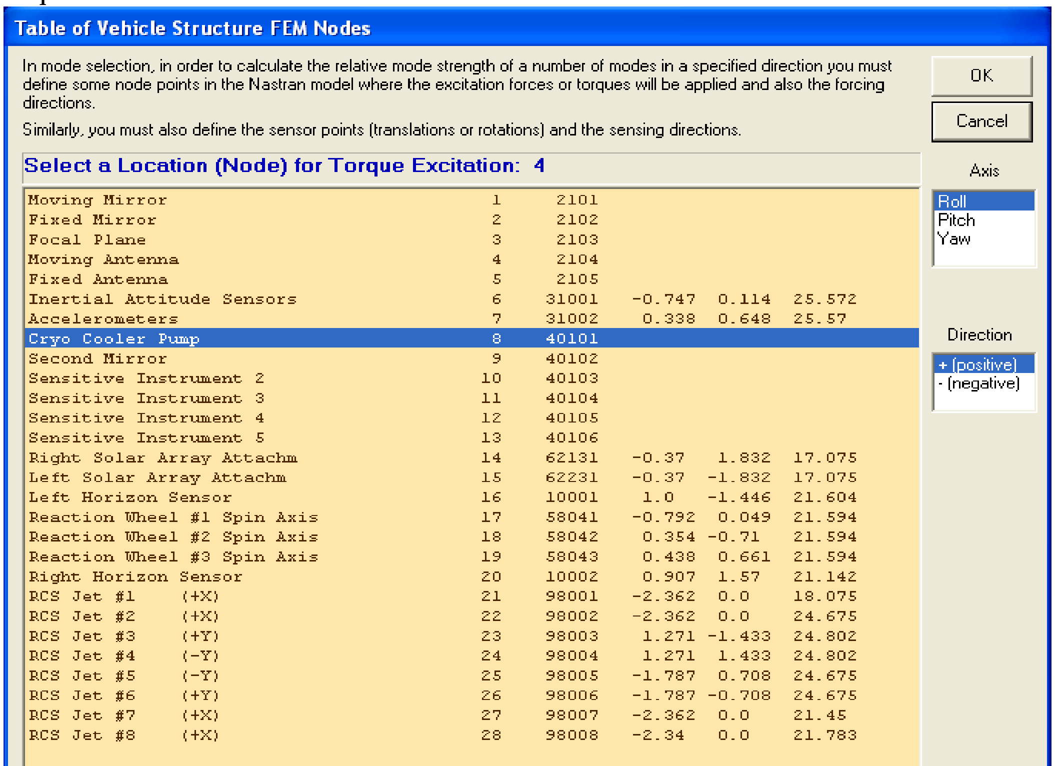

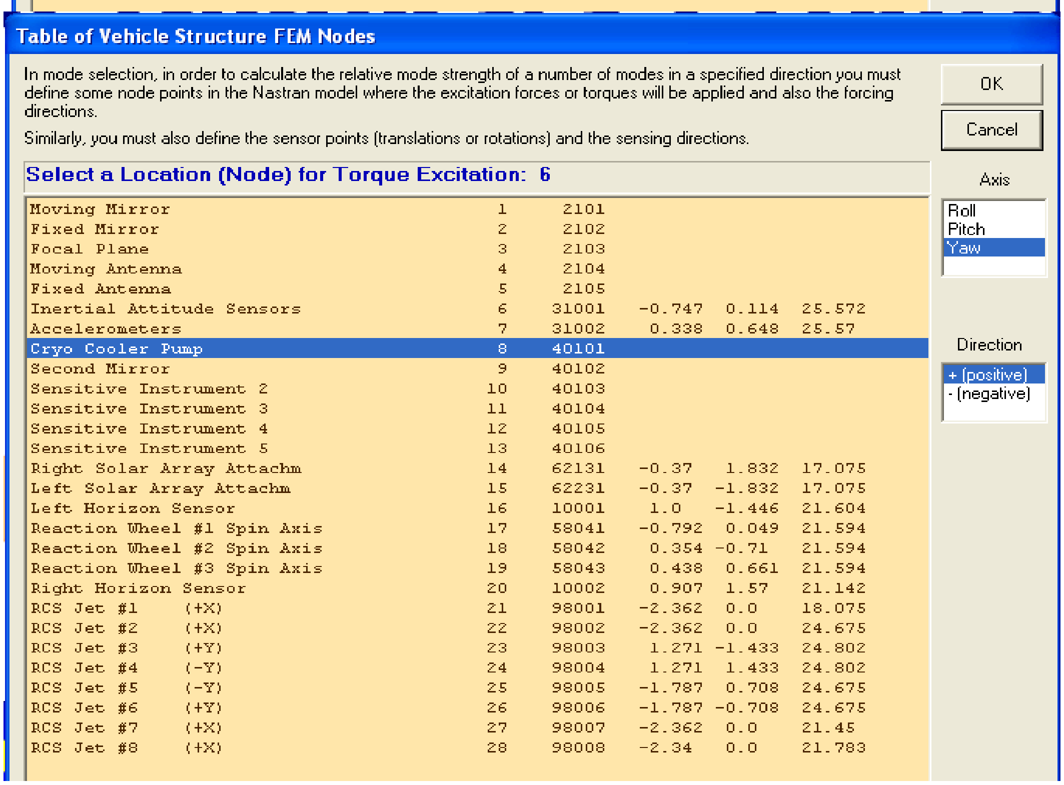

The next step is to identify nodes and directions for the 6 rotational sensors which were defined only for mode selection purposes. Node #6 was selected for the rotational sensors (1, 2, 3), measuring in the +roll, +pitch, and +yaw directions respectively.

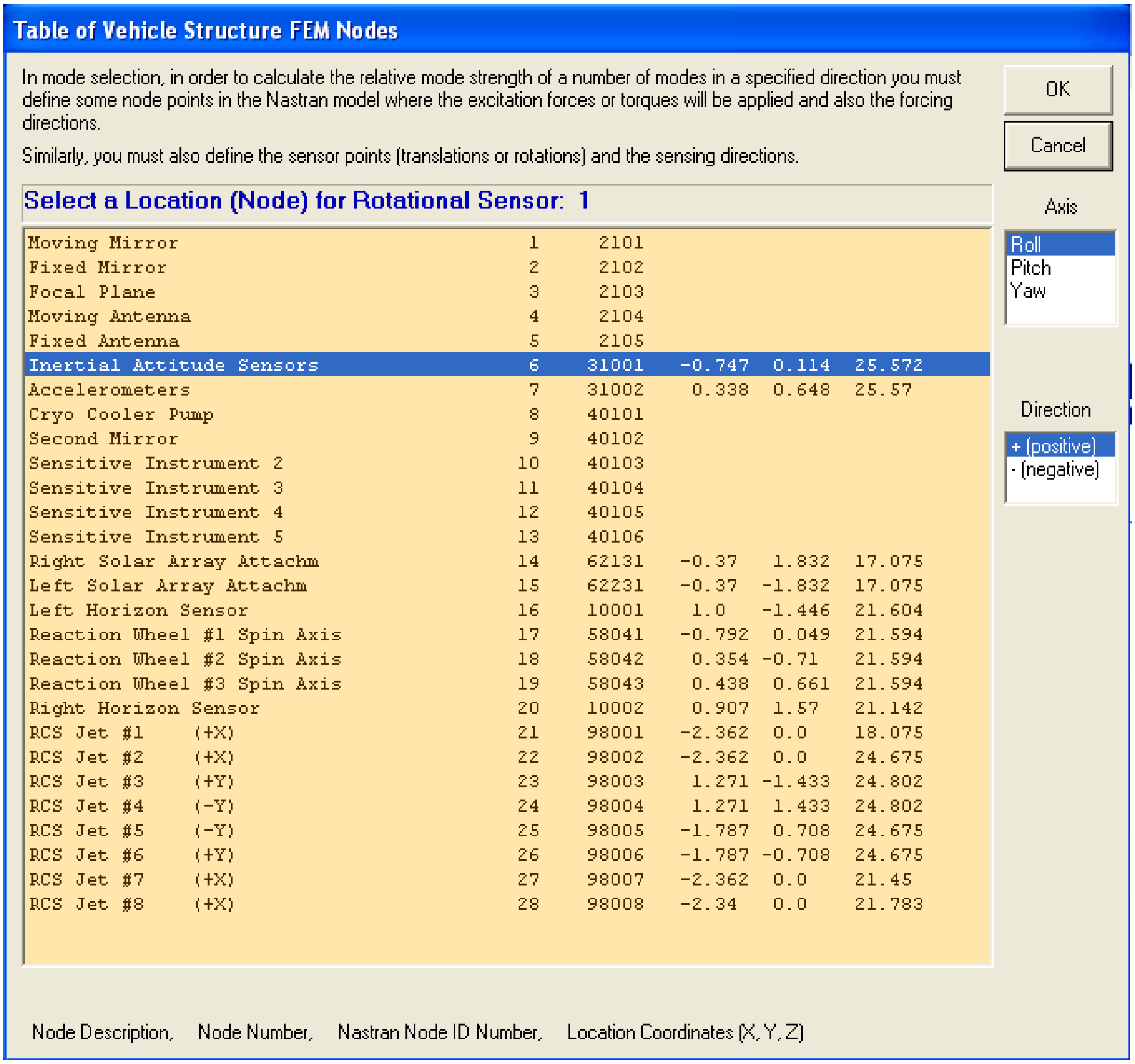

Similarly, nodes #11, #12, and #13 were selected to represent the rotational sensors (4, 5, 6), measuring in +roll, +pitch, and +yaw directions respectively.

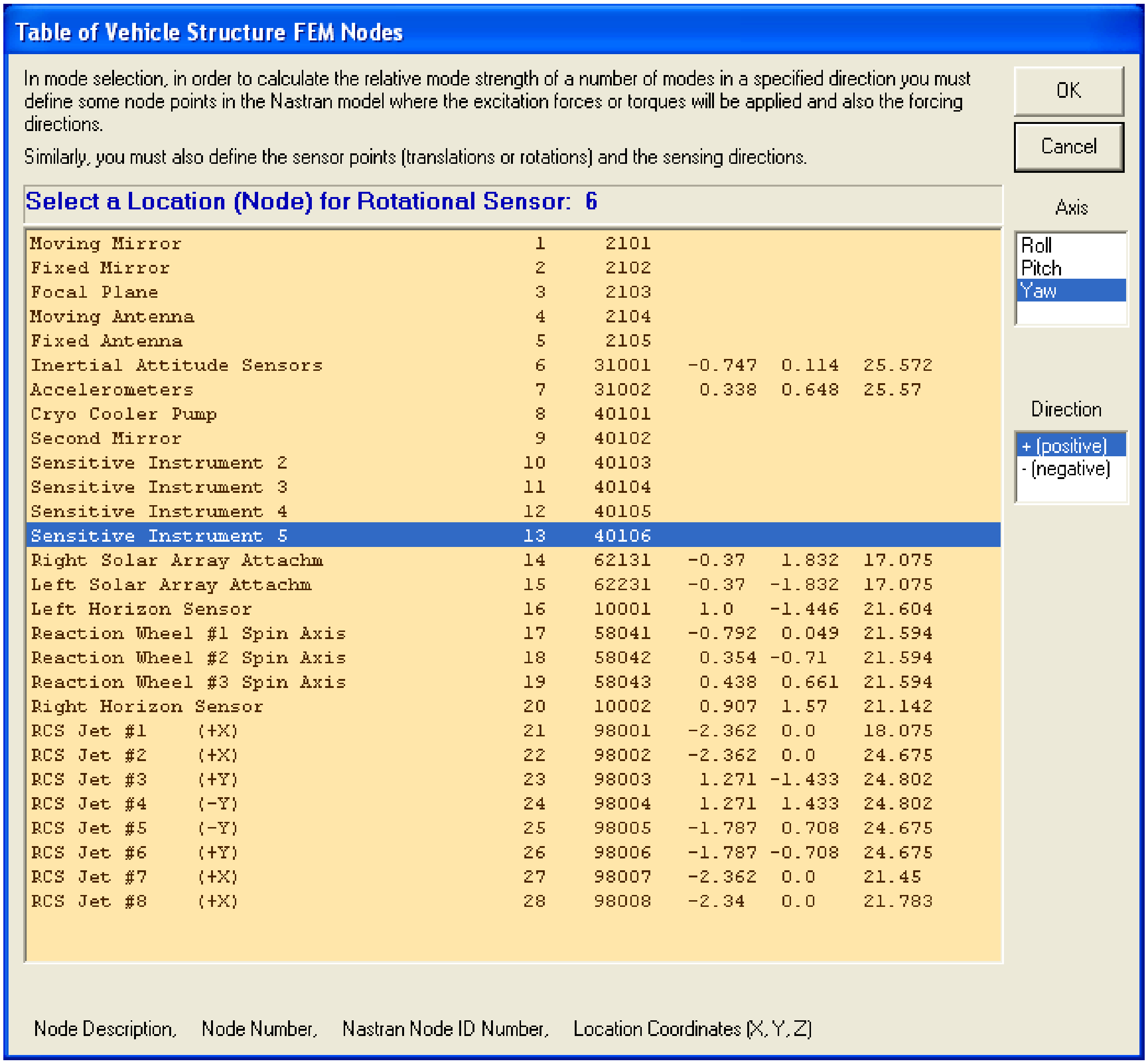

Moving Mirror	1	2101			
Fixed Mirror	2	2102			
Focal Plane	3	2103			
Moving Antenna	4	2104			
Fixed Antenna	5	2105			
Inertial Attitude Sensors	6	31001	-0.747	0.114	25.572
Accelerometers	7	31002	0.338	0.648	25.57
Cryo Cooler Pump	8	40101			
Second Mirror	9	40102			
Sensitive Instrument 2	10	40103			
Sensitive Instrument 3	11	40104			
Sensitive Instrument 4	12	40105			
Sensitive Instrument 5	13	40106			
Right Solar Array Attachm	14	62131	-0.37	1.832	17.075
Left Solar Array Attachm	15	62231	-0.37	-1.832	17.075
Left Horizon Sensor	16	10001	1.0	-1.446	21.604
Reaction Wheel #1 Spin Axis	17	58041	-0.792	0.049	21.594
Reaction Wheel #2 Spin Axis	18	58042	0.354	-0.71	21.594
Reaction Wheel #3 Spin Axis	19	58043	0.438	0.661	21.594
Right Horizon Sensor	20	10002	0.907	1.57	21.142
RCS Jet #1 (+X)	21	98001	-2.362	0.0	18.075
RCS Jet #2 (+X)	22	98002	-2.362	0.0	24.675
RCS Jet #3 (+Y)	23	98003	1.271	-1.433	24.802
RCS Jet #4 (-Y)	24	98004	1.271	1.433	24.802
RCS Jet #5 (-Y)	25	98005	-1.787	0.708	24.675
RCS Jet #6 (+Y)	26	98006	-1.787	-0.708	24.675
RCS Jet #7 (+X)	27	98007	-2.362	0.0	21.45
RCS Jet #8 (+X)	28	98008	-2.34	0.0	21.783

At this point the program has all the information needed to compute the modal strengths, but there is one more thing that needs to be defined before it will allow the user to select the dominant modes. In order to create the state-space model the program needs to know the locations of the inputs and outputs defined in the spacecraft configuration data. That is, to associate the 8 RCS jet forces, the 6 torque application points, the two accelerometer measurements, and the 13 rotational sensors defined in the beginning of this process, with structural locations in the modal data file. Similar dialog menus which display the nodes table are used here to select these locations. The background color is different (light blue) to avoid mix-up with the previous menus which were for mode selection purposes. The next two dialogs show how to select nodes and directions for the RCS jet forces. Node numbers #21 through #28 are chosen for the RCS forces 1 through 8. Node #21 is selected for Force Excitation #1, which represents RCS jet #1. The force direction is along x: (1, 0, 0).

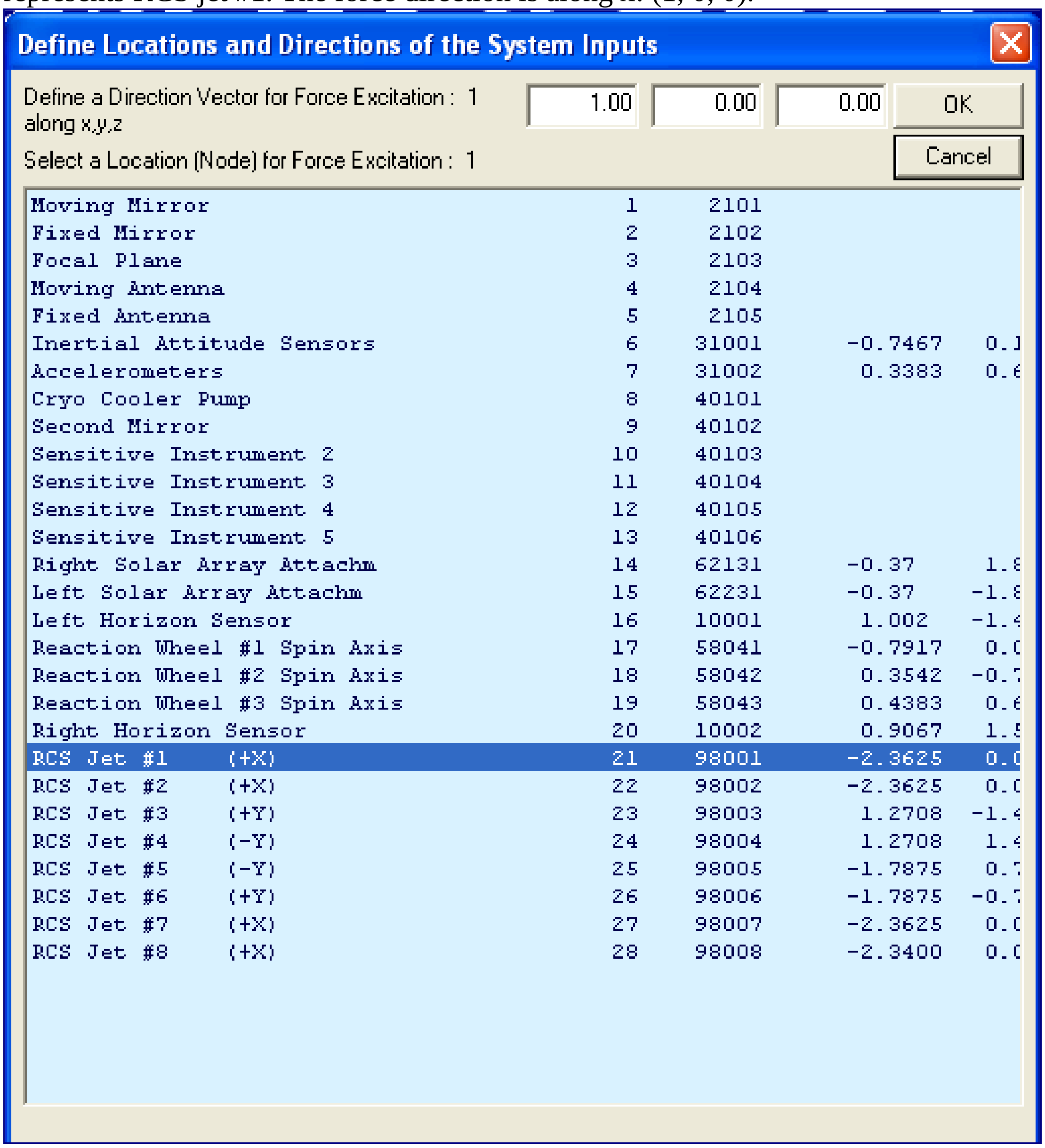

Similarly, Force Excitation #7 is associated with node #27 representing the RCS jet #7. The force direction is also along x (1, 0, 0).

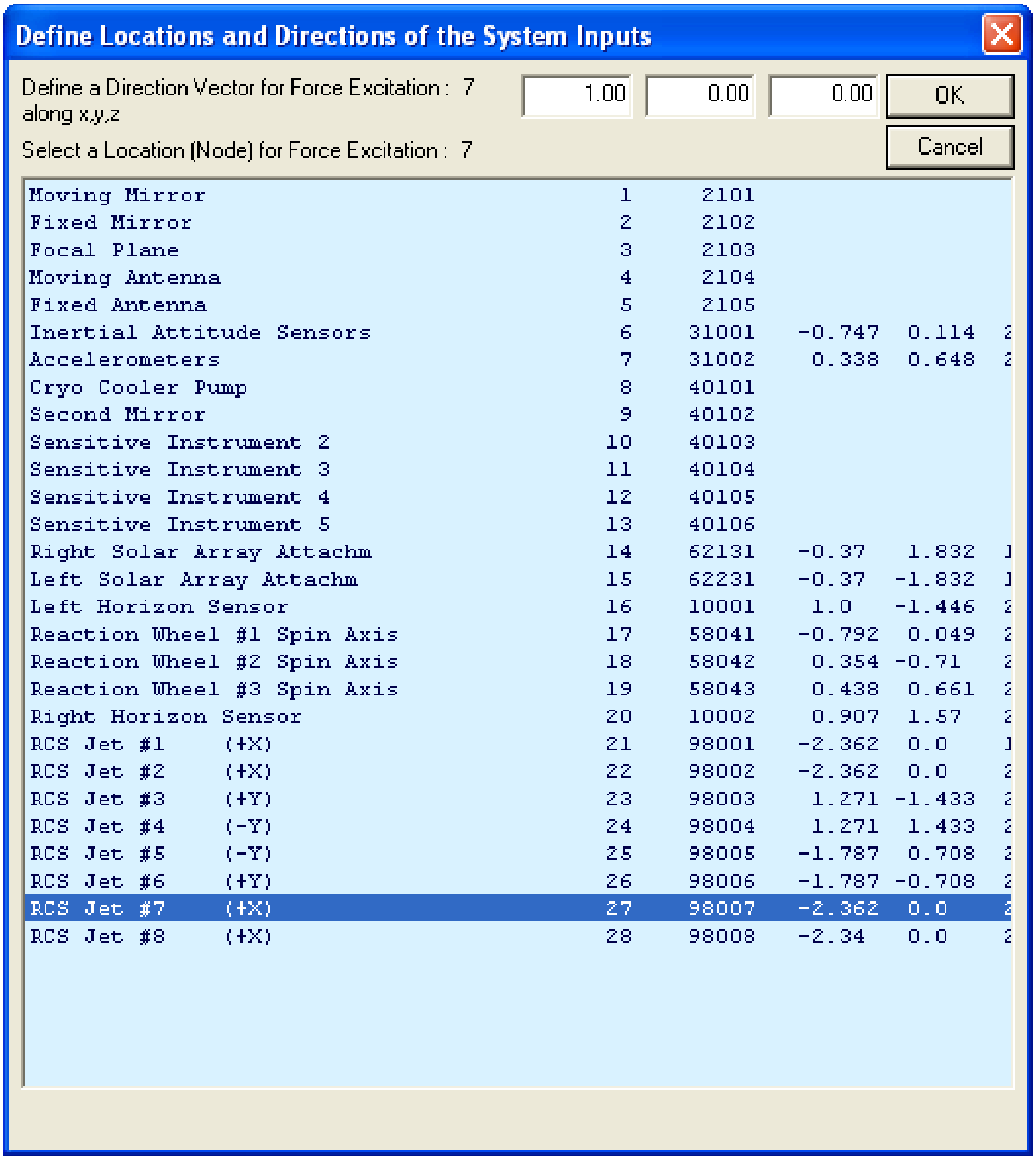

In the next three dialogs we select locations and directions for the first 3 torques which are reaction wheel torques. Nodes #17, #18, #19, are selected corresponding to wheels #1, #2, and #3. The torque directions are in the body axes, about x, y, and z respectively. The selection of the first wheel is shown in the dialog below. The other two are selected from similar menus. Note, that the wheels are usually mounted together inside a solid structure and they are very near each other, and therefore, a single node should be sufficient to identify the reaction wheel array, but for tutorial purposes we selected 3 separate nodes to apply the roll, pitch, and yaw torques.

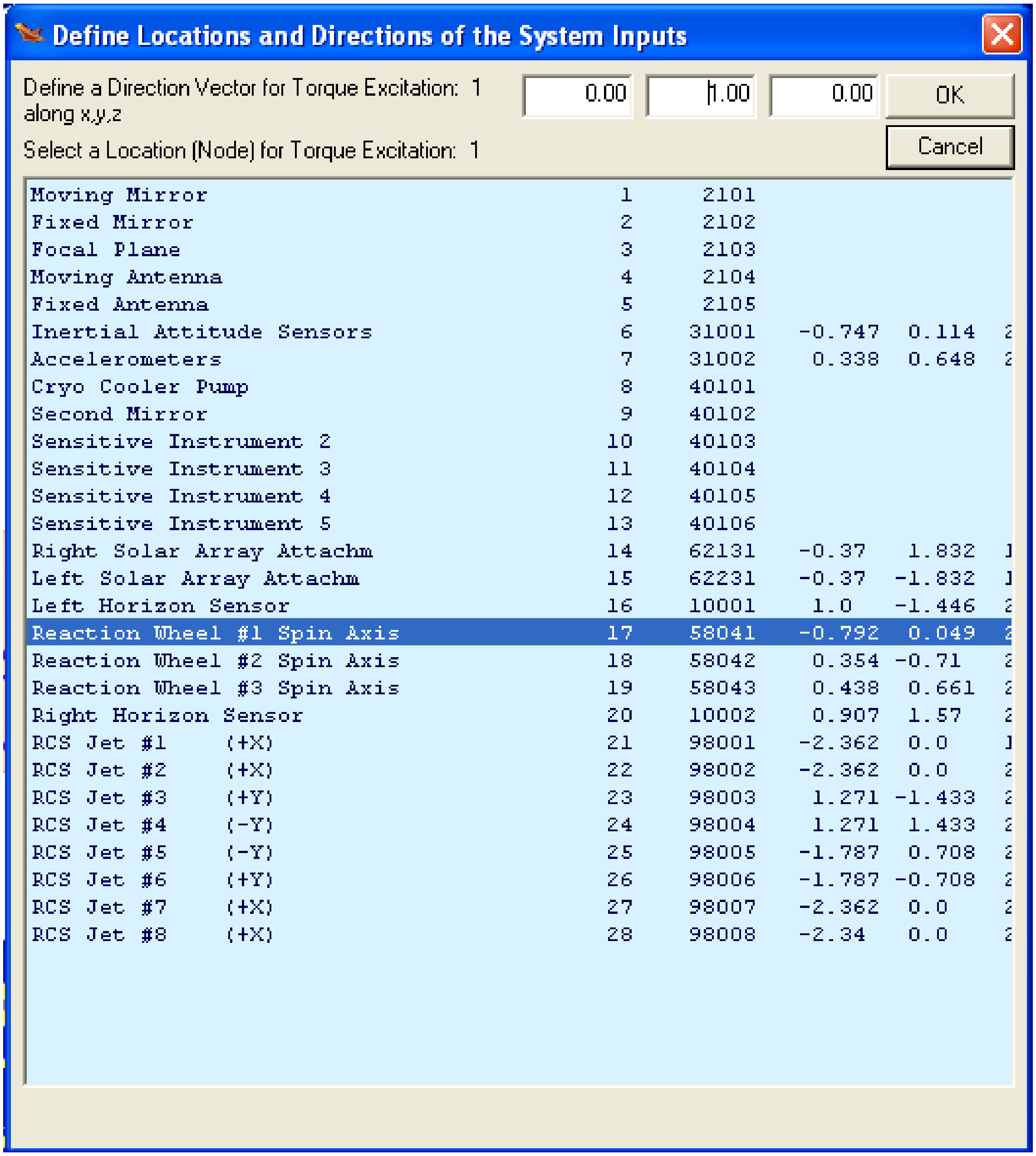

We also select 3 structural locations for the cryo-cooler disturbance torques. The cryo-cooler is located at node #8. The disturbance torques, (4, 5, and 6) are applied in roll, pitch, and yaw respectively. Only the first selection is shown below for the roll (1, 0, 0) disturbance torque. Pitch (0, 1, 0) and yaw (0, 0, 1) torques are also applied in the same location.

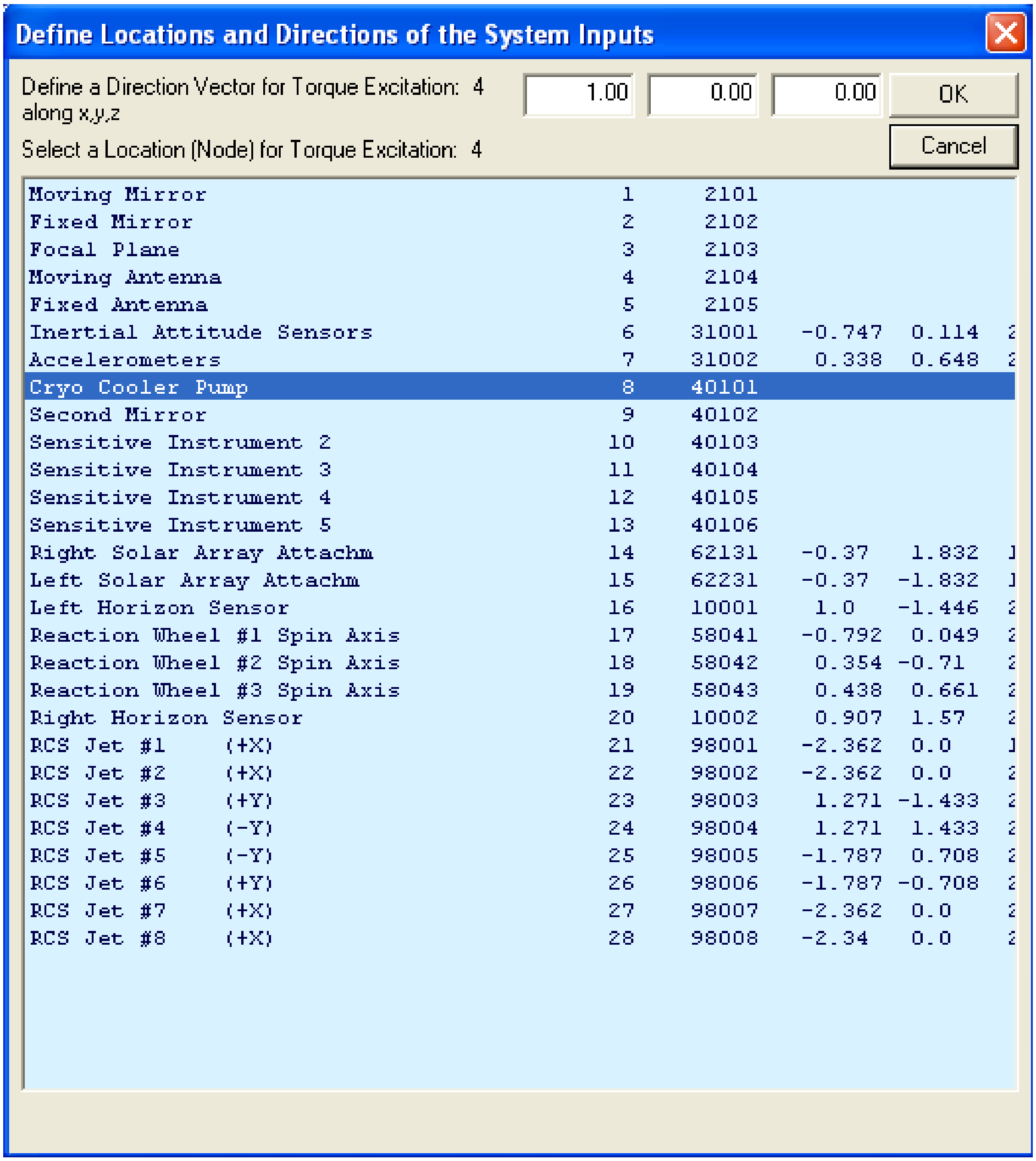

For the translational sensors (1 and 2) we select node #7 to define two accelerometers measuring along the x and y axes respectively. The selection of the first one, measuring acceleration in the x direction is shown below.

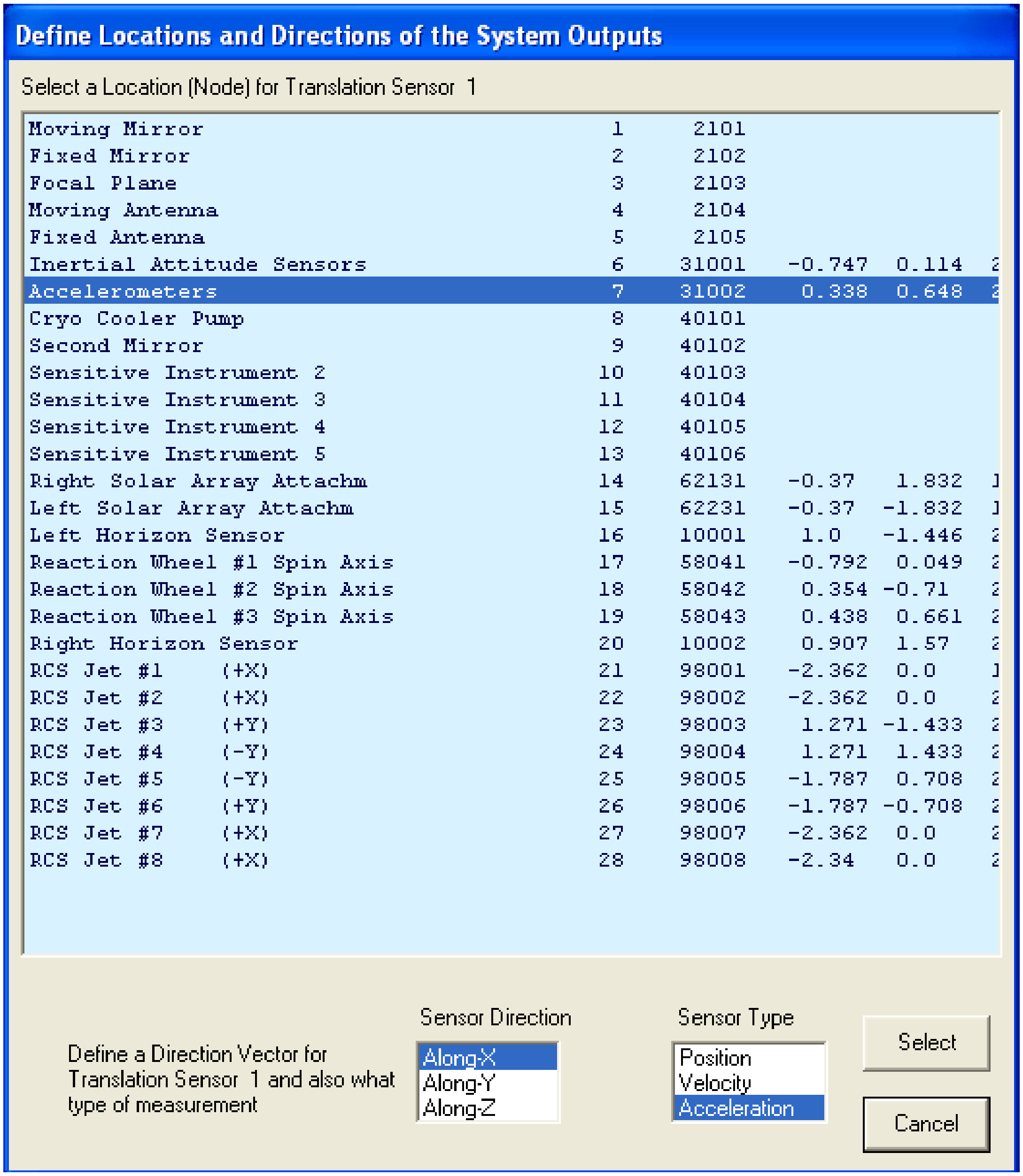

We finally have to define locations for our 13 rotational sensors. We have 3 rate gyros at node #6 measuring roll, pitch, and yaw rates, 3 gyro measurements also at node #6 measuring roll, pitch, and yaw rotation angles. They are used for attitude control. We also have two angular measurements in pitch and yaw at node #9, another two angular measurements in pitch and yaw at node #10, and 3 angular measurements at nodes #11, #12, and #13 measuring roll, pitch, and yaw respectively. They are used for sensitivity measurements. The next five menus below show the node selection for some of these 13 rotational sensors.

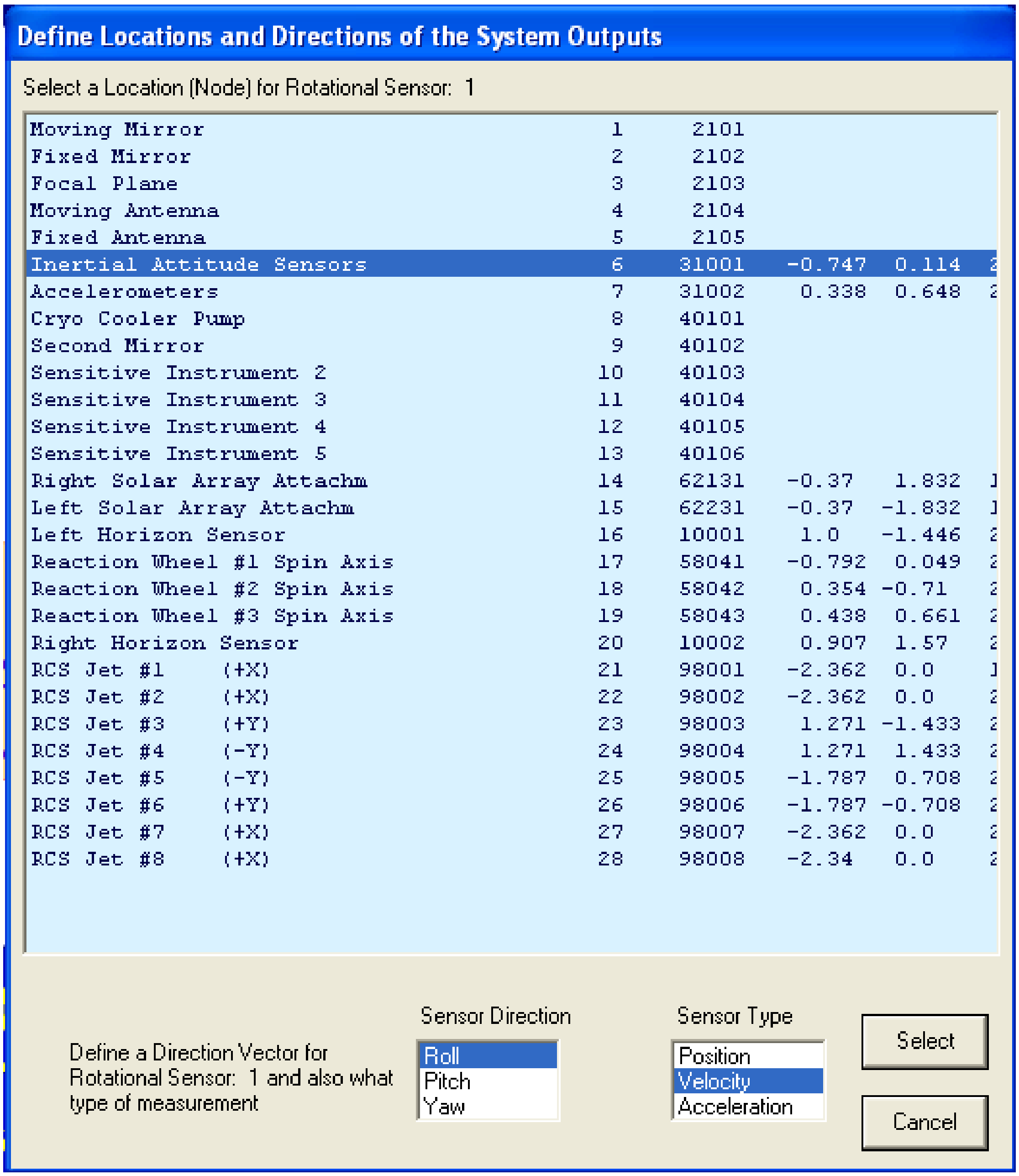

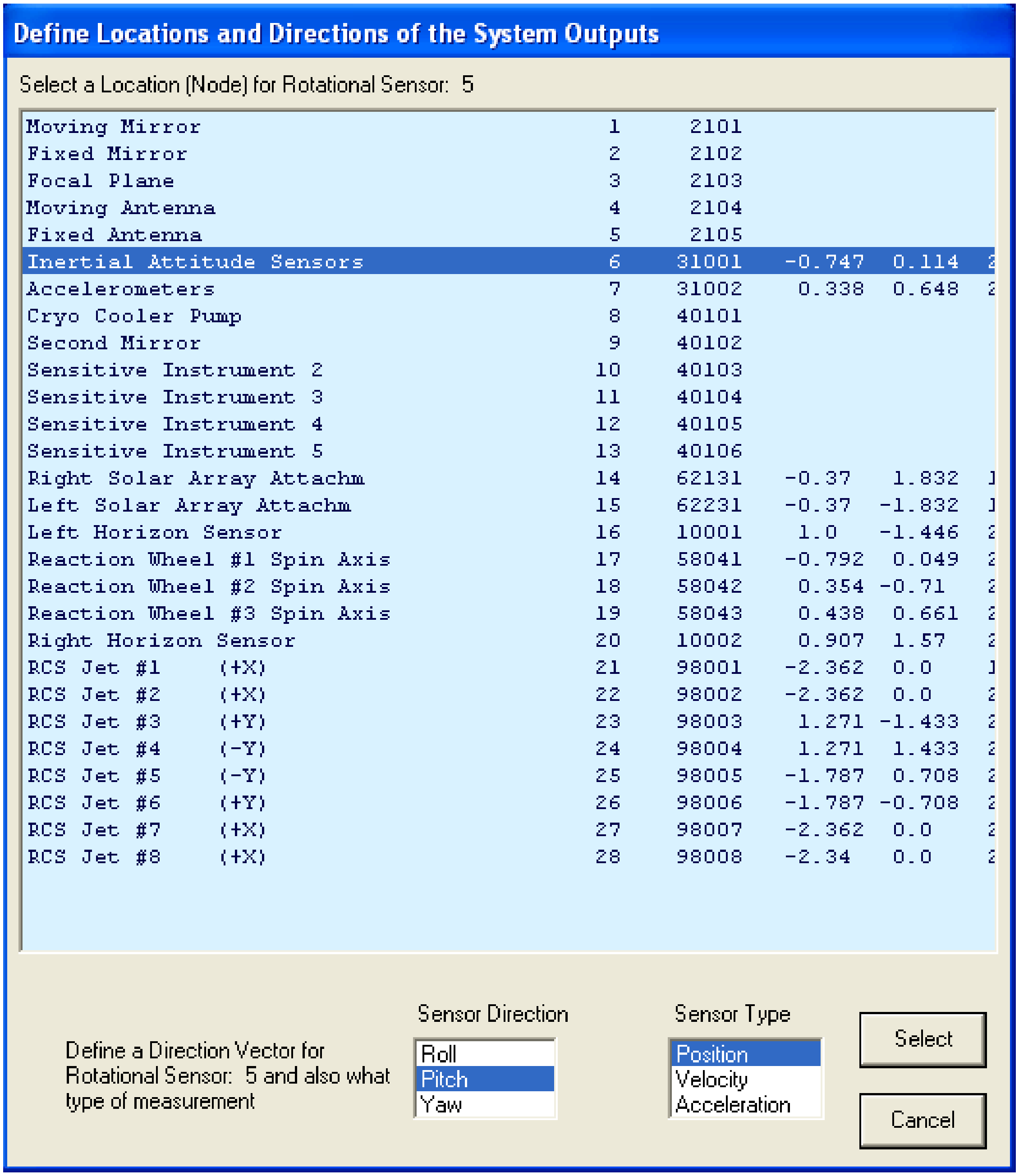
Define Locations and Directions of the System Outputs
Select a Location (Node) for Rotational Sensor: 5
Moving Mirror 1 2101
Fixed Mirror 2 2102
Focal Plane 3 2103
Moving Antenna 4 2104
Fixed Antenna 5 2105
Inertial Attitude Sensors 6 31001 -0.747 0.114
Accelerometers 7 31002 0.338 0.648
Cryo Cooler Pump 8 40101
Second Mirror 9 40102
Sensitive Instrument 2 10 40103
Sensitive Instrument 3 11 40104
Sensitive Instrument 4 12 40105
Sensitive Instrument 5 13 40106
Right Solar Array Attachm 14 62131 -0.37 1.832
Left Solar Array Attachm 15 62231 -0.37 -1.832
Left Horizon Sensor 16 10001 1.0 -1.446
Reaction Wheel #1 Spin Axis 17 58041 -0.792 0.049
Reaction Wheel #2 Spin Axis 18 58042 0.354 -0.71
Reaction Wheel #3 Spin Axis 19 58043 0.438 0.661
Right Horizon Sensor 20 10002 0.907 1.57
RCS Jet #1 (+X) 21 98001 -2.362 0.0
RCS Jet #2 (+X) 22 98002 -2.362 0.0
RCS Jet #3 (+Y) 23 98003 1.271 -1.433
RCS Jet #4 (-Y) 24 98004 1.271 1.433
RCS Jet #5 (-Y) 25 98005 -1.787 0.708
RCS Jet #6 (+Y) 26 98006 -1.787 -0.708
RCS Jet #7 (+X) 27 98007 -2.362 0.0
RCS Jet #8 (+X) 28 98008 -2.34 0.0
Sensor Direction
Sensor Type
Define a Direction Vector for Rotational Sensor: 5 and also what type of measurement
Roll
Pitch
Yaw
Position
Velocity
Acceleration
Select
Cancel

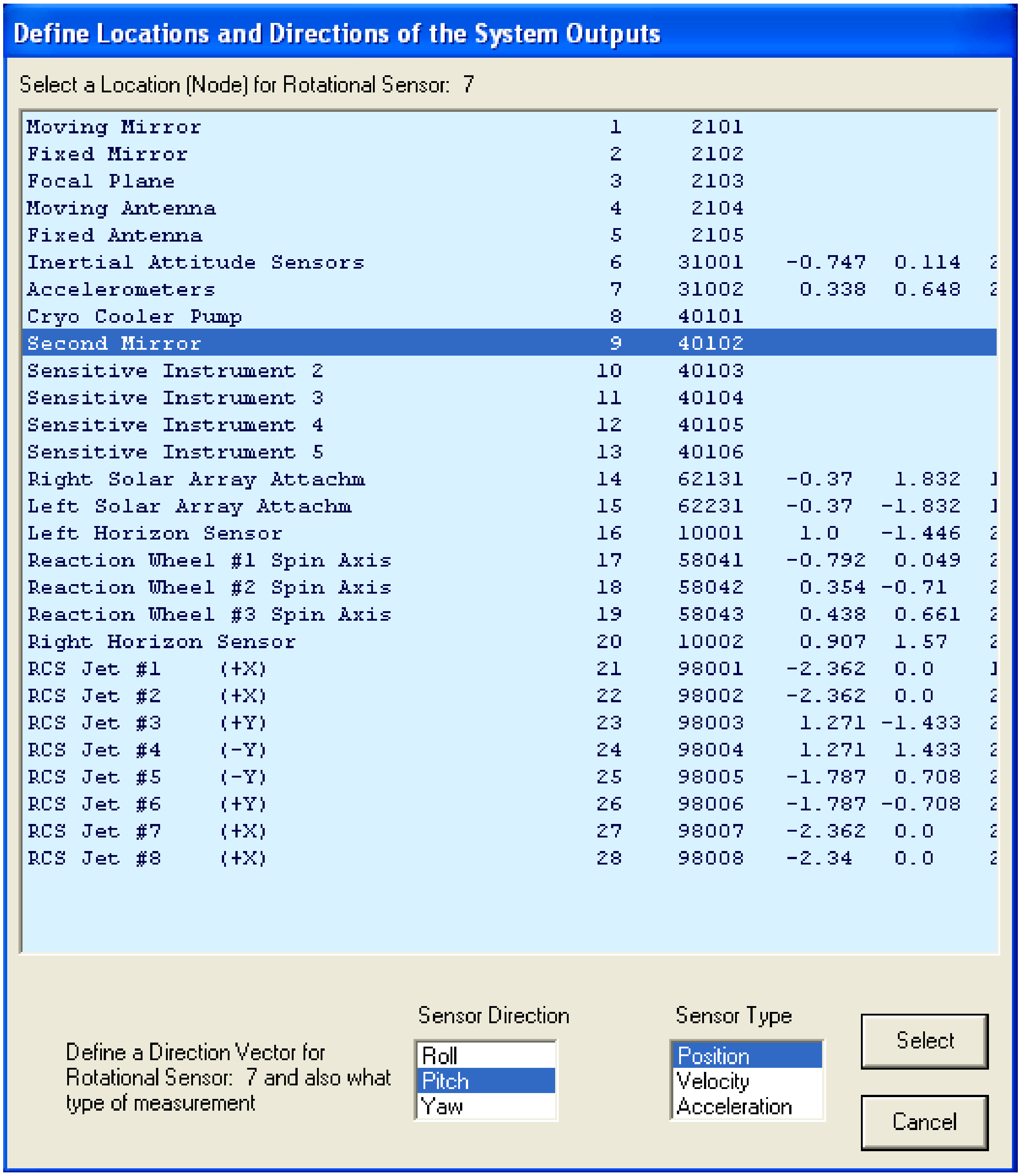
Define Locations and Directions of the System Outputs
Select a Location (Node) for Rotational Sensor: 7
Moving Mirror 1 2101
Fixed Mirror 2 2102
Focal Plane 3 2103
Moving Antenna 4 2104
Fixed Antenna 5 2105
Inertial Attitude Sensors 6 31001 -0.747 0.114
Accelerometers 7 31002 0.338 0.648
Cryo Cooler Pump 8 40101
Second Mirror 9 40102
Sensitive Instrument 2 10 40103
Sensitive Instrument 3 11 40104
Sensitive Instrument 4 12 40105
Sensitive Instrument 5 13 40106
Right Solar Array Attachm 14 62131 -0.37 1.832
Left Solar Array Attachm 15 62231 -0.37 -1.832
Left Horizon Sensor 16 10001 1.0 -1.446
Reaction Wheel #1 Spin Axis 17 58041 -0.792 0.049
Reaction Wheel #2 Spin Axis 18 58042 0.354 -0.71
Reaction Wheel #3 Spin Axis 19 58043 0.438 0.661
Right Horizon Sensor 20 10002 0.907 1.57
RCS Jet #1 (+X) 21 98001 -2.362 0.0
RCS Jet #2 (+X) 22 98002 -2.362 0.0
RCS Jet #3 (+Y) 23 98003 1.271 -1.433
RCS Jet #4 (-Y) 24 98004 1.271 1.433
RCS Jet #5 (-Y) 25 98005 -1.787 0.708
RCS Jet #6 (+Y) 26 98006 -1.787 -0.708
RCS Jet #7 (+X) 27 98007 -2.362 0.0
RCS Jet #8 (+X) 28 98008 -2.34 0.0
Sensor Direction
Sensor Type
Define a Direction Vector for Rotational Sensor: 7 and also what type of measurement
Roll
Pitch
Yaw
Position
Velocity
Acceleration
Select
Cancel

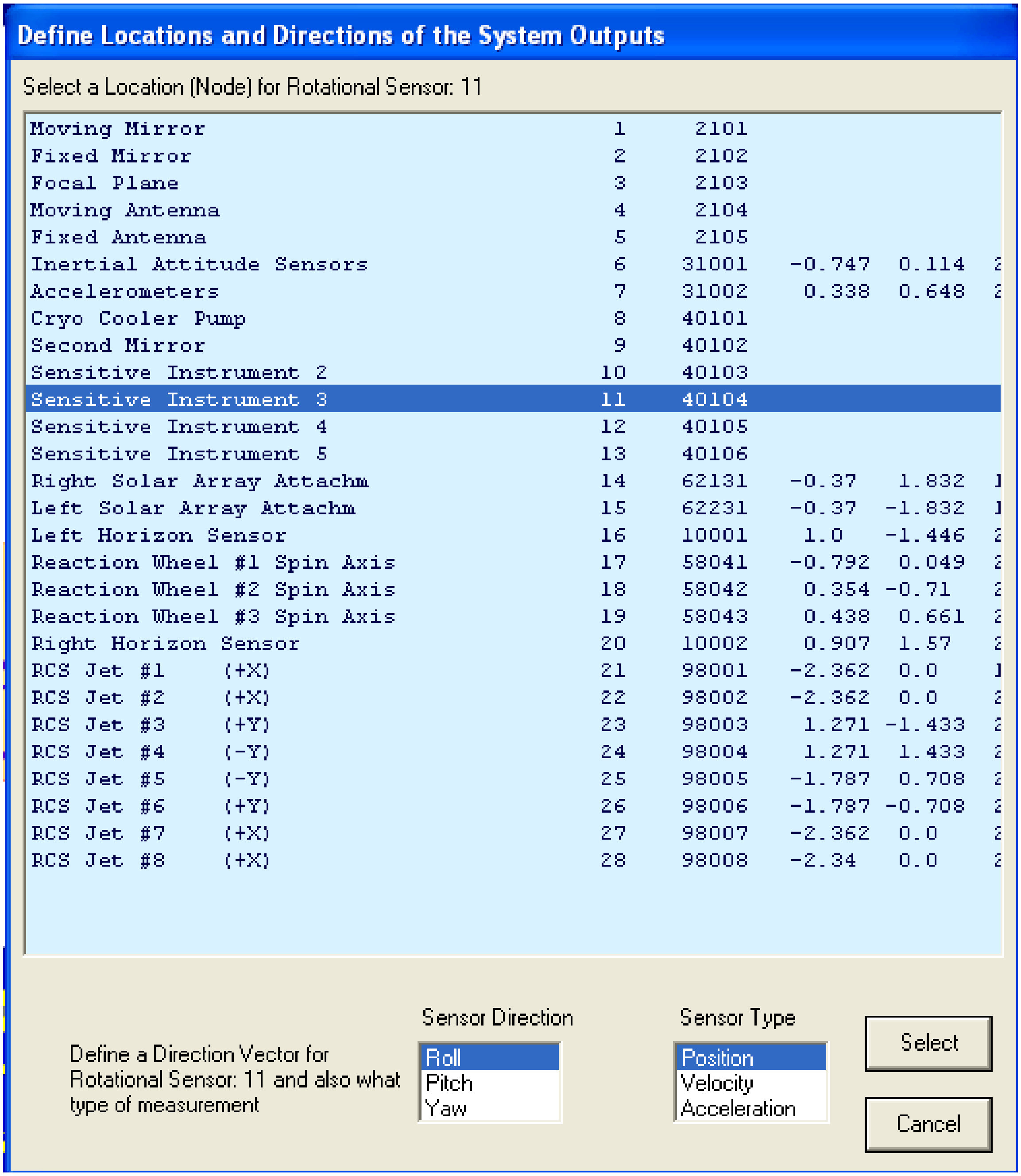
Define Locations and Directions of the System Outputs
Select a Location (Node) for Rotational Sensor: 11
Moving Mirror 1 2101
Fixed Mirror 2 2102
Focal Plane 3 2103
Moving Antenna 4 2104
Fixed Antenna 5 2105
Inertial Attitude Sensors 6 31001 -0.747 0.114
Accelerometers 7 31002 0.338 0.648
Cryo Cooler Pump 8 40101
Second Mirror 9 40102
Sensitive Instrument 2 10 40103
Sensitive Instrument 3 11 40104
Sensitive Instrument 4 12 40105
Sensitive Instrument 5 13 40106
Right Solar Array Attachm 14 62131 -0.37 1.832
Left Solar Array Attachm 15 62231 -0.37 -1.832
Left Horizon Sensor 16 10001 1.0 -1.446
Reaction Wheel #1 Spin Axis 17 58041 -0.792 0.049
Reaction Wheel #2 Spin Axis 18 58042 0.354 -0.71
Reaction Wheel #3 Spin Axis 19 58043 0.438 0.661
Right Horizon Sensor 20 10002 0.907 1.57
RCS Jet #1 (+X) 21 98001 -2.362 0.0
RCS Jet #2 (+X) 22 98002 -2.362 0.0
RCS Jet #3 (+Y) 23 98003 1.271 -1.433
RCS Jet #4 (-Y) 24 98004 1.271 1.433
RCS Jet #5 (-Y) 25 98005 -1.787 0.708
RCS Jet #6 (+Y) 26 98006 -1.787 -0.708
RCS Jet #7 (+X) 27 98007 -2.362 0.0
RCS Jet #8 (+X) 28 98008 -2.34 0.0
Define a Direction Vector for Rotational Sensor: 11 and also what type of measurement
Sensor Direction
Roll
Pitch
Yaw
Sensor Type
Position
Velocity
Acceleration
Select
Cancel

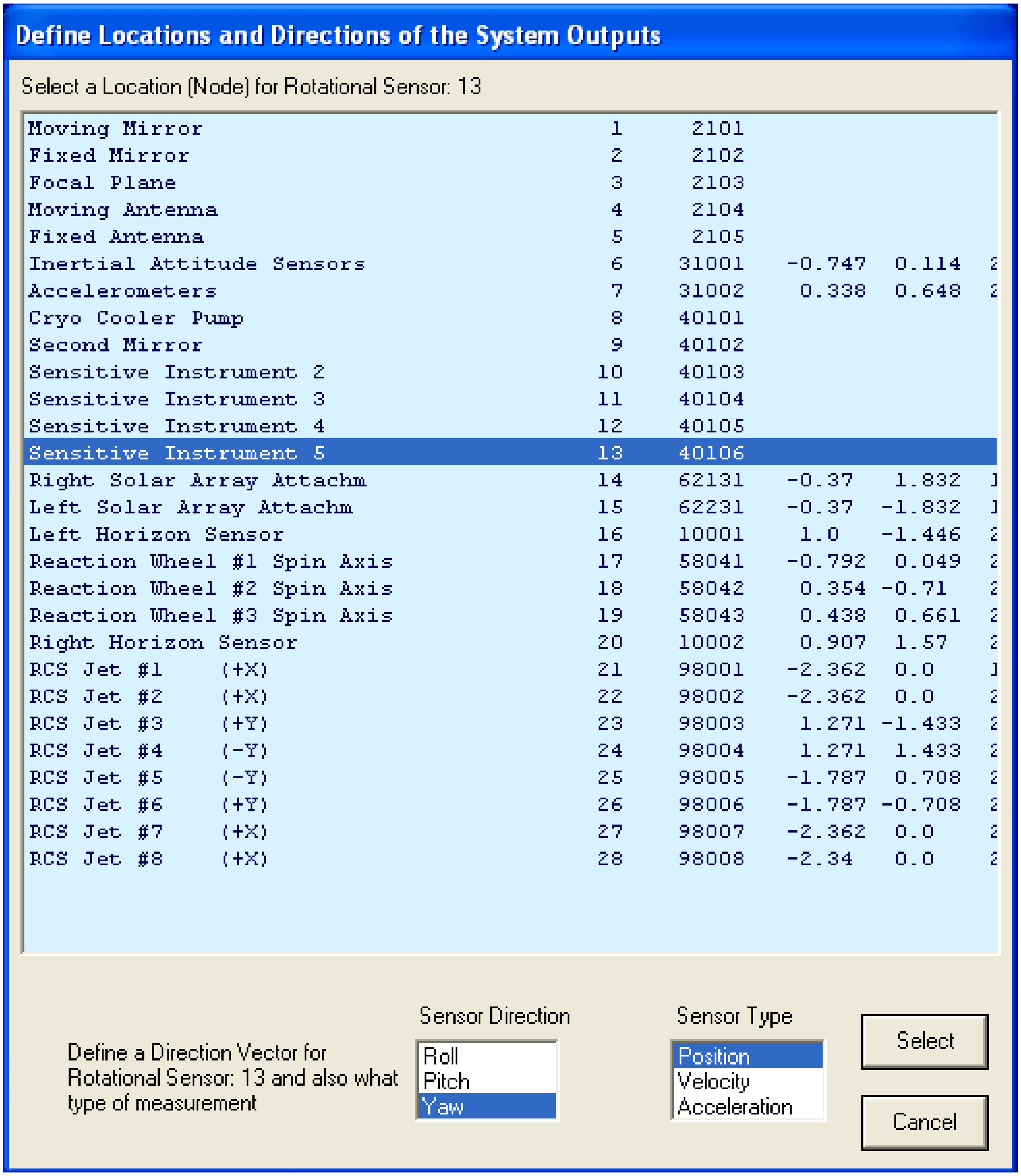

At this point the program displays the mode selection bar chart that shows each mode number and its corresponding mode strength. The mode strength is a relative number in a logarithmic scale. Initially all the modes appear in red. The user can select some of the modes by clicking with the mouse on the corresponding bar and the color of the selected mode changes to green. Notice, that the first 6 rigid-body modes were included in this model. Later we are going to create a flex model without the rigid-body modes that will be used in the following sections. When the mode selection is complete the user presses the "Enter" key to complete the creation of the spacecraft data. After saving the spacecraft input data in file "*Surveillance-Sat.Inp*", the program continues to process it and to create the state-space model. It displays a menu of spacecraft titles already existing in the input data file. In this case there is only one title, the one just created. The user selects the title and clicks on "Run Input Set" to compute the flex spacecraft state-space model in file "*Surveillance_Sat.Qdr*".

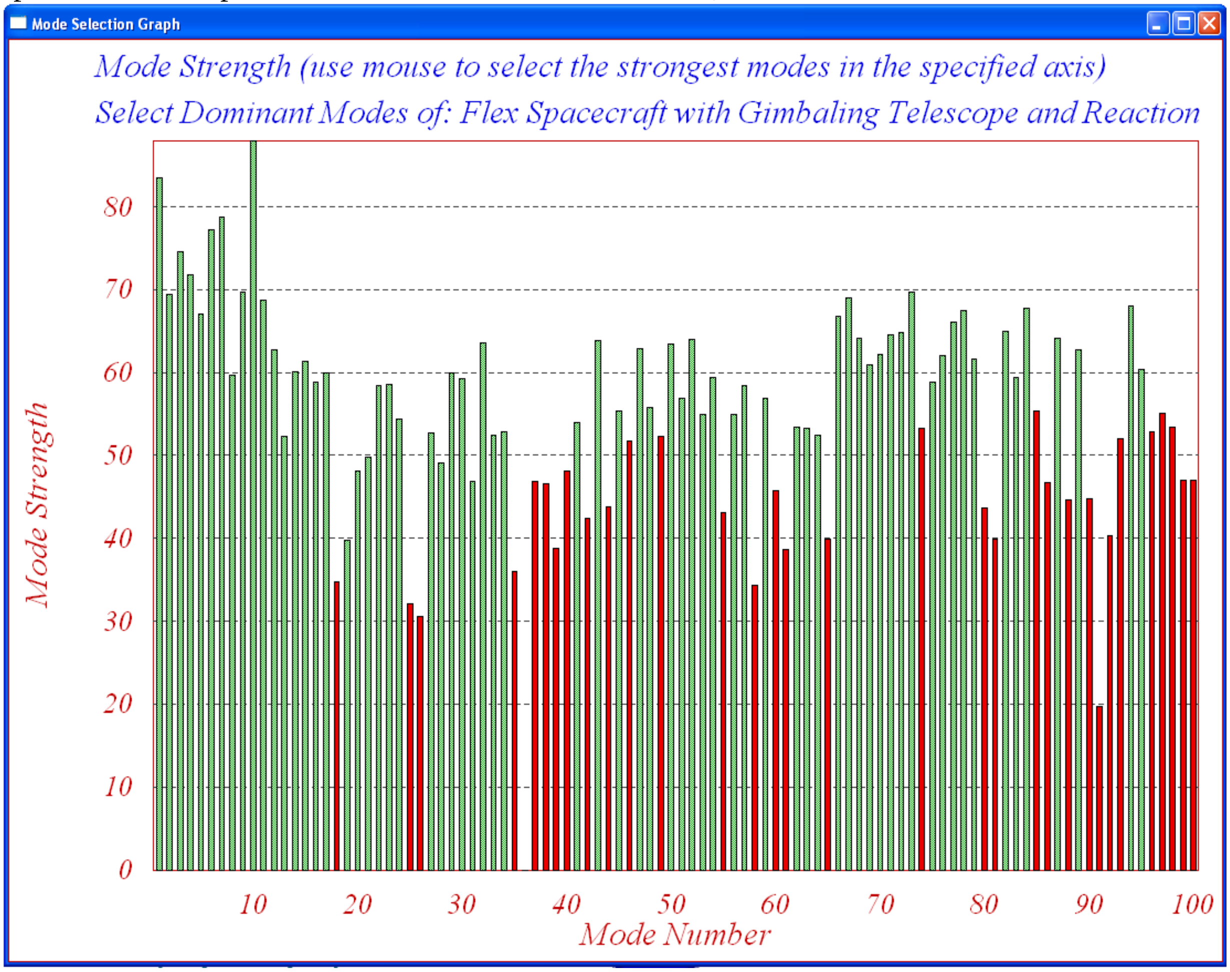

Figure 3.1 Flexible Spacecraft Mode Comparison and Selection Chart

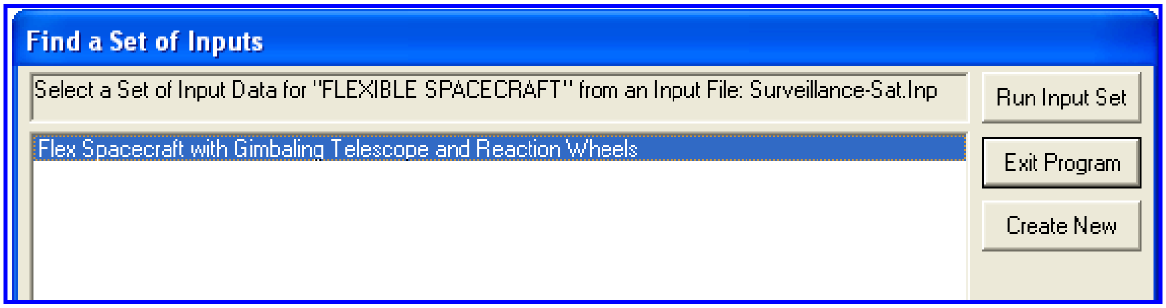

Figure 3.2 Flexible Spacecraft Data Selection Menu

3.3 Conversion to Matlab Format

The flex spacecraft model will be analyzed in Matlab and we must, therefore, convert the state-space systems in file "*Surveillance-Sat.Qdr*" to a format that can be loaded into Matlab. The "*Export to Matlab*" utility program is used for the data conversion. From the Flixan bar menu select "*File*", "*Matlab Conversions*", and then "*Export to Matlab*". Select the current project folder "*…\Examples\ Surveillance Satellite React-Wheels\Flex Model*", and from the filename selection menu (right) select the systems file "*Surveillance-Sat.Qdr*" and click "OK".

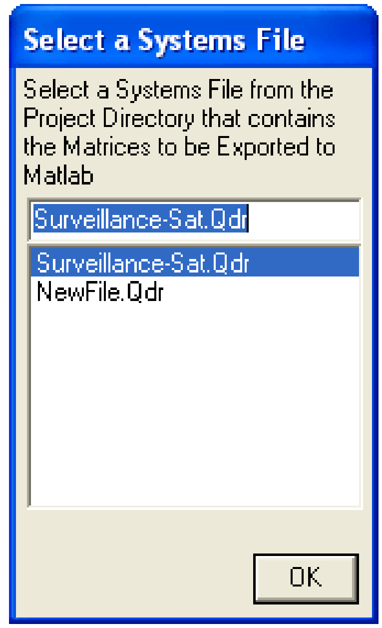

The next step is to define the folder where m-file with the state-space system will be placed and where the Matlab analysis will be performed. That is, in the "*Flex Model*" folder (show below). Click "OK" to continue.

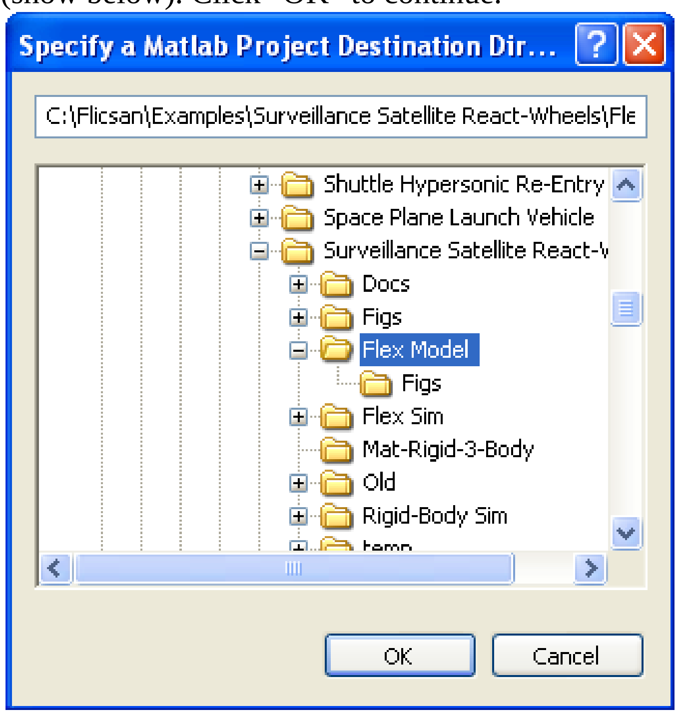

In the dialog on the right you let the program know that you are transforming a state-space system, rather than just a single matrix, and that it will be saved as a 4-matrix function m-file instead of 4 separate matrices.

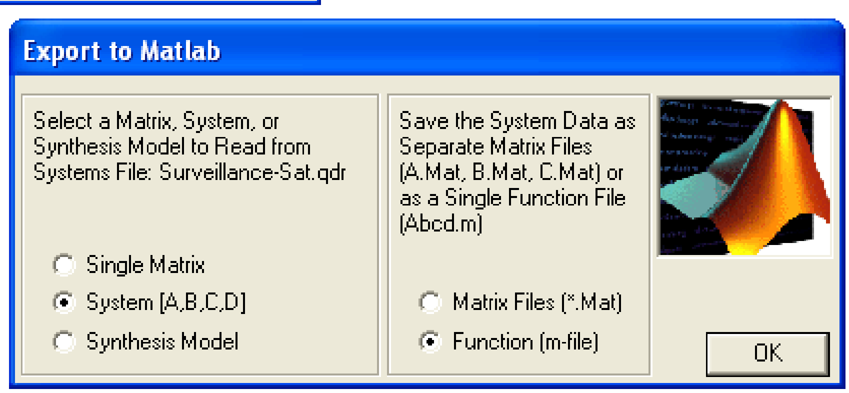

In the following menu we select the system to be converted for Matlab. There are four systems in file "*Surveillance_Sat.Qdr*". We select the first one that has 67 modes including the rigid-body modes. Click "OK" to read the data and continue.

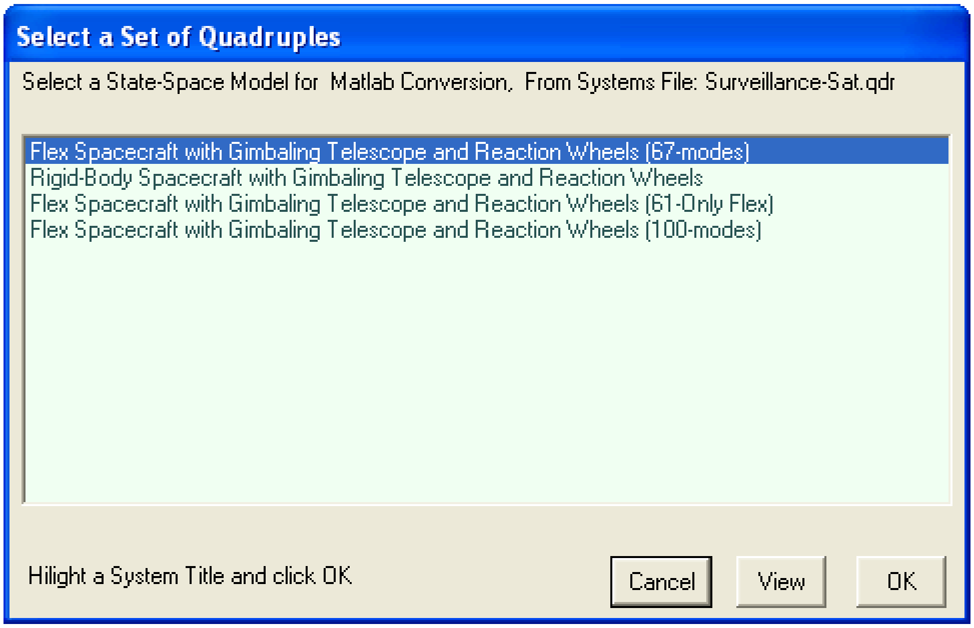

The final question of the Matlab conversion utility program is the filename where the four-matrix m-function will be saved. We enter "flex67" without the (.m). The program reformats the data and saves it as a system function "*flex67.m*" in the destination folder chosen.

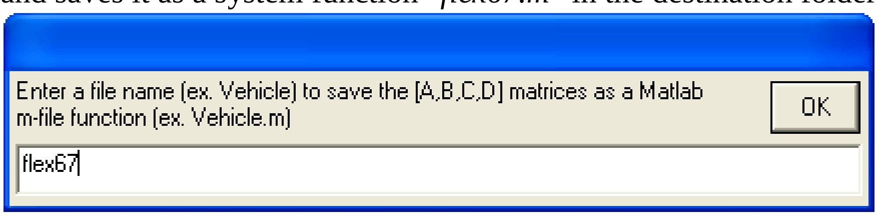

The system is loaded into Matlab by executing the following statement in Matlab.

```
[Avf, Bvf, Cvf, Dvf]= flex67;    % Load Flex Model from Flixan
```

Batch Mode

In file "*Surveillance-Sat.Inp*" there is a set of batch instructions that automates and speeds up the systems creation process. Its title is "*Batch for the Flex Surveillance Satellite*". By running this batch the other 3 systems in file "*Surveillance-Sat.Qdr*" are also created, converted to Matlab and saved in folder "*…\Examples\ Surveillance Satellite React-Wheels\Flex Model*". There filenames are "*rigid_body.m*", "*flex61.m*", and "*flex100.m*".

3.4 Flexible Spacecraft Simulation Analysis

In the previous section we used the flex spacecraft modeling program to create a 67-mode state-space model of our surveillance spacecraft in file "*Surveillance_Sat.Qdr*". Actually there are more than 67 modes because we introduced four additional gimbal modes to unlock the hinges of the four rotating appendages using the H-parameters contained in file "*Surveillance_Sat.Hpr*". The H-parameters allow dynamic coupling between gimbal rotations and the flex modes. This multi-body spacecraft model is linear, at a fixed gimbal orientation, and it includes 6 rigid-body modes (3 rotations and 3 translations) implemented like the flex modes using modal data. It is used for small angle analysis, for gimbal rotations up to 5 degrees or so. For large angle slewing, we obviously need a non-linear multi-body simulation. This will be studied later in Section 5. The linear model, however, is very useful for stability and sensitivity analysis to disturbances. The total number of states in the linear model is 142. The last 8 states are rotations and rates at the four gimbals (optical sensor elevation and azimuth gimbals, and two solar array gimbals). The model has 18 inputs: 8 RCS jet forces, 3 Reaction Wheel torques, 3 disturbance torques at the cryo-cooler, and 4 torques at the appendage gimbals. The system has 23 outputs: two accelerometers, three rate gyros at the navigation platform, three rotational gyros also at the nav-base, four rotational gyros at nodes #9 and #10, and another 3 rotational gyros at nodes #11 to #13. The last 8 outputs are gimbal angles and gimbal rates at the 4 hinges. The title of this system is "*Flex Spacecraft with Gimbaling Telescope and Reaction Wheels (67-modes)*".

We will now use this flexible state-space model to perform a simple simulation. The Matlab analysis files are in folder "*…\Examples\Surveillance Satellite React-Wheels\ Flex Model*". The Simulink model "*Flex_RCS.mdl*" in Figure (3.3) is used to analyze the flex spacecraft state-space system. The spacecraft state-space model is loaded from file "*flex67.m*" by executing the m-file "*runf.m*". Other parameters are also loaded into Matlab, such as: jet locations, jet directions, and gimbal servo gains. The 100 mode system and the rigid-body system, which were created in files: "*flex100.m*" and "*rigid_body.m*" are also saved in that folder and they can be loaded instead using "*runf.m*". The 100 flex modes model has 208 states. It was used for comparison purposes and it will not be discussed here. The biggest disadvantage of this linear spacecraft model derived from a FEM is that it is missing the nutation dynamics, which are created by the pitch momentum bias (H_{y0}), and dynamically couple the roll and yaw axis. In the Section 4 we will couple the flex model with the momentum biased non-linear model, but in this section we shall analyze the linear flex model by itself. The simulation model has the RCS jets loop closed and also the payload gimbal loops are closed. The reaction-wheel ACS loop is not implemented because it cannot work efficiently in the lateral directions without the gyroscopic coupling. The flex spacecraft (cyan) and the gimbal control blocks (pink) are shown in detail in Figure (3.4 & 4.3).

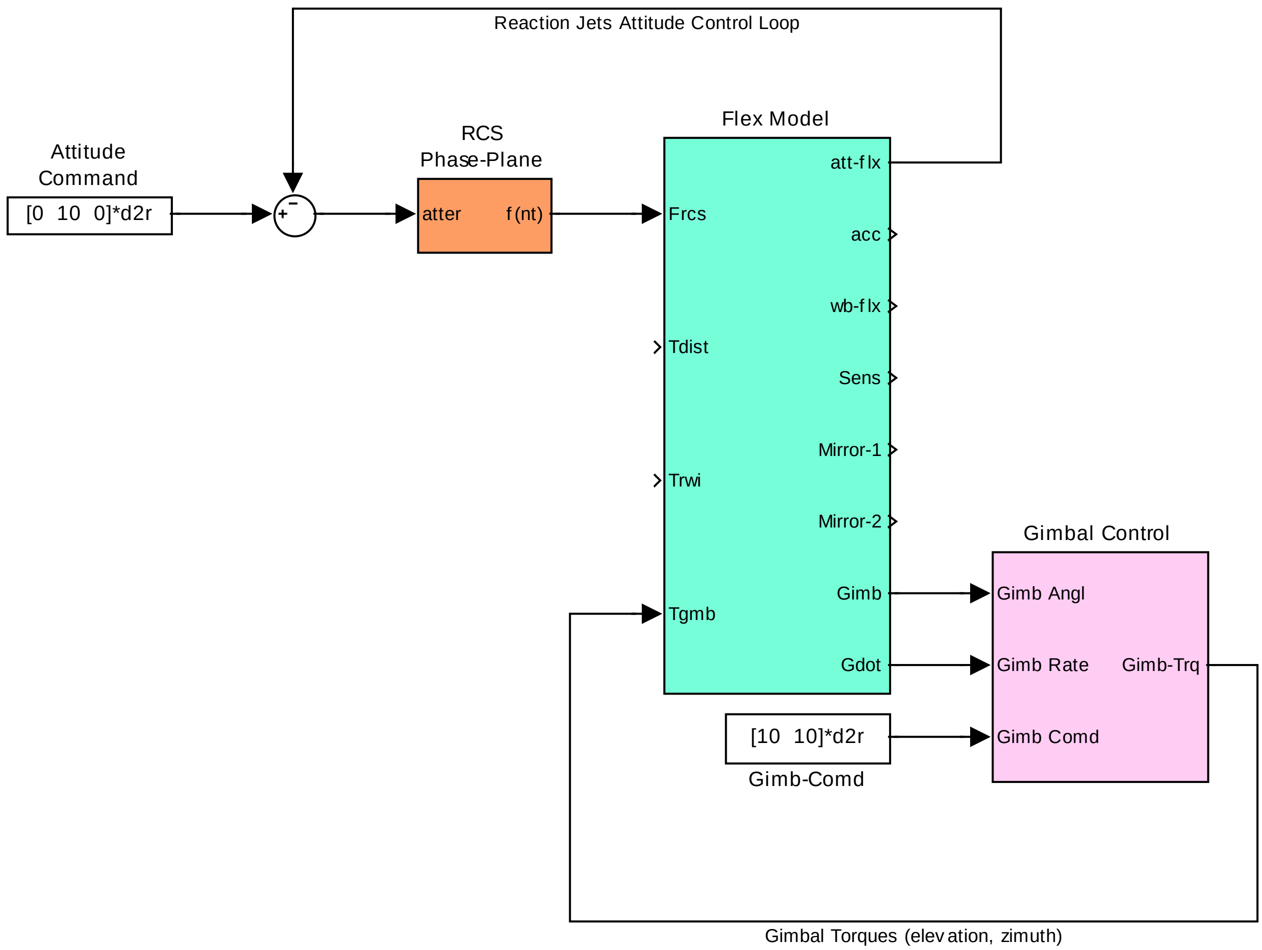

Figure 3.3 Model for Analyzing the Flex Spacecraft System with RCS and Gimbal Loops Closed. The Reaction Wheels are not used in this model.

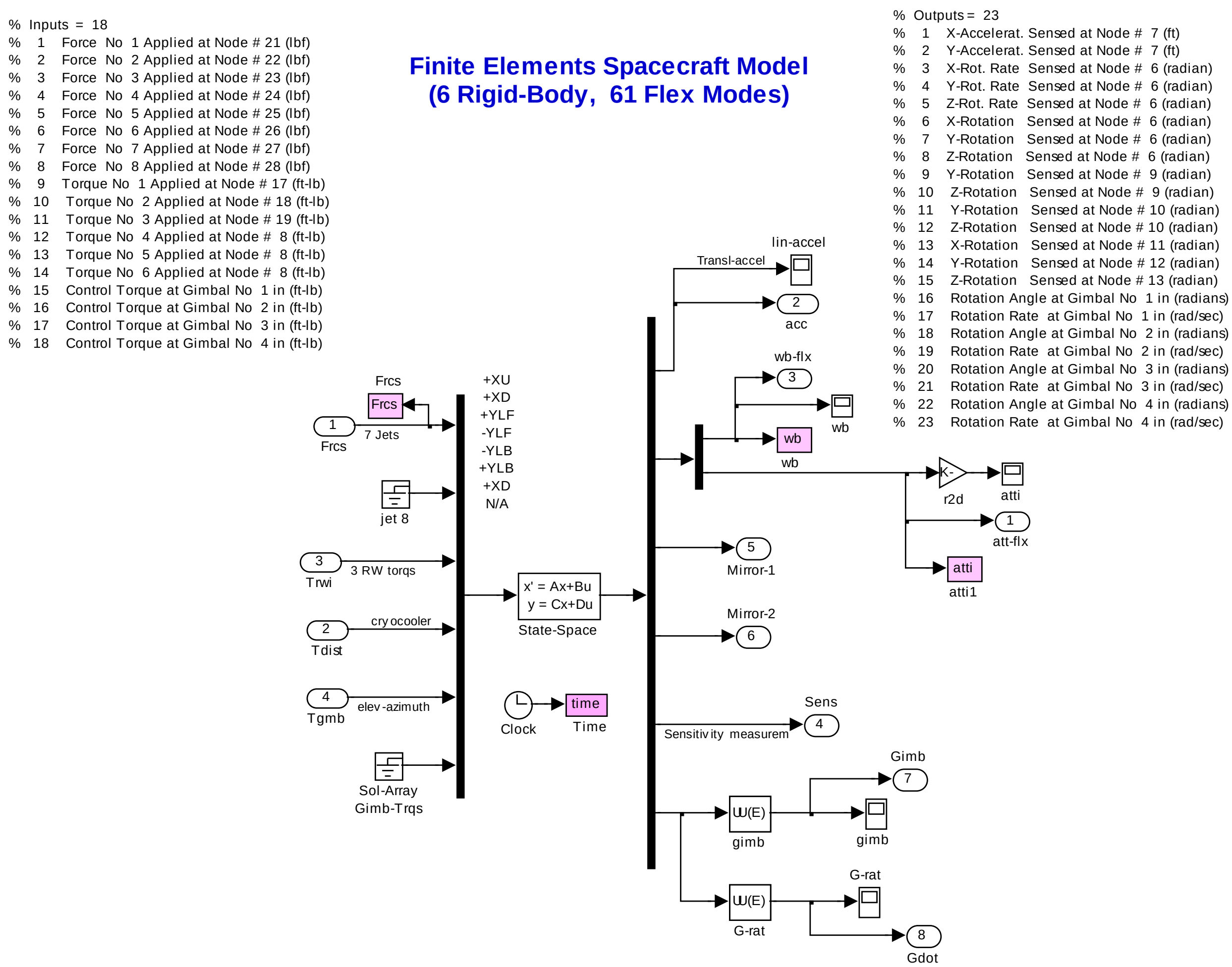

Figure 3.4 Flex Spacecraft Model from file: Flex67.m" Consisting of 61 Flex Modes and 6 Rigid Modes

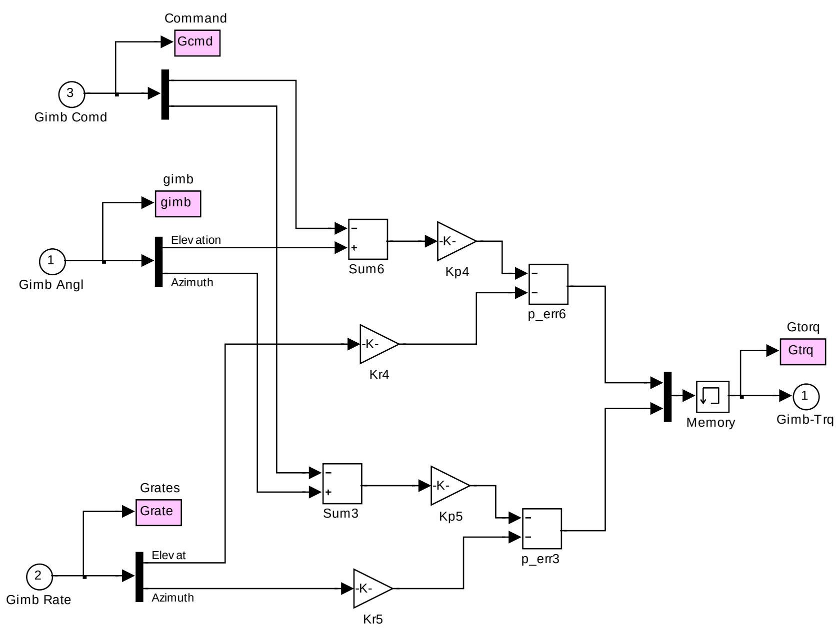

Figure 3.5 Gimbal Controller

The following results were obtained by commanding the RCS attitude control system to perform a 10 (degrees) rotation in pitch. The payload elevation and azimuth gimbals were also commanded to perform a 10 (deg) slew each. Figure (3.6) shows the spacecraft attitude and rate as it performs the 10 (deg) slew. The attitude response is rate limited. Flex oscillations are visible in the rate measurement in response to jet firing. Notice, blue is roll, and red is yaw. Figure (3.7) shows the azimuth and elevation gimbal responses to 10º commands. The gimbal response is much faster than RCS bandwidth.

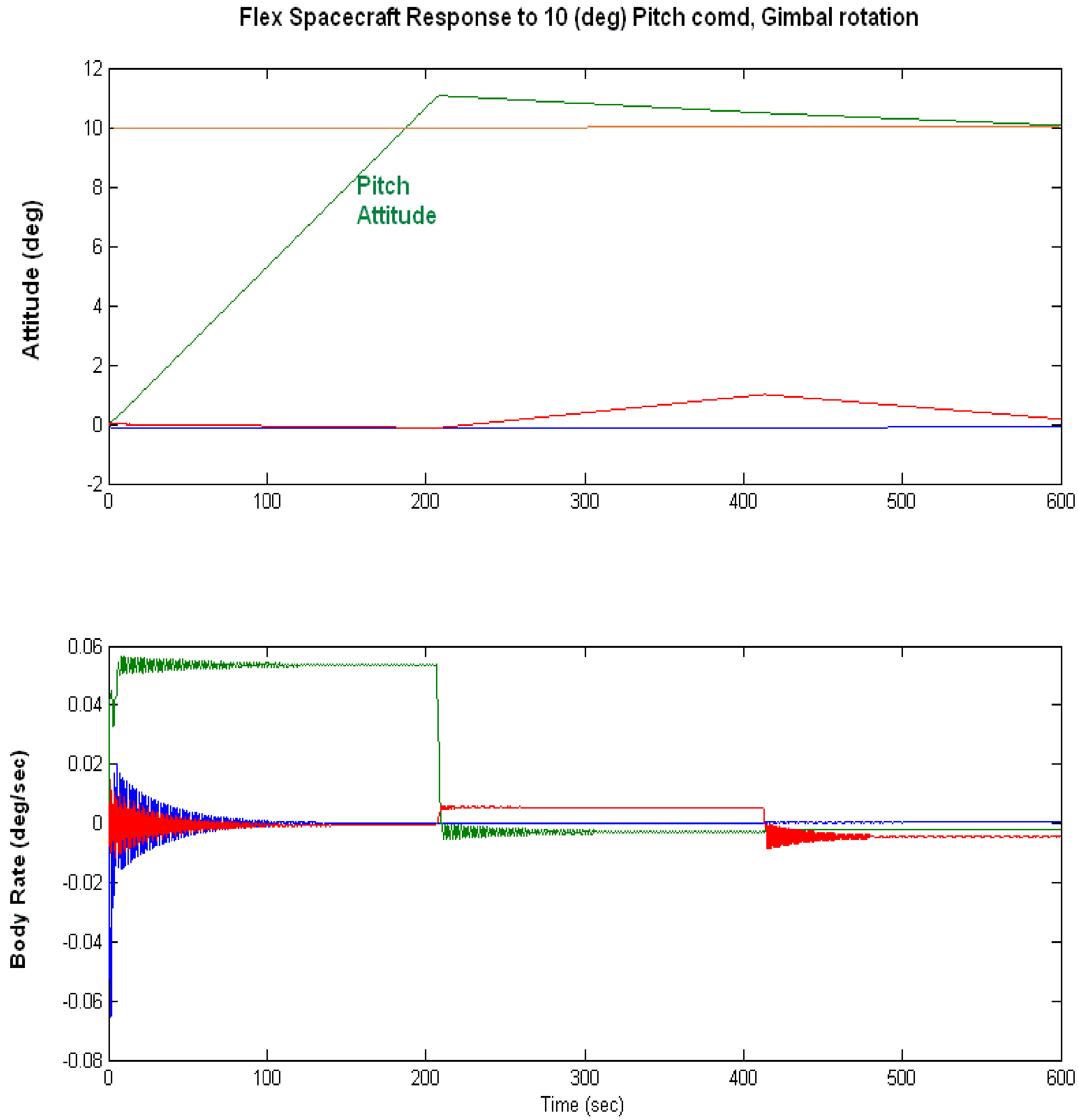

Figure 3.6 Flex Spacecraft Attitude and Rate Response to a 10 (deg) Command

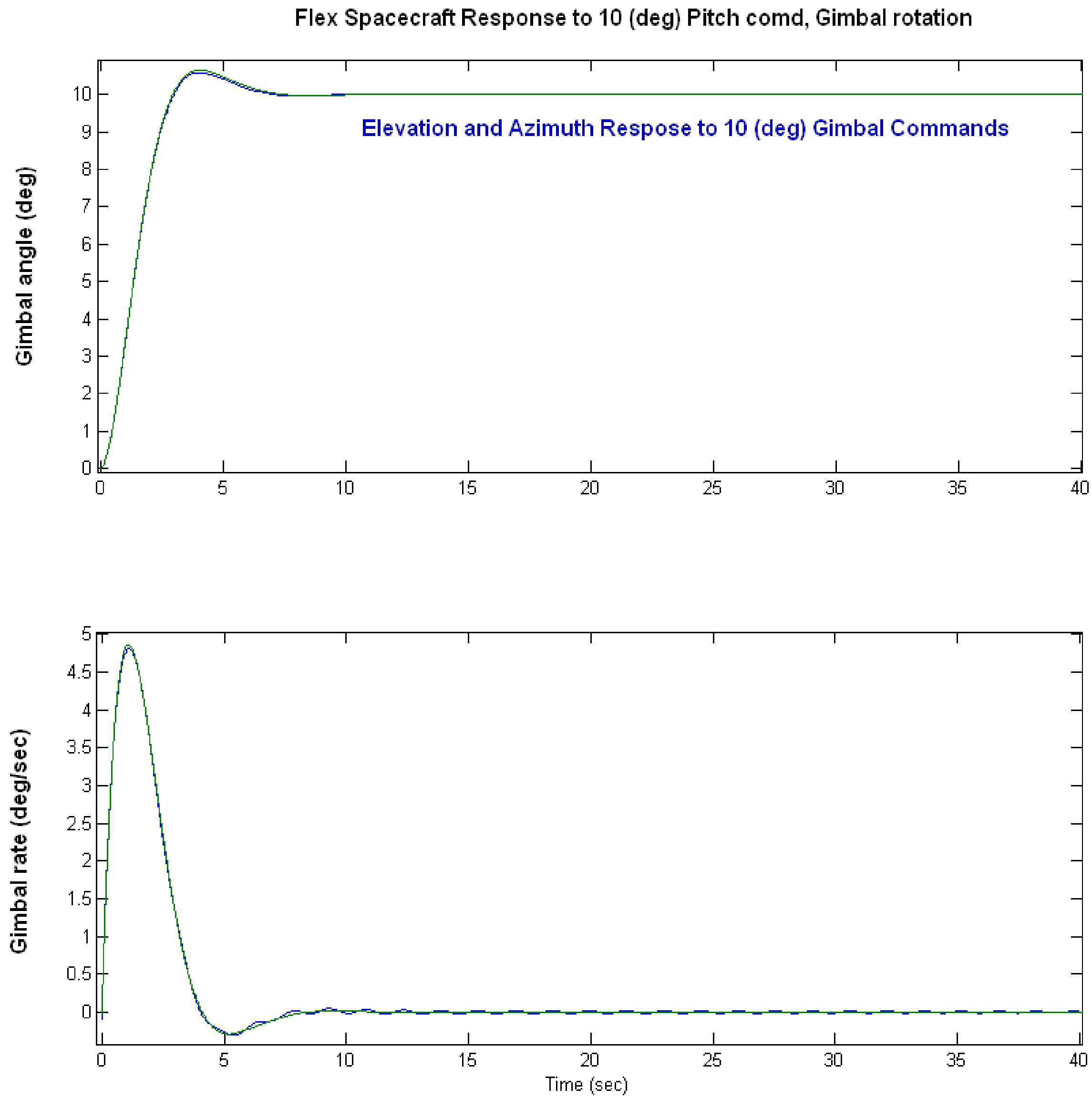

Figure 3.7 Elevation and Azimuth Gimbal Position and Rate responses to a 10 (deg) command in both directions

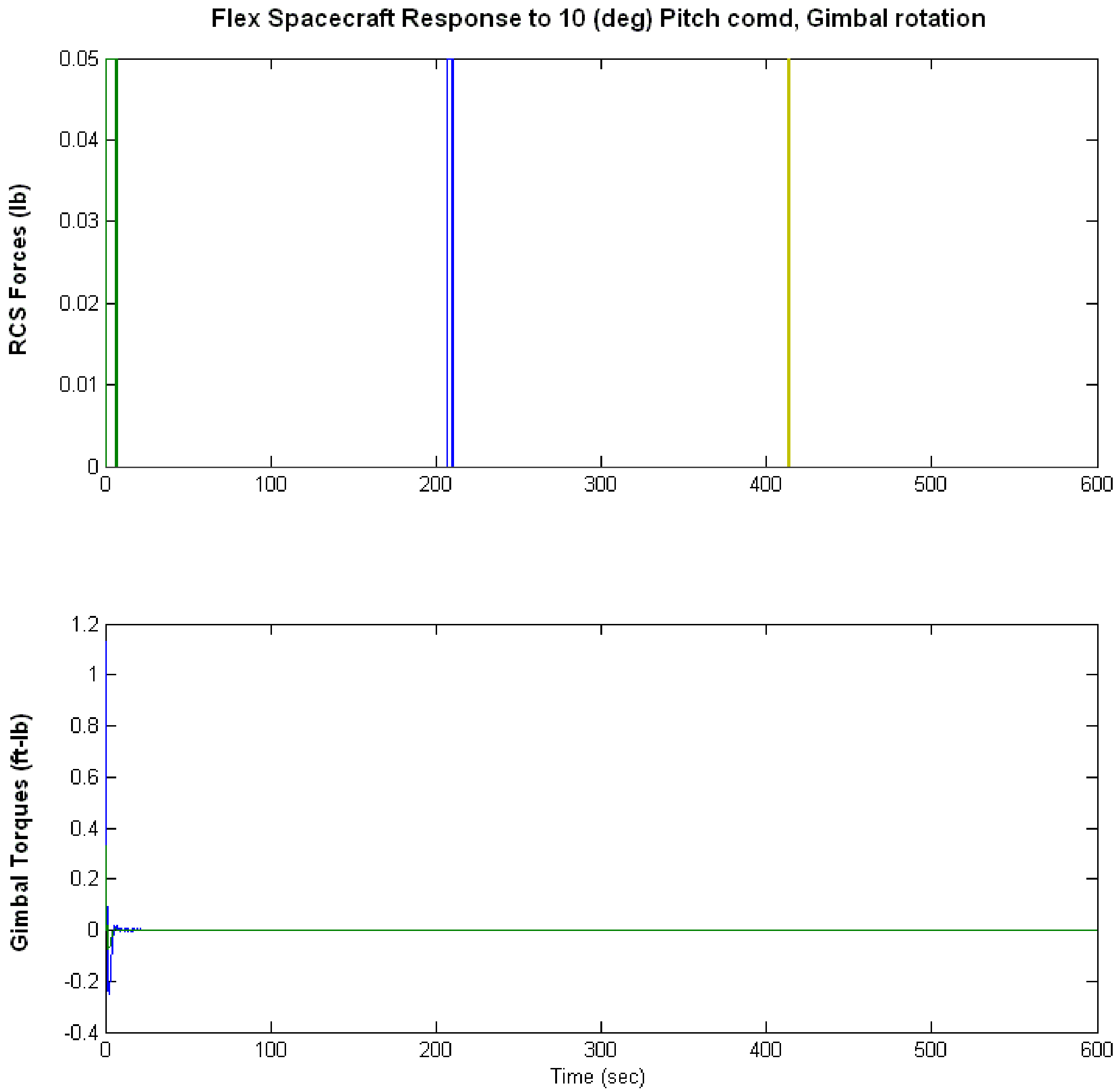

Figure 3.8 RCS jet forces during attitude control and gimbal torques to rotate the payload

3.5 Gimbal Sensitivity to Solar Array Stepper Motor Disturbances

The two solar arrays rotate about the spacecraft y axis and they perform a full 360º rotation with respect to the spacecraft for every orbit. The rotation is controlled by stepper motors at each solar array joint which generate a train of torque pulses that rotate the arrays at constant rate. The pulses frequency is at 2 Hz and they consist of a 0.08 (ft-lb) positive pulse followed by a similar negative pulse. The train of pulses generates a disturbance on the spacecraft which degrates the telescope image by creating a jitter on the Line-of-Sight (LOS). The purpose of this sensitivity analysis is to simulate the stepper motor torque pulses and apply them at the solar array joints and observe its effect on the azimuth and elevation jitter at the telescope gimbals. The Simulink model "*Flex_Solar.mdl*", shown in figure (3.9), is used to perform sensitivity to stepper motor disturbance analysis. It is excited by a disturbance model that simulates the Solar Array stepper motor torque pulses. Only the gimbal control loops are closed because the RCS creates much bigger disturbances and it is not active during telescope operations.

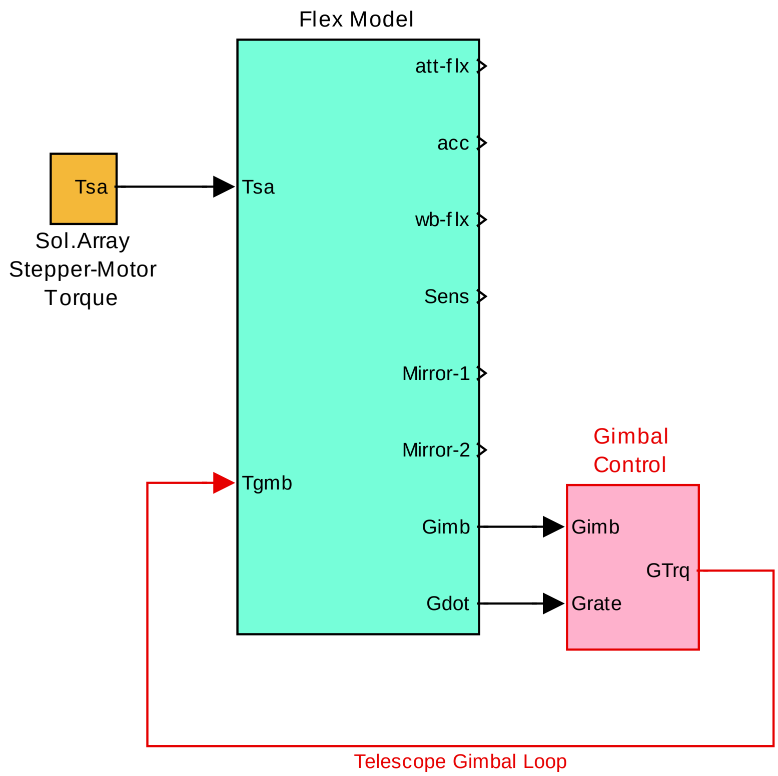

Figure 3.9 Sensitivity Analysis Model "Flex_Solar.mdl"

After running the model for a while we execute file "plf.m" to plot the data. Figure (3.10) shows the jitter effect on the telescope gimbals. It shows the gimbal rates versus rotation error in both: elevation (blue) and azimuth (green). Obviously, the azimuth is affected more because the disturbance pulses from the SA gimbals are in pitch.

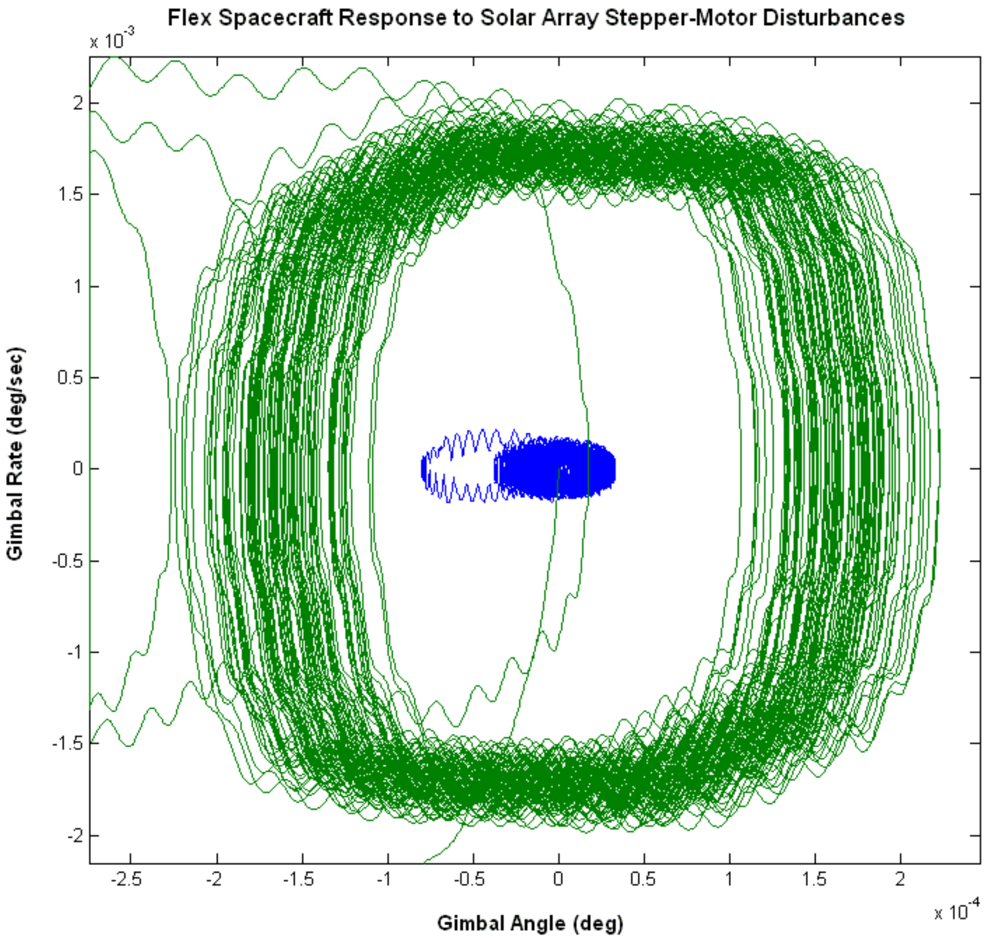

Figure 3.10 Azimuth and Elevation Jitter on the Telescope Gimbals

Figure (3.11) shows the solar array rotation angle and rate. The rate oscillations are due to the stepper motor pulses. Figure (3.12) shows the effect of the disturbance torque on the telescope gimbal torques.

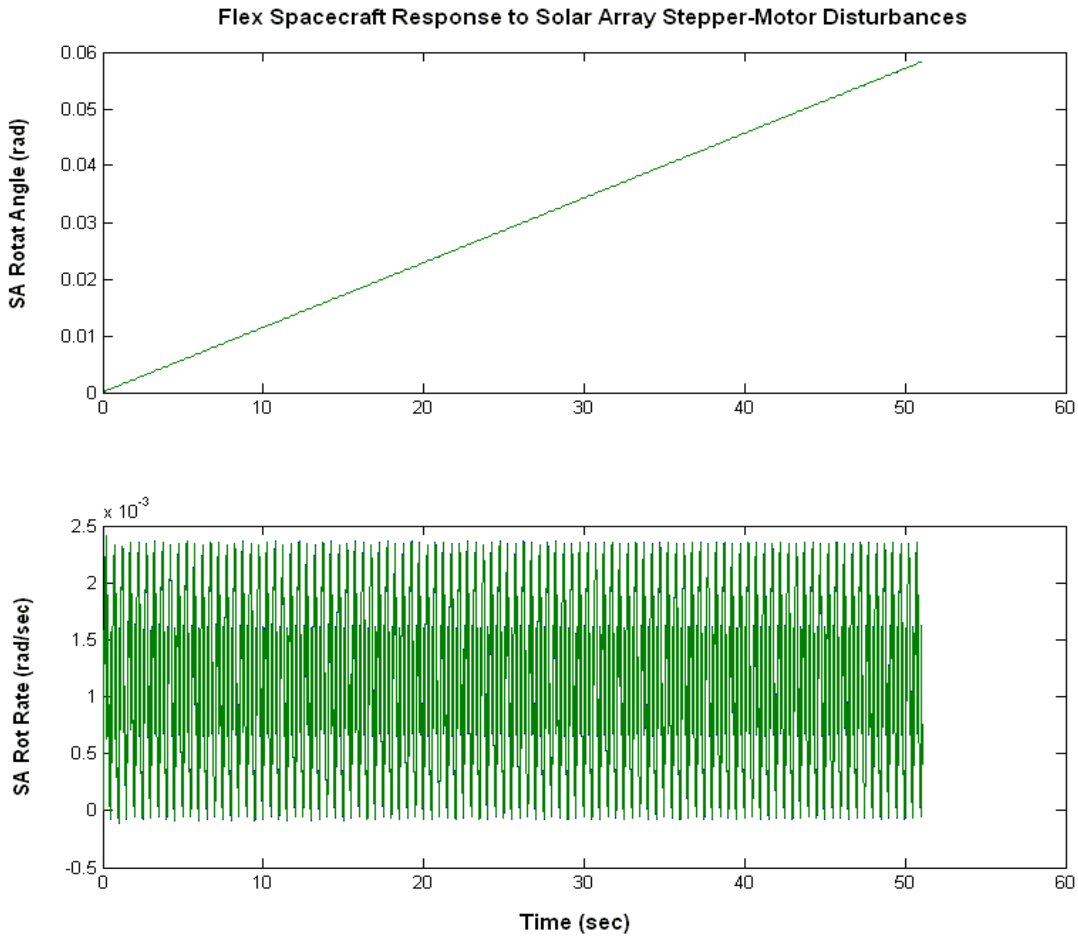

Figure 3.11 Solar Array Rotation Angle in (rad) and Rate in (rad/sec)

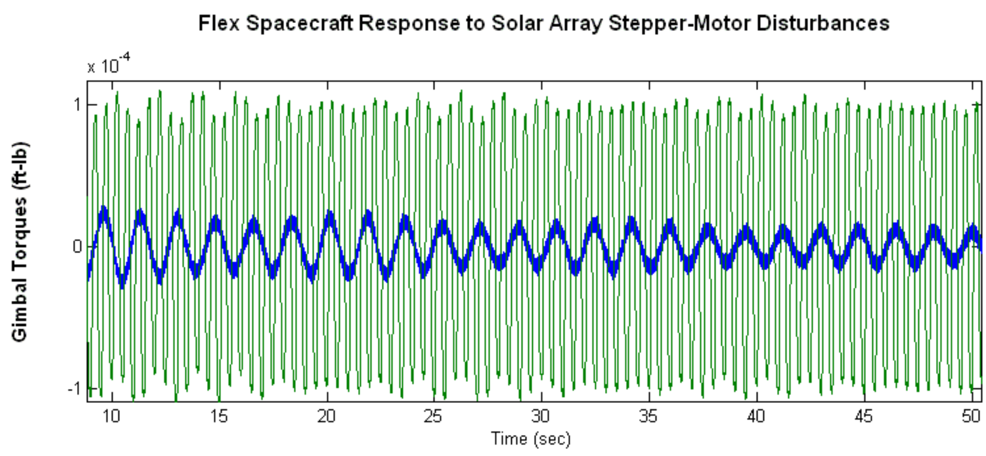

Figure 3.12 Azimuth and Elevation Gimbal Torques resulting from the Stepper-Motor Disturbance

4 Analysis of Rigid-Body with Flex Modes Combined

In Section 2 we developed a non-linear dynamic model of the orbiting spacecraft in the LVLH attitude. In Section 3 we created flexible spacecraft systems from modal data. Flex systems that include rigid-body modes, a system with only rigid modes, and a system with only flex modes that does not include the 6 rigid-body modes. This flex only system contains 61 flex modes starting from mode #7. It will be used in this Section and also in Section 5 combined in parallel with the non-linear rigid-body models to capture both, flexibility and non-linear dynamics. Its title is "*Flex Spacecraft with Gimbaling Telescope and Reaction Wheels (61-Only Flex)*" and it was saved in file "*flex61.m*". The Matlab analysis in this section is performed in subdirectory: "*\Examples\ Surveillance Satellite React-Wheels\Coupled Models*".

4.1 Rigid + Flex Non-Linear Simulation Model

Figure (4.1) shows the non-linear simulation model with flexibility "*NonLinear-Flex-Sim.mdl*". The spacecraft dynamics block is shown in Figure (4.1a). It consists of the non-linear spacecraft dynamics block in parallel with the flex state-space system from "flex61.m". Both systems receive the same RCS forces and RW torques, and their outputs are combined together representing the rigid plus flex motion. The RW torques are in body coordinates and they are generated by the RW Dynamics block shown in Figure (4.1b). It uses the function "*Wheel_Dynamics.m*" to calculate the wheel torque in body, including also the gyroscopic effect due to body rate coupling with the bias momentum. It calculates also the wheel rates relative to the spacecraft. The wheel friction is also included in the model. The RW/RCS control law is identical to the one used in section 2. The file "*run.m*" in the "*Coupled Models*" subdirectory initializes the model.

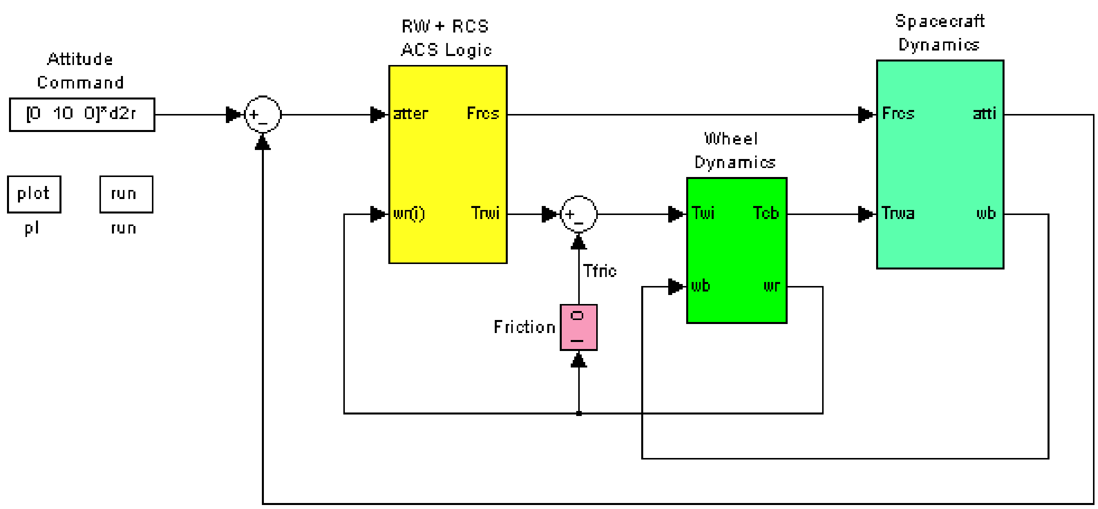

Figure 4.1 Non-Linear Simulation Model with Flexibility "NonLinear_Flex_Sim.mdl"

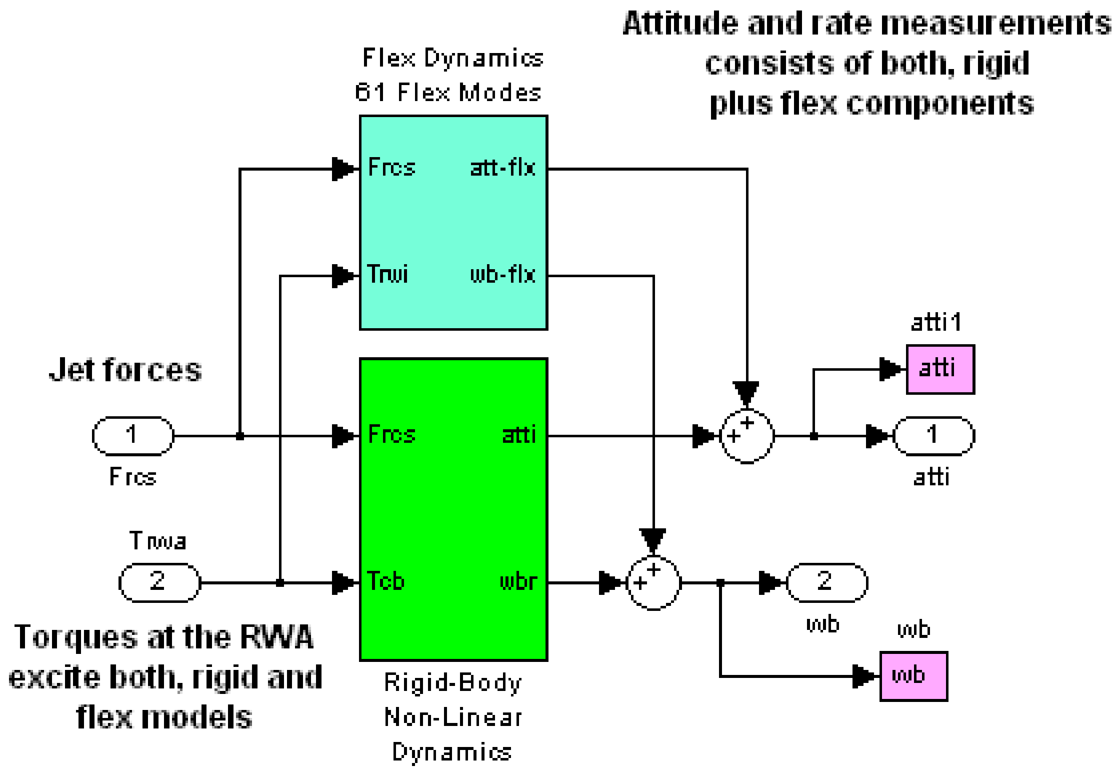

Figure 4.1a Spacecraft Dynamics Consisting of Flex System in Parallel with the Non-Linear Model

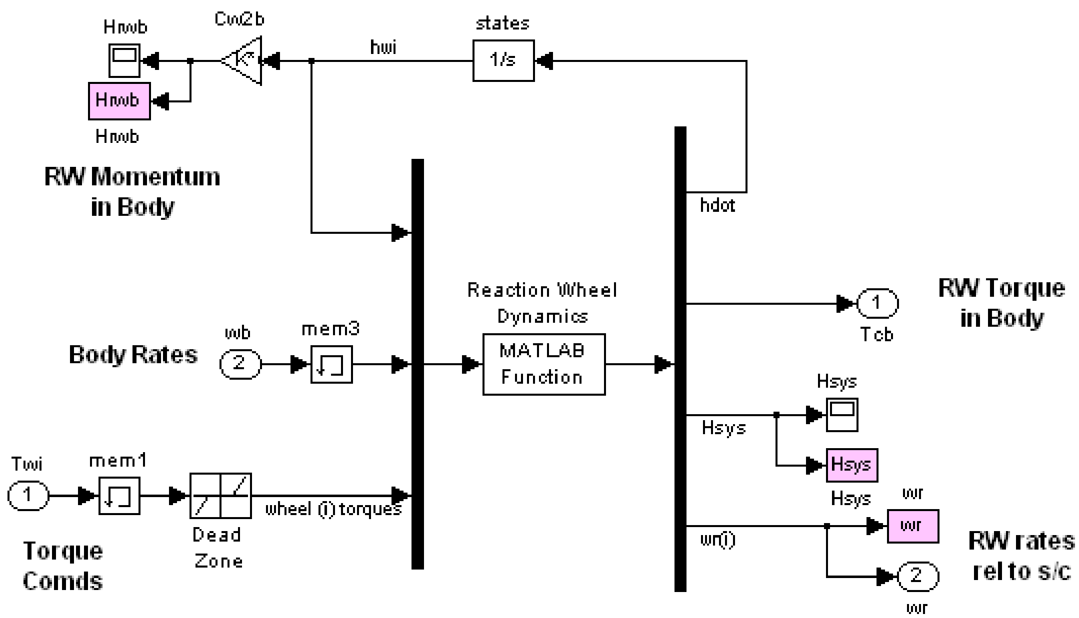

Figure 4.1b Reaction Wheel Dynamics Block Calculates the RW Torques in Body Coordinates

Figures (4.2a through 4.2c) show simulation results using the Simulink model “NonLinear_Flex_Sim.mdl”. This model is obviously a lot slower than its rigid-body equivalent because it contains 60 flex modes, so we initialized it at non-zero RW #2 and #3 rates in order to speed up the time it takes to reach the momentum dump level. We are commanding it to go to a 10° change in LVLH pitch attitude. It starts by using the reaction wheels to control attitude. Wheel #1 is maintained at constant speed throughout to provide the -40 (ft-lb-sec) bias, by commanding it a small torque to overcome the friction torques. The external disturbance torques on the spacecraft cause the momentum magnitude to drift. When it exceeds 10 (ft-lb-sec) from its biased value the ACS switches to the RCS mode to bring the RW #2 and #3 rates back to zero. When the momentum dump is achieved it switches back to the RW control mode.

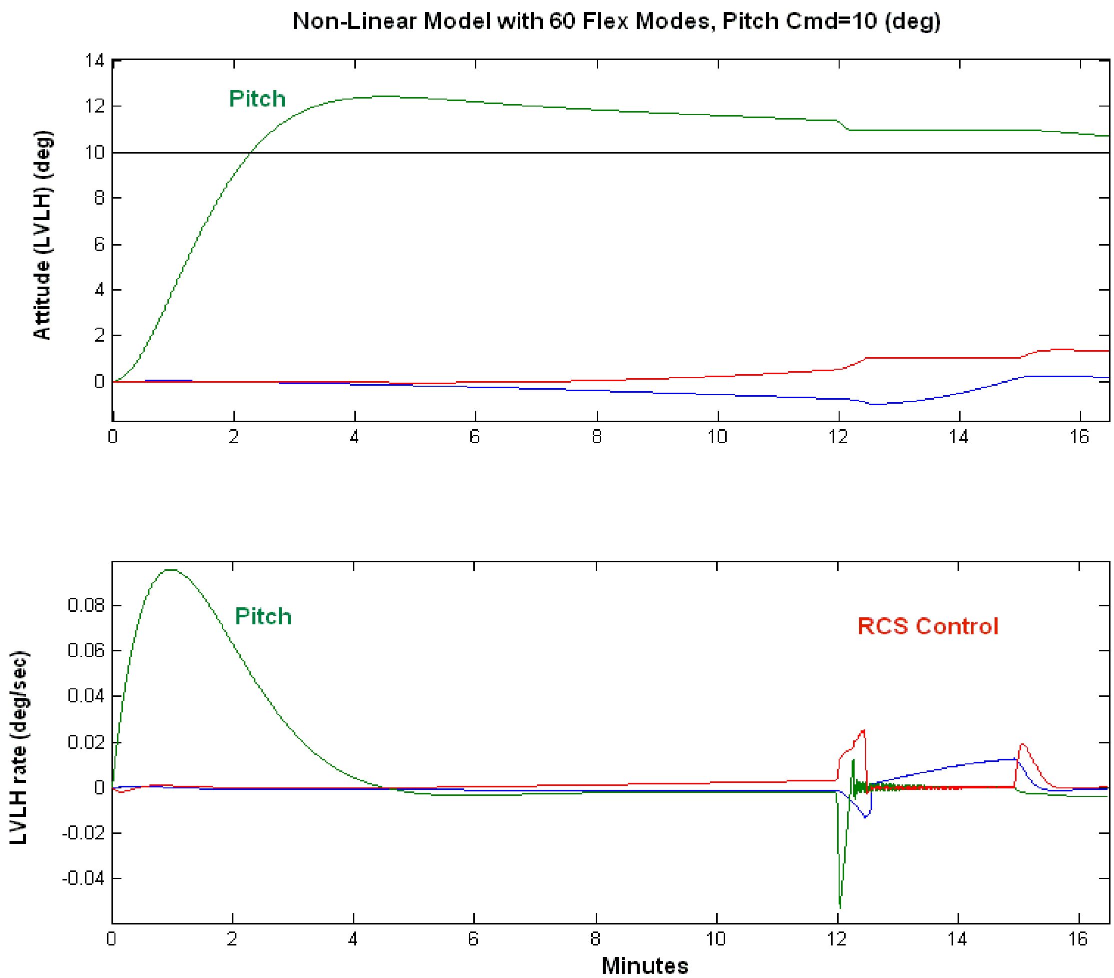

Figure 4.2a Spacecraft attitude and Rate relative to the LVLH frame after being commanded 10° in pitch

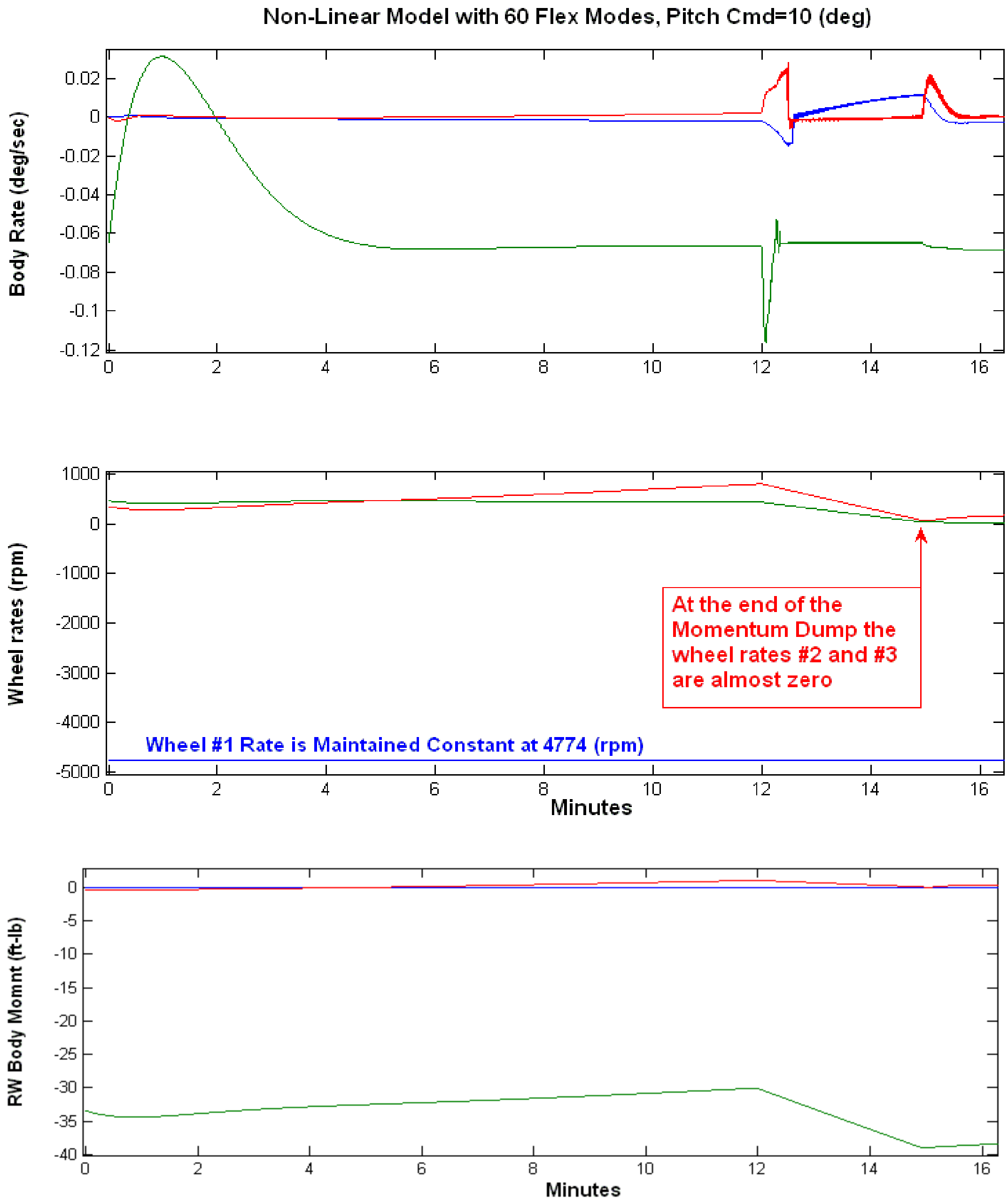

Figure 4.2b At the end of the RCS burn the Pitch Momentum is -40 (ft-lb-sec). The Roll and Yaw Momentum is zero

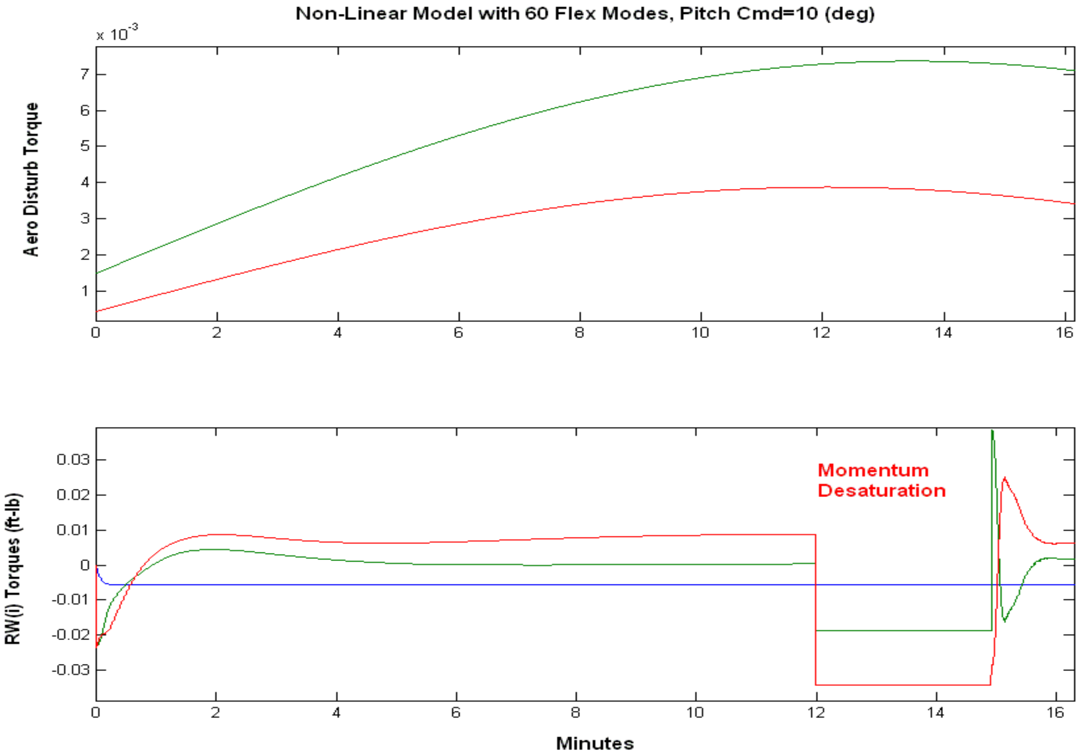

Figure 4.2c Wheel #1 (blue) is commanded a small torque to overcome internal friction and to maintain a constant speed. Wheels #2 and #3 (green & red) are torqued in order to control attitude and to overcome external disturbances. During RCS control Wheels #2 and #3 are torqued in the direction required to bring their speeds to zero in unison.

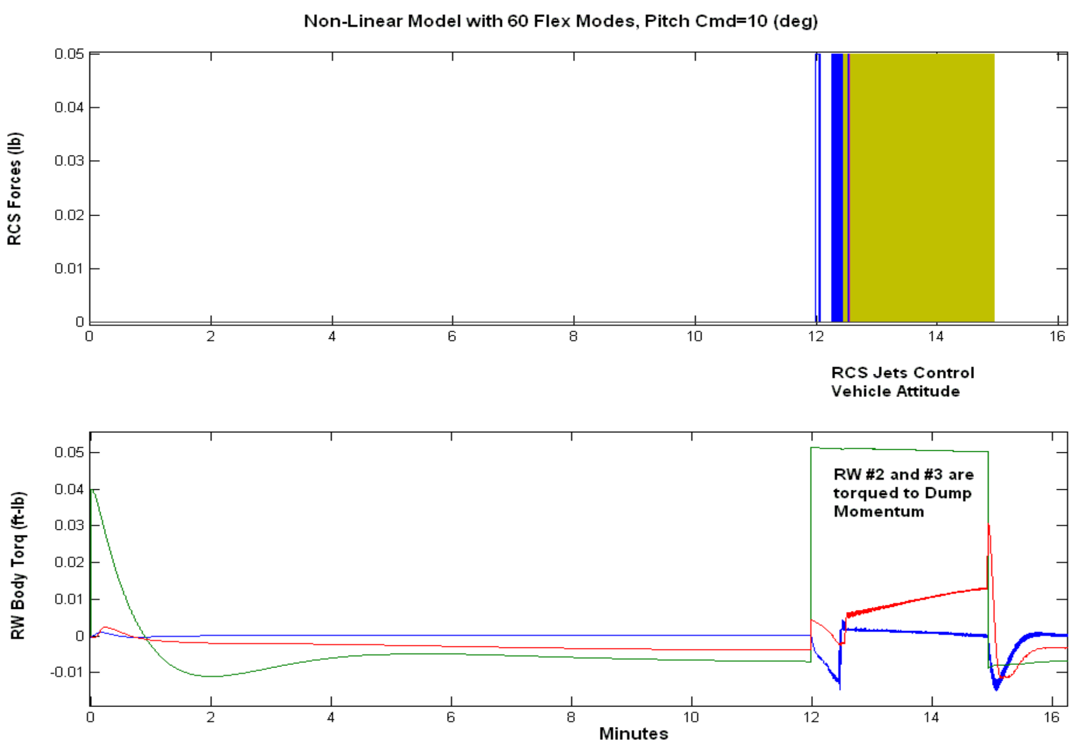

Figure 4.2d The RW Desaturation Torque is mainly in the Spacecraft Pitch direction (green). The Roll torque (blue) is gyroscopic due to yaw body rate coupling with the pitch momentum.

4.2 Rigid + Flex Linear Stability Analysis

For linear stability analysis we will repeat the idea of combining the 61-flex-mode state-space model in parallel with a linearized model of the spacecraft dynamics. We will ignore the RCS stability for now and focus mainly on the RW control analysis. We will develop two linear models, a closed-loop and an open-loop model, and perform linear analysis. The analysis files for this section are included in subdirectory: "… *\Examples\ Surveillance Satellite React-Wheels\Linear Flex Anal*".

4.3 Linearized Rigid-Body Equations of Motion

The following equations describe the linear motion of the spacecraft in circular orbit around the earth relative to the LVLH frame. The angular acceleration is a function of various external torques, as follows:

$$I\,\dot{\omega}_b = -\omega_b \times I\omega_b + T_{sc} + T_{gg} + T_d + T_{bias}$$

Where: the first term on the RHS is the gyroscopic torque on spacecraft

T_{sc} is the torques on the spacecraft from the RWA

T_{gg} is the gravity gradient torques on the spacecraft as a function of attitude

T_d is the aerodynamic torque

T_{sc} is a bias torque due to linearization

w_0 is the orbital rate in (rad/sec)

The linearized gyroscopic term is:

$$-\omega_b \times I\omega_b =$$

$$\omega_0 \begin{bmatrix} I_{XZ} & 2I_{YZ} & I_{ZZ} - I_{YY} \\ -I_{YZ} & 0 & I_{XY} \\ I_{YY} - I_{XX} & -2I_{XY} & I_{XZ} \end{bmatrix} \begin{pmatrix} \omega_x \\ \omega_y \\ \omega_z \end{pmatrix} + \omega_0^2 \begin{pmatrix} -I_{YZ} \\ 0 \\ I_{XY} \end{pmatrix}_{bias}$$

The torque applied on the spacecraft from the reaction wheel assembly consists of: reaction torques due to rotor acceleration plus lateral gyroscopic torques due to pitch momentum bias. In this case we only have H_{Y0}.

$$T_{sc} = \begin{bmatrix} \omega_z H_{Y0} - \omega_y H_{Z0} + \omega_0 H_z \\ \omega_x H_{Z0} - \omega_z H_{X0} \\ \omega_y H_{X0} - \omega_x H_{Y0} - \omega_0 H_x \end{bmatrix}_{gyro} - C_w^b\, \underline{T}_{wi}$$

The rate of change in reaction wheel momentum in body frame is a function of the applied RW torques:

$$\begin{pmatrix} \dot{H}_{RWX} \\ \dot{H}_{RWY} \\ \dot{H}_{RWZ} \end{pmatrix} = \begin{pmatrix} T_{RWX} \\ T_{RWY} \\ T_{RWZ} \end{pmatrix}$$

The gravity gradient torque is a function of the LVLH attitude

$$T_{gg} = 3\omega_0^2 \begin{bmatrix} I_{ZZ} - I_{YY} & I_{XY} & 0 \\ I_{ZZ} & I_{ZZ} - I_{XX} & 0 \\ -I_{XZ} & -I_{YZ} & 0 \end{bmatrix} \begin{pmatrix} \phi \\ \theta \\ \psi \end{pmatrix}_{LVLH} + \omega_0^2 \begin{pmatrix} -I_{YZ} \\ 3I_{XZ} \\ -2I_{XY} \end{pmatrix}_{bias}$$

The combined bias term after linearization from the gyroscopic and the gravity gradient equations is

$$T_{bias} = \omega_0^2 \begin{pmatrix} -2I_{YZ} \\ 3I_{XZ} \\ -I_{XY} \end{pmatrix}$$

The LVLH attitude is obtained by integrating the following equations:

$$\begin{pmatrix} \dot{\phi} \\ \dot{\theta} \\ \dot{\psi} \end{pmatrix}_{LVLH} = \begin{pmatrix} \omega_x + \omega_0 \psi \\ \omega_y + \omega_0 \\ \omega_z - \omega_0 \phi \end{pmatrix}$$

4.4 Linear Closed-Loop Model

In this section we shall examine the in-plane and out-of-plane system stability of the satellite using linear models and design filters to attenuate the structural modes. Folder "*Linear Flex Anal*" contains a linear simulation model "*Sim_Flex.mdl*", shown in Figure (4.4). It consists of three blocks, the flexible spacecraft dynamics, the reaction wheel dynamics, and the RW control law which was described earlier.

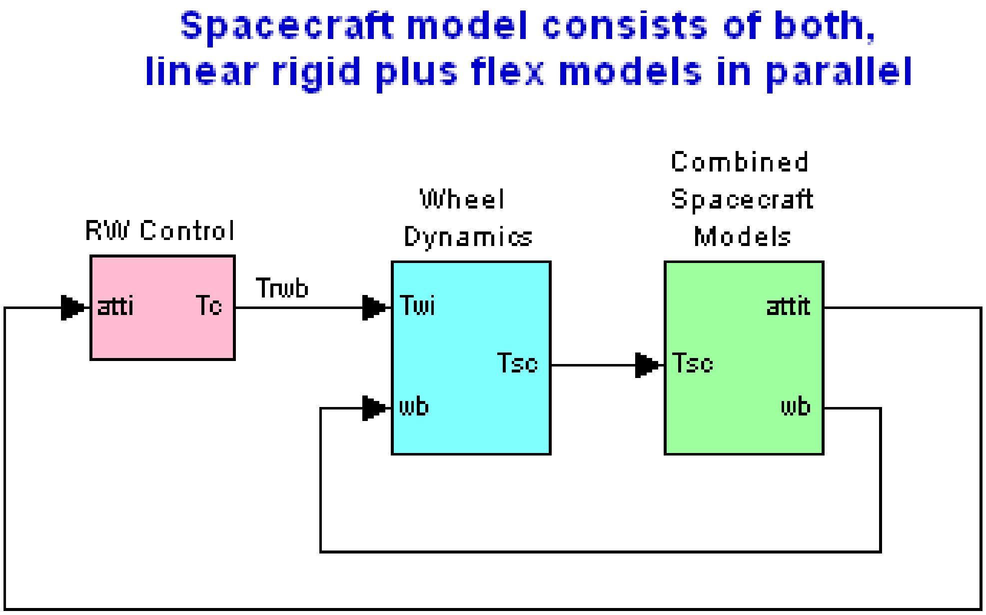

Figure 4.4 Linear Reaction-Wheel Closed-Loop Simulation Model "Sim_Linear.mdl"

It is different from a previous rigid-body analysis model in folder "*Linear-Anal-2*", where the RW model was included in the spacecraft block. In this model, the output (T_{sc}) from the RW dynamics block (cyan) consists of two components: the control torques due to the RW (2 & 3) rotor accelerations, and also the gyroscopic torques in yaw and roll due to the 40 (ft-lb-sec) pitch momentum wheel#1 bias coupling with the body rate (ω_b x H_{rw}). The Matlab function "*Wheel_Dynamics.m*" calculates the linearized wheel momentum (in the spacecraft frame) and the total torque is applied to the spacecraft at the reaction wheel assembly.

This torque drives both: rigid and flex spacecraft models in the body frame. The spacecraft block (green), in figure (4.4), consists of two subsystems in parallel, the rigid-body dynamics and the flex dynamics, as shown in figure (4.5).

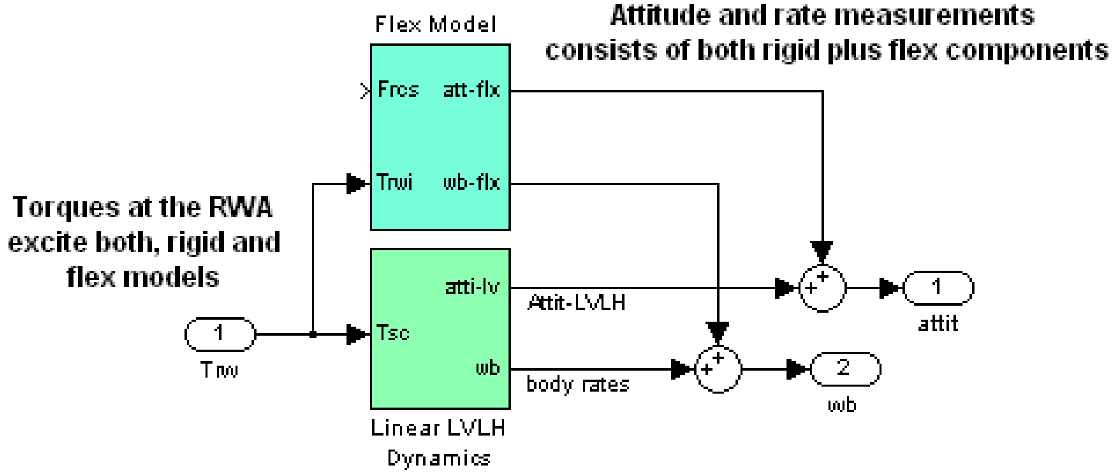

Figure 4.5 Combined Spacecraft dynamics consisting of linear plus flex subsystems in parallel

The linear spacecraft dynamics with respect to the LVLH frame (equations in section 4.3) is implemented in the Matlab function "*Spacecraft.m*", which generates the body rates and the spacecraft LVLH attitude as a function of the torques at the RW assembly (RWA). The gravity-gradient and the linearized spacecraft gyroscopic torques (ω_b x $J\omega_b$) are calculated in this file as a function of attitude and body rate by means of matrices (M_{gg} and M_1), which are calculated in file "run.m" as a function of mass properties. T_d and T_{bs} are disturbance and bias torques respectively. The torque T_{sc} is the control torque coming from the RWA and it includes also the gyroscopic effects due to the bias momentum of wheel #1. The spacecraft model outputs are: body rates, and LVLH attitude. The flex dynamics block is the FEM state-space model used in section (4.1). It uses the system from file "*flex61.m*" in folder "*Linear Flex Anal*", that has the 6 rigid-body modes removed. The reason for replacing the FEM rigid-body modes with the spacecraft LVLH dynamics is because the FEM is missing the gyroscopic, gravity-gradient, and orbital effects. The rates and attitudes from the flex model are added to the rates and attitudes of the rigid-body model to simulate the sensor outputs which measure both, rigid and flex motion.

Figure (4.6) shows a simulation analysis of the linear model initialized from an LVLH attitude [2, 1, -2] degrees. The system sustains an oscillation because it has a critically damped resonance at orbital rate 0.00113 (rad/sec). The period of the oscillation, however, is long and the RCS (not included here) is able to control it. The roll and yaw attitude oscillations converge to a zero mean. The nutation mode at 0.055 (rad/sec) is well damped by the RW attitude control system. The structural modes are attenuated by the low-pass filter. The pitch momentum is building up because of the gravity gradient torque. The simulation sample rate Ts was set to 0.001 seconds.

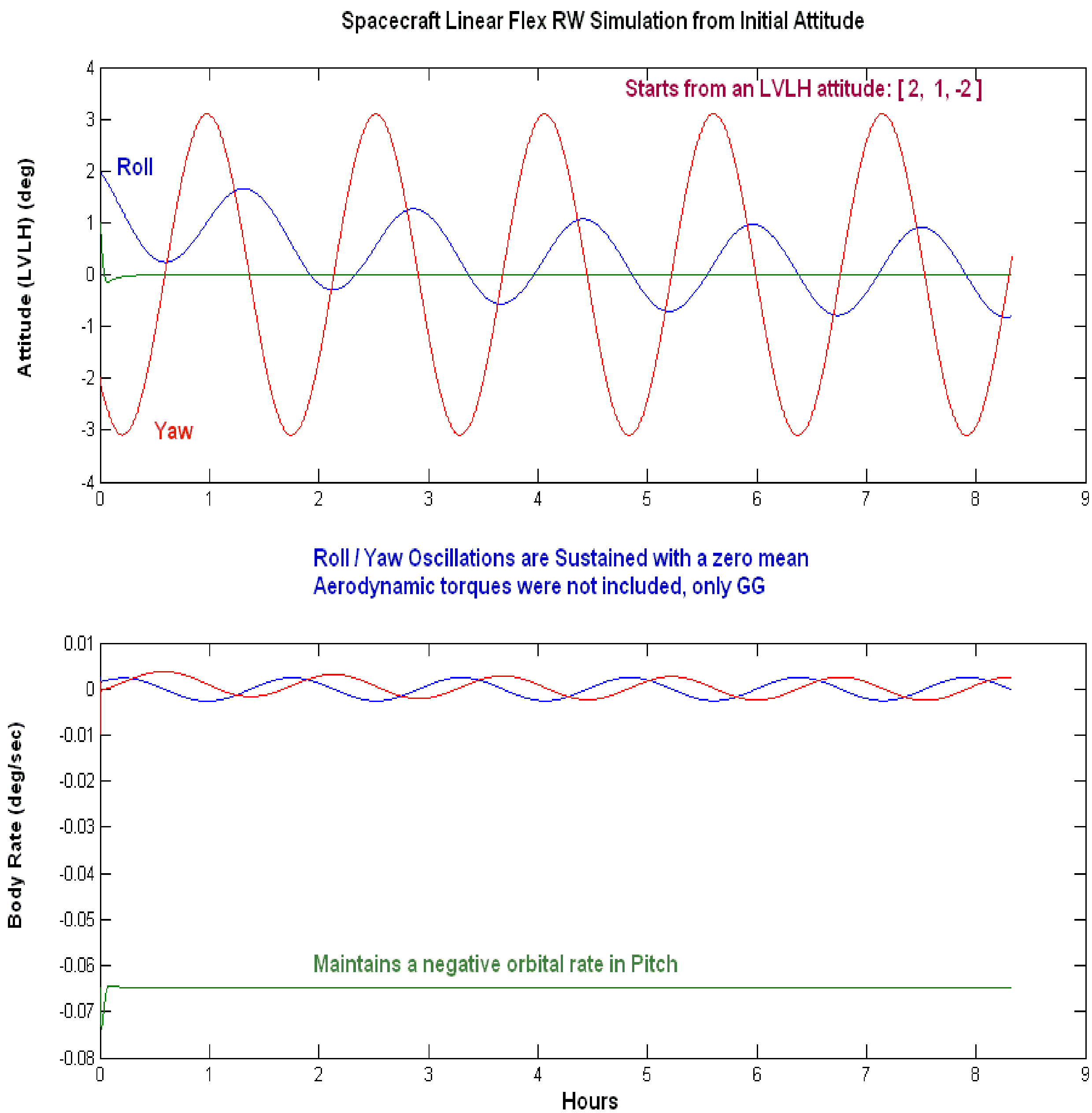

Figure 4.6 Linear Simulation using model "Sim_Flex.Mdl" shows spacecraft response from an initial LVLH attitude

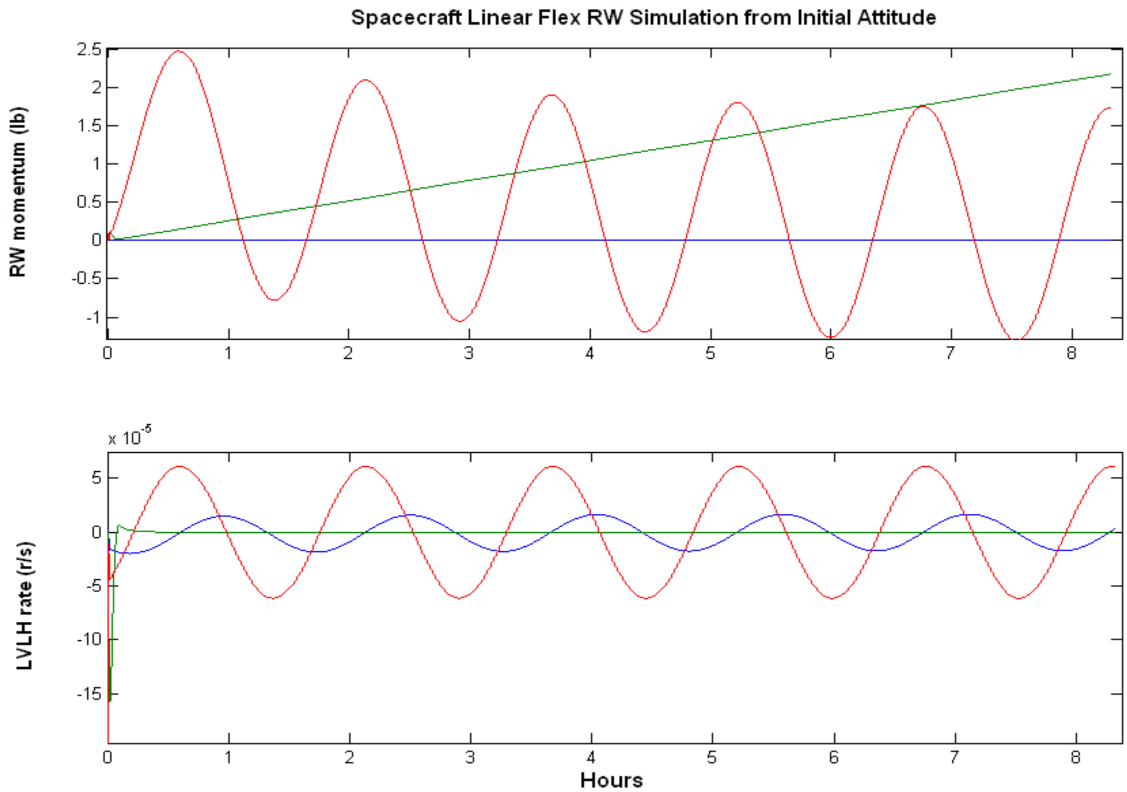
Spacecraft Linear Flex RW Simulation from Initial Attitude
RW momentum (lb)
x 10^-5
LVLH rate (r/s)
Hours

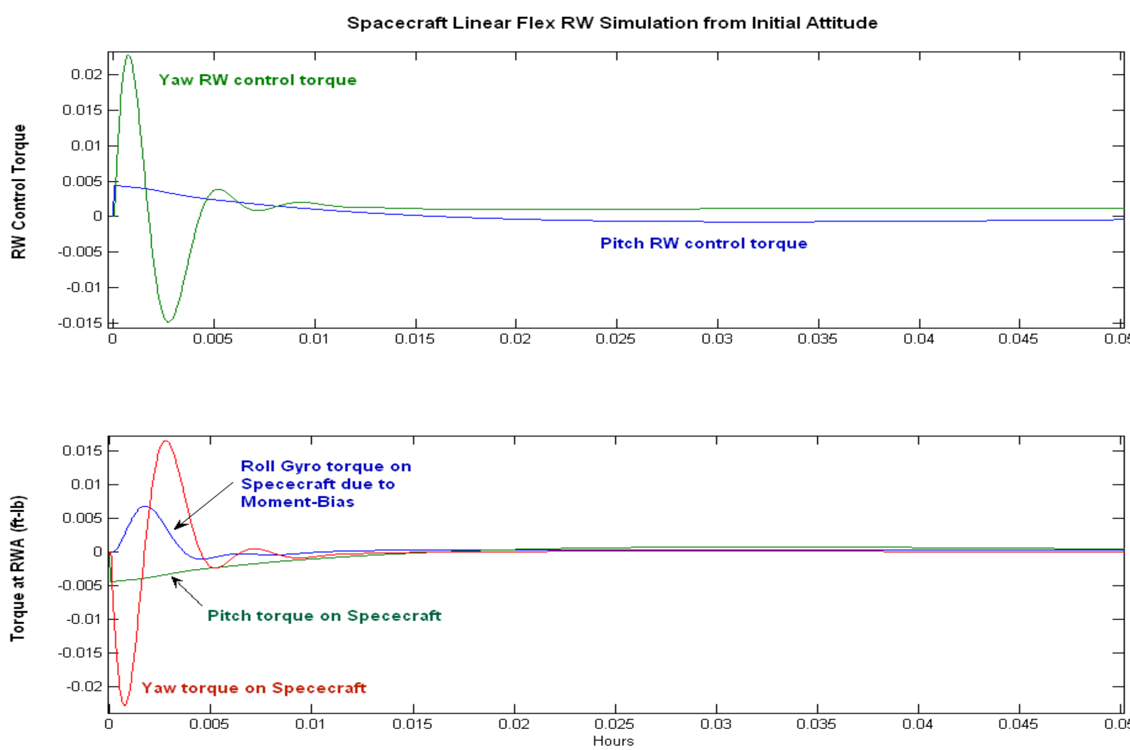
Spacecraft Linear Flex RW Simulation from Initial Attitude
RW Control Torque
Yaw RW control torque
Pitch RW control torque
Torque at RWA (ft-lb)
Roll Gyro torque on Spececraft due to Moment-Bias
Pitch torque on Spececraft
Yaw torque on Spececraft
Hours

4.5 Stability Analysis in Frequency Domain

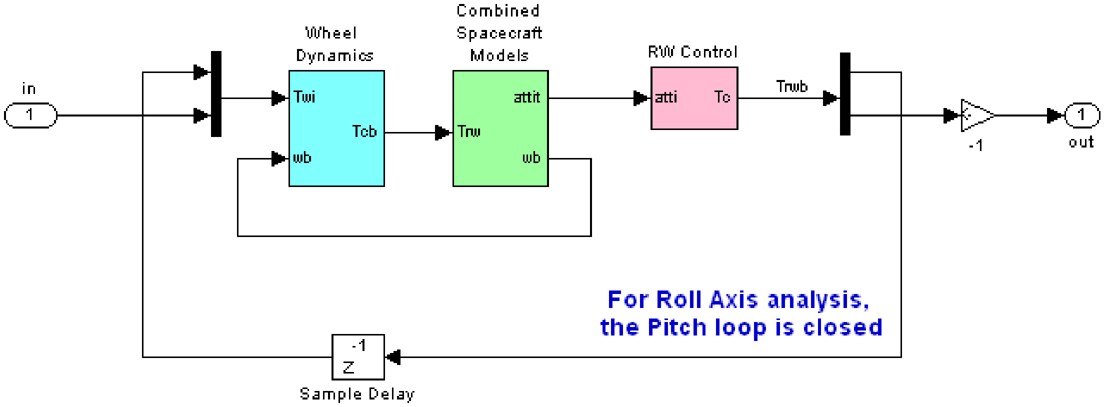

Figure 4.7 Model "Open_Anal.mdl" used for frequency domain stability analysis

Figure (4.7) is another linear Simulink model consisting of the same subsystems as figure (4.4) and it is used for open-loop frequency response analysis. The controller consists of two loops, the pitch (in-plane) loop and the out-of-plane (lateral) loop. The control loops are cut at the RW controller output, one loop at a time. The Matlab file "*LinAna.m*" is used to calculate the frequency response. The above configuration is for analyzing the out-of-plane stability with the pitch loop closed. Preliminary stability analysis in the lateral axis predicts flex mode instability, as shown in the Nichols plot in figure (4.10). The instability, however, is attenuated by introducing a low pass filter in the out-of-plane RW control loop, as shown in figure (4.11). The pitch axis, shown in figure (4.9), does not require any compensation.

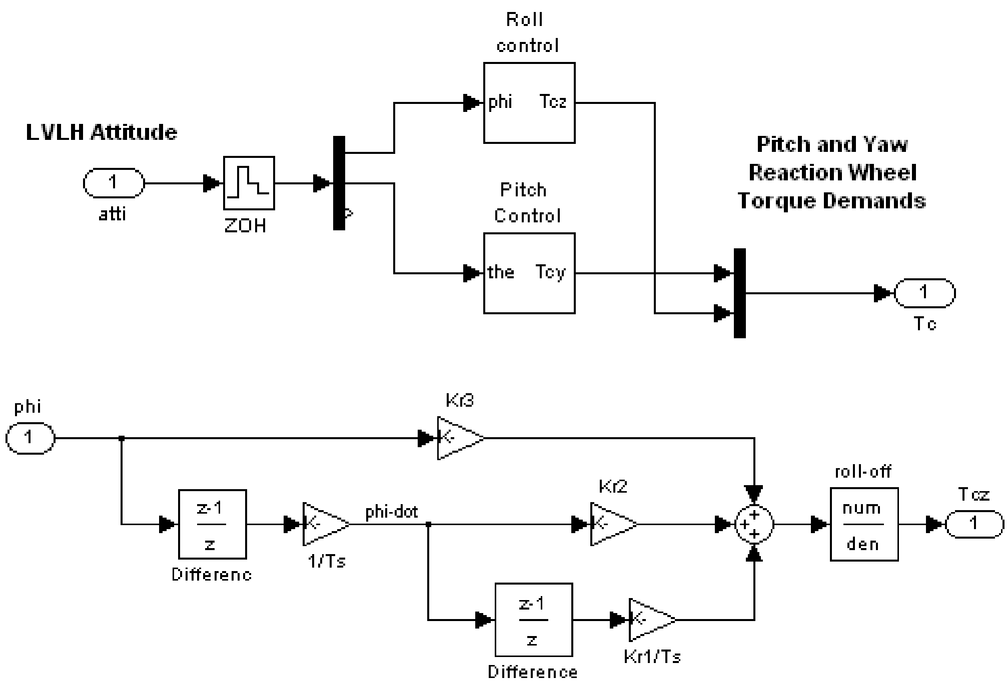

Figure 4.8 RW Control Law with additional low-pass filter to attenuate flex mode instability in roll

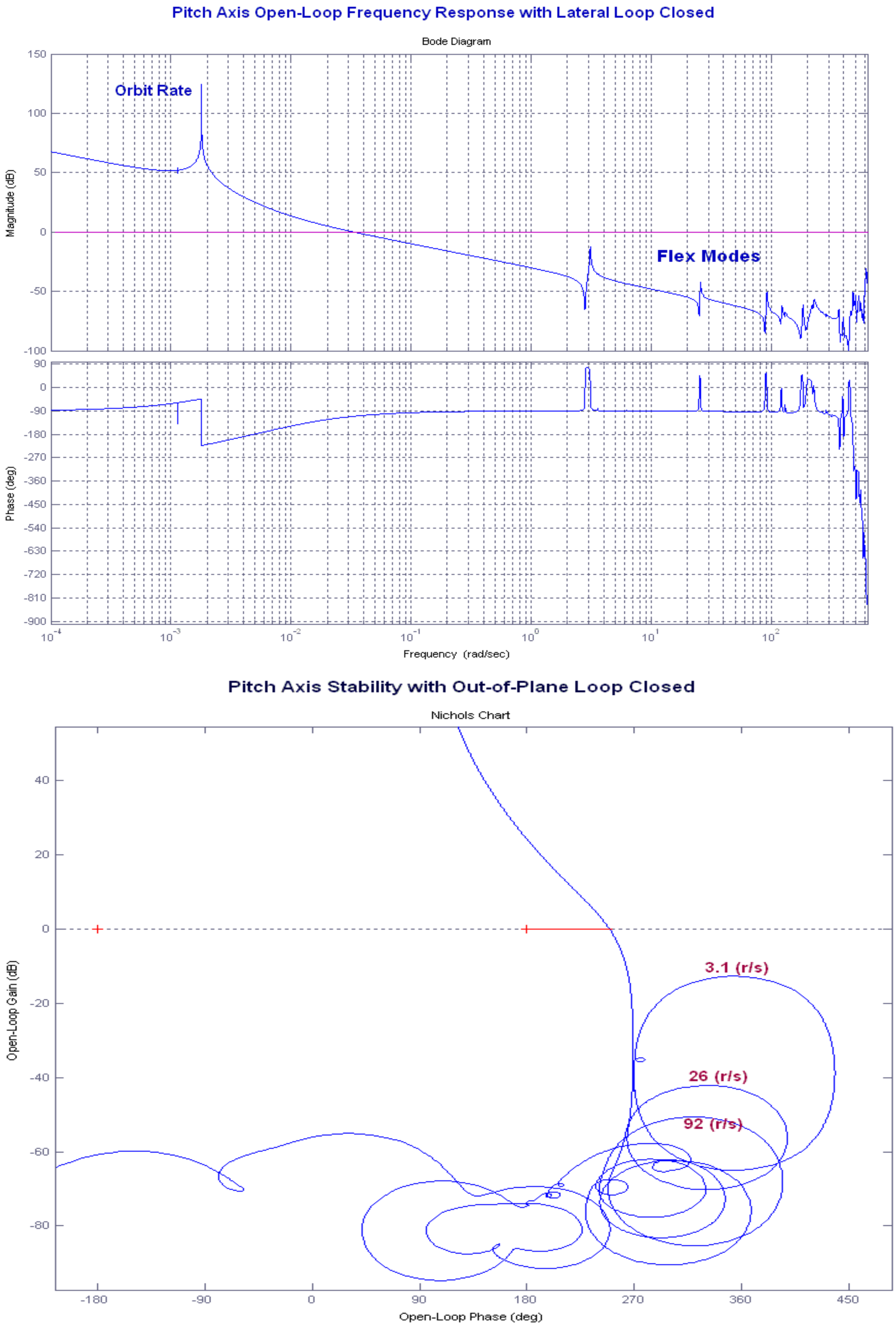

Figure 4.9 Pitch Axis Frequency Response Analysis

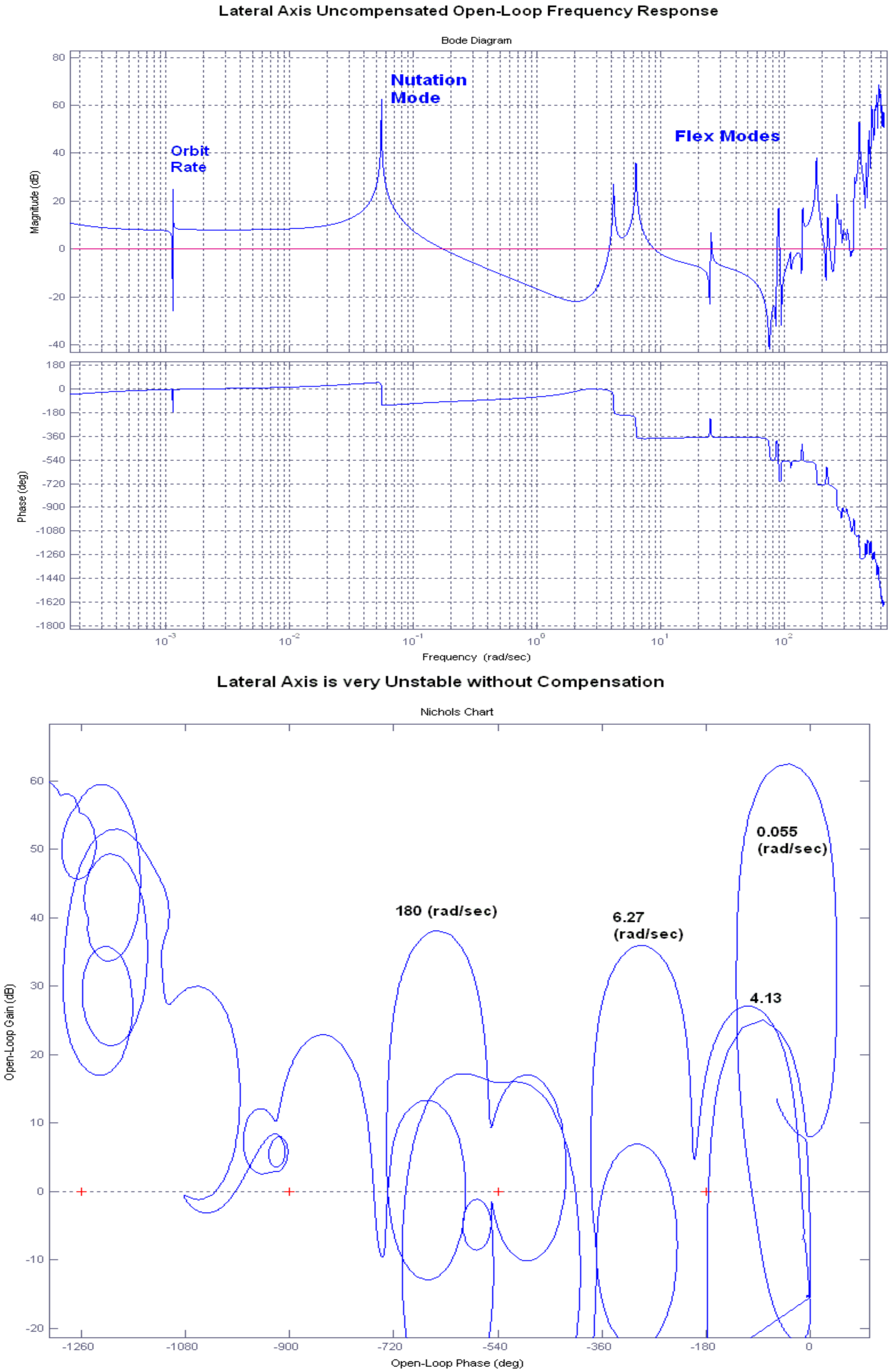

Figure 4.10 Frequency Response of the Lateral Loop without Compensation

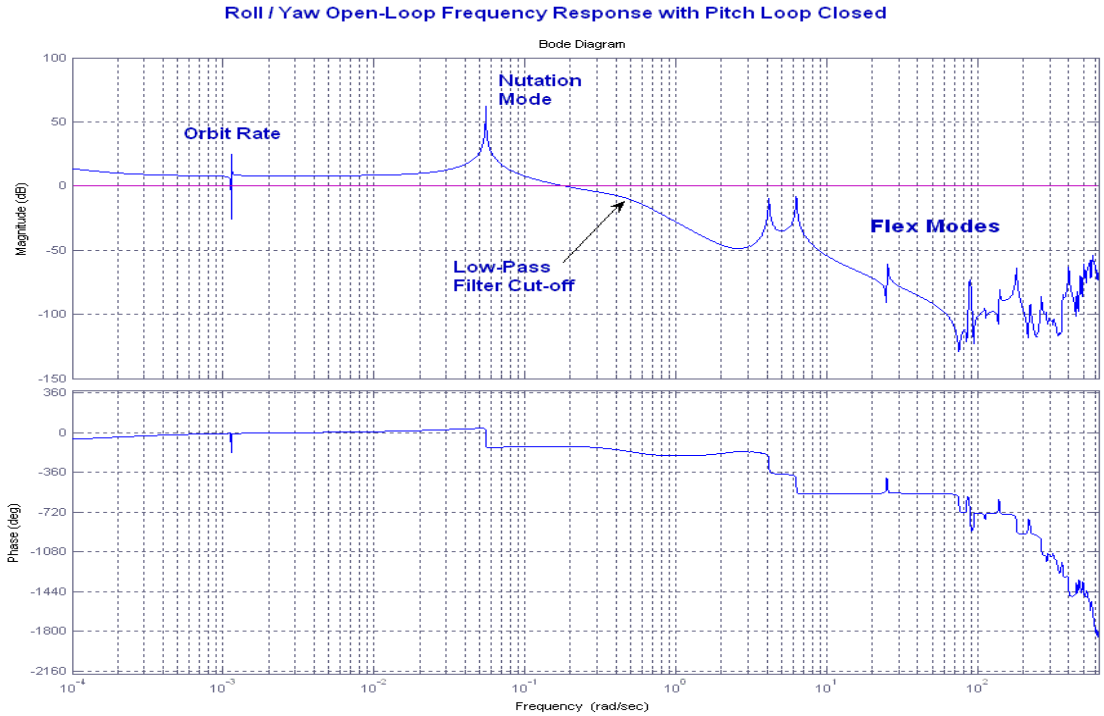

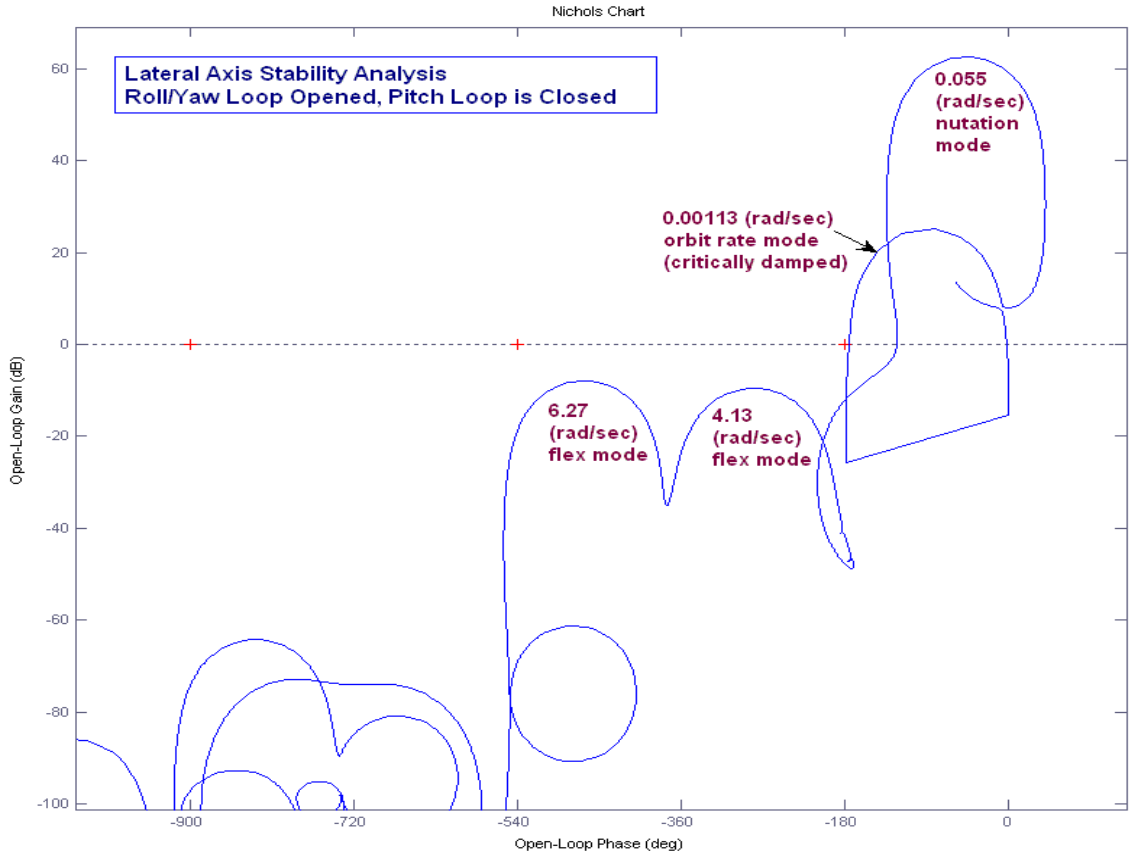

Figure 4.11 Frequency Response Analysis of the Compensated Lateral Axis Loop

5 Multi-Body Analysis

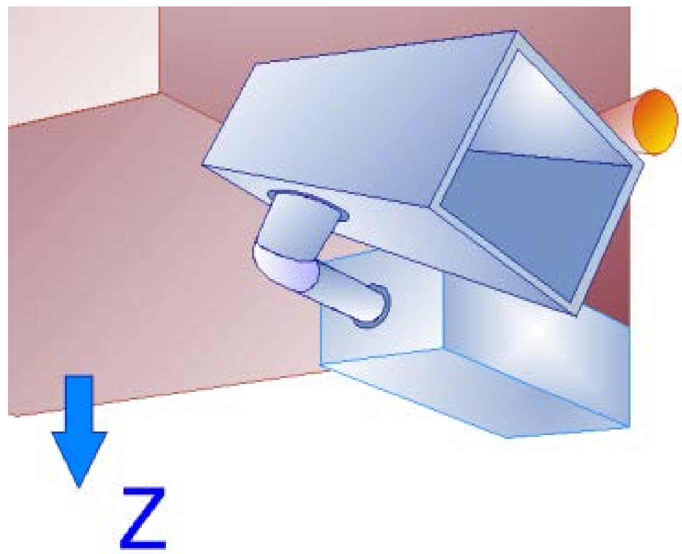

The next step in the surveillance satellite analysis is to improve the dynamic model by introducing two additional rotational degrees of freedom for the optical telescope. The telescope is attached to the spacecraft bus by means of a 2-hinge mechanical system that allows it to rotate about two orthogonal axes. The inner hinge is parallel to the spacecraft x axis. The outer hinge is orthogonal to the first hinge. When the hinges are at zero position the telescope is pointing towards the earth (+z) and the direction of the outer hinge is along the spacecraft –y axis. Typically, a multi-body non-linear simulation tool should be used to simulate the relative motion between the satellite bus and the moving sensor, but for simplicity we will use a 3-rigid-body non-linear Simulink model and introduce flexibility by coupling it with the flex model in parallel. We will also design simple PD control laws for the two gimbals, elevation (inner) and azimuth (outer) and analyze system performance and stability using the attitude control laws that were developed in previous sections. We will first model the rigid-body dynamics for the 3-body system and simulate it in Matlab using the previously designed control laws. Then we will combine the 3-rigid-body model with the flex model in parallel and analyze flex stability and performance to gimbal commands. We will also analyze the telescope Line-of-Sight (LOS) sensitivity to mechanical disturbances.

5.1 Rigid-Body Simulation

The analysis data files for this section are in folder *"…\Flixan\Examples\Surveillance Satellite React-Wheels\3_Body+Flex_NLSim*". The 3-body spacecraft dynamics is in file "*Vehi-3B3W.m*". The two solar arrays are not hinged in the model because their motion is very slow and do not create disturbances while rotating. Their masses and inertias were included in the spacecraft bus mass properties. The dynamic model consists of spacecraft attitude, gimbal dynamics, reaction wheels, orbital dynamics, reaction control jets, and gravity gradient effects. The model mass properties, hinge directions, etc, is initialized by running file "Dynamics-Data.m". The file "run.m" in addition to the "Dynamics-Data" it also initializes all the other parameters needed in this analysis. The wheels are initialized with -40 (ft-lb-sec) initial momentum in the pitch direction and the spacecraft with a negative pitch rate -0.00113 (rad/sec). The initial position and velocity are initialized for a 215 N-miles circular orbit. The flex state-space model "flex61.m" is also loaded (generated from previous analysis). This model consists of 61 flex modes. It starts from mode #7 and excludes the FEM rigid-body modes. The “run” file initializes also the RCS and reaction wheel parameters and initializes the state-vector in the simulation (Int_IC).

The inputs to this model are: RCS jet forces, reaction wheel torques (individual wheel axes), 2 telescope gimbal torques, and disturbance torques. The outputs of the spacecraft model are: attitudes (LVLH), body rates, RW momentum, RW rates relative to spacecraft, spacecraft position and velocity (ECI), altitude, telescope gimbal angles, and rates. The rigid spacecraft dynamics is in file “Vehi-3B3W.m” is embedded in the rigid Simulink model “RigBody3_Sim.mdl”, shown in Figure (5.1) below.

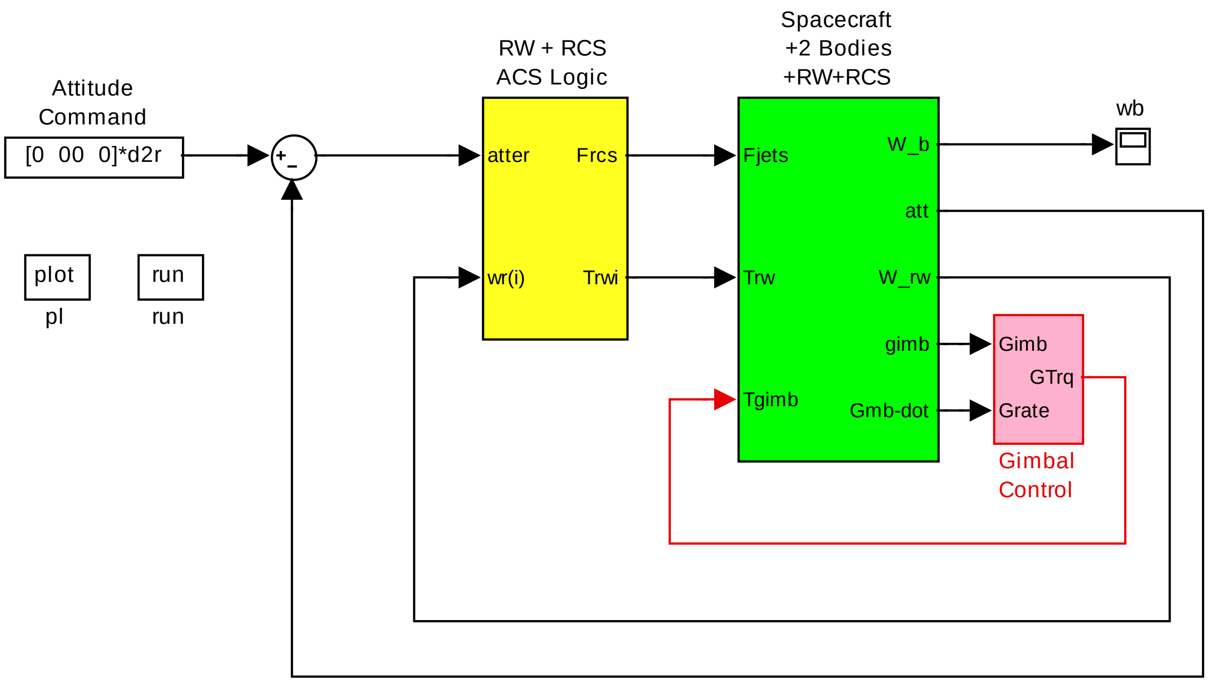

Figure 5.1 3-Rigid-Body 6-dof Simulation model (RigBody3_Sim.mdl)

The attitude control logic (yellow block) is identical to the control system used in section 4 so it will not be discussed here. The green dynamics block is shown expanded below.

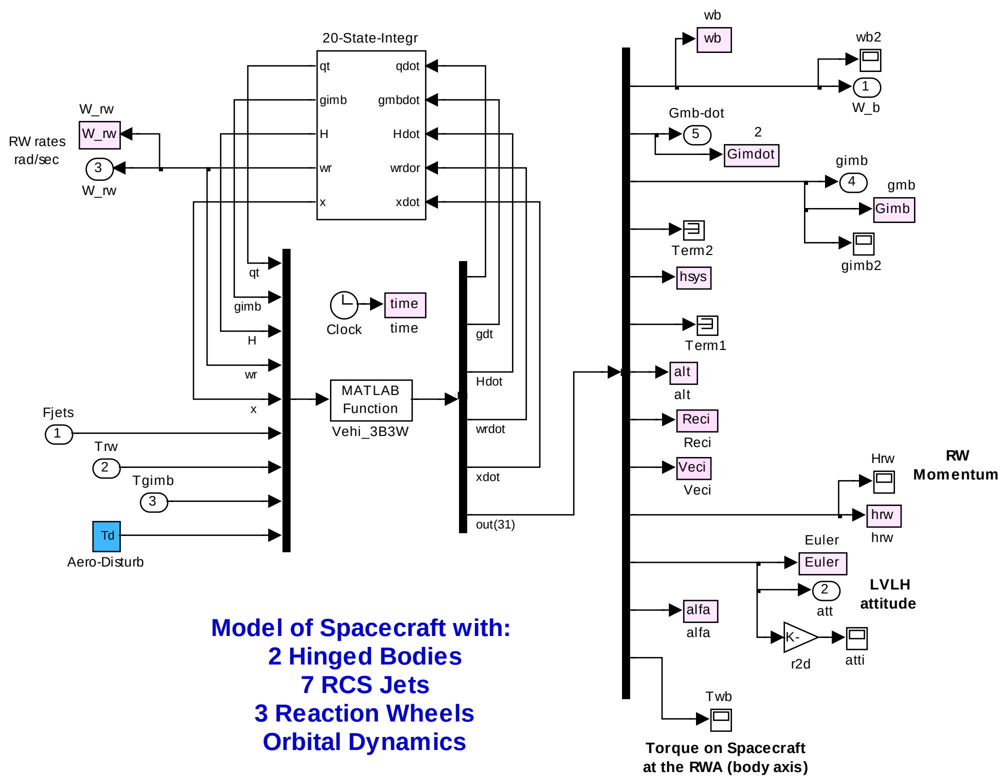

Figure 5.2 Multi-body Spacecraft Model (file: Vehi-3B3W.m)

The gimbal control system is a PD controller, shown in Figure (5.3), designed to rotate the gimbals at the commanded gimbal angles relative to the spacecraft. The gains of gimbal servo system are designed for a 0.25 Hz bandwidth. The telescope system has its own inertial navigation and guidance system independent of the spacecraft in order to guide the telescope LOS. It is not discussed here because it is beyond the scope of this analysis, which is to evaluate stability, performance and LOS sensitivity to disturbances.

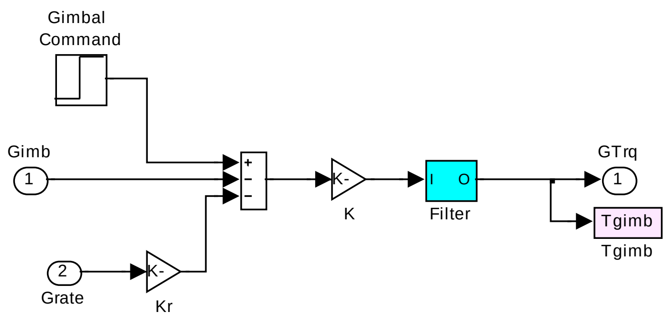

Figure 5.3 Gimbal Control System

5.2 Rigid-Body Analysis

Before analyzing flexibility we must first make sure that the multi-rigid-body dynamic model behavior is acceptable. We will therefore run the above simulation model for a while under the influence of external environmental torques (aero and gravity gradient disturbances) to test that the controls are functioning properly and verify that the model is stable in the time domain and also that the RW momentum desaturation works as expected to re-adjust the RW momentum when it exceeds a certain level (10 ft-lb-sec) from its nominal biased value. Then we can go ahead and combine it with the flex model. Figure (5.4a) shows the spacecraft attitude and rate. A yaw attitude error of 6 (deg) is within the acceptable range. Pitch and roll attitude is controlled more tightly.

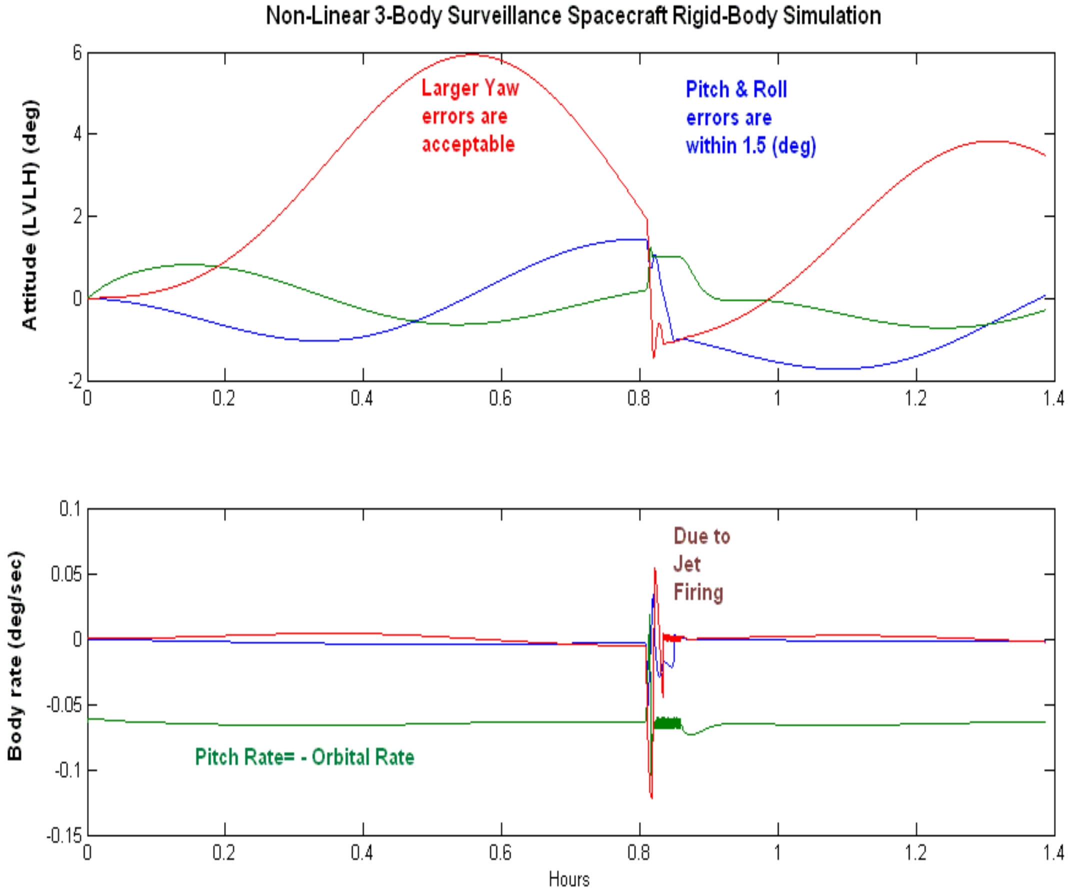

Figure 5.4a Spacecraft Attitude and Rate in presence of Aero and Gravity Gradient torques

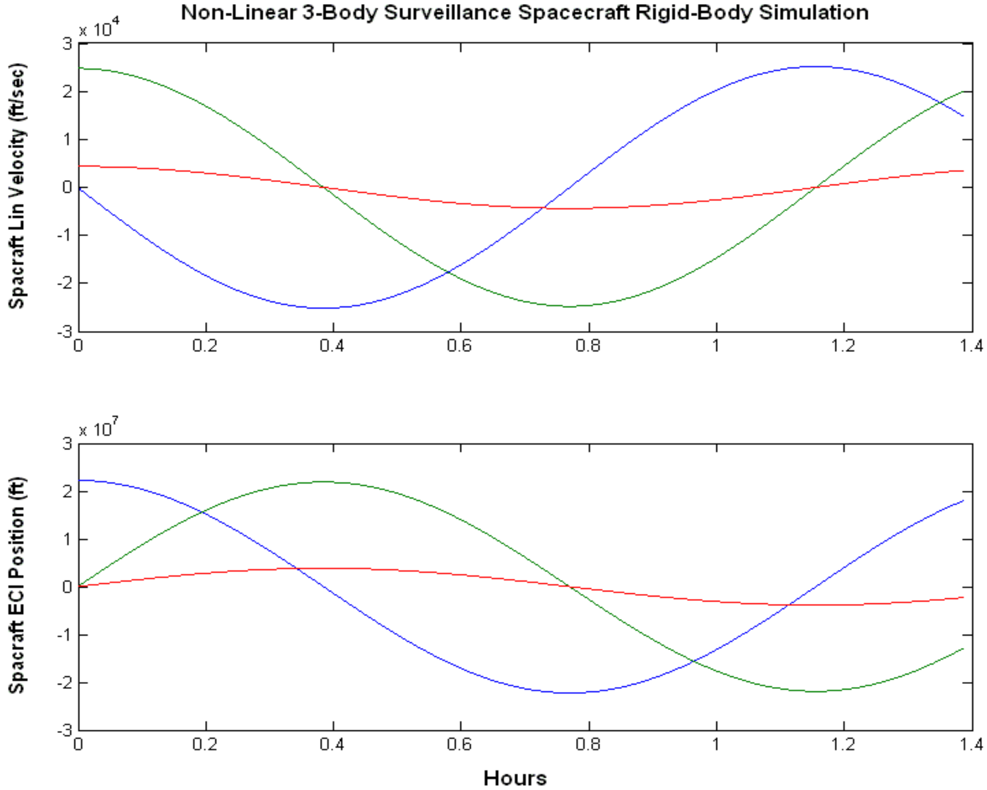

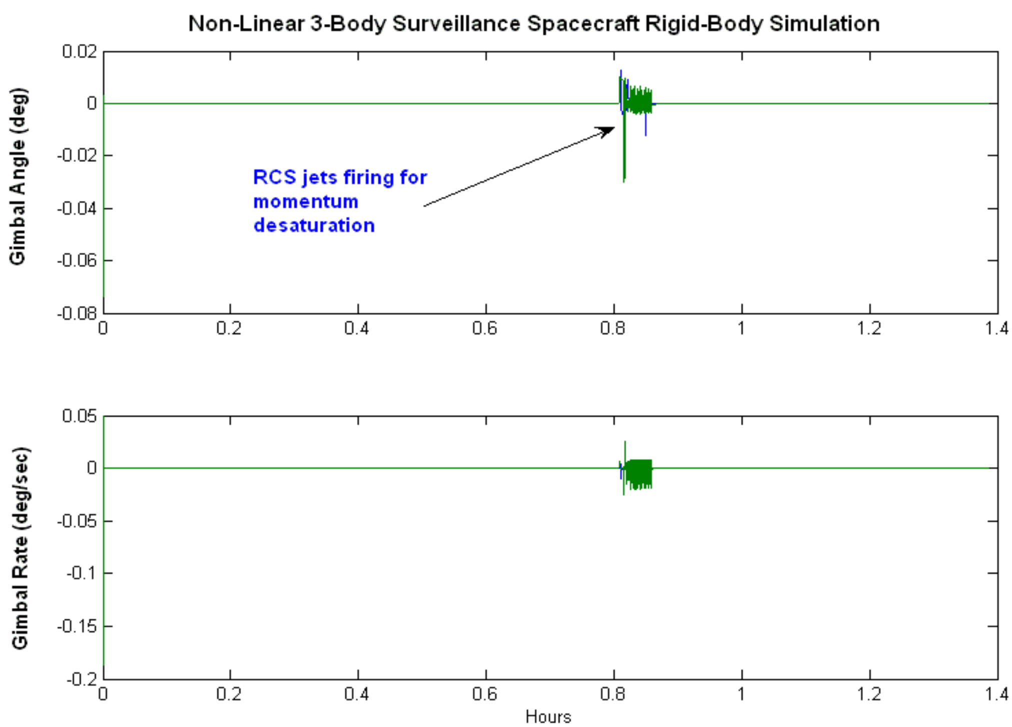

Figure 5.4(c) Jitter at the telescope gimbals due to RCS jets firing

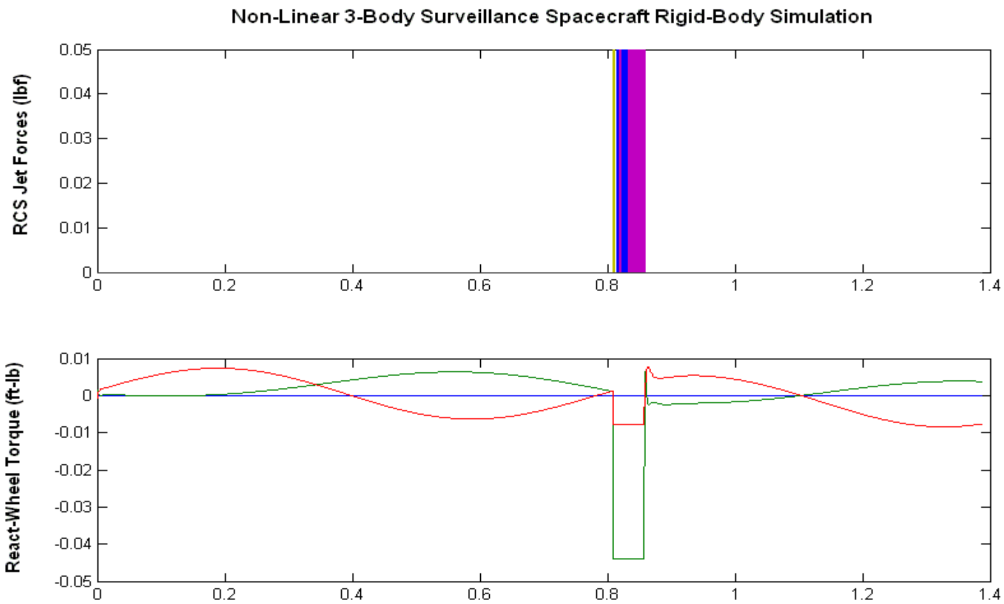

Figure 5.4(d) RW pitch and yaw torques are cycling to balance the aero torques. RCS jets are firing during RW momentum desaturation while the wheels are torqued in the direction to remove excess momentum

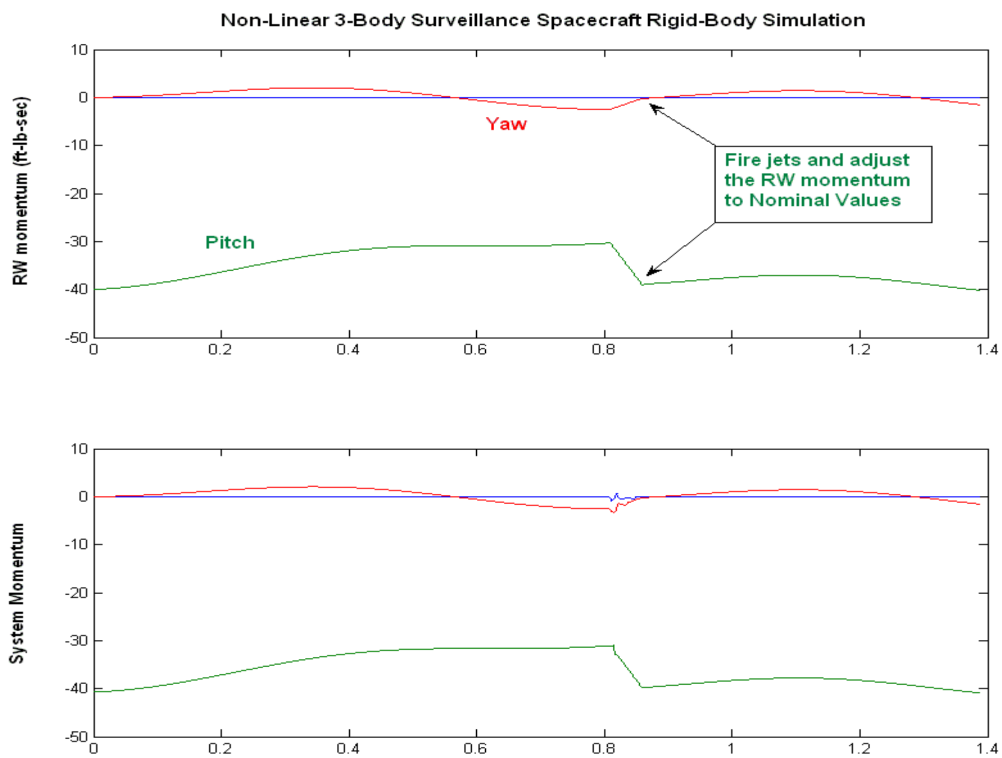

Figure 5.4(e) RW momentum drifts during RW control. Desaturation brings it back near its nominal value

5.3 Flex Multi-Body Simulation Model

The flex multi-body simulation model is in file "*Body3_Flex_Sim.mdl*" in folder "*Examples\Surveillance Satellite React-Wheels\3_Body+Flex_NLSim*". It is very similar to the rigid-body model "*RigBody3_Sim.mdl*", shown in Figure(5.1), except that the spacecraft dynamics block contains the 61-mode flexible model in parallel with the 3-body model, as shown in Figure (5.5). The flex state-space model is loaded from file "*flex61.m*" and was derived in Section 3. It does not include the 6 rigid-body modes (since they are replaced by the multi-body model). The same jet force inputs and gimbal torques are applied to both rigid and flex models. The RW input torques, however, are different. The rigid model requires the wheel control torques about their individual RW axis which comes directly from the control law. The flex model requires the combined RW assembly torque in body axis. This torque also includes the gyroscopic torques due to momentum bias coupling with body rates. It is calculated in the rigid-body model (Twb) and is connected to the equivalent flex model input. The outputs from the two models are combined. Although this model includes also the low frequency orbital dynamics, the flex modes are slowing down the simulation because its sampling period is Ts=0.001 (sec), and we therefore use it only for short periods.

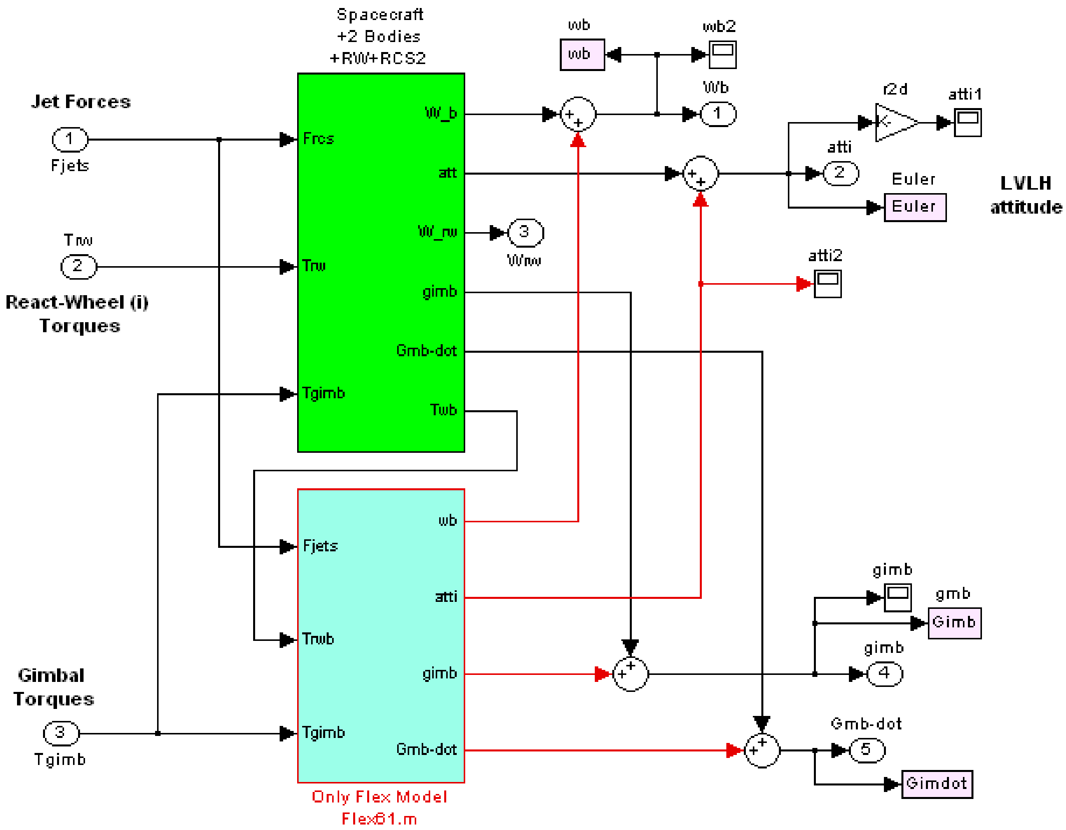

Figure 5.5 Rigid Multi-Body spacecraft dynamics combined in parallel with the 61-mode flex spacecraft model

5.4 Performance of the Gimbals Position Control System

The 3-body flex spacecraft model "*Body3_Flex_Sim.mdl*" is used here to analyze the spacecraft response to 5 (deg) gimbal commands at both, inner and outer gimbals simultaneously. The gimbal torque reaches a peak value of 0.7 (ft-lb) which causes the reaction wheel torque to saturate. A torque limiter is needed here to soften the impact to the reaction wheel control system, but this is left as an exercise to the reader.

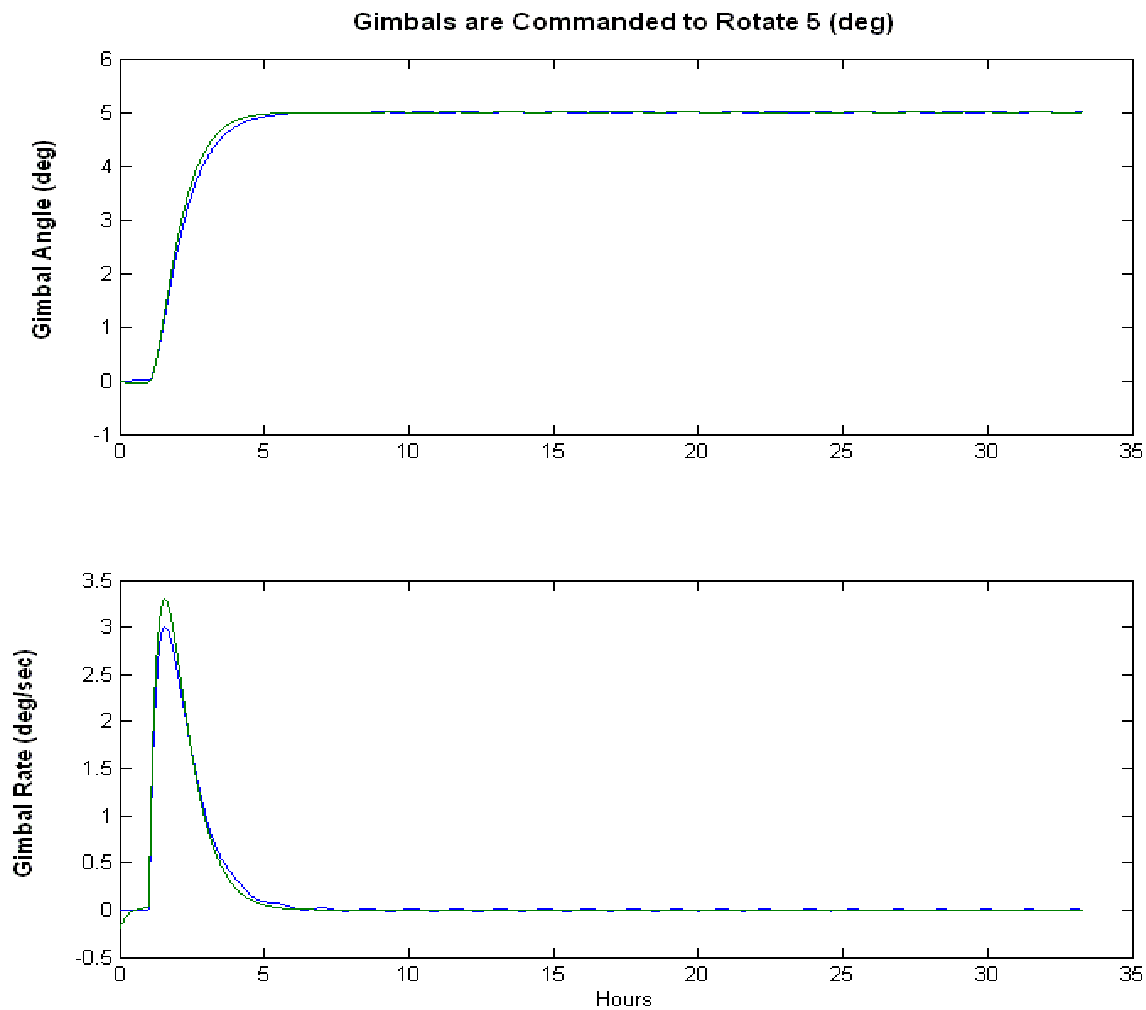

Figure 5.6a Gimbal Responses to a Simultaneous 5 (deg) Azimuth and Elevation Command

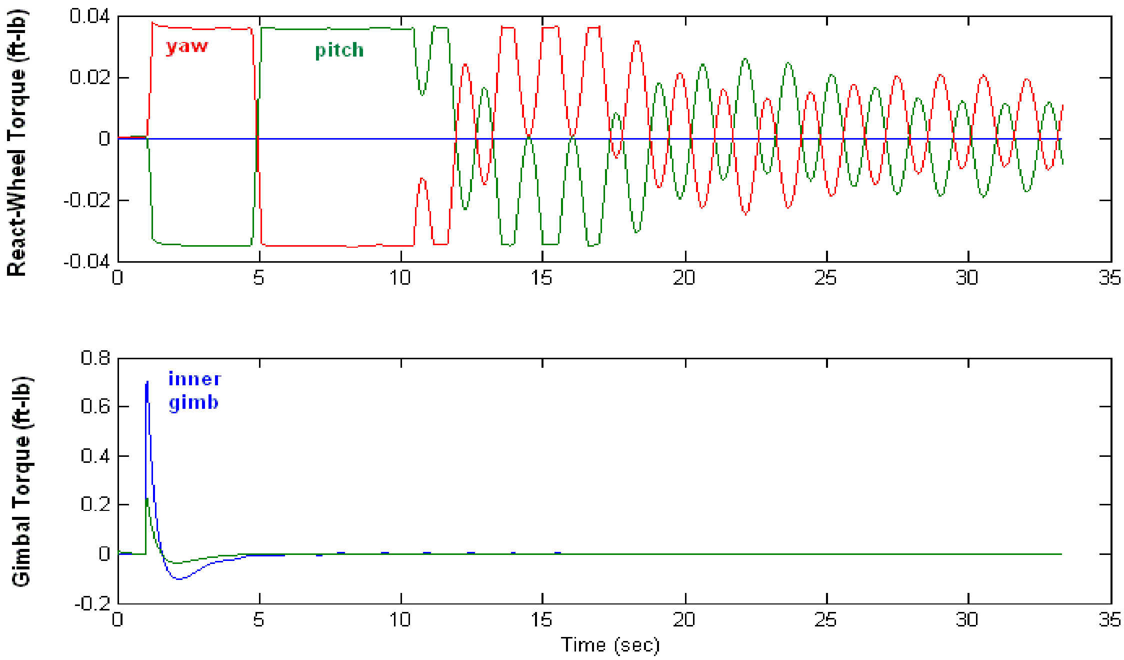

Figure 5.6(b) Gimbaling torques and RW reaction torques

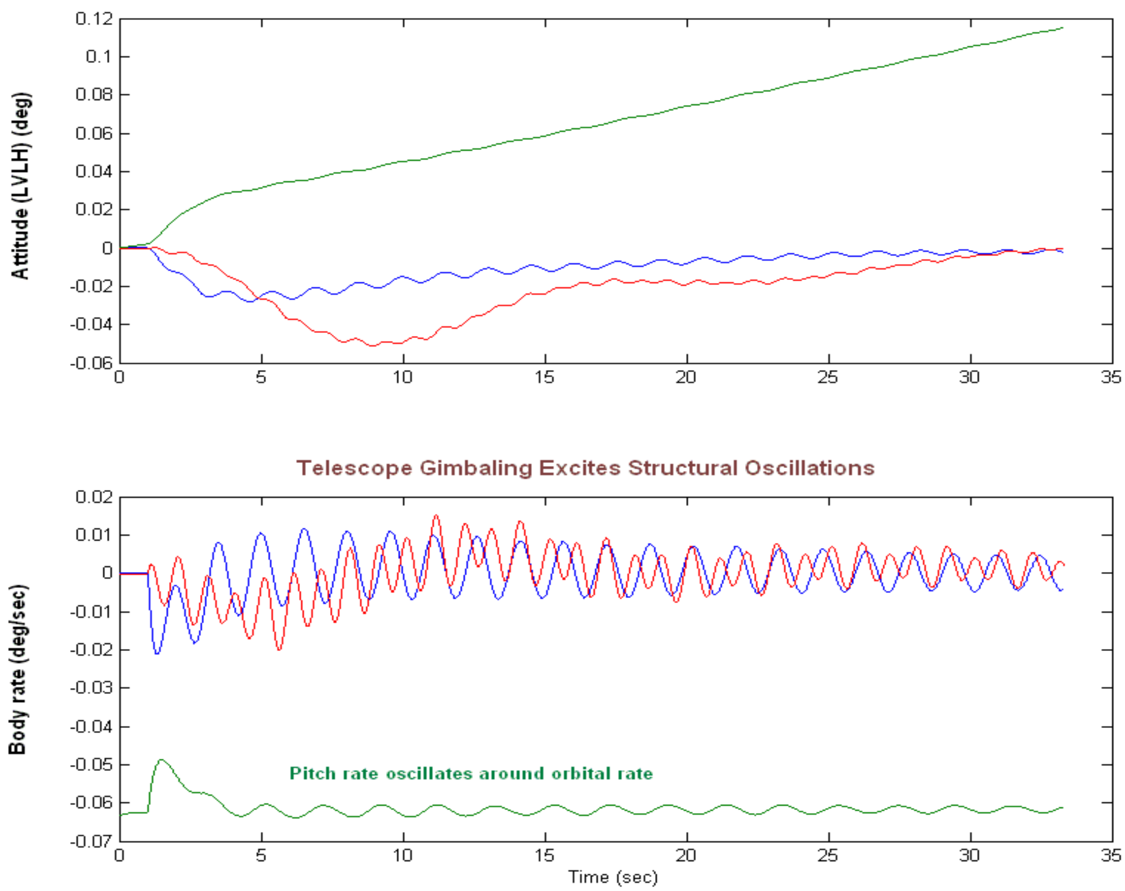

Figure 5.6(c) Effect of Telescope Gimbaling on the Spacecraft Rate

5.5 Stability Analysis of the RW System

Figure (5.7) shows a Simulink model "*Lin_Analysis.mdl*" used for linear frequency domain stability analysis under reaction wheel control. A similar analysis using the Describing Function method can also be performed for the RCS loops but it will not be shown here. The model includes the RW steering logic, the RW controls, and the telescope gimbal loops which are closed. One of the two RW control loops is opened. It is the lateral loop that feeds roll error into yaw RW torque. The pitch loop is closed. This model is used to evaluate stability of the lateral loop by calculating the frequency response across the opened loop. The Matlab script file "liana.m" is used to calculate the Bode and Nichols charts as shown in Figure (5.8). The results look very similar to the results obtained using the previous flex analysis in Figure (x). The biggest difference is at low frequencies near the orbital frequency region because of the additional orbital dynamics included in this model which were not included in the previous model. Figure (5.9) shows a similar plot obtained after modifying Figure (5.7), by closing the lateral loop and opening the pitch loop. Figures (5.10, and 5.11) show similar stability plots for the two gimbals, by opening one gimbal loop and closing all the other loops. It appears that the gimbal loops have plenty of stability margin.

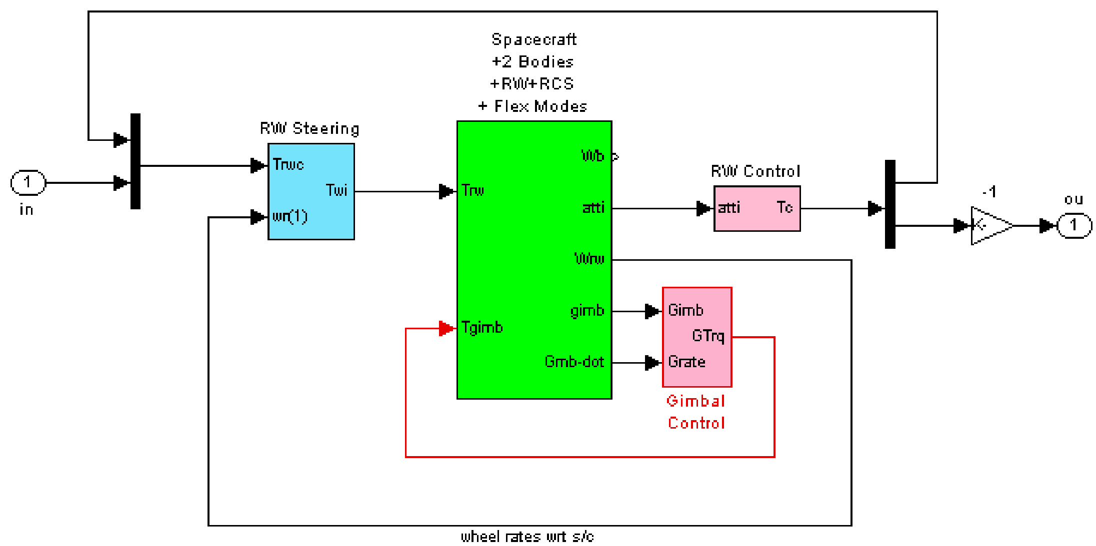

Figure 5.7 Linear Stability Analysis Model (Lin_Analysis.mdl)

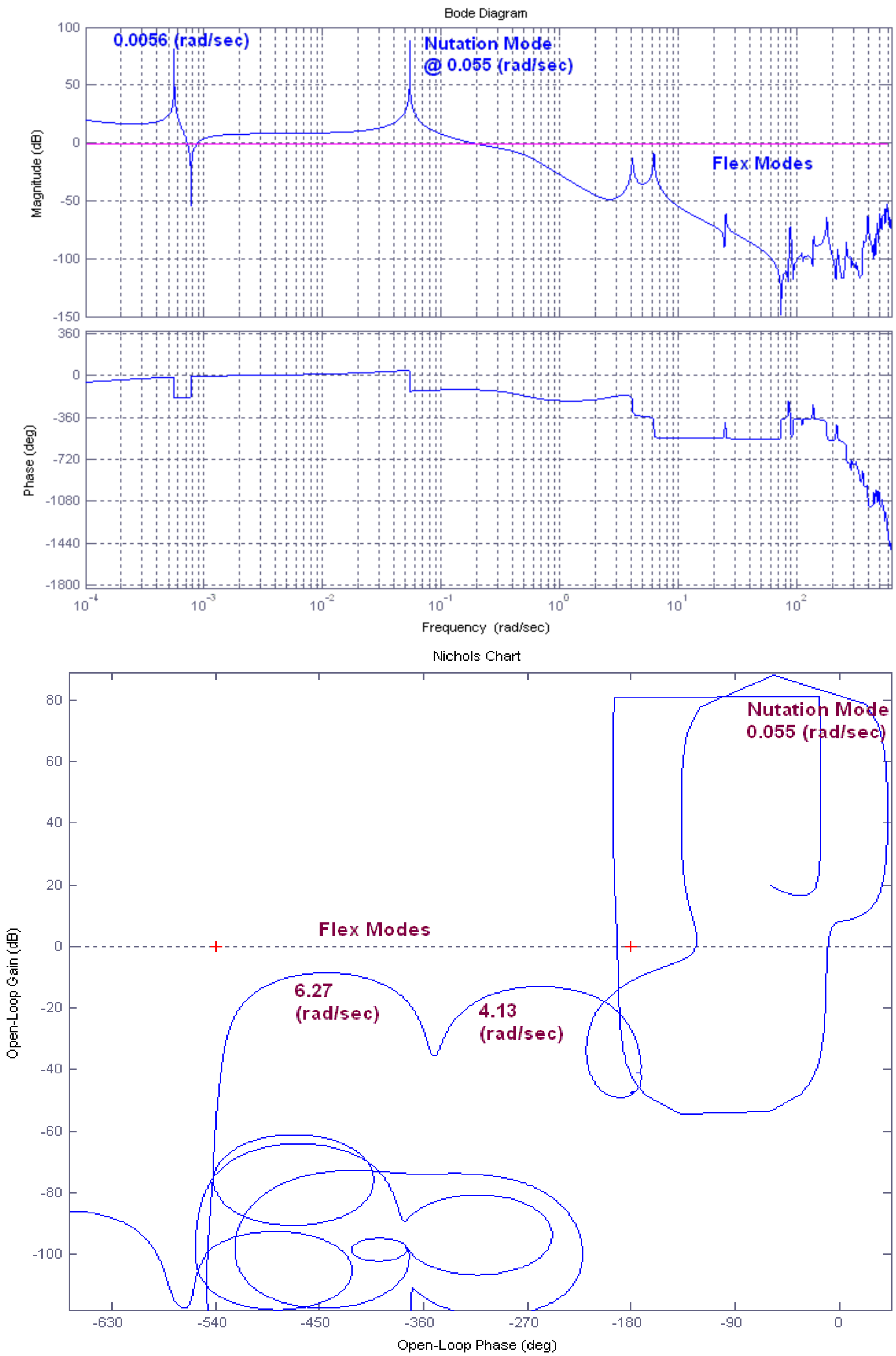

Figure 5.8 Bode and Nichols Plots show the RW system stability in the lateral axis with the pitch loop closed

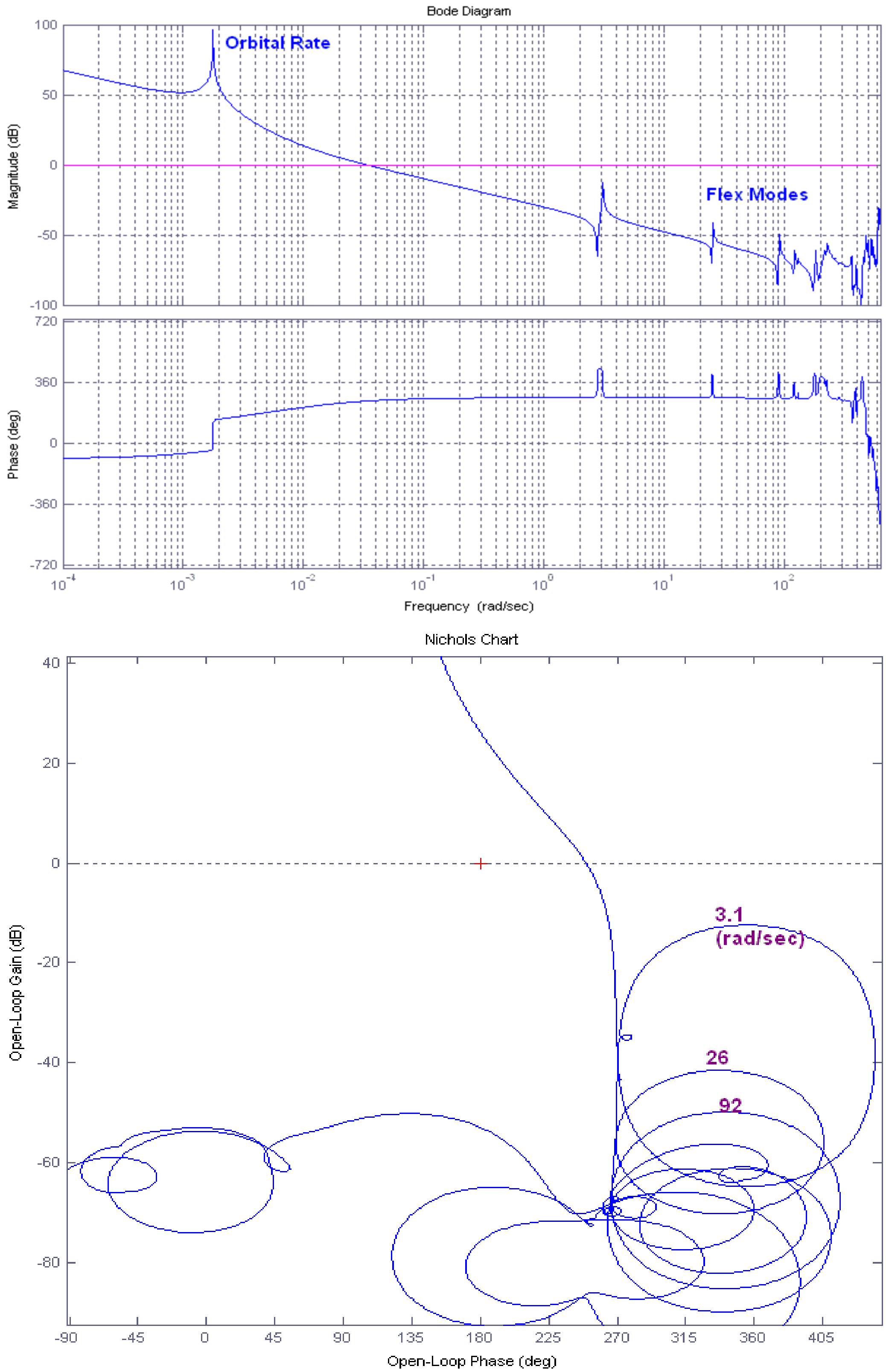

Figure 5.9 Bode and Nichols Plots show the RW system stability in the Pitch axis with the Lateral loop closed

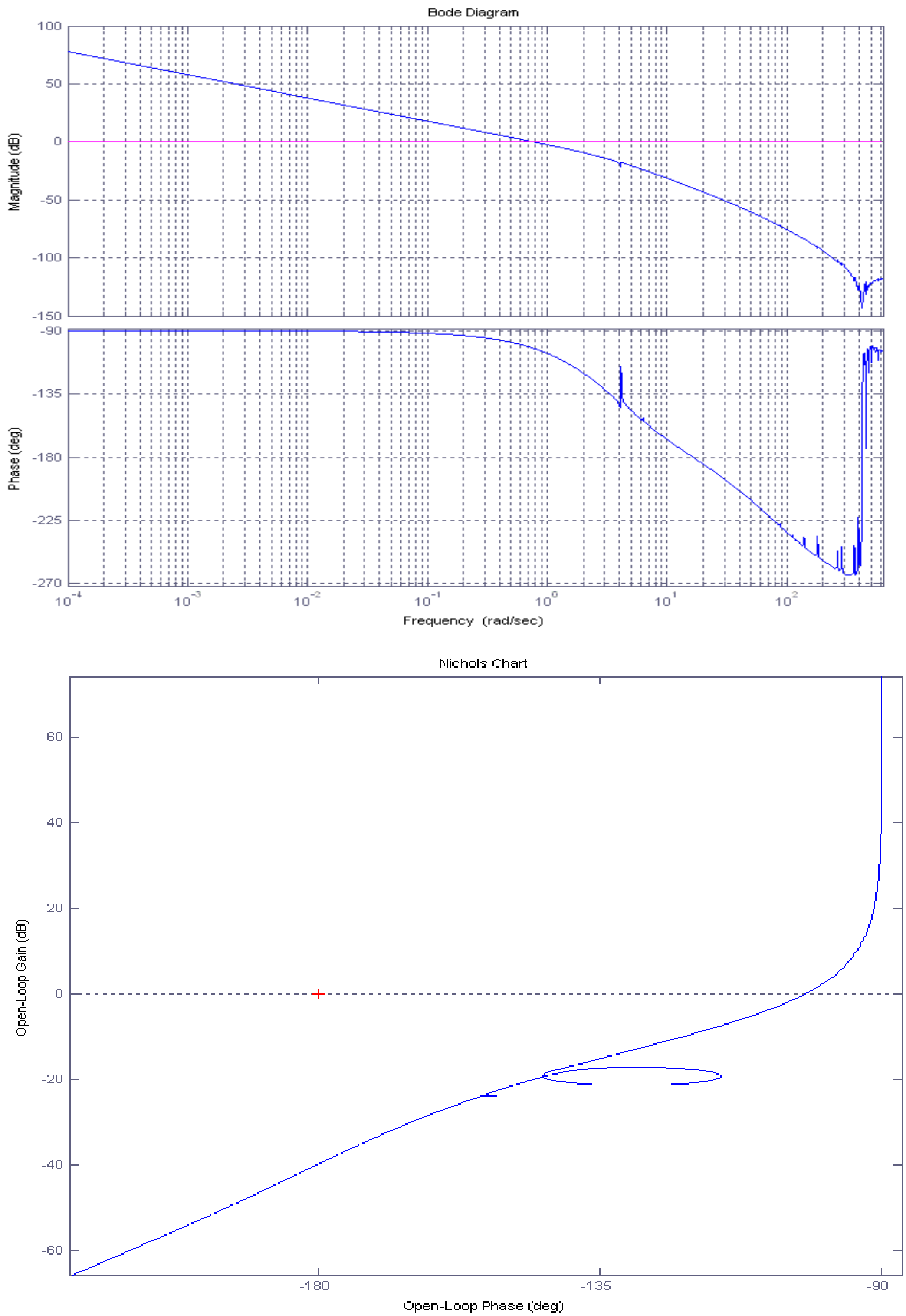

Figure 5.10 Bode and Nichols Plots show the Inner Gimbal system open-loop stability with all other loops closed

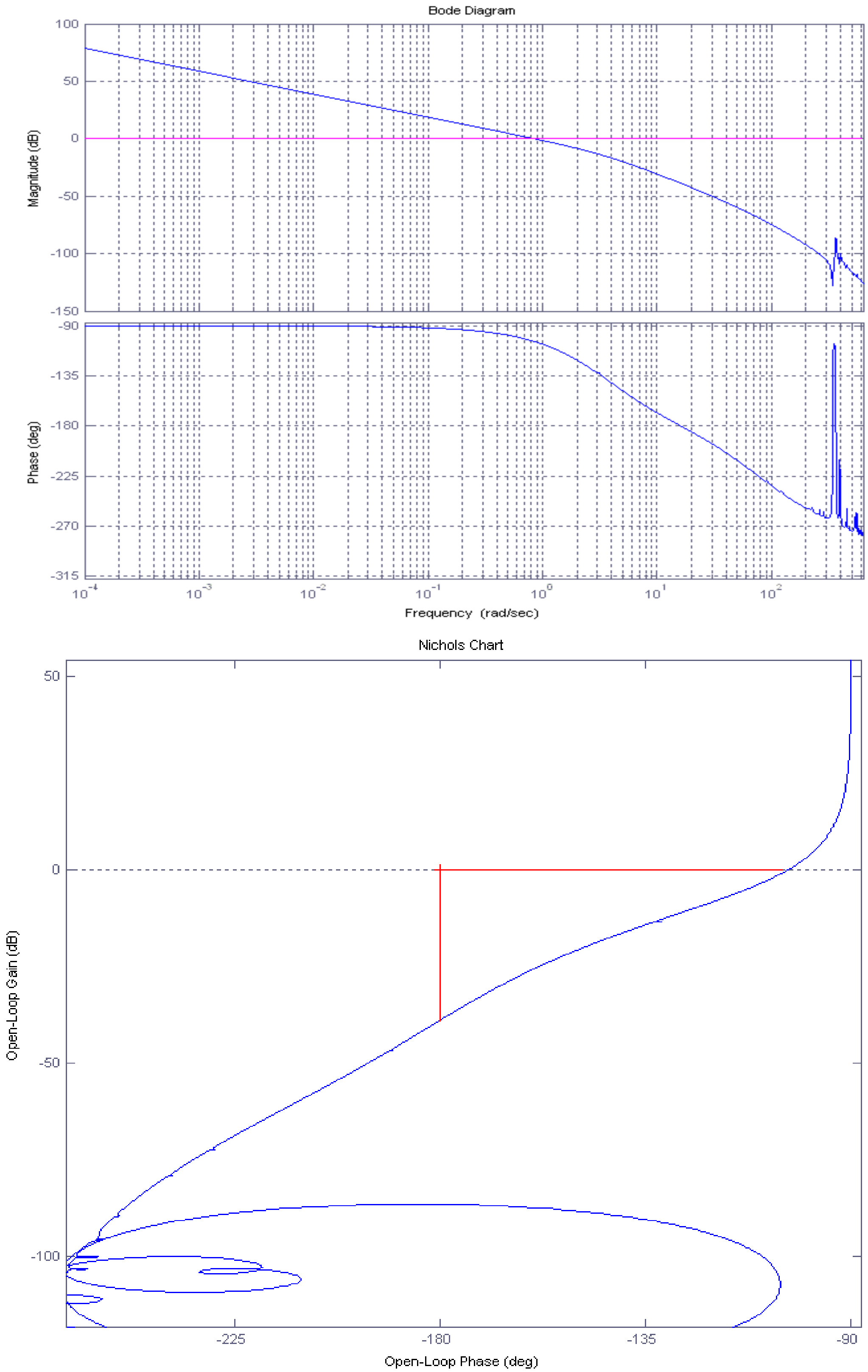

Figure 5.11 Bode and Nichols Plots show the Outer Gimbal system open-loop stability with all other loops closed

5.6 Sensitivity Analysis to Mechanical Disturbances

The spacecraft has several disturbance sources on board causing jitter on the telescope image during RW control. The LOS jitter during jet firing is much bigger and for this reason the telescope is not being used during this short period of time. The main disturbance source is a cryo-cooler, which circulates a coolant fluid around the spacecraft, but there are also disturbances coming from the reaction wheels. Figure (5.12) shows the frequency response characteristics of the combined disturbance torque which can be represented as a transfer function $W_d(s)$.

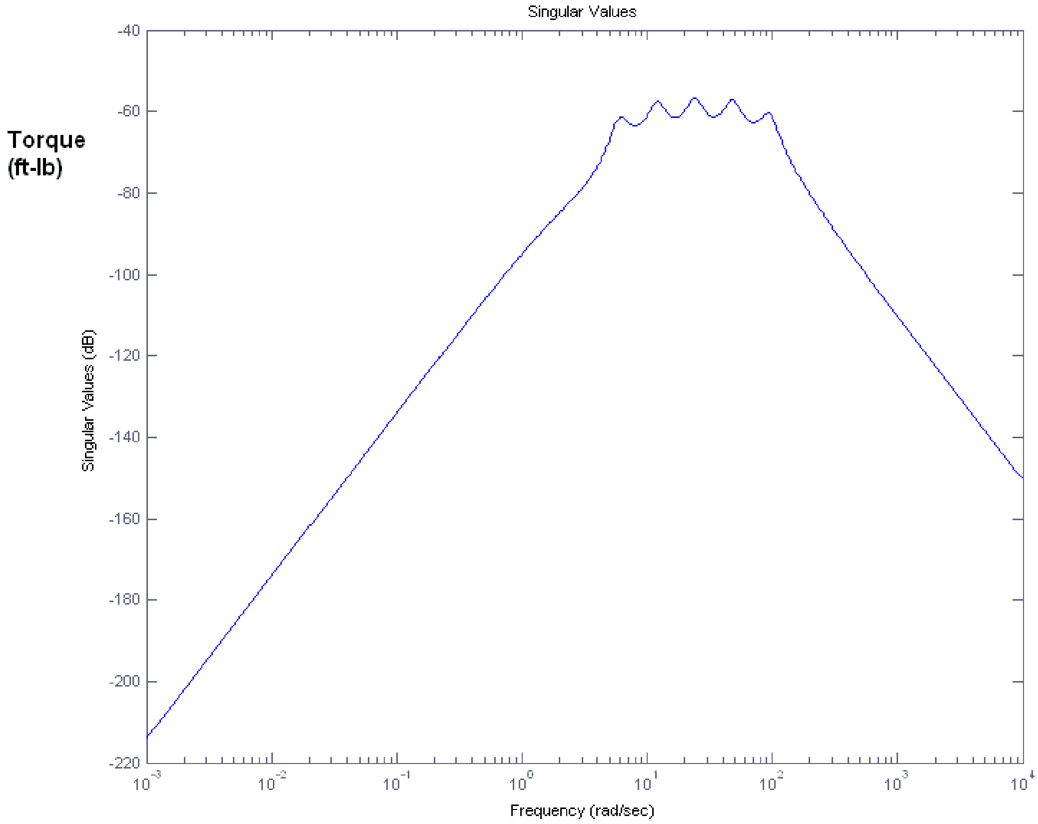

Figure 5.12 Frequency Response Characteristics of the Disturbances $W_d(\omega)$

There is also a requirement that the LOS attitude error should be less than 2 (micro-radians) in the presence of the disturbances. If e_{max} is the maximum allowable line-of-sight error and S(s) is the sensitivity transfer function of the closed-loop spacecraft between the disturbance torque and the telescope gimbal angles, then the equation $W_d(\omega)S(\omega) < e_{\max}$ must be satisfied at all frequencies. The Simulink model "*Sensitiv-Analysis.m*", shown in Figure (5.13), is used to evaluate the system LOS sensitivity to disturbances. Figure (5.14) shows the normalized sensitivity response which was obtained by running the Matlab script file "liana.m". It shows that the sensitivity function is less than 1 at all frequencies meeting the jitter requirement.

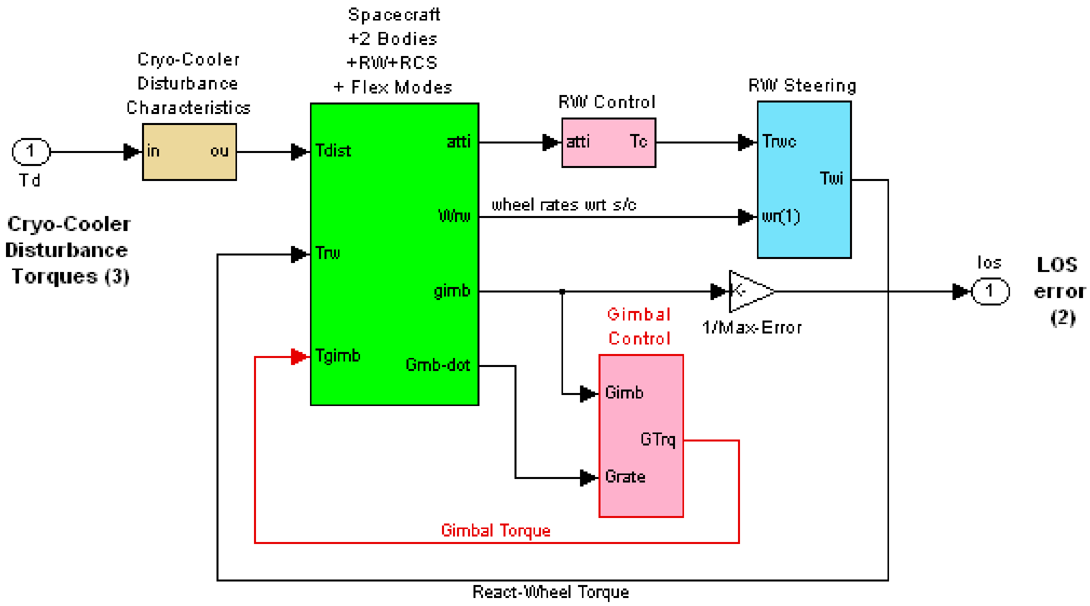

Figure 5.13 Disturbance Sensitivity Analysis Model

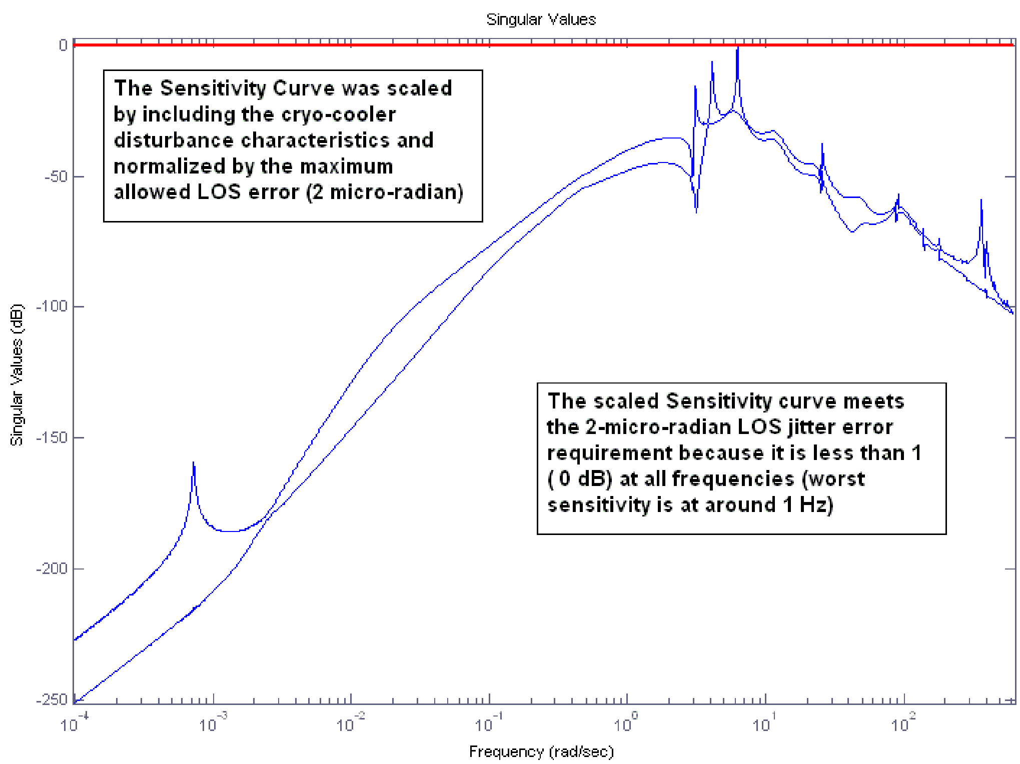

Figure 5.14 Scaled Sensitivity Response between the disturbance torques and the LOS attitude shows that the system barely meets the 2 (micro-radians) requirement.

6 Further Analysis of the Surveillance Spacecraft Using the Flight Vehicle Modeling Program

In this section we will complete the analysis of the surveillance satellite using another modeling approach. This time the spacecraft state-space model is derived using the Flixan Flight Vehicle Modeling Program. This model consists of both: rigid-body and flex dynamics. It includes also the momentum biased wheel, the two reaction wheels, the rotating telescope which is gimbaling in elevation and azimuth, the two solar arrays rotating in pitch, the RCS jet forces, Gravity-Gradient torques, and the LVLH attitude. The input data to the Flixan Flight Vehicle Modeling Program implementing the spacecraft configuration are in file: "*Surv_Sat_RB+Flx.Inp*" in folder "*\Examples\ Surveillance Satellite React-Wheels*". There are three sets of Flight Vehicle data in that file: (a) a rigid-body model, (b) a rigid-body model that includes rotating appendages, and (c) a flexible spacecraft model with the 4 gimbaling appendages. The analysis in this section focuses on the last system, whose title is "*Space Surveillance Satellite with RCS and Reaction Wheels (Gimbals & 60 Flex Modes)*".

If you look in the input data file "*Surv_Sat_RB+Flx.Inp*" below the title and the comment lines, the flag "*LVLH Attitude*" is included. This turns on the Gravity Gradient torques (internally) and the LVLH attitude dynamics. The vehicle pitch rate is set to be equal to the orbital rate which is ω_o= -0.064744 (deg/sec). There are 7 jets which are defined as "Throttling" because their thrust varies from zero to 0.05 (lb). Actually it is either zero or max thrust, being turned on and off by the jet control logic. There are 3 external disturbance torques about x, y, and z, which are used to apply the aerodynamic disturbances on the spacecraft. The spacecraft is also defined to have 3 reaction wheels. The first one is actually a momentum wheel because it has a constant negative rate of -4774 (rpm) and its spin axis is in the y direction which provides pitch momentum biasing on the spacecraft. The other two reaction wheels are tilted in the y-z plane to provide pitch and yaw torques. None of the wheels has a roll momentum component. They all have the same moment of inertia about their spin axes, 0.08 (slug-ft^2). The spacecraft is also defined to have 13 rotational sensors, 3 rate-gyros and 10 attitude measurements, and two accelerometers along the x and y axes.

Near the end of the vehicle data set there is a line that specifies the H-parameters filename "*Surveillance-Sat.Hpr*". This file defines the dynamic coupling between the spacecraft flexibility and the gimbaling bodies, and it was also used to develop the spacecraft models in Section 3. It contains the (100x4) H-parameters matrix, the gimbaling appendages moments of inertia matrix (slug-ft^2), the masses (slugs), the hinge direction unit vectors in spacecraft body, the locations of the 4 hinges in (ft), and the CG locations of the 4 appendages in (ft) in spacecraft coordinates. Some of the data in the (Hpr) file were not used in Section 3 but they are needed here. If the H-parameters filename line is missing from the input data file or if the program cannot locate the (Hpr) file with the coupling coefficients, it will assume that there are no gimbaling bodies and the state variables associated with the gimbaling appendages will be excluded from the state-space model. The last two lines in the vehicle data set specify that 60 flex modes will be included in the model, and that the flex modes will be read from the modal data set "*Space Surveillance Satellite with RCS and Reaction Wheels (60 Flex Pre-Selected Modes)*", which is also located in file "*Surv_Sat_RB+Flx.Inp*".

The selected modal data is an already processed set of data located in the same input file. There may be more than one set of selected modes in the same input data file. They were extracted from the original modal data file "*Surveillance-Sat.Mod*" by means of a mode selection process that is described in Section 6.1. The modal data set in this case consists of 60 pre-selected modes. Each mode consists of mode frequencies and shapes at key vehicle locations, like the RCS jets, the reaction wheels, the disturbance locations, and the gyro and accelerometer sensors.

6.1 Mode Selection Process

Before we select the bending modes we assume that the spacecraft vehicle data is already saved in file "*Surv_Sat_RB+Flx.Inp*" because the mode selection program needs to identify the vehicle effectors and sensors. The data files for this analysis are in directory "*…\Flixan\Examples\Surveillance Satellite React-Wheels*" and the Matlab analysis is performed in subdirectory "*\Linear Flex Anal FV*". The file that contains the finite element structural modes for the Satellite is "*Surveillance-Sat.Mod*". It contains the mode shapes and slopes for the first 100 modes, at 28 locations (also known as nodes). This file is formatted to be recognizable by the mode selection program. The modal data file contains frames of data for every mode frequency. Each frame consists of the mode frequency in (rad/sec), the modal damping coefficient (they are originally all set to ζ=0.005 but they can be modified as needed), the generalized mass (all set to 12), followed by the mode shapes and slopes at the 28 vehicle locations (translations along x, y, z, and rotations about x, y, z). The locations which are important for flight control analysis are the RCS jets, the RW locations, the external disturbance torque, and the sensors. The locations (nodes) in the modal data file are listed in the map file "*Surveillance-Sat.Nod*". This file contains a description for each node, the node numbers (in this case 1 to 28), a node identification number (which is a node number created in the FEM), and the node location in vehicle coordinates (this is only for reference and it is not used by the program). To execute the mode selection program you must first start the Flixan program and select the folder "*…\Examples\ Surveillance Satellite React-Wheels*", as shown on the right. The mode selection program is under the "*Flight Vehicle Model Options*" group.

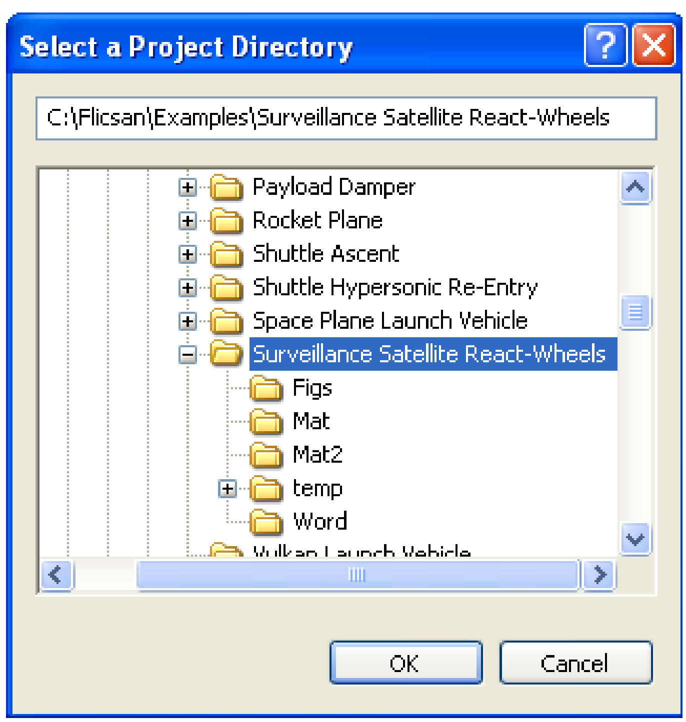

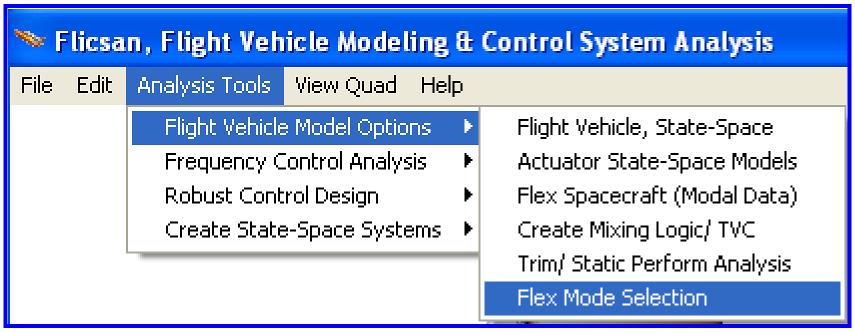

It starts with a small filenames menu where the user selects the modal data filename which must have an extension (.Mod), the nodes file (.Nod), the flight vehicle input data file (.Inp), and an output filename (Modsel.Msl), as shown below. This is where the program will save the relative mode strength at the completion of mode selection. The modal data and nodes map files are the same ones that were used in Section (3).

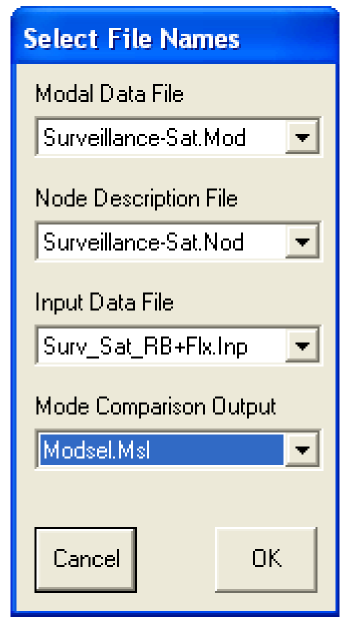

After selecting the filenames the next step is to locate the flight vehicle input data set in file "*Surv_Sat_RB+Flx.Inp*". This data set is normally used to define and create the vehicle state-space model, but it is also used by the mode selection program because the program needs info regarding the RCS jets, the reaction wheels, the disturbance torques, the gyros and accelerometers, which are defined in the input data. From the menu below select the title "*Space Surveillance Satellite with RCS and Reaction Wheels (Gimbals & 60 Flex Modes)*" and click the "*Run Input Set*" button.

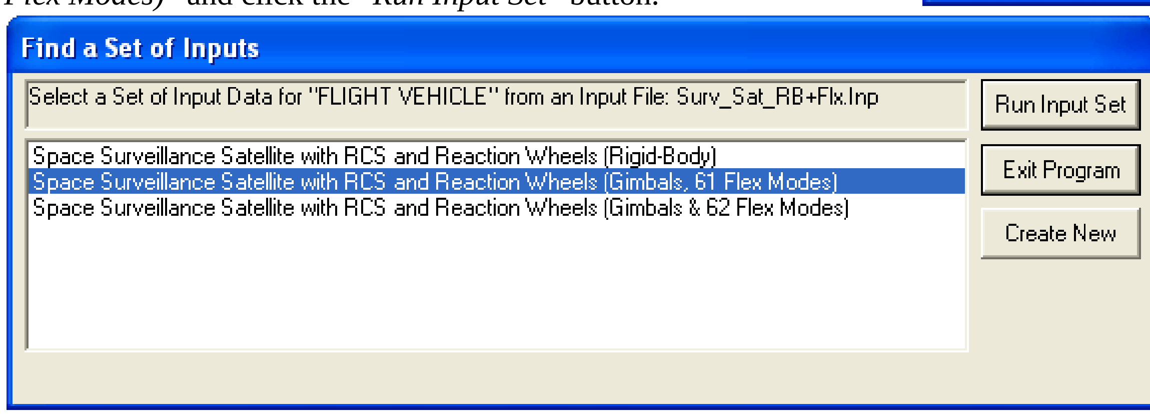

The dialog below is used to define the number of excitation, and the number of sensor points to be used for mode selection. This does not have to be equal to the number of actual vehicle effectors and sensors used in the model. It is only for mode selection purposes. We must also define the range of modes to be evaluated (1 to 100 modes in this case). We will not select, however, the first 6 modes because they are rigid body modes and we should only include structural modes in the flex mode set. We must enter the number of forces excitations (1 force in this case), the number of torque excitations (1 torque locations in this case), and three rotational sensors for gyros. No translational sensors. These locations are only for mode selection. We will also select the graphic mode selection option where the user selects the modes from a bar chart using the mouse. The number of modes to be selected does not apply in this case. We click “OK” to continue.

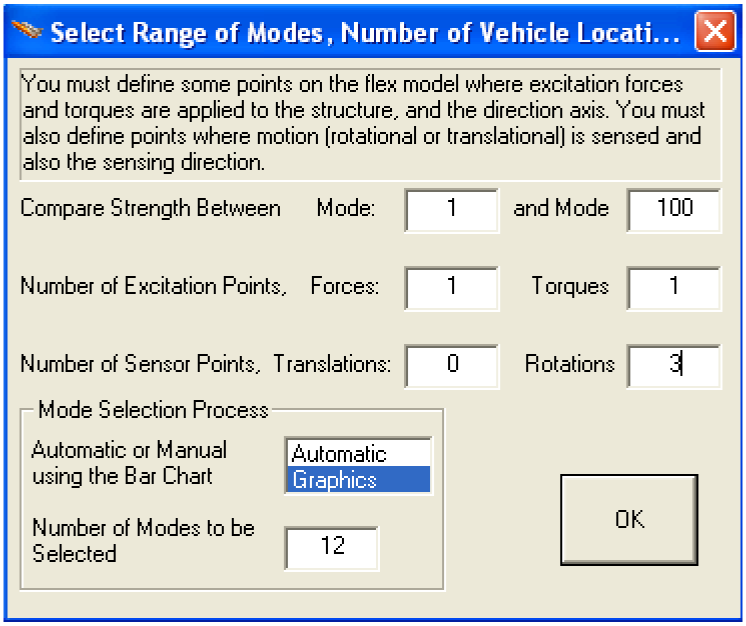

The purpose of the following dialog is in case there is a need to convert the units of the modal data or to modify the direction of the coordinate axes of the finite elements model to match the rigid-body analysis model. In this case the units and directions are the same in both models. There is no need to scale the modal data, and the answer is “No”.

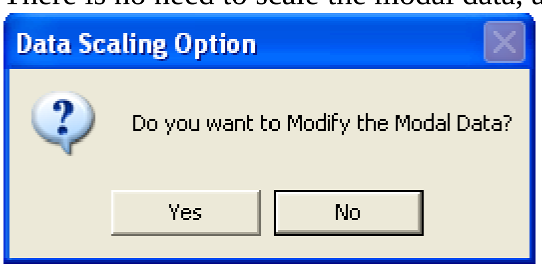

The next step is to identify the nodes for the 1 force excitation and the 1 torque excitation points. The nodes map, which is the file “*Surveillance-Sat.Nod*” is used by the mode selection program to assist the user identifying the excitation and sensor nodes in the modal data file by means of menus. The first RCS jet in node #21 is selected to apply the force excitation in the +y direction. We also define the 1 torque excitation point to be the cooler disturbance pump, node #8, in the +roll direction. Remember, that these locations are only for mode selection purposes. At this point they are arbitrary because we are planning to select the same modes as we selected in Section 3. Next, we select 3 locations to define the 3 rotational measurements for mode selection. All 3 are in the same location, the Inertial Attitude Sensors, node #6 (31001), selected 3 times in +roll, +pitch, and +yaw directions.

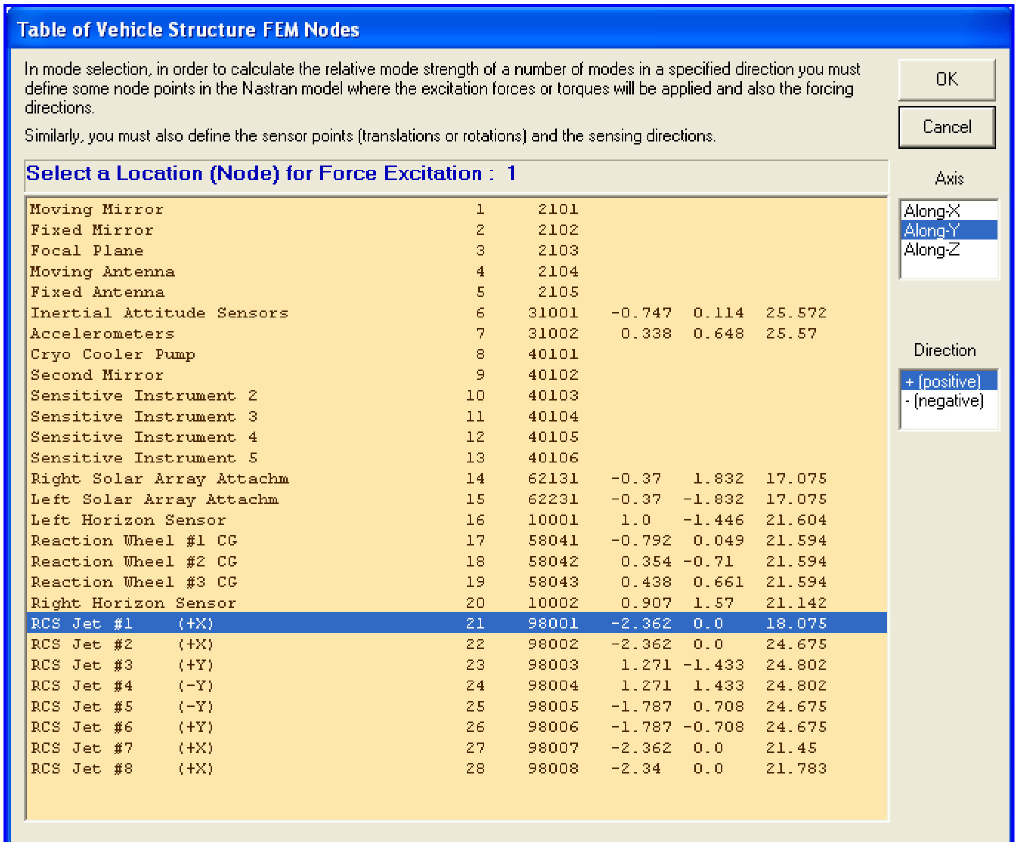

Table of Vehicle Structure FEM Nodes

In mode selection, in order to calculate the relative mode strength of a number of modes in a specified direction you must define some node points in the Nastran model where the excitation forces or torques will be applied and also the forcing directions.

Similarly, you must also define the sensor points (translations or rotations) and the sensing directions.

OK

Cancel

Select a Location (Node) for Force Excitation : 1

Moving Mirror	1	2101			
Fixed Mirror	2	2102			
Focal Plane	3	2103			
Moving Antenna	4	2104			
Fixed Antenna	5	2105			
Inertial Attitude Sensors	6	31001	-0.747	0.114	25.572
Accelerometers	7	31002	0.338	0.648	25.57
Cryo Cooler Pump	8	40101			
Second Mirror	9	40102			
Sensitive Instrument 2	10	40103			
Sensitive Instrument 3	11	40104			
Sensitive Instrument 4	12	40105			
Sensitive Instrument 5	13	40106			
Right Solar Array Attachm	14	62131	-0.37	1.832	17.075
Left Solar Array Attachm	15	62231	-0.37	-1.832	17.075
Left Horizon Sensor	16	10001	1.0	-1.446	21.604
Reaction Wheel #1 CG	17	58041	-0.792	0.049	21.594
Reaction Wheel #2 CG	18	58042	0.354	-0.71	21.594
Reaction Wheel #3 CG	19	58043	0.438	0.661	21.594
Right Horizon Sensor	20	10002	0.907	1.57	21.142
RCS Jet #1 (+X)	21	98001	-2.362	0.0	18.075
RCS Jet #2 (+X)	22	98002	-2.362	0.0	24.675
RCS Jet #3 (+Y)	23	98003	1.271	-1.433	24.802
RCS Jet #4 (-Y)	24	98004	1.271	1.433	24.802
RCS Jet #5 (-Y)	25	98005	-1.787	0.708	24.675
RCS Jet #6 (+Y)	26	98006	-1.787	-0.708	24.675
RCS Jet #7 (+X)	27	98007	-2.362	0.0	21.45
RCS Jet #8 (+X)	28	98008	-2.34	0.0	21.783

Axis

Along-X
Along-Y
Along-Z

Direction

+ (positive)
- (negative)

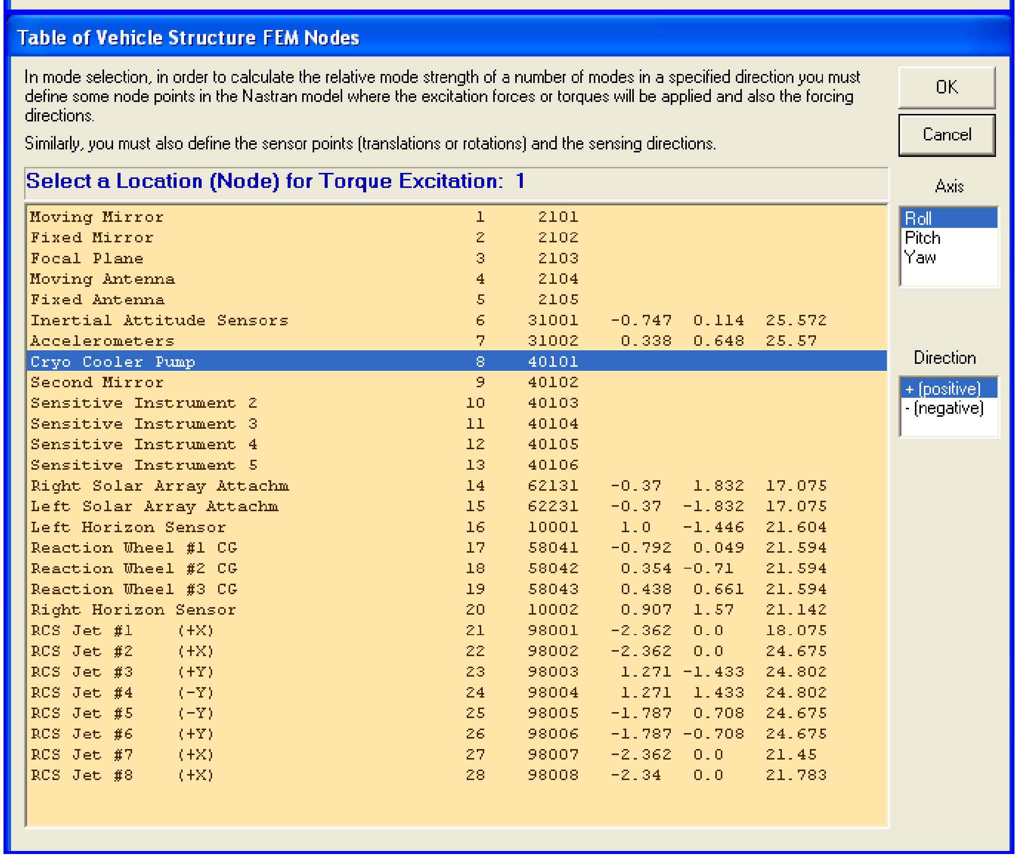

Table of Vehicle Structure FEM Nodes

In mode selection, in order to calculate the relative mode strength of a number of modes in a specified direction you must define some node points in the Nastran model where the excitation forces or torques will be applied and also the forcing directions.

Similarly, you must also define the sensor points (translations or rotations) and the sensing directions.

OK

Cancel

Select a Location (Node) for Torque Excitation: 1

Moving Mirror	1	2101			
Fixed Mirror	2	2102			
Focal Plane	3	2103			
Moving Antenna	4	2104			
Fixed Antenna	5	2105			
Inertial Attitude Sensors	6	31001	-0.747	0.114	25.572
Accelerometers	7	31002	0.338	0.648	25.57
Cryo Cooler Pump	8	40101			
Second Mirror	9	40102			
Sensitive Instrument 2	10	40103			
Sensitive Instrument 3	11	40104			
Sensitive Instrument 4	12	40105			
Sensitive Instrument 5	13	40106			
Right Solar Array Attachm	14	62131	-0.37	1.832	17.075
Left Solar Array Attachm	15	62231	-0.37	-1.832	17.075
Left Horizon Sensor	16	10001	1.0	-1.446	21.604
Reaction Wheel #1 CG	17	58041	-0.792	0.049	21.594
Reaction Wheel #2 CG	18	58042	0.354	-0.71	21.594
Reaction Wheel #3 CG	19	58043	0.438	0.661	21.594
Right Horizon Sensor	20	10002	0.907	1.57	21.142
RCS Jet #1 (+X)	21	98001	-2.362	0.0	18.075
RCS Jet #2 (+X)	22	98002	-2.362	0.0	24.675
RCS Jet #3 (+Y)	23	98003	1.271	-1.433	24.802
RCS Jet #4 (-Y)	24	98004	1.271	1.433	24.802
RCS Jet #5 (-Y)	25	98005	-1.787	0.708	24.675
RCS Jet #6 (+Y)	26	98006	-1.787	-0.708	24.675
RCS Jet #7 (+X)	27	98007	-2.362	0.0	21.45
RCS Jet #8 (+X)	28	98008	-2.34	0.0	21.783

Axis

Roll
Pitch
Yaw

Direction

+ (positive)
- (negative)

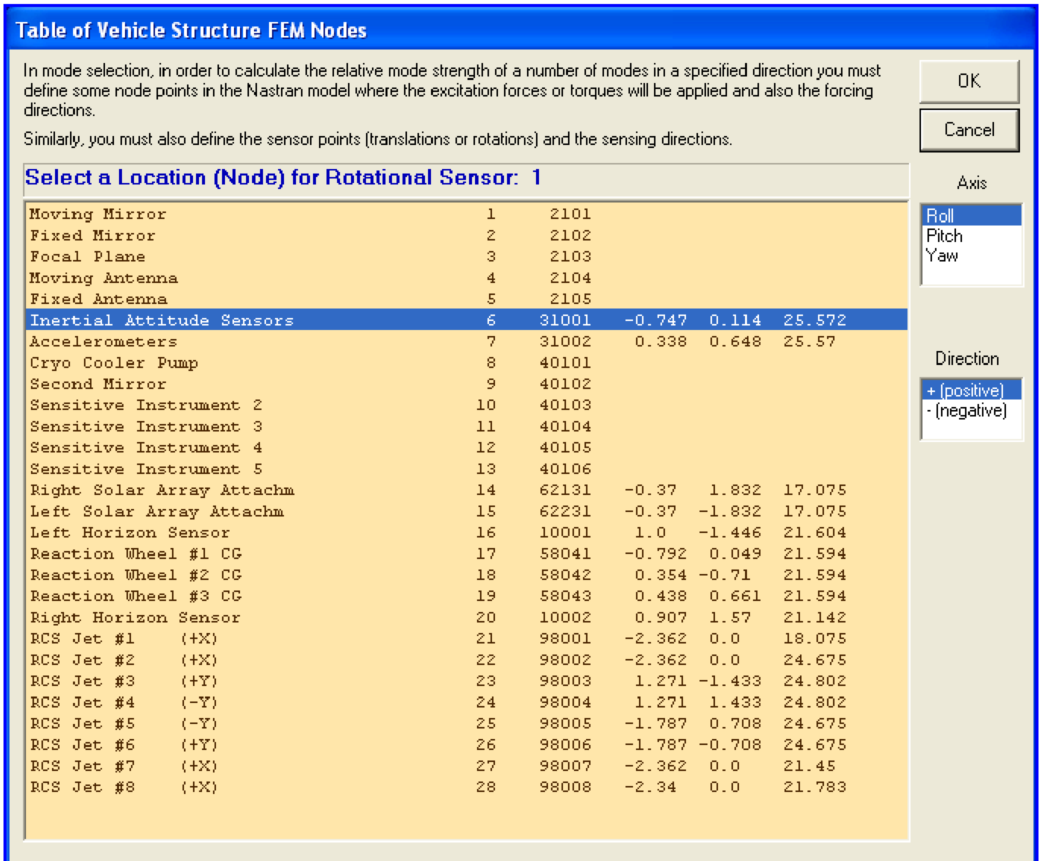
Table of Vehicle Structure FEM Nodes
In mode selection, in order to calculate the relative mode strength of a number of modes in a specified direction you must define some node points in the Nastran model where the excitation forces or torques will be applied and also the forcing directions.
Similarly, you must also define the sensor points (translations or rotations) and the sensing directions.
OK
Cancel
Select a Location (Node) for Rotational Sensor: 1
Axis
Roll
Pitch
Yaw
Direction
+ (positive)
- (negative)
Moving Mirror 1 2101
Fixed Mirror 2 2102
Focal Plane 3 2103
Moving Antenna 4 2104
Fixed Antenna 5 2105
Inertial Attitude Sensors 6 31001 -0.747 0.114 25.572
Accelerometers 7 31002 0.338 0.648 25.57
Cryo Cooler Pump 8 40101
Second Mirror 9 40102
Sensitive Instrument 2 10 40103
Sensitive Instrument 3 11 40104
Sensitive Instrument 4 12 40105
Sensitive Instrument 5 13 40106
Right Solar Array Attachm 14 62131 -0.37 1.832 17.075
Left Solar Array Attachm 15 62231 -0.37 -1.832 17.075
Left Horizon Sensor 16 10001 1.0 -1.446 21.604
Reaction Wheel #1 CG 17 58041 -0.792 0.049 21.594
Reaction Wheel #2 CG 18 58042 0.354 -0.71 21.594
Reaction Wheel #3 CG 19 58043 0.438 0.661 21.594
Right Horizon Sensor 20 10002 0.907 1.57 21.142
RCS Jet #1 (+X) 21 98001 -2.362 0.0 18.075
RCS Jet #2 (+X) 22 98002 -2.362 0.0 24.675
RCS Jet #3 (+Y) 23 98003 1.271 -1.433 24.802
RCS Jet #4 (-Y) 24 98004 1.271 1.433 24.802
RCS Jet #5 (-Y) 25 98005 -1.787 0.708 24.675
RCS Jet #6 (+Y) 26 98006 -1.787 -0.708 24.675
RCS Jet #7 (+X) 27 98007 -2.362 0.0 21.45
RCS Jet #8 (+X) 28 98008 -2.34 0.0 21.783

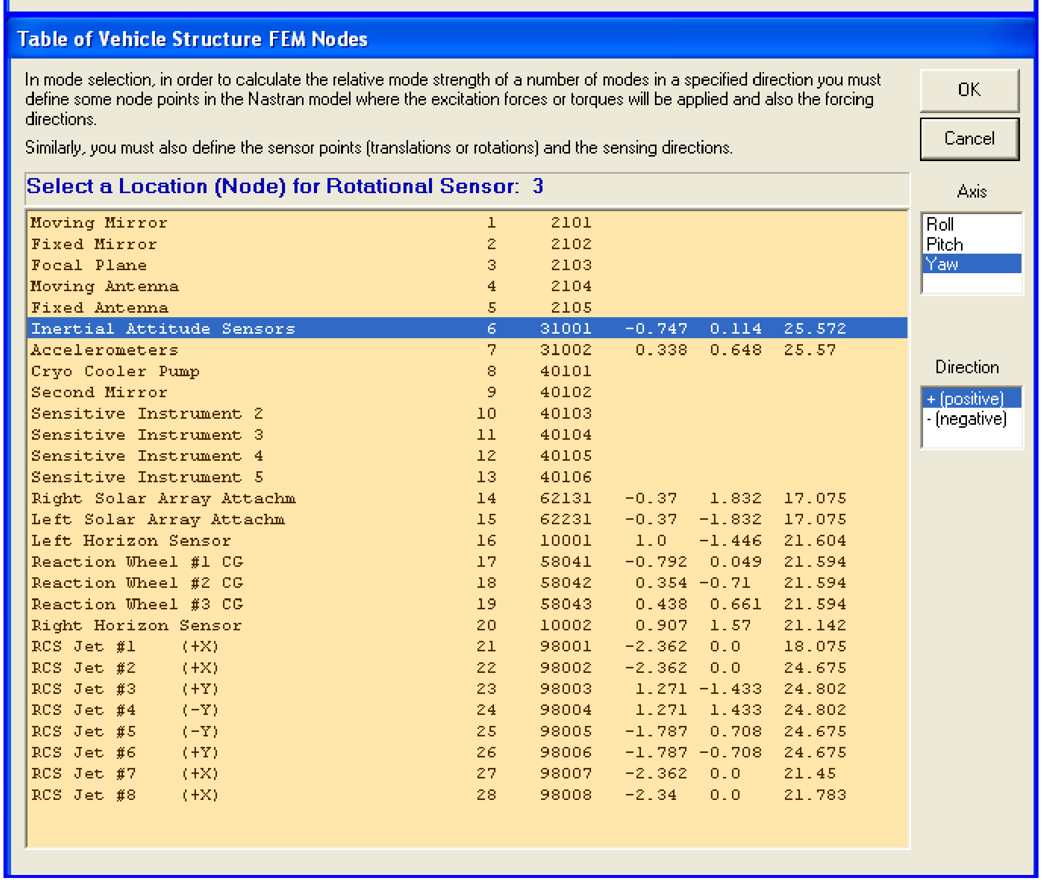
Table of Vehicle Structure FEM Nodes
In mode selection, in order to calculate the relative mode strength of a number of modes in a specified direction you must define some node points in the Nastran model where the excitation forces or torques will be applied and also the forcing directions.
Similarly, you must also define the sensor points (translations or rotations) and the sensing directions.
OK
Cancel
Select a Location (Node) for Rotational Sensor: 3
Axis
Roll
Pitch
Yaw
Direction
+ (positive)
- (negative)
Moving Mirror 1 2101
Fixed Mirror 2 2102
Focal Plane 3 2103
Moving Antenna 4 2104
Fixed Antenna 5 2105
Inertial Attitude Sensors 6 31001 -0.747 0.114 25.572
Accelerometers 7 31002 0.338 0.648 25.57
Cryo Cooler Pump 8 40101
Second Mirror 9 40102
Sensitive Instrument 2 10 40103
Sensitive Instrument 3 11 40104
Sensitive Instrument 4 12 40105
Sensitive Instrument 5 13 40106
Right Solar Array Attachm 14 62131 -0.37 1.832 17.075
Left Solar Array Attachm 15 62231 -0.37 -1.832 17.075
Left Horizon Sensor 16 10001 1.0 -1.446 21.604
Reaction Wheel #1 CG 17 58041 -0.792 0.049 21.594
Reaction Wheel #2 CG 18 58042 0.354 -0.71 21.594
Reaction Wheel #3 CG 19 58043 0.438 0.661 21.594
Right Horizon Sensor 20 10002 0.907 1.57 21.142
RCS Jet #1 (+X) 21 98001 -2.362 0.0 18.075
RCS Jet #2 (+X) 22 98002 -2.362 0.0 24.675
RCS Jet #3 (+Y) 23 98003 1.271 -1.433 24.802
RCS Jet #4 (-Y) 24 98004 1.271 1.433 24.802
RCS Jet #5 (-Y) 25 98005 -1.787 0.708 24.675
RCS Jet #6 (+Y) 26 98006 -1.787 -0.708 24.675
RCS Jet #7 (+X) 27 98007 -2.362 0.0 21.45
RCS Jet #8 (+X) 28 98008 -2.34 0.0 21.783

At this point the excitation and sensor points and directions for the mode selection process have been defined. The modal strength for each mode is determined by the values of the mode shapes at the nodes where the forces and torques are applied, the force direction, and also by the values of the mode shapes at the 3 rotational sensors in the directions measured. High mode shape magnitudes at the excitation and sensor points, at a mode frequency, imply strong contributions from that mode. The mode selection program computes the mode strength at each mode frequency and saves it in file "*Modsel.Msl*".

The mode selection process, however, is not finished yet because the program needs additional info before allowing the user to select by means of a bar-chart which modes to retain from the big modal data file. The program will create a smaller subset of the original modal data set and save it in the input data file "*Surv_Sat_RB+Flx.Inp*". At the end of this process the selected set of modal data will contain only the dominant modes (between the excitation and sensor points defined), and mode shapes only at the locations which are required by the flexible satellite model, such as: the RCS jets, the RW locations, the external disturbances, the attitude control sensors, and other sensitive locations for performance evaluation. The program will display similar menus (in light blue color) that display the nodes map from where the user can identify nodes at the required vehicle locations.

From the following menus the user must identify 7 nodes (#21 to #27) that correspond to the 7 RCS jet locations defined in the input data file "*Surv_Sat_RB+Flx.Inp*". The selection of the first and the 7th jets are shown below. The user must also define 3 locations, node numbers (#17, #18, and #19) for the 3 reaction wheels.

Table of Vehicle Structure FEM Nodes

You must now identify some points on the finite element model that correspond to the important locations on the vehicle (as specified in the vehicle data) where the forces are being applied and the motion is being sensed. Such as TVC gimbals, gyros, etc.

Select a Location (Node) for Thruster Engine : 1 OK

Moving Mirror	1	2101			
Fixed Mirror	2	2102			
Focal Plane	3	2103			
Moving Antenna	4	2104			
Fixed Antenna	5	2105			
Inertial Attitude Sensors	6	31001	-0.747	0.114	25.572
Accelerometers	7	31002	0.338	0.648	25.57
Cryo Cooler Pump	8	40101			
Second Mirror	9	40102			
Sensitive Instrument 2	10	40103			
Sensitive Instrument 3	11	40104			
Sensitive Instrument 4	12	40105			
Sensitive Instrument 5	13	40106			
Right Solar Array Attachm	14	62131	-0.37	1.832	17.075
Left Solar Array Attachm	15	62231	-0.37	-1.832	17.075
Left Horizon Sensor	16	10001	1.0	-1.446	21.604
Reaction Wheel #1 CG	17	58041	-0.792	0.049	21.594
Reaction Wheel #2 CG	18	58042	0.354	-0.71	21.594
Reaction Wheel #3 CG	19	58043	0.438	0.661	21.594
Right Horizon Sensor	20	10002	0.907	1.57	21.142
RCS Jet #1 (+X)	21	98001	-2.362	0.0	18.075
RCS Jet #2 (+X)	22	98002	-2.362	0.0	24.675
RCS Jet #3 (+Y)	23	98003	1.271	-1.433	24.802
RCS Jet #4 (-Y)	24	98004	1.271	1.433	24.802
RCS Jet #5 (-Y)	25	98005	-1.787	0.708	24.675
RCS Jet #6 (+Y)	26	98006	-1.787	-0.708	24.675
RCS Jet #7 (+X)	27	98007	-2.362	0.0	21.45
RCS Jet #8 (+X)	28	98008	-2.34	0.0	21.783

Table of Vehicle Structure FEM Nodes

You must now identify some points on the finite element model that correspond to the important locations on the vehicle (as specified in the vehicle data) where the forces are being applied and the motion is being sensed. Such as TVC gimbals, gyros, etc.

Select a Location (Node) for Thruster Engine : 7 OK

Moving Mirror	1	2101			
Fixed Mirror	2	2102			
Focal Plane	3	2103			
Moving Antenna	4	2104			
Fixed Antenna	5	2105			
Inertial Attitude Sensors	6	31001	-0.747	0.114	25.572
Accelerometers	7	31002	0.338	0.648	25.57
Cryo Cooler Pump	8	40101			
Second Mirror	9	40102			
Sensitive Instrument 2	10	40103			
Sensitive Instrument 3	11	40104			
Sensitive Instrument 4	12	40105			
Sensitive Instrument 5	13	40106			
Right Solar Array Attachm	14	62131	-0.37	1.832	17.075
Left Solar Array Attachm	15	62231	-0.37	-1.832	17.075
Left Horizon Sensor	16	10001	1.0	-1.446	21.604
Reaction Wheel #1 CG	17	58041	-0.792	0.049	21.594
Reaction Wheel #2 CG	18	58042	0.354	-0.71	21.594
Reaction Wheel #3 CG	19	58043	0.438	0.661	21.594
Right Horizon Sensor	20	10002	0.907	1.57	21.142
RCS Jet #1 (+X)	21	98001	-2.362	0.0	18.075
RCS Jet #2 (+X)	22	98002	-2.362	0.0	24.675
RCS Jet #3 (+Y)	23	98003	1.271	-1.433	24.802
RCS Jet #4 (-Y)	24	98004	1.271	1.433	24.802
RCS Jet #5 (-Y)	25	98005	-1.787	0.708	24.675
RCS Jet #6 (+Y)	26	98006	-1.787	-0.708	24.675
RCS Jet #7 (+X)	27	98007	-2.362	0.0	21.45
RCS Jet #8 (+X)	28	98008	-2.34	0.0	21.783

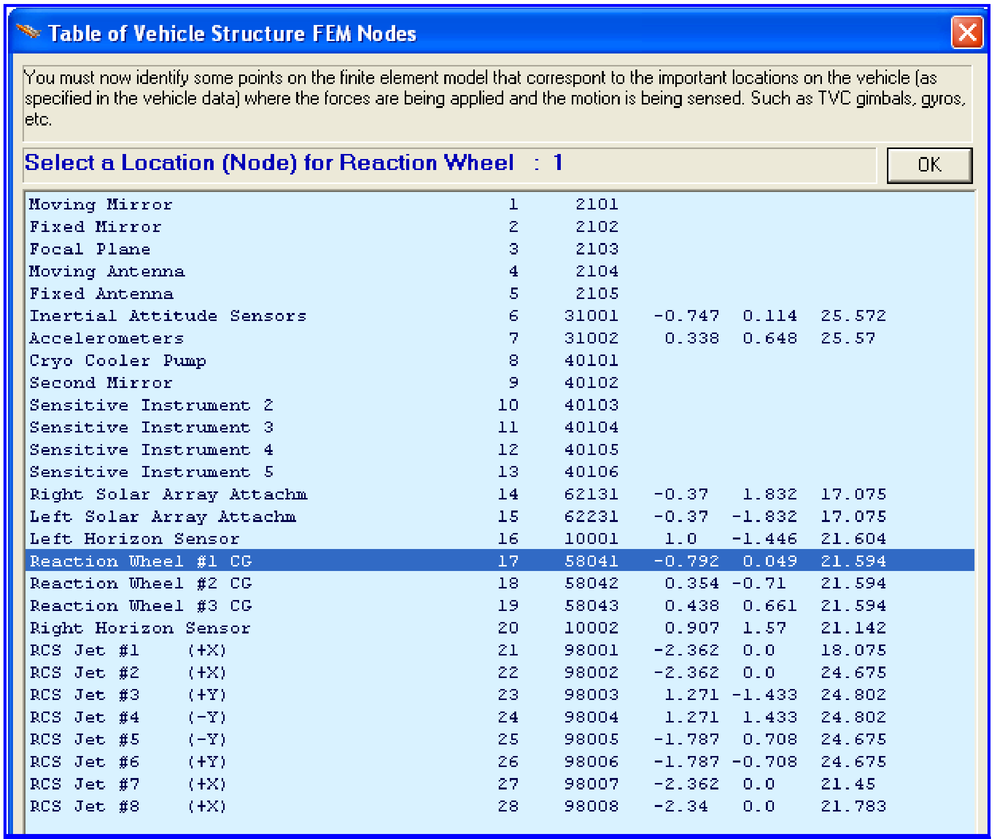

Table of Vehicle Structure FEM Nodes

You must now identify some points on the finite element model that correspont to the important locations on the vehicle (as specified in the vehicle data) where the forces are being applied and the motion is being sensed. Such as TVC gimbals, gyros, etc.

Select a Location (Node) for Reaction Wheel : 1 OK

Moving Mirror	1	2101			
Fixed Mirror	2	2102			
Focal Plane	3	2103			
Moving Antenna	4	2104			
Fixed Antenna	5	2105			
Inertial Attitude Sensors	6	31001	-0.747	0.114	25.572
Accelerometers	7	31002	0.338	0.648	25.57
Cryo Cooler Pump	8	40101			
Second Mirror	9	40102			
Sensitive Instrument 2	10	40103			
Sensitive Instrument 3	11	40104			
Sensitive Instrument 4	12	40105			
Sensitive Instrument 5	13	40106			
Right Solar Array Attachm	14	62131	-0.37	1.832	17.075
Left Solar Array Attachm	15	62231	-0.37	-1.832	17.075
Left Horizon Sensor	16	10001	1.0	-1.446	21.604
Reaction Wheel #1 CG	17	58041	-0.792	0.049	21.594
Reaction Wheel #2 CG	18	58042	0.354	-0.71	21.594
Reaction Wheel #3 CG	19	58043	0.438	0.661	21.594
Right Horizon Sensor	20	10002	0.907	1.57	21.142
RCS Jet #1 (+X)	21	98001	-2.362	0.0	18.075
RCS Jet #2 (+X)	22	98002	-2.362	0.0	24.675
RCS Jet #3 (+Y)	23	98003	1.271	-1.433	24.802
RCS Jet #4 (-Y)	24	98004	1.271	1.433	24.802
RCS Jet #5 (-Y)	25	98005	-1.787	0.708	24.675
RCS Jet #6 (+Y)	26	98006	-1.787	-0.708	24.675
RCS Jet #7 (+X)	27	98007	-2.362	0.0	21.45
RCS Jet #8 (+X)	28	98008	-2.34	0.0	21.783

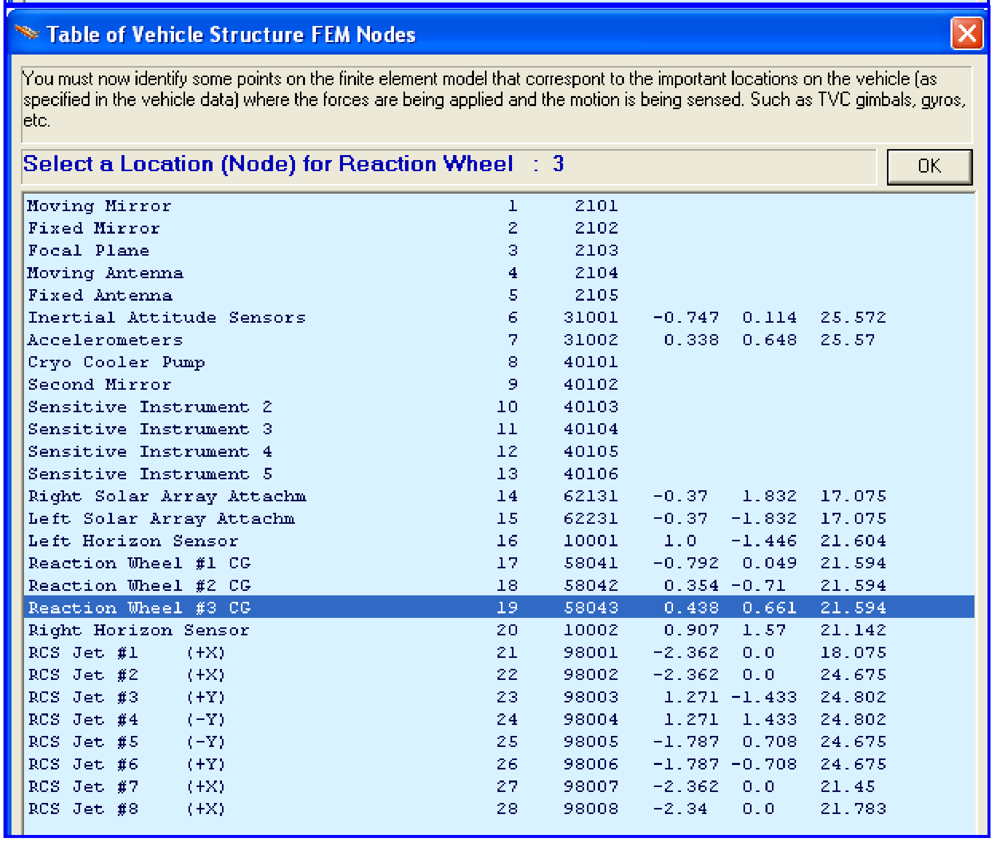

Table of Vehicle Structure FEM Nodes

You must now identify some points on the finite element model that correspont to the important locations on the vehicle (as specified in the vehicle data) where the forces are being applied and the motion is being sensed. Such as TVC gimbals, gyros, etc.

Select a Location (Node) for Reaction Wheel : 3 OK

Moving Mirror	1	2101			
Fixed Mirror	2	2102			
Focal Plane	3	2103			
Moving Antenna	4	2104			
Fixed Antenna	5	2105			
Inertial Attitude Sensors	6	31001	-0.747	0.114	25.572
Accelerometers	7	31002	0.338	0.648	25.57
Cryo Cooler Pump	8	40101			
Second Mirror	9	40102			
Sensitive Instrument 2	10	40103			
Sensitive Instrument 3	11	40104			
Sensitive Instrument 4	12	40105			
Sensitive Instrument 5	13	40106			
Right Solar Array Attachm	14	62131	-0.37	1.832	17.075
Left Solar Array Attachm	15	62231	-0.37	-1.832	17.075
Left Horizon Sensor	16	10001	1.0	-1.446	21.604
Reaction Wheel #1 CG	17	58041	-0.792	0.049	21.594
Reaction Wheel #2 CG	18	58042	0.354	-0.71	21.594
Reaction Wheel #3 CG	19	58043	0.438	0.661	21.594
Right Horizon Sensor	20	10002	0.907	1.57	21.142
RCS Jet #1 (+X)	21	98001	-2.362	0.0	18.075
RCS Jet #2 (+X)	22	98002	-2.362	0.0	24.675
RCS Jet #3 (+Y)	23	98003	1.271	-1.433	24.802
RCS Jet #4 (-Y)	24	98004	1.271	1.433	24.802
RCS Jet #5 (-Y)	25	98005	-1.787	0.708	24.675
RCS Jet #6 (+Y)	26	98006	-1.787	-0.708	24.675
RCS Jet #7 (+X)	27	98007	-2.362	0.0	21.45
RCS Jet #8 (+X)	28	98008	-2.34	0.0	21.783

The next step is to define the location of the cryo-cooler disturbance torque. We select node #8 (40101) three times in order to apply roll, pitch, and yaw torques, as defined in the input data.

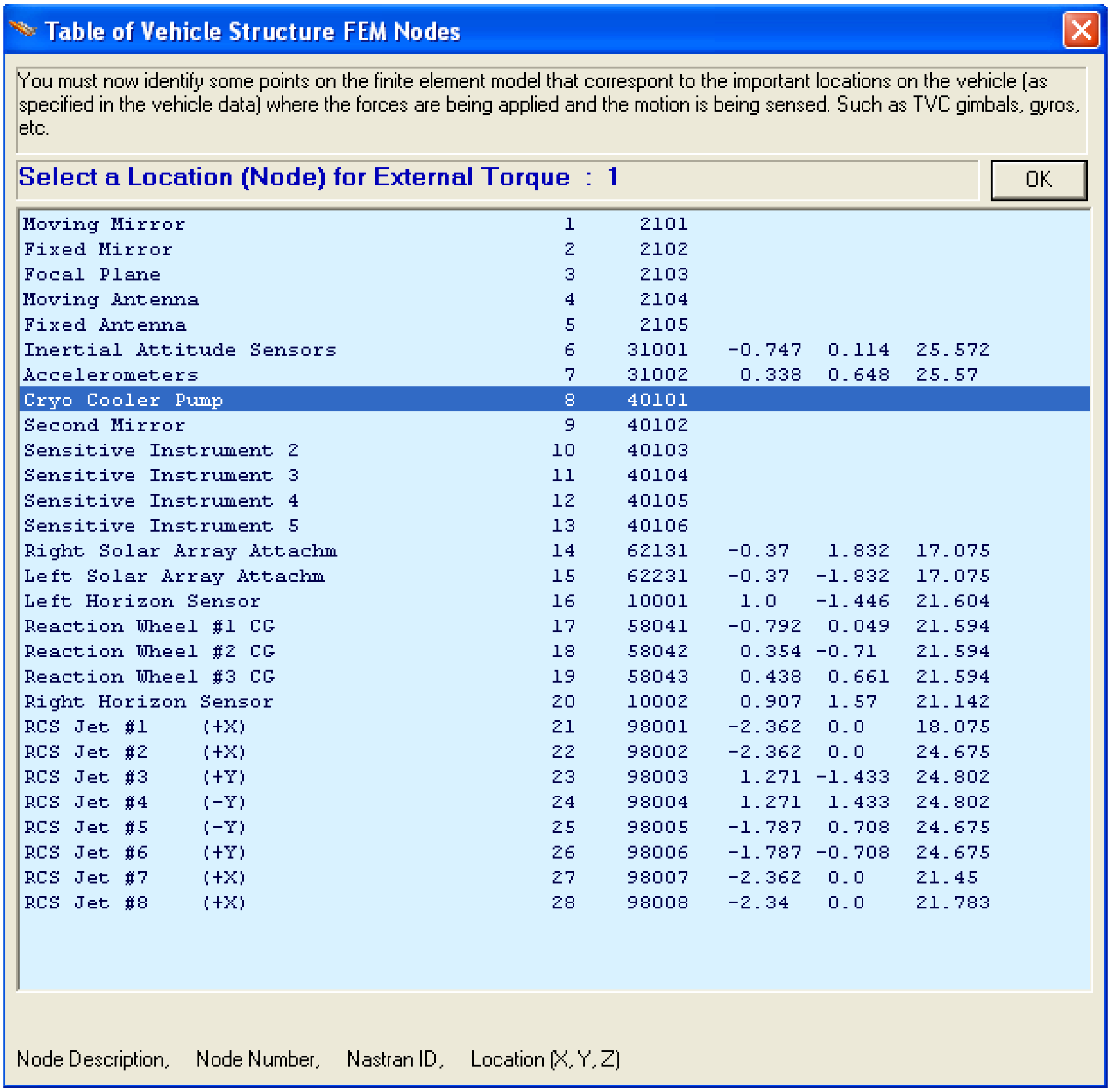

Node Description,	Node Number,	Nastran ID,	Location (X, Y, Z)		
Moving Mirror	1	2101			
Fixed Mirror	2	2102			
Focal Plane	3	2103			
Moving Antenna	4	2104			
Fixed Antenna	5	2105			
Inertial Attitude Sensors	6	31001	-0.747	0.114	25.572
Accelerometers	7	31002	0.338	0.648	25.57
Cryo Cooler Pump	8	40101			
Second Mirror	9	40102			
Sensitive Instrument 2	10	40103			
Sensitive Instrument 3	11	40104			
Sensitive Instrument 4	12	40105			
Sensitive Instrument 5	13	40106			
Right Solar Array Attachm	14	62131	-0.37	1.832	17.075
Left Solar Array Attachm	15	62231	-0.37	-1.832	17.075
Left Horizon Sensor	16	10001	1.0	-1.446	21.604
Reaction Wheel #1 CG	17	58041	-0.792	0.049	21.594
Reaction Wheel #2 CG	18	58042	0.354	-0.71	21.594
Reaction Wheel #3 CG	19	58043	0.438	0.661	21.594
Right Horizon Sensor	20	10002	0.907	1.57	21.142
RCS Jet #1 (+X)	21	98001	-2.362	0.0	18.075
RCS Jet #2 (+X)	22	98002	-2.362	0.0	24.675
RCS Jet #3 (+Y)	23	98003	1.271	-1.433	24.802
RCS Jet #4 (-Y)	24	98004	1.271	1.433	24.802
RCS Jet #5 (-Y)	25	98005	-1.787	0.708	24.675
RCS Jet #6 (+Y)	26	98006	-1.787	-0.708	24.675
RCS Jet #7 (+X)	27	98007	-2.362	0.0	21.45
RCS Jet #8 (+X)	28	98008	-2.34	0.0	21.783

We must also select locations for the 13 rotational sensors. The first 6 are at the Inertial Attitude Sensors, node #6 (31001), measuring attitude and rate in roll, pitch, and yaw directions. The next two (7 and 8) are in the Second Mirror, node #9 (40102). The next two (9 and 10) are in the Sensitive Instrument 2, node #10 (40103). The last three rotational sensors (11, 12, and 13) are located in nodes (#11, #12, and #13).

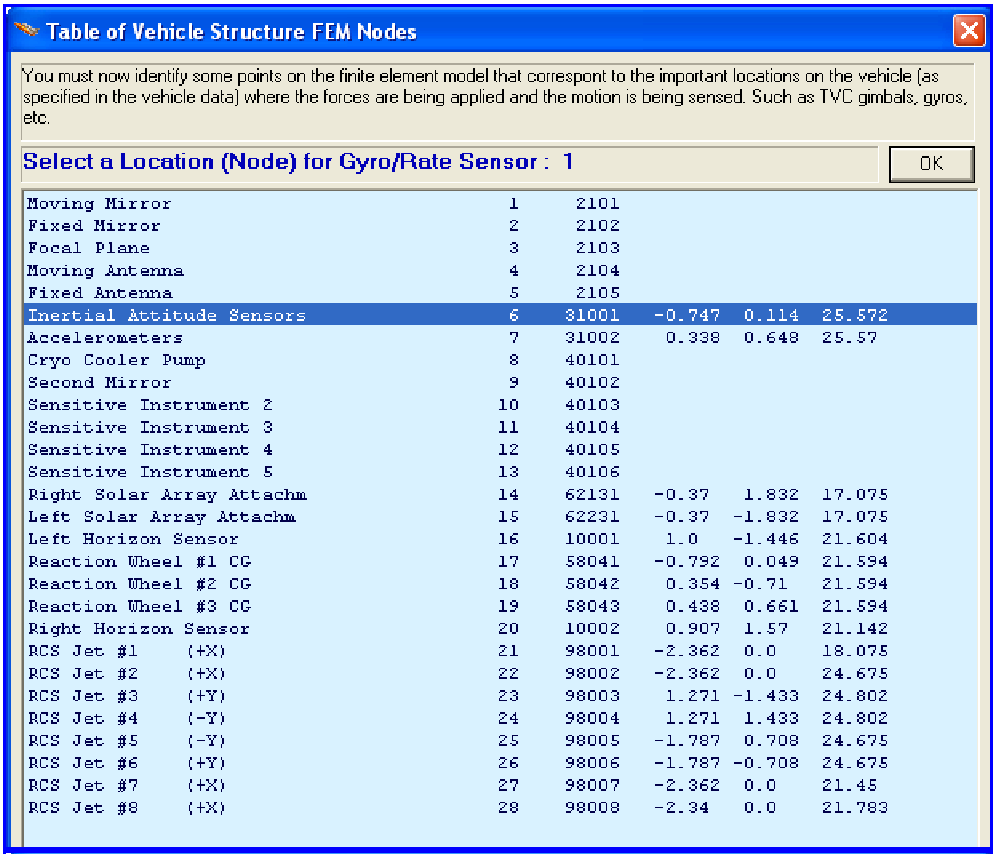
Table of Vehicle Structure FEM Nodes
You must now identify some points on the finite element model that corresport to the important locations on the vehicle (as specified in the vehicle data) where the forces are being applied and the motion is being sensed. Such as TVC gimbals, gyros, etc.
Select a Location (Node) for Gyro/Rate Sensor : 1
OK
Moving Mirror 1 2101
Fixed Mirror 2 2102
Focal Plane 3 2103
Moving Antenna 4 2104
Fixed Antenna 5 2105
Inertial Attitude Sensors 6 31001 -0.747 0.114 25.572
Accelerometers 7 31002 0.338 0.648 25.57
Cryo Cooler Pump 8 40101
Second Mirror 9 40102
Sensitive Instrument 2 10 40103
Sensitive Instrument 3 11 40104
Sensitive Instrument 4 12 40105
Sensitive Instrument 5 13 40106
Right Solar Array Attachm 14 62131 -0.37 1.832 17.075
Left Solar Array Attachm 15 62231 -0.37 -1.832 17.075
Left Horizon Sensor 16 10001 1.0 -1.446 21.604
Reaction Wheel #1 CG 17 58041 -0.792 0.049 21.594
Reaction Wheel #2 CG 18 58042 0.354 -0.71 21.594
Reaction Wheel #3 CG 19 58043 0.438 0.661 21.594
Right Horizon Sensor 20 10002 0.907 1.57 21.142
RCS Jet #1 (+X) 21 98001 -2.362 0.0 18.075
RCS Jet #2 (+X) 22 98002 -2.362 0.0 24.675
RCS Jet #3 (+Y) 23 98003 1.271 -1.433 24.802
RCS Jet #4 (-Y) 24 98004 1.271 1.433 24.802
RCS Jet #5 (-Y) 25 98005 -1.787 0.708 24.675
RCS Jet #6 (+Y) 26 98006 -1.787 -0.708 24.675
RCS Jet #7 (+X) 27 98007 -2.362 0.0 21.45
RCS Jet #8 (+X) 28 98008 -2.34 0.0 21.783

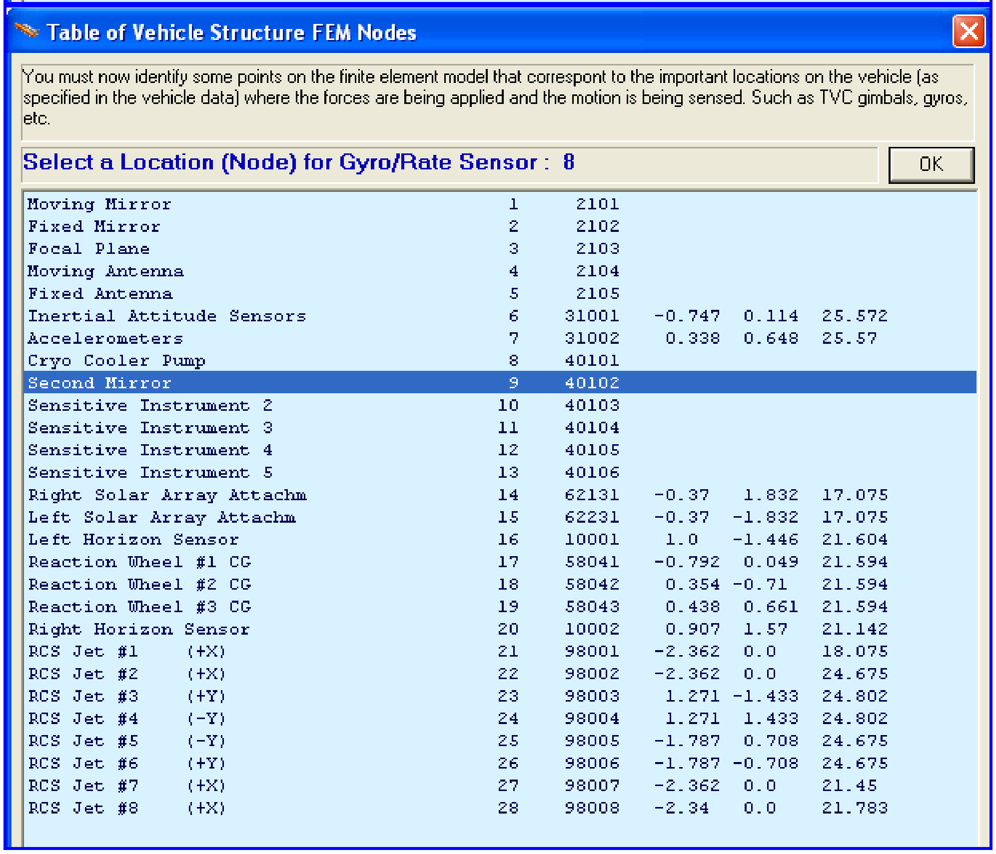
Table of Vehicle Structure FEM Nodes
You must now identify some points on the finite element model that corresport to the important locations on the vehicle (as specified in the vehicle data) where the forces are being applied and the motion is being sensed. Such as TVC gimbals, gyros, etc.
Select a Location (Node) for Gyro/Rate Sensor : 8
OK
Moving Mirror 1 2101
Fixed Mirror 2 2102
Focal Plane 3 2103
Moving Antenna 4 2104
Fixed Antenna 5 2105
Inertial Attitude Sensors 6 31001 -0.747 0.114 25.572
Accelerometers 7 31002 0.338 0.648 25.57
Cryo Cooler Pump 8 40101
Second Mirror 9 40102
Sensitive Instrument 2 10 40103
Sensitive Instrument 3 11 40104
Sensitive Instrument 4 12 40105
Sensitive Instrument 5 13 40106
Right Solar Array Attachm 14 62131 -0.37 1.832 17.075
Left Solar Array Attachm 15 62231 -0.37 -1.832 17.075
Left Horizon Sensor 16 10001 1.0 -1.446 21.604
Reaction Wheel #1 CG 17 58041 -0.792 0.049 21.594
Reaction Wheel #2 CG 18 58042 0.354 -0.71 21.594
Reaction Wheel #3 CG 19 58043 0.438 0.661 21.594
Right Horizon Sensor 20 10002 0.907 1.57 21.142
RCS Jet #1 (+X) 21 98001 -2.362 0.0 18.075
RCS Jet #2 (+X) 22 98002 -2.362 0.0 24.675
RCS Jet #3 (+Y) 23 98003 1.271 -1.433 24.802
RCS Jet #4 (-Y) 24 98004 1.271 1.433 24.802
RCS Jet #5 (-Y) 25 98005 -1.787 0.708 24.675
RCS Jet #6 (+Y) 26 98006 -1.787 -0.708 24.675
RCS Jet #7 (+X) 27 98007 -2.362 0.0 21.45
RCS Jet #8 (+X) 28 98008 -2.34 0.0 21.783

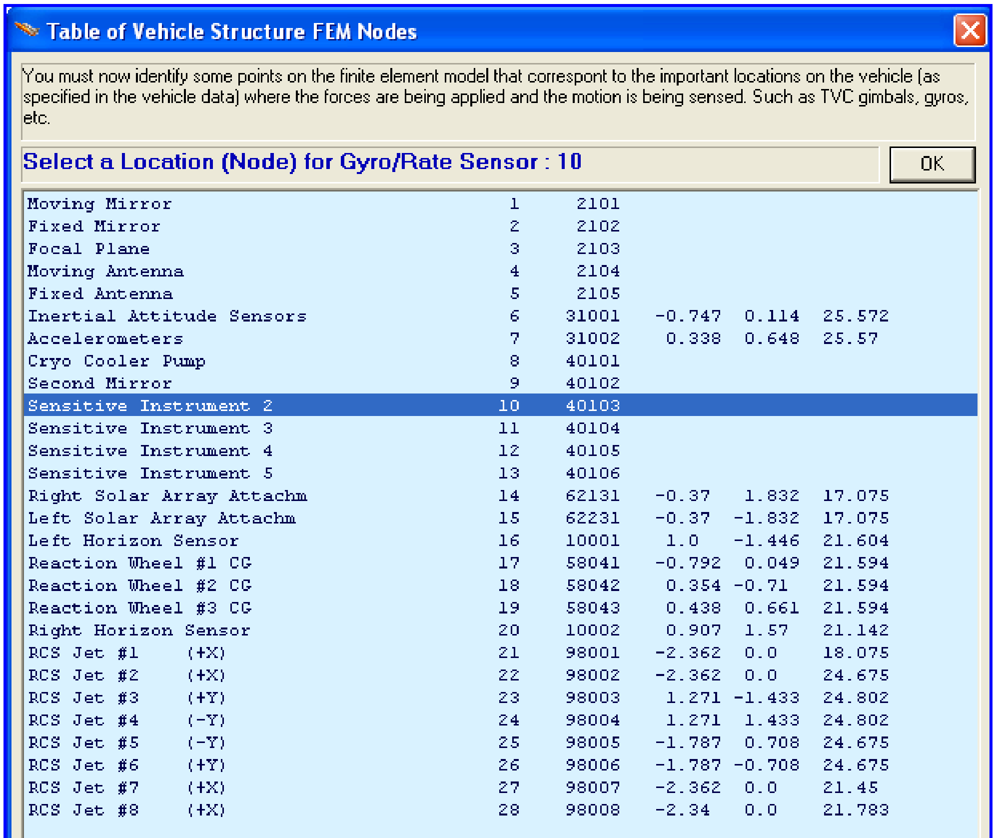

Table of Vehicle Structure FEM Nodes

You must now identify some points on the finite element model that correspont to the important locations on the vehicle (as specified in the vehicle data) where the forces are being applied and the motion is being sensed. Such as TVC gimbals, gyros, etc.

Select a Location (Node) for Gyro/Rate Sensor : 10

OK

Moving Mirror	1	2101			
Fixed Mirror	2	2102			
Focal Plane	3	2103			
Moving Antenna	4	2104			
Fixed Antenna	5	2105			
Inertial Attitude Sensors	6	31001	-0.747	0.114	25.572
Accelerometers	7	31002	0.338	0.648	25.57
Cryo Cooler Pump	8	40101			
Second Mirror	9	40102			
Sensitive Instrument 2	10	40103			
Sensitive Instrument 3	11	40104			
Sensitive Instrument 4	12	40105			
Sensitive Instrument 5	13	40106			
Right Solar Array Attachm	14	62131	-0.37	1.832	17.075
Left Solar Array Attachm	15	62231	-0.37	-1.832	17.075
Left Horizon Sensor	16	10001	1.0	-1.446	21.604
Reaction Wheel #1 CG	17	58041	-0.792	0.049	21.594
Reaction Wheel #2 CG	18	58042	0.354	-0.71	21.594
Reaction Wheel #3 CG	19	58043	0.438	0.661	21.594
Right Horizon Sensor	20	10002	0.907	1.57	21.142
RCS Jet #1 (+X)	21	98001	-2.362	0.0	18.075
RCS Jet #2 (+X)	22	98002	-2.362	0.0	24.675
RCS Jet #3 (+Y)	23	98003	1.271	-1.433	24.802
RCS Jet #4 (-Y)	24	98004	1.271	1.433	24.802
RCS Jet #5 (-Y)	25	98005	-1.787	0.708	24.675
RCS Jet #6 (+Y)	26	98006	-1.787	-0.708	24.675
RCS Jet #7 (+X)	27	98007	-2.362	0.0	21.45
RCS Jet #8 (+X)	28	98008	-2.34	0.0	21.783

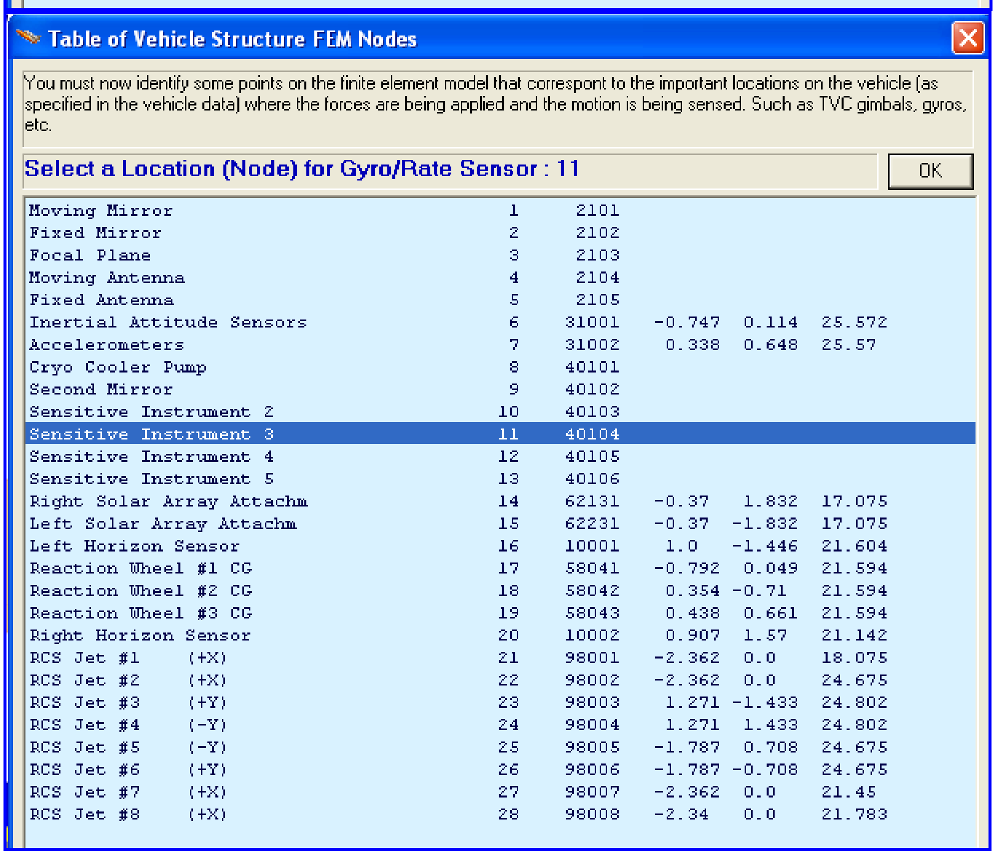

Table of Vehicle Structure FEM Nodes

You must now identify some points on the finite element model that correspont to the important locations on the vehicle (as specified in the vehicle data) where the forces are being applied and the motion is being sensed. Such as TVC gimbals, gyros, etc.

Select a Location (Node) for Gyro/Rate Sensor : 11

OK

Moving Mirror	1	2101			
Fixed Mirror	2	2102			
Focal Plane	3	2103			
Moving Antenna	4	2104			
Fixed Antenna	5	2105			
Inertial Attitude Sensors	6	31001	-0.747	0.114	25.572
Accelerometers	7	31002	0.338	0.648	25.57
Cryo Cooler Pump	8	40101			
Second Mirror	9	40102			
Sensitive Instrument 2	10	40103			
Sensitive Instrument 3	11	40104			
Sensitive Instrument 4	12	40105			
Sensitive Instrument 5	13	40106			
Right Solar Array Attachm	14	62131	-0.37	1.832	17.075
Left Solar Array Attachm	15	62231	-0.37	-1.832	17.075
Left Horizon Sensor	16	10001	1.0	-1.446	21.604
Reaction Wheel #1 CG	17	58041	-0.792	0.049	21.594
Reaction Wheel #2 CG	18	58042	0.354	-0.71	21.594
Reaction Wheel #3 CG	19	58043	0.438	0.661	21.594
Right Horizon Sensor	20	10002	0.907	1.57	21.142
RCS Jet #1 (+X)	21	98001	-2.362	0.0	18.075
RCS Jet #2 (+X)	22	98002	-2.362	0.0	24.675
RCS Jet #3 (+Y)	23	98003	1.271	-1.433	24.802
RCS Jet #4 (-Y)	24	98004	1.271	1.433	24.802
RCS Jet #5 (-Y)	25	98005	-1.787	0.708	24.675
RCS Jet #6 (+Y)	26	98006	-1.787	-0.708	24.675
RCS Jet #7 (+X)	27	98007	-2.362	0.0	21.45
RCS Jet #8 (+X)	28	98008	-2.34	0.0	21.783

We must also select locations for the two accelerometers to be used in sensitivity analysis. The accelerometers node #7 (31002) is selected twice. We finally select node #8 (98008) for the disturbance torque location, which is not used in this analysis.

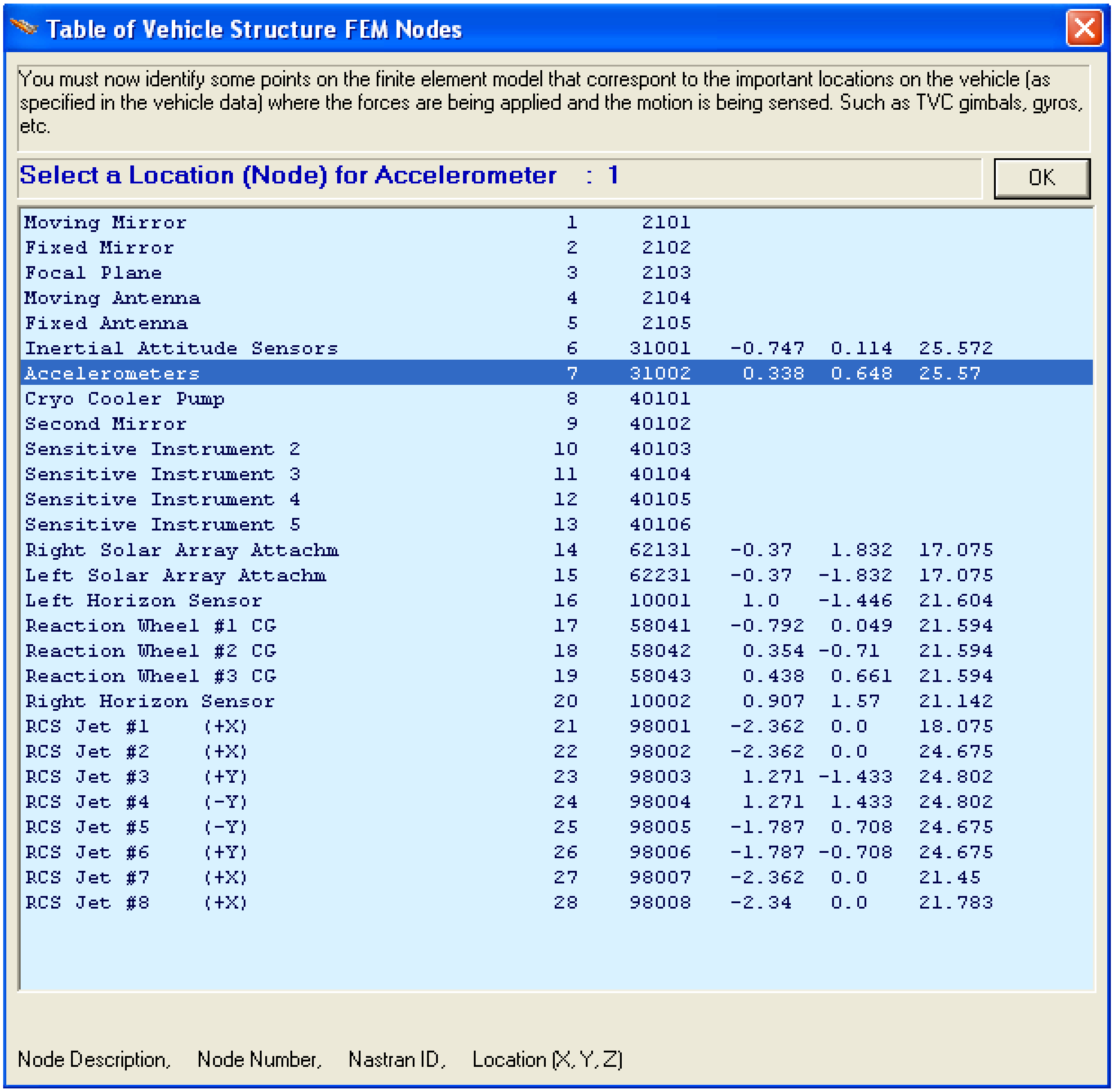
Table of Vehicle Structure FEM Nodes

You must now identify some points on the finite element model that correspont to the important locations on the vehicle (as specified in the vehicle data) where the forces are being applied and the motion is being sensed. Such as TVC gimbals, gyros, etc.

Select a Location (Node) for Accelerometer : 1

OK

Moving Mirror	1	2101			
Fixed Mirror	2	2102			
Focal Plane	3	2103			
Moving Antenna	4	2104			
Fixed Antenna	5	2105			
Inertial Attitude Sensors	6	31001	-0.747	0.114	25.572
Accelerometers	7	31002	0.338	0.648	25.57
Cryo Cooler Pump	8	40101			
Second Mirror	9	40102			
Sensitive Instrument 2	10	40103			
Sensitive Instrument 3	11	40104			
Sensitive Instrument 4	12	40105			
Sensitive Instrument 5	13	40106			
Right Solar Array Attachm	14	62131	-0.37	1.832	17.075
Left Solar Array Attachm	15	62231	-0.37	-1.832	17.075
Left Horizon Sensor	16	10001	1.0	-1.446	21.604
Reaction Wheel #1 CG	17	58041	-0.792	0.049	21.594
Reaction Wheel #2 CG	18	58042	0.354	-0.71	21.594
Reaction Wheel #3 CG	19	58043	0.438	0.661	21.594
Right Horizon Sensor	20	10002	0.907	1.57	21.142
RCS Jet #1 (+X)	21	98001	-2.362	0.0	18.075
RCS Jet #2 (+X)	22	98002	-2.362	0.0	24.675
RCS Jet #3 (+Y)	23	98003	1.271	-1.433	24.802
RCS Jet #4 (-Y)	24	98004	1.271	1.433	24.802
RCS Jet #5 (-Y)	25	98005	-1.787	0.708	24.675
RCS Jet #6 (+Y)	26	98006	-1.787	-0.708	24.675
RCS Jet #7 (+X)	27	98007	-2.362	0.0	21.45
RCS Jet #8 (+X)	28	98008	-2.34	0.0	21.783

Node Description, Node Number, Nastran ID, Location (X, Y, Z)

At this point the mode selection program displays the results of the mode strength comparison between the excitation points and directions to the sensor points and directions (defined in earlier menu dialogs), and it saves the relative mode strength for each mode in file "Modsel.Dat". Then it displays a mode strength bar chart (shown below) where the relative mode strength of each mode is plotted versus the mode number. All bars are initially red before selection. The height of each bar is logarithmically proportional to the relative mode strength. The strong modes appear tall and the weak modes are short. The modal strength is a relative number adjusted with respect to the minimum and maximum modal strengths. The user selects some of the strongest modes from the chart by pointing the mouse cursor at the bar and clicking the mouse to select it. The modes change color from red to green when they are selected. Notice that the first six modes are not selected because they are rigid-body modes, and the rigid-body dynamics have already been included in the vehicle model. We select 60 flex modes, the same flex modes that we selected in section (3) using the Flex Spacecraft Program, and press the enter button to complete the mode selection.

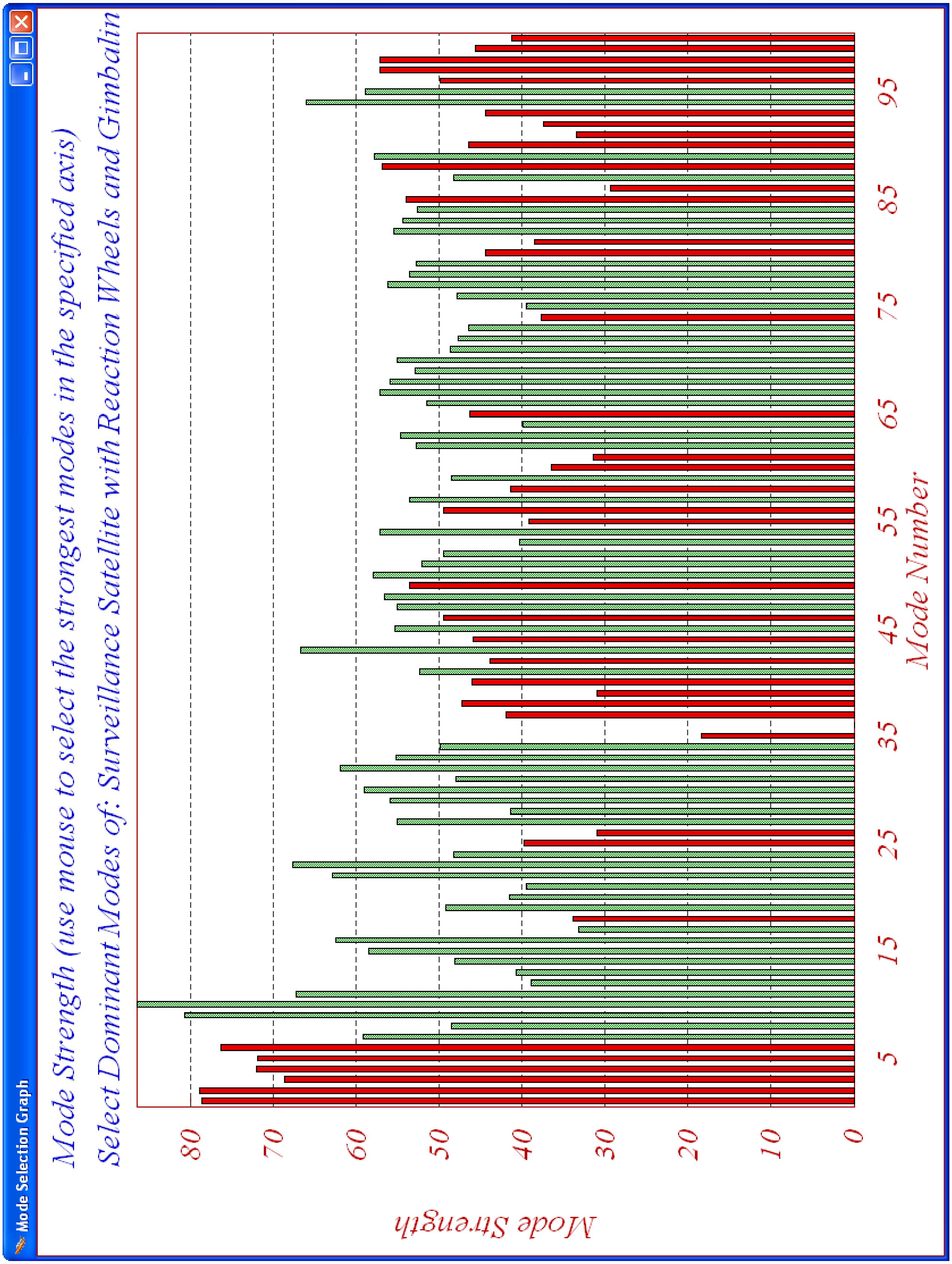
Mode Selection Graph
Mode Strength (use mouse to select the strongest modes in the specified axis)
Select Dominant Modes of: Surveillance Satellite with Reaction Wheels and Gimbalin
Mode Strength
0
10
20
30
40
50
60
70
80
Mode Number
5
15
25
35
45
55
65
75
85
95

The final step before exiting mode selection is to complete the dialog below where the user enters some reference notes regarding the mode selection process. Describing, for example what type of modes were selected, and the conditions of mode selection, excitation points, measurement points, directions, etc. This information will be included as comments below the title in the selected modes set, which is saved in the input data file "*Surv_Sat_RB+Flx.Inp*". The title of the selected modes set is "*Space Surveillance Satellite with RCS and Reaction Wheels (60 Flex Pre-Selected Modes)*". It contains the frequencies and mode shapes of the selected modes at important vehicle locations. The title of the selected modes must also be included at the bottom of the Satellite input data set (below the number of flex modes) in order for the flight vehicle modeling program to associate the selected modes with the spacecraft input data.

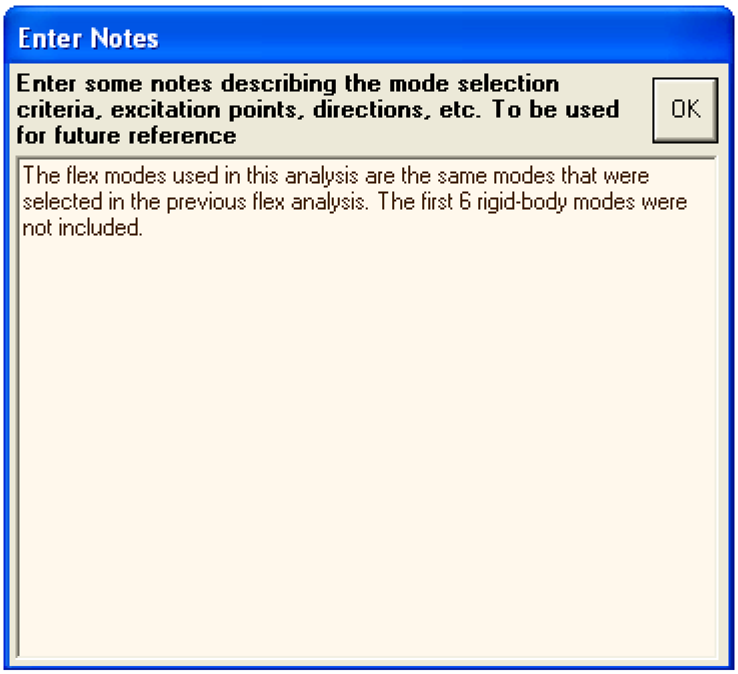

6.2 Creating the Spacecraft Systems

On the top of the input data file "*Surv_Sat_RB+Flx.Inp*" there is a batch set of instruction data that can be used to speed up the execution of the spacecraft systems by running them in batch mode, instead of executing them separately, discretizing them, and transforming them for Matlab. Its title is "*Batch for the Surveillance Satellite*". The batch creates 3 spacecraft systems, "*Space Surveillance Satellite with RCS and Reaction Wheels (Rigid-Body)*" for the rigid-body model without gimbaling appendages, "*Space Surveillance Satellite with RCS and Reaction Wheels (Gimbals, No Flex)*" for the rigid-body model with the four gimbaling appendages, and "*Space Surveillance Satellite with RCS and Reaction Wheels (Gimbals & 60 Flex Modes)*" for the 60 mode flex spacecraft with the four gimbaling appendages. The systems are saved in file "*Surv_Sat_RB+Flx.Qdr*". The batch then calls the S to Z transformation program to discretize the above systems using 10 msec sampling rate and saves them in the same systems file. The discrete system titles are: "*Space Surveill Satellite with RCS and Reaction Wheels (Rigid-Body, Z-Transf)*", "*Space Surveill Satellite with RCS and Reaction Wheels (Gimbals, No Flex, Z-*

Transf)", and "*Space Surveill Satellite with RCS and Reaction Wheels (Gimbals, 60 Modes, Z-Transf)*" respectively. The batch finally transforms the 3 discrete systems from file "*Surv_Sat_RB+Flx.Qdr*" to Matlab format for further analysis. The system function filenames for the 3 discrete systems are "*fv_rb.m*", "*fv_grb.m*", and "*fv_60.m*" respectively. They are saved in subdirectory: "*…\Examples\Surveillance Satellite React-Wheels\Linear Flex Anal FV*".

Start the Flixan program and go to directory: "*…\Examples\Surveillance Satellite React-Wheels*". Go to "Edit", "Manage Input Files", and select "Process/ Edit Input Data".

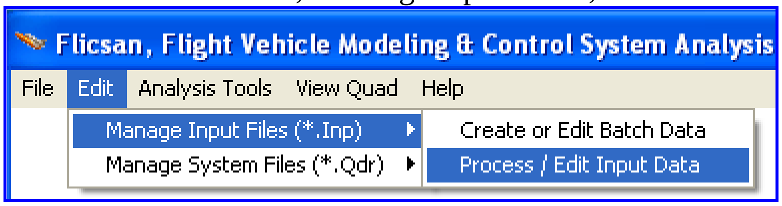

From the following dialog in the filename selection menu (upper left) select file "*Surv-Sat_RB+Flx.Inp*" and click the "*Select Input File*" button. Then from the right menu select the top option "*Batch for the Surveillance Satellite*" and then click on the "*Execute/ View Input Data*" button.

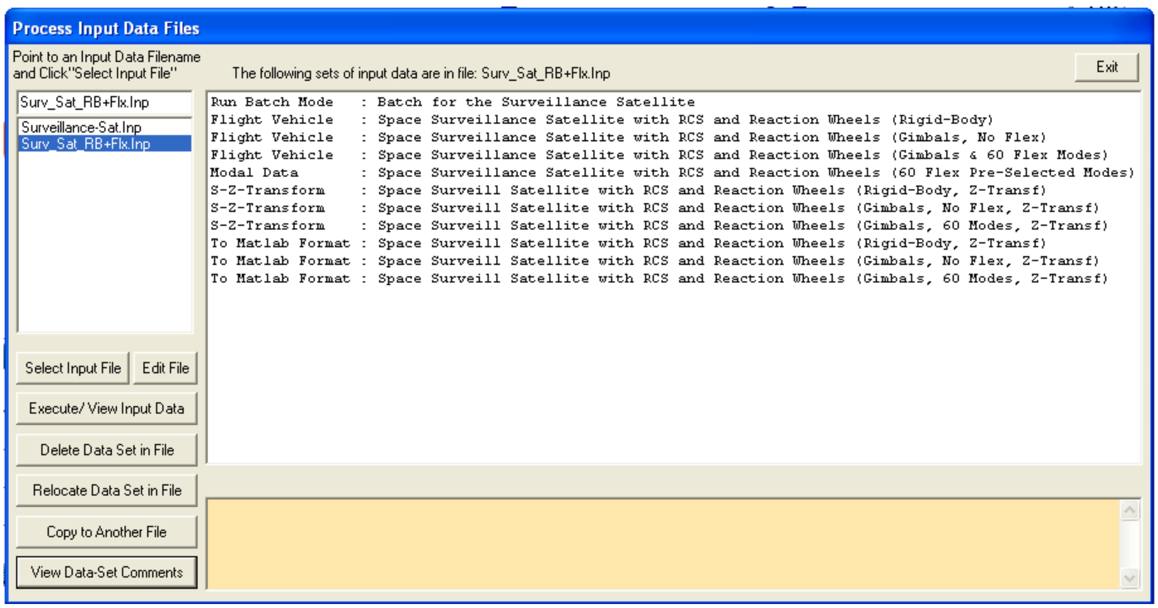

The program will execute the batch set of instructions which are on the top of file "*Surv-Sat_RB+Flx.Inp*". It will ask the user if it is acceptable to recreate the state-space systems file "*Surv_Sat_RB+Flx.Qdr*". You may answer "Yes", and the program will run the batch set of instructions as shown below. When it finishes click on "Exit" to complete the execution. The 3 systems "*fv_rb.m*", "*fv_grb.m*", and "*fv_60.m*" will be saved in the root directory. From there you may move them to subdirectory "*…\Examples\Surveillance Satellite React-Wheels\Linear Flex Anal FV*" for further Matlab analysis.

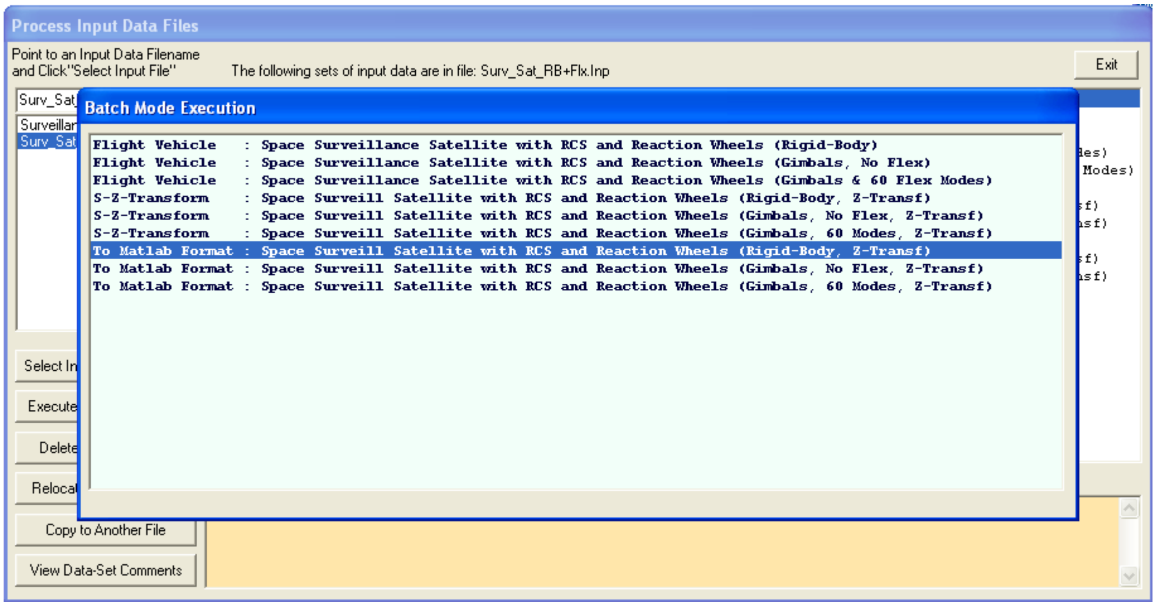

6.3 The Simulation Model

The flexible spacecraft simulation model is shown in figure (6.1). The vehicle block (green) consists of the discrete state-space model which is loaded from file "*fv_60.m*". Its title is "*Space Surveill Satellite with RCS and Reaction Wheels (Gimbals, 60 Modes, Z-Transf)*", extracted from the systems file "*Surv_Sat_RB+Flx.Qdr*". The vehicle block is shown opened in figure (6.4). Before running the simulation model you must execute the file "run.m" to load the state-space matrices and to initialize the spacecraft parameters.

Flex Simulation with Gimbals, RW, and RCS

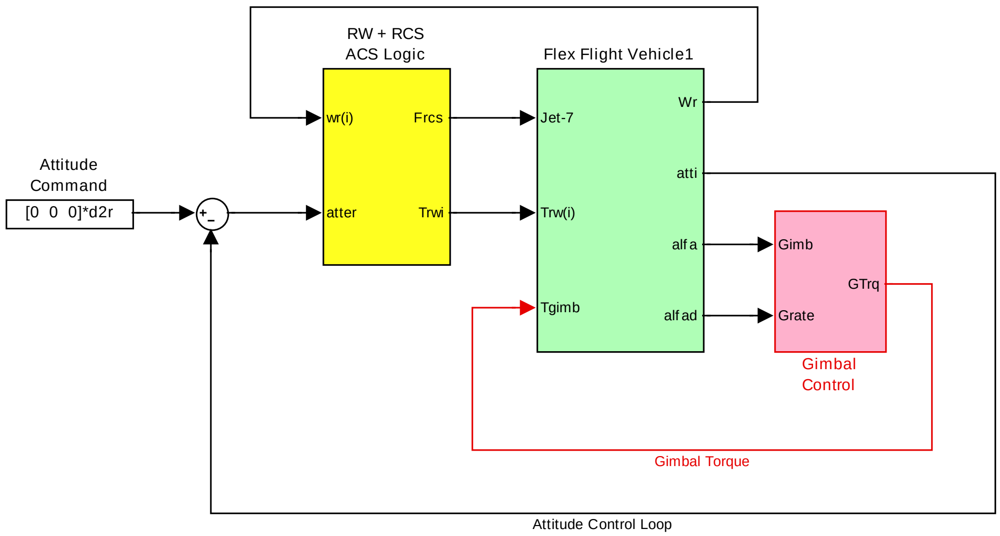

Figure 6.1 Flex Spacecraft Simulation Model "Flex_Sim_Mdl"

The model has the two telescope gimbal loops closed via PD gains designed to provide a 2 (rad/sec) bandwidth. There is also a low-pass filter in the telescope position control loop.

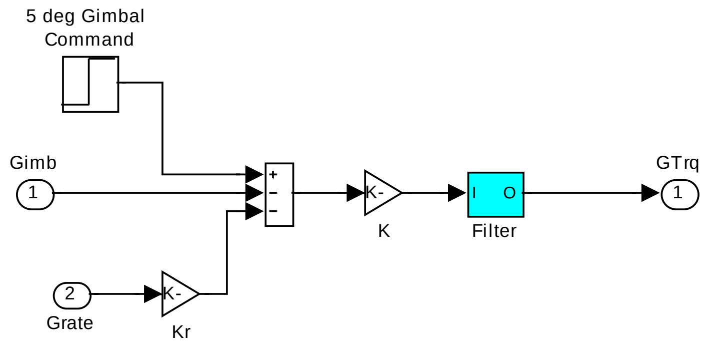

Figure 6.2 Telescope Gimbal Control System

Figure (6.3) shows the combined RCS/ RW Attitude Control logic. It consists of a state-flow mode switching logic that determines which controller will remain active and which one will be turned off based on the magnitude of the RW momentum. The RW steering logic converts the pitch and yaw torque commands to RW#2 and RW#3 torque commands.

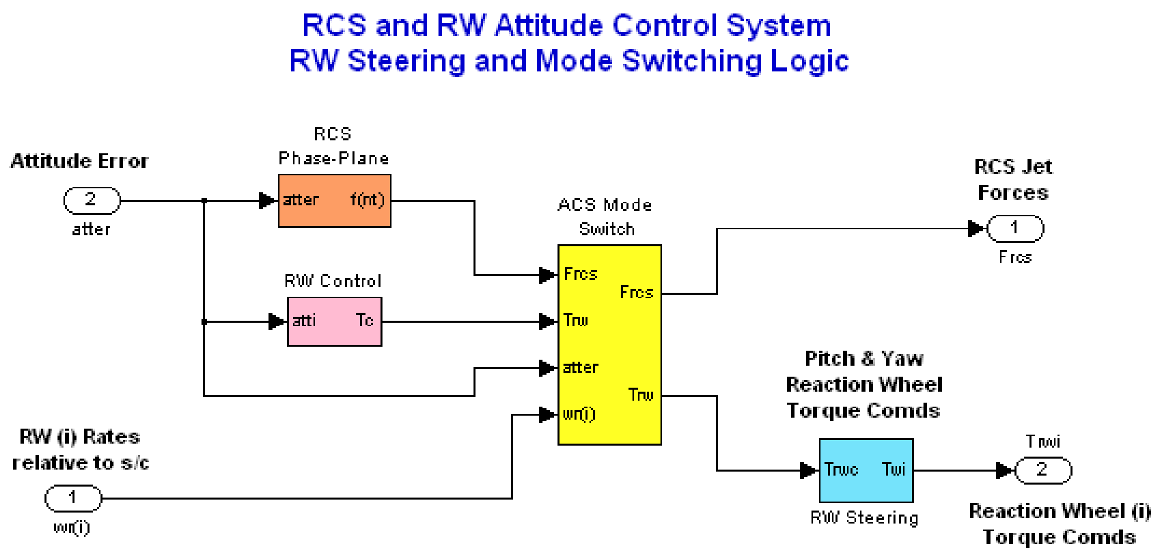

Figure 6.3 RW/ RCS Combined Attitude Control System

Figure (6.3) shows the RW/RCS control state-flow switching logic. It starts in the reaction wheel mode. When the wheel momentum magnitude exceeds the max momentum H_{max} it switches to RCS1 mode. In this mode the jets control the vehicle attitude while the wheels are torqued in the direction to reduce the reaction wheel momentum in unison. It remains in RCS1 mode as long as the RW momentum is greater than Hmax/10 or the spacecraft rate is greater than Rlim. If the RW momentum drops below Hmax/10 and the spacecraft rate is below Rlim it switches back to the RW mode. Otherwise, if the momentum reaches below Hmax/10 but the rate is still higher than Rlim it switches to the RCS2 mode where the jets still control the attitude but the RW torque is set to zero. It remains in RCS2 mode until the rate magnitude drops below Rlim and then it switches back to the RW control mode.

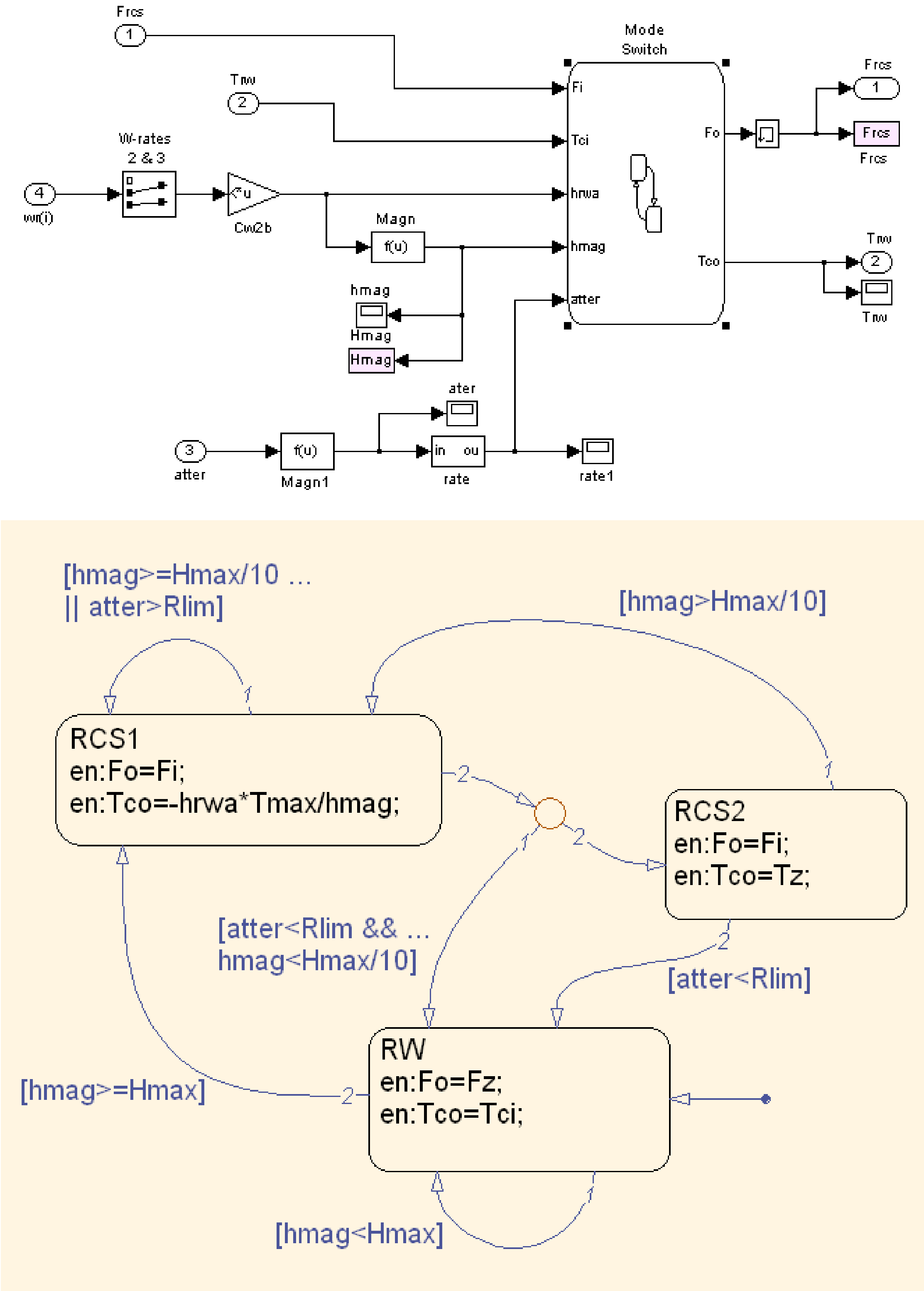

Figure 6.3 Attitude Control Mode State-Flow Switching Logic

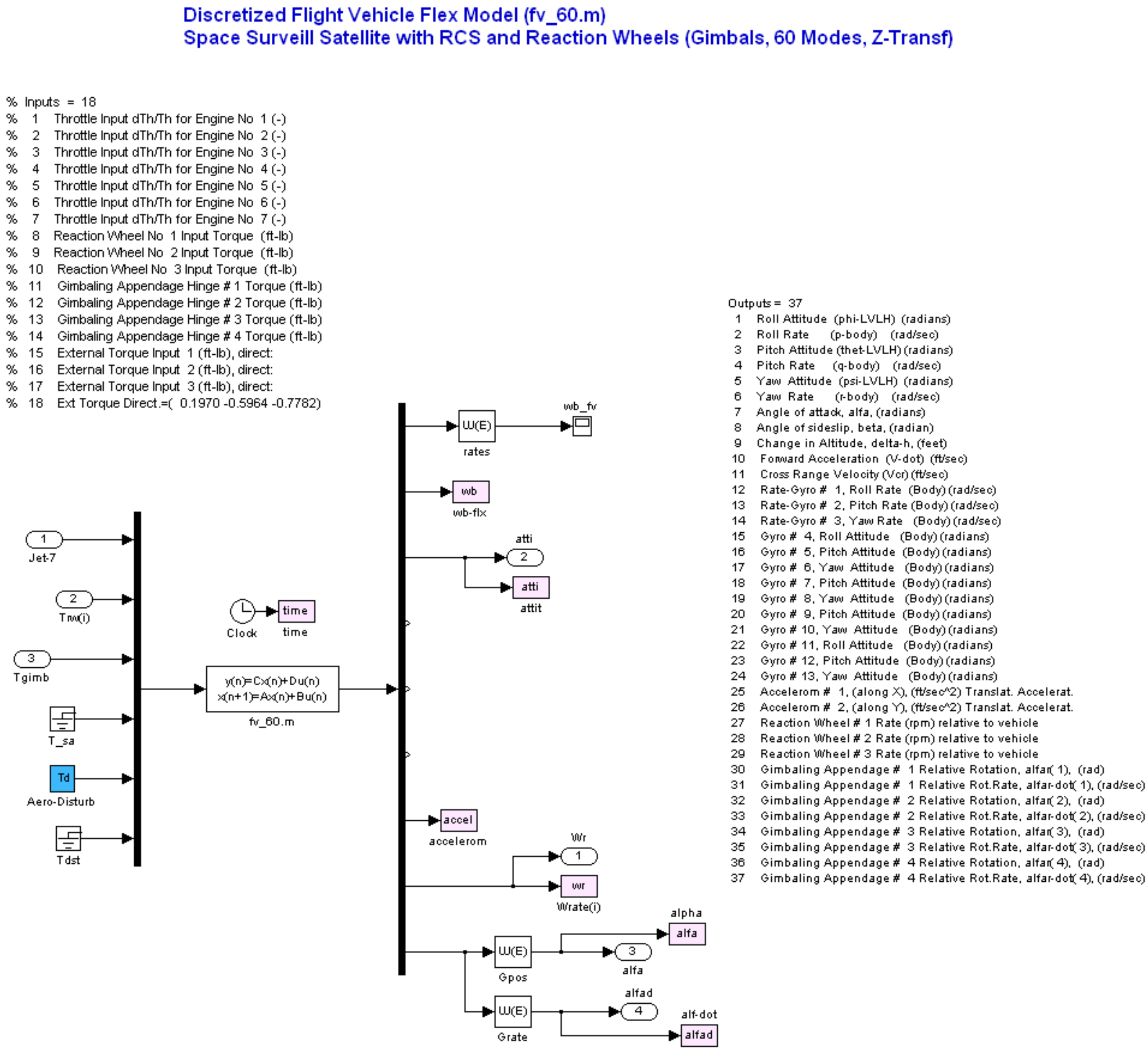

Figure 6.4 Discrete Spacecraft State-Space Model from file “fv_60.m”

Figures (6.5 and 6.6) show some time domain simulation results. Figure (6.5) shows the switching between the RW and the RCS modes, when the RW momentum exceeds 10 (ft-lb-sec). During the RCS control period the wheels are torqued in the direction to reduce the wheel momentum, and the telescope gimbals are also torqued to maintain constant gimbal angles. Figure (6.6) shows the telescope gimbal response to 5 (deg) gimbal commands in both: Elevation and Azimuth directions.

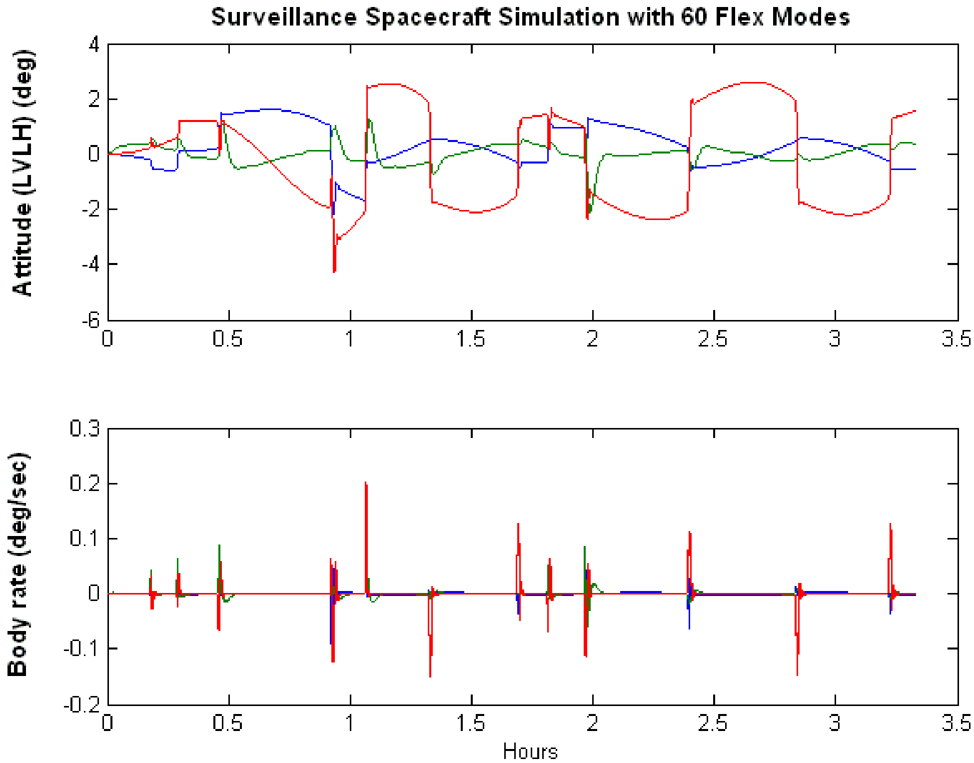
Surveillance Spacecraft Simulation with 60 Flex Modes
Attitude (LVLH) (deg)
Body rate (deg/sec)
Hours

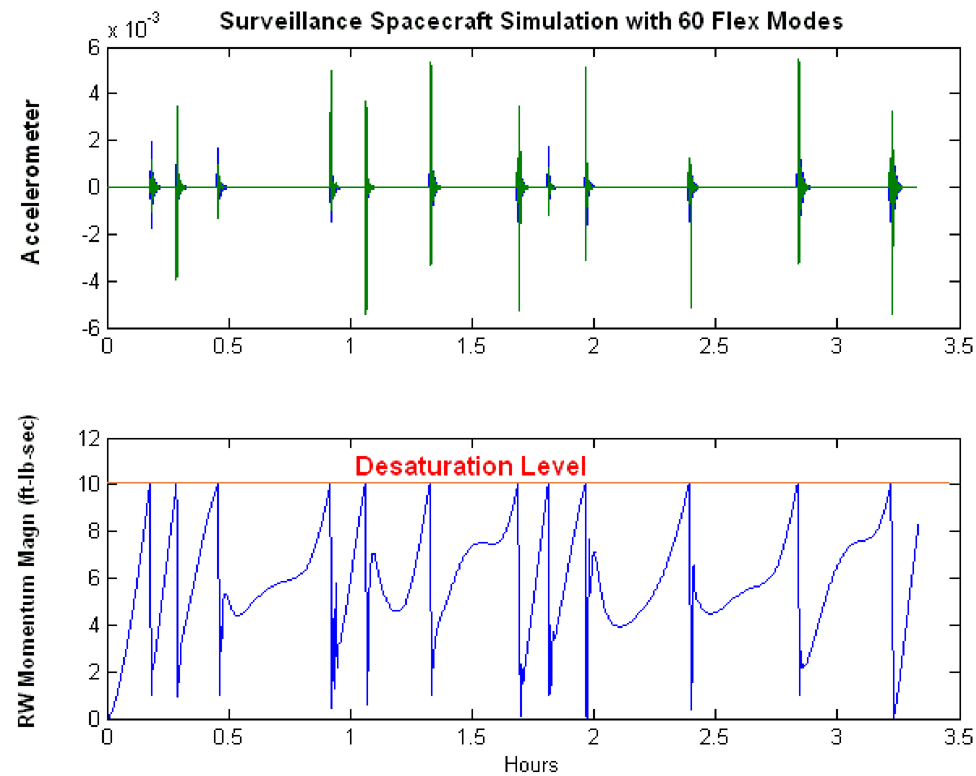
Surveillance Spacecraft Simulation with 60 Flex Modes
x 10^-3
Accelerometer
RW Momentum Magn (ft-lb-sec)
Desaturation Level
Hours

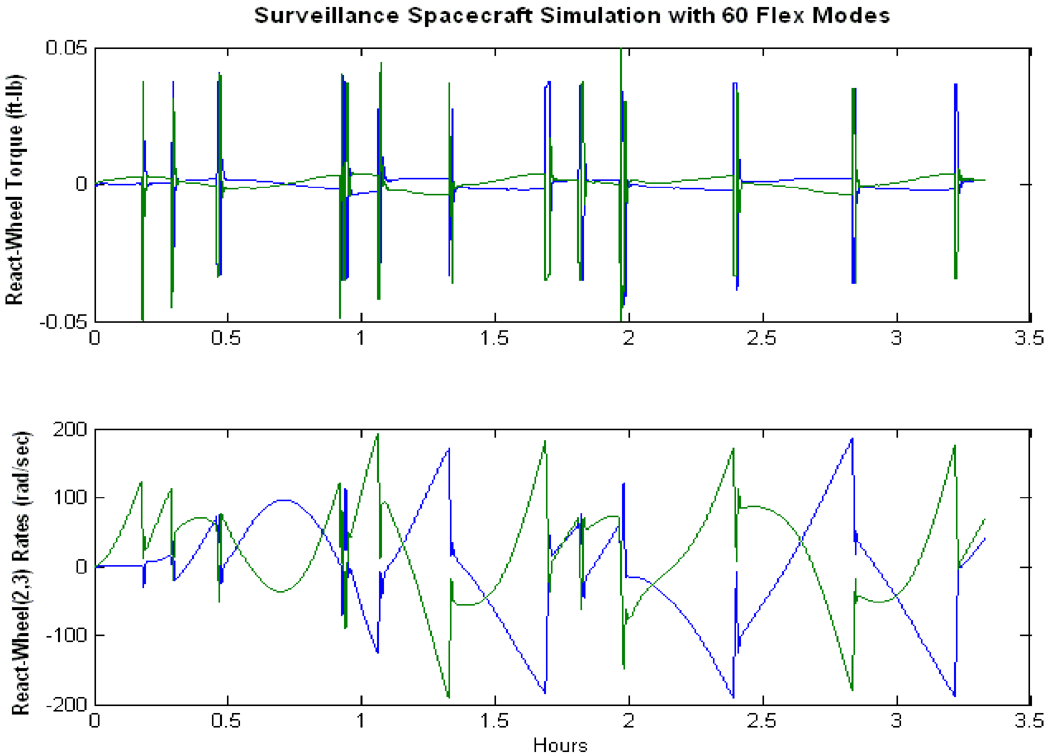
Surveillance Spacecraft Simulation with 60 Flex Modes
React-Wheel Torque (ft-lb)
React-Wheel(2,3) Rates (rad/sec)
Hours

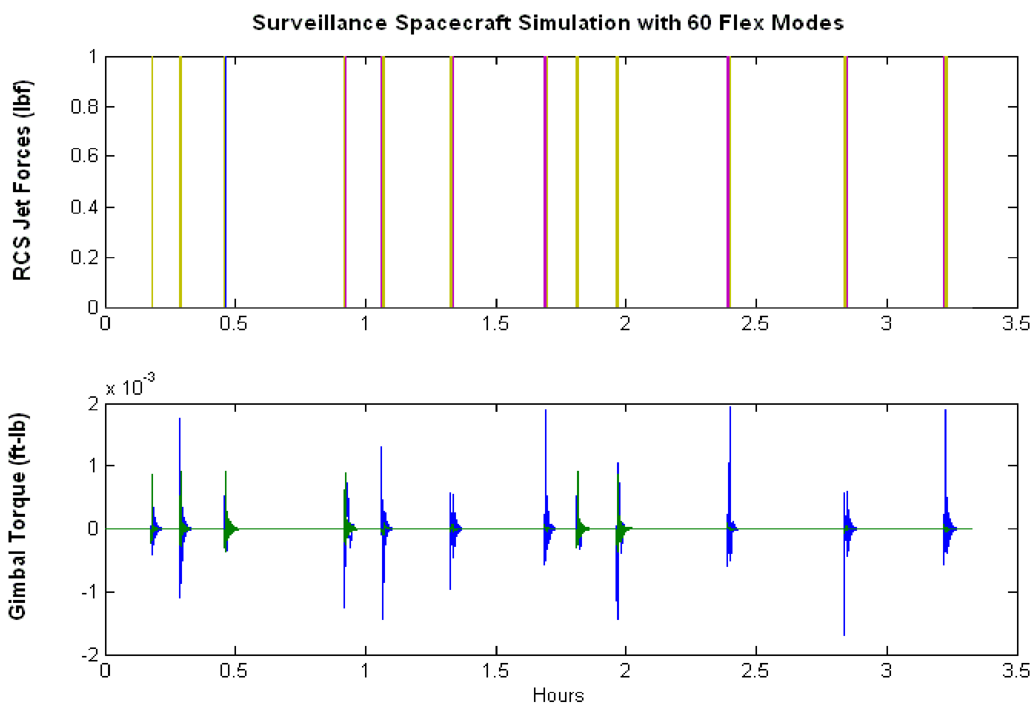
Surveillance Spacecraft Simulation with 60 Flex Modes
RCS Jet Forces (lbf)
Gimbal Torque (ft-lb)
x 10^-3
Hours

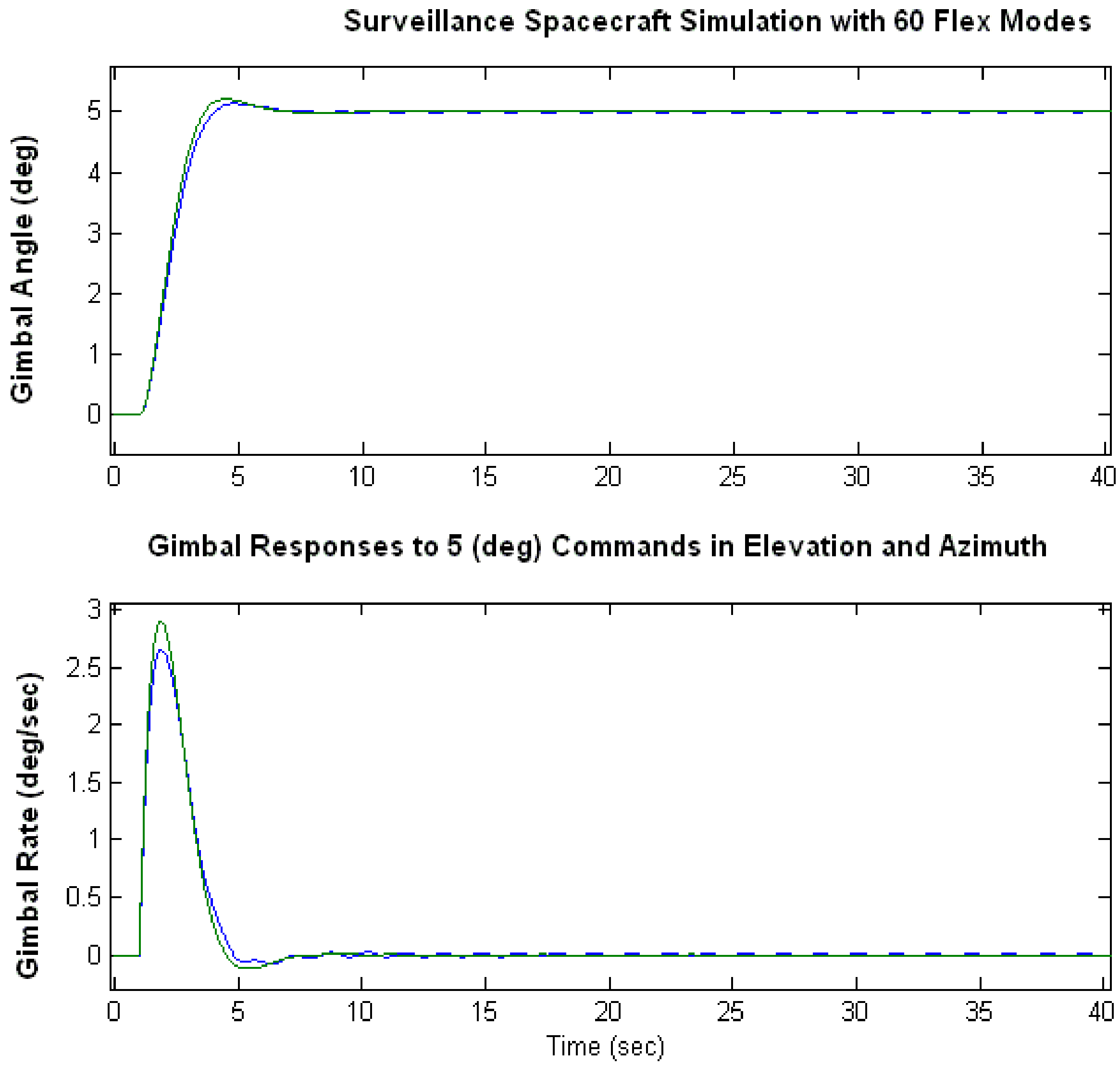

Figure 6.6 Telescope Gimbals Response to a Simultaneous 5 (deg) Command in both Elevation and Azimuth.

6.4 Stability Analysis

The Simulink model "*Open_Anal_Flx.Mdl*" shown in figure (6.7) is used for RW attitude control stability analysis in the frequency domain. The RCS control loop is not included, only the RW control system. The vehicle model is the same as the one used in figure (6.6). The telescope positioning control loop is closed. In the configuration shown below for lateral loop stability analysis, the lateral loop is opened and the pitch loop is closed. For pitch loop stability analysis the model must be modified by closing the lateral loop and opening the pitch loop. The frequency responses are obtained by running the Matlab file "*Lin_Ana_Flx.m*". There is also a similar model "*Open_Anal_GRB.Mdl*" used for rigid-body stability analysis that uses the rigid-body system in file "*fv_rb.m*", and a similar file "*Lin_Ana_GRB.m*" for calculating the rigid-body frequency response plots.

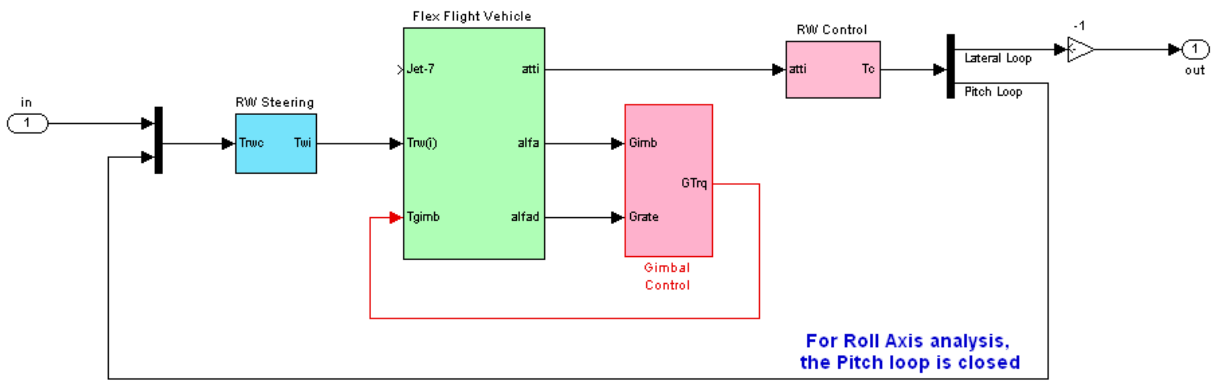

Figure 6.7 Simulink Model "Open_Anal_Flx.Mdl" for Linear ACS Flex Stability Analysis

Figure (6.8a) shows the open-loop frequency response and Nichols plot for the pitch axis. It looks very similar to previous results shown in figures (4.11 and 5.9). There is more phase lag at high frequencies because of an additional (z^{-1}) sample delay included in the loop. All modes are gain stable and there is a big resonance at orbital rate since the dynamics are with respect to the LVLH frame. Similarly, figure (6.8b) shows the open-loop frequency response and Nichols plot for the lateral axis, and it looks similar to previous results shown in figures (4.13 and 5.8). Figure (6.9) shows flex versus rigid-body models comparison of stability margins using Nichols charts.

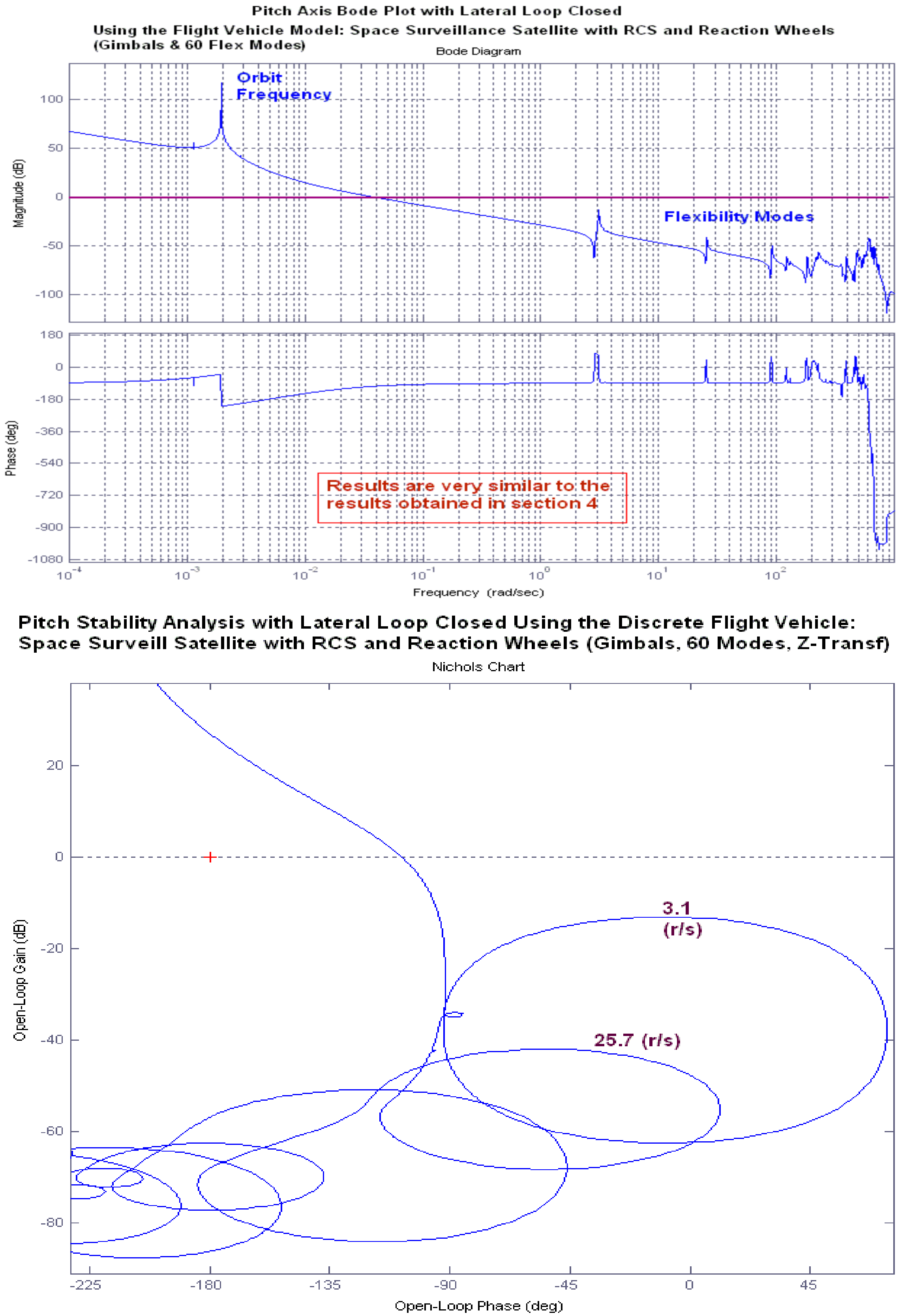

Figure 6.8a Stability analysis of the Pitch loop with the Lateral loop Opened

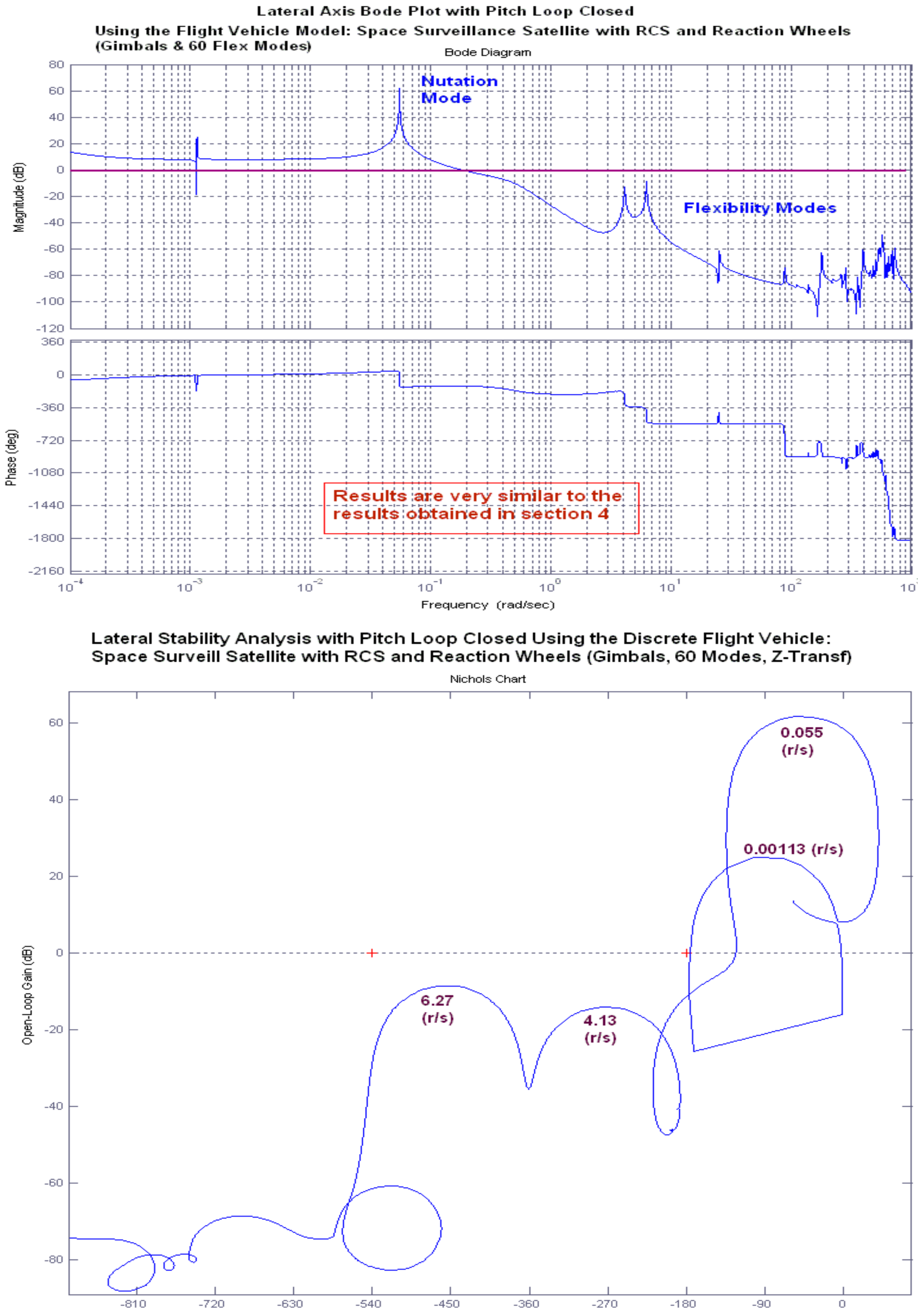

Figure 6.8b Stability analysis of the Lateral loop with the Pitch loop Opened

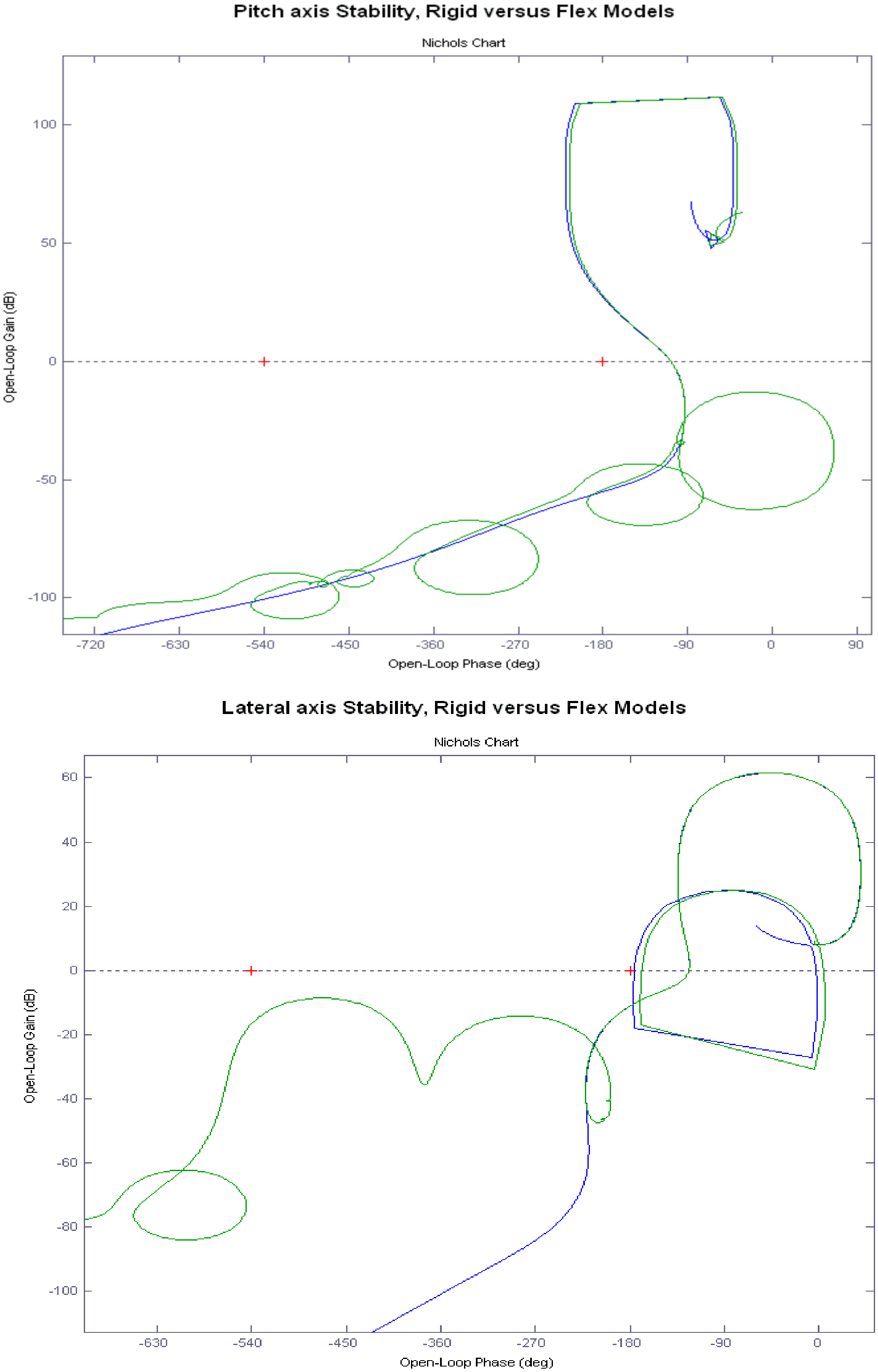

Figure 6.9 Stability Margins Comparison between Rigid and Flex Models Using Nichols Charts

The telescope gimbal loop stability is obtained by closing the attitude control loop and opening the gimbal loop, one axis a time, as shown in the Simulink model "*Open-Anal-Gimb.mdl*". In the case of azimuth loop stability analysis the azimuth loop is opened and the elevation loop is closed, as shown in figure (6.10). The stability margins of the azimuth and elevation loops are shown in figures (6.11 and 6.12) respectively. Both gimbal loops have a bandwidth of approximately 2 (rad/sec).

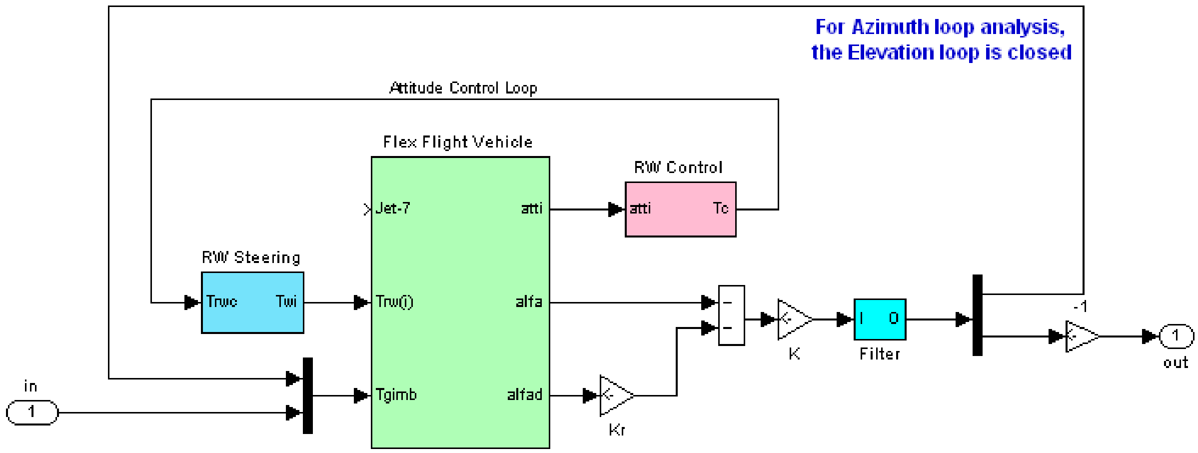

Figure 6.10 Simulink model "Open_Anal_Gimb.mdl" for gimbal frequency response analysis

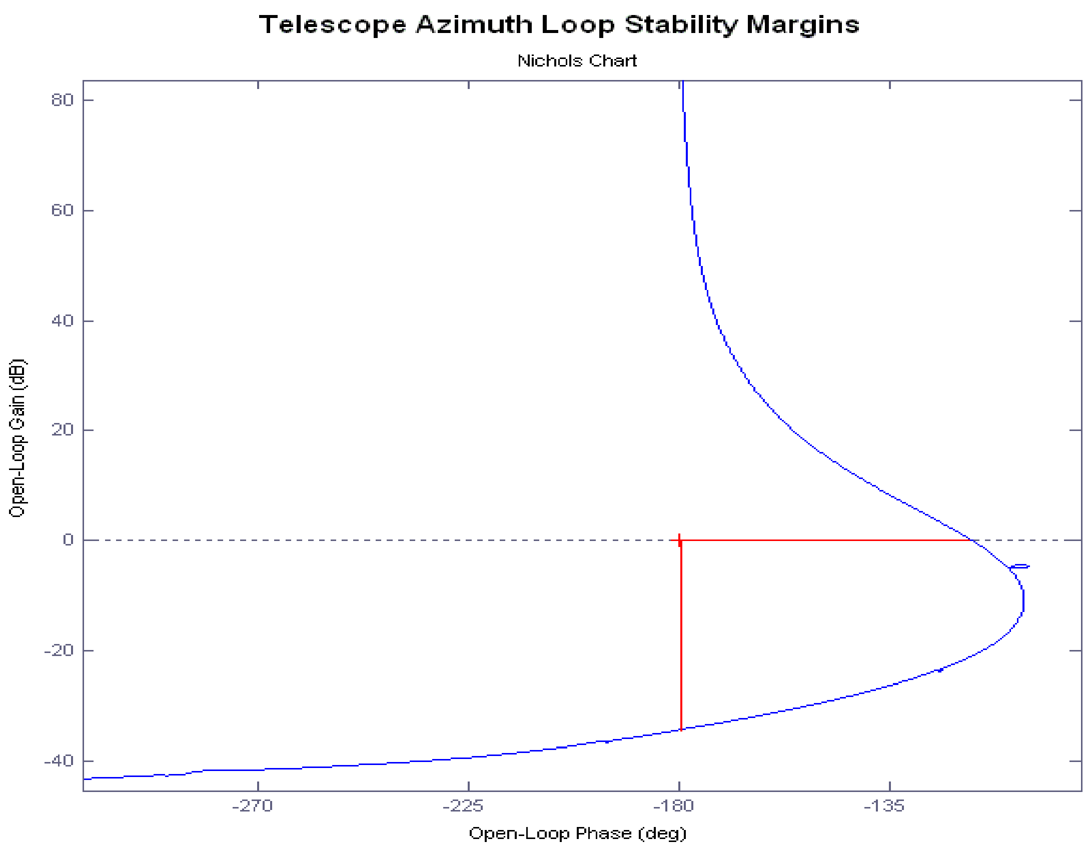

Figure 6.11 Azimuth loop stability margins, (all other loops are closed)

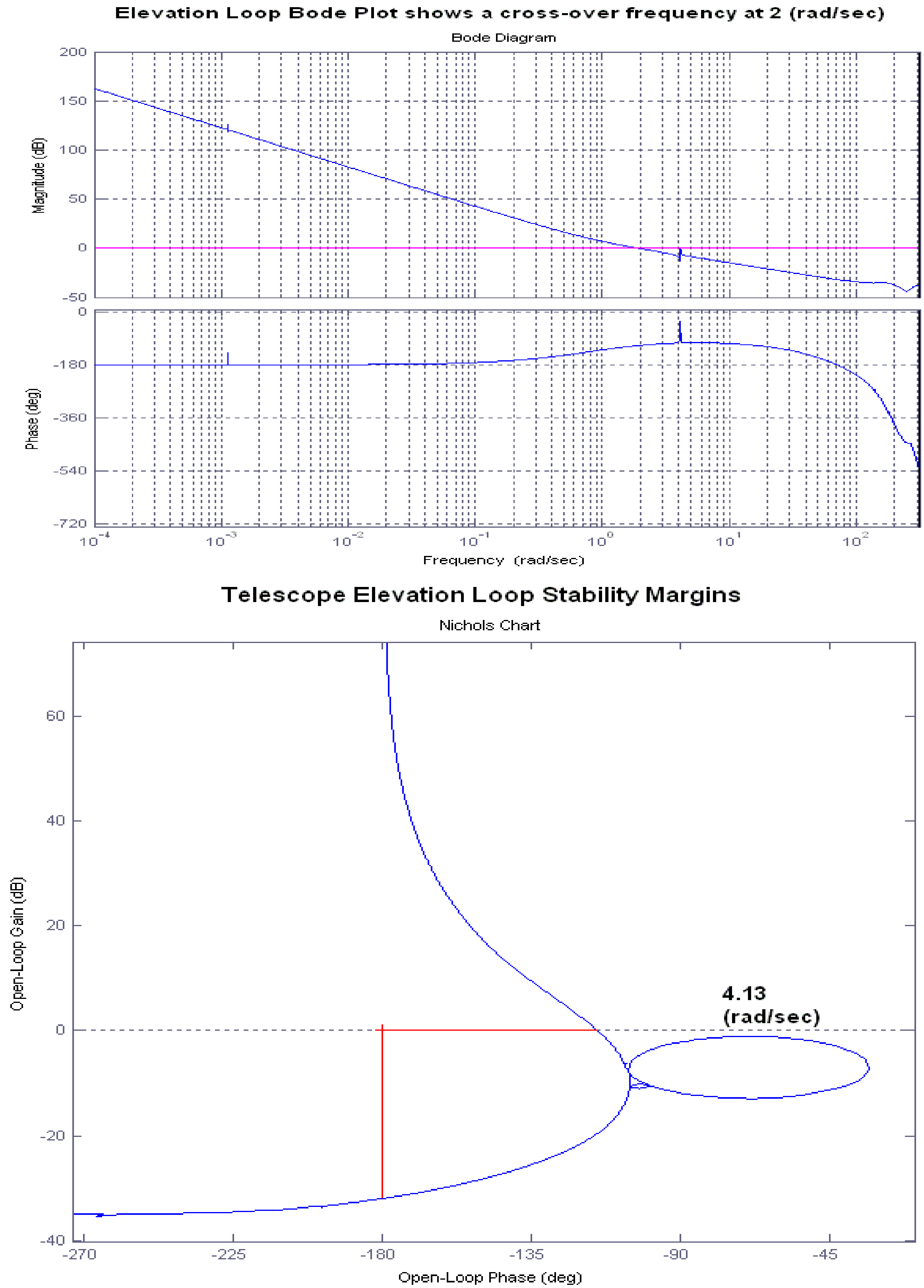

Figure 6.12 Elevation Loop Stability Margins, (all other loops are closed)

6.5 LOS Sensitivity to Solar Array Stepper Motor Disturbances

The two solar arrays rotate about the spacecraft y axis and they perform a full 360º rotation with respect to the spacecraft for every orbit. The rate of rotation is 0.00113 (rad/sec). The rotation is controlled by a stepper motors at each solar array joint which generate a train of torque pulses that rotate the arrays at constant average rate. The pulses frequency is at 2 Hz and they consist of a 0.08 (ft-lb) positive pulse followed by a similar negative pulse. The train of pulses generates a disturbance on the spacecraft which distorts the telescope image by creating a jitter on the Line-of-Sight (LOS). The purpose of the following sensitivity analysis is to simulate the stepper motor torque pulses and apply them at the two solar array joints and observe its effect on the azimuth and elevation jitter at the telescope gimbals which represent the LOS sensitivity.

The following time-domain Simulink model "*Sensitivity_Sim.mdl*", shown in figure (6.13) is used to perform this sensitivity to disturbance analysis. It has the attitude control loops and the gimbal control loops closed. It is excited by disturbance models for the Solar Array stepper motor pulses, and also for the cryo-cooler pump.

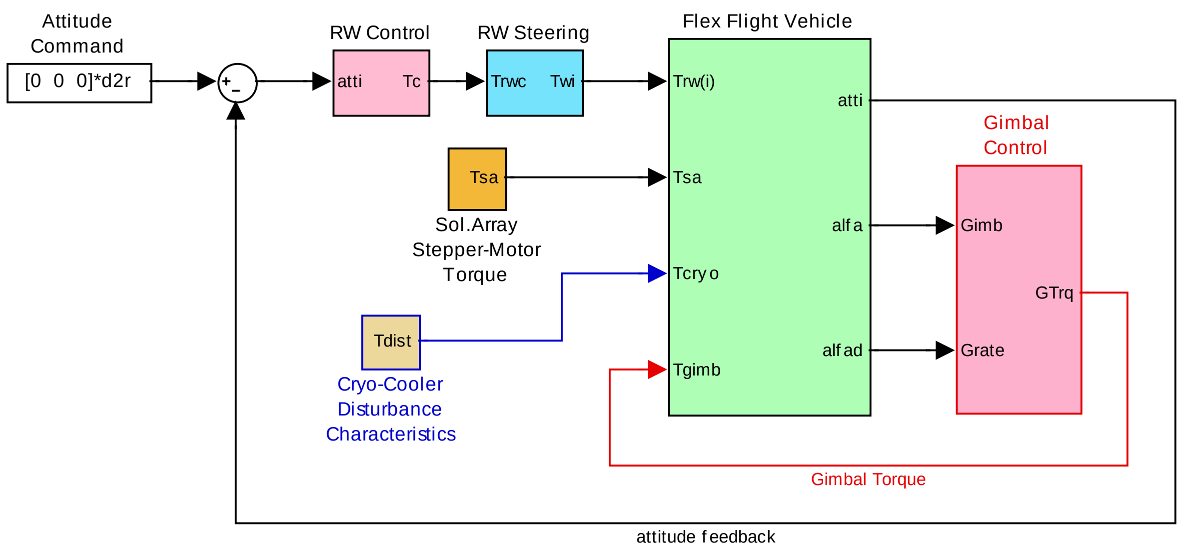

Figure 6.13 Sensitivity Analysis Model (Sensitivity_Sim.mdl)

In this analysis we disconnect the cryo-cooler in the Simulink model and we apply only the stepper motor disturbance torque. After running the model for a while we execute file "pld.m" to plot the data. Figure (6.14) shows the disturbance effect on the Line-of-Sight jitter. It shows the telescope gimbal rates versus angle jitter in both: elevation (blue) and azimuth (green). Obviously, the azimuth is affected more because the disturbance pulses are in pitch. Figure (6.15) shows the solar array rotation and rate. The average rate is equal to the orbital rate, 0.00113 (rad/sec), but it oscillates because of the stepper motor pulses. Figure (6.16) shows the stepper motor effect on the spacecraft rate. Figure (6.17) shows its effect on the reaction wheels. Figure (6.18) shows the magnitude of the SA stepper motor torque pulses and the telescope gimbal torques.

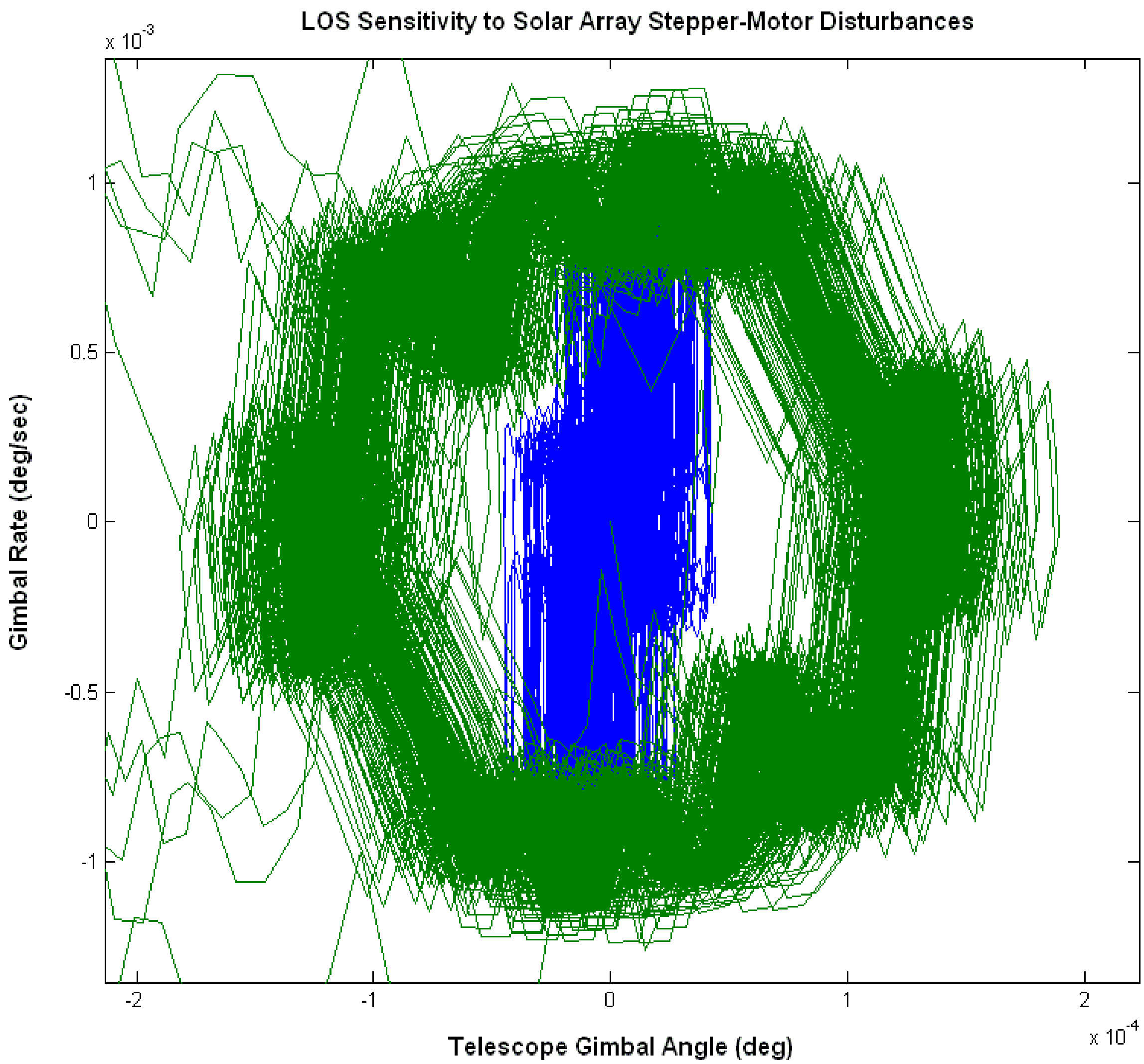

Figure 6.14 Azimuth and Elevation LOS Jitter on the Telescope Gimbals

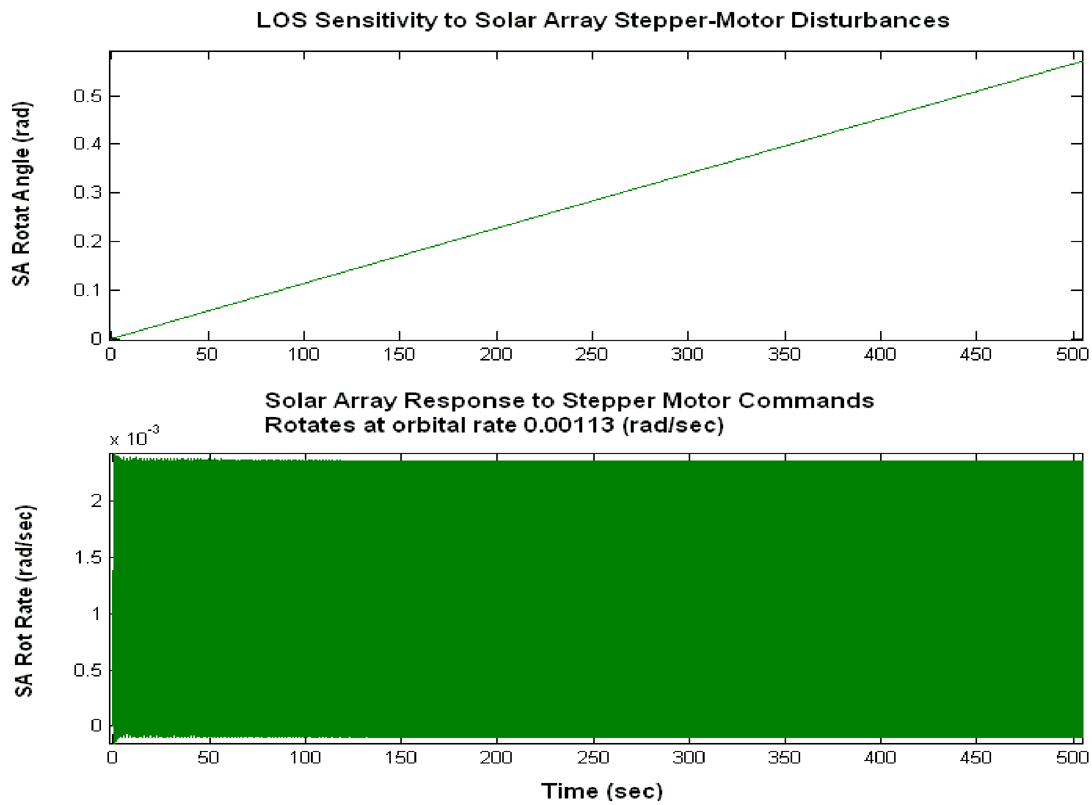

Figure 6.15 Solar Array rotation angle and rate which has an average rate equal to the orbital rate 0.00113 (rad/sec)

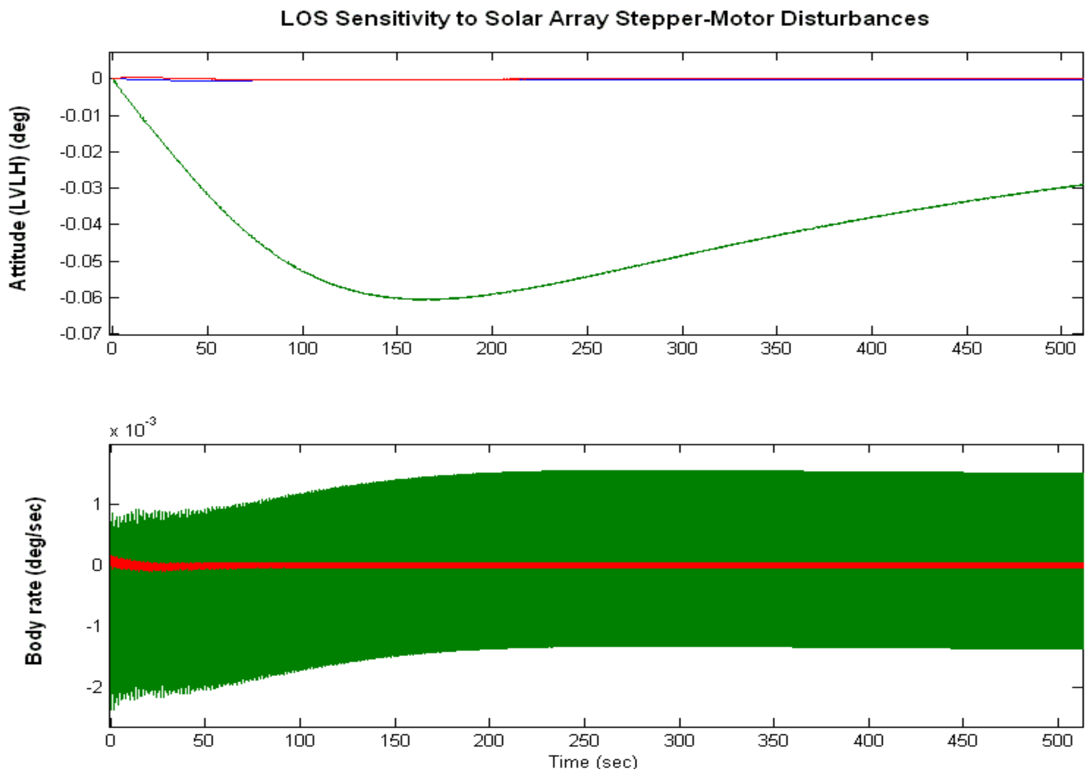

Figure 6.16 Spacecraft Attitude and Rate, shows the effect of the stepper motor on the spacecraft rate

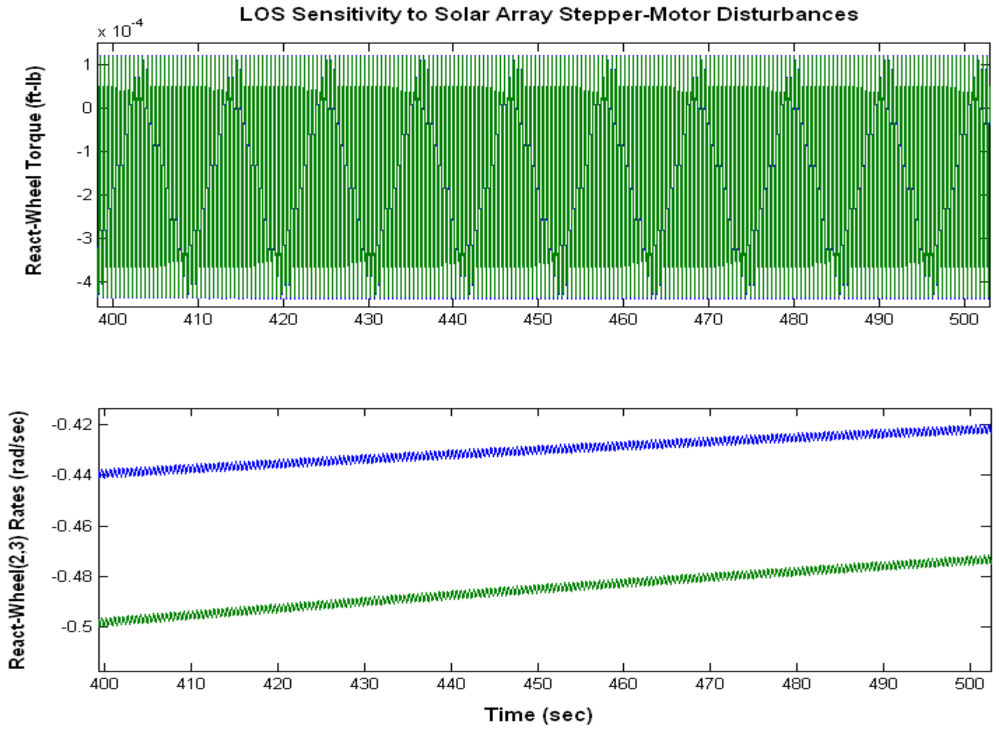

Figure 6.17 Reaction Wheel (2 & 3) Torques and Rates

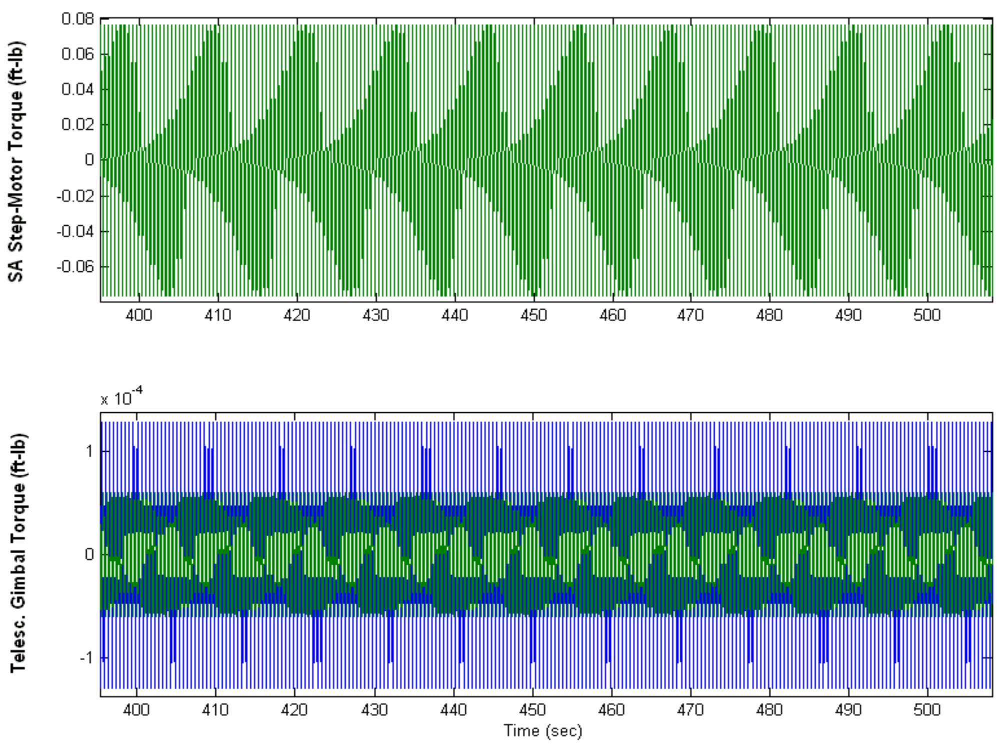

Figure 6.18 Control Torques on the Solar Array (open-loop) and at the Telescope Gimbals

6.6 LOS Sensitivity to the Cryo-Cooler Disturbances

The cryo-cooler is a mechanical pump that circulates fluid around the spacecraft for cooling purposes. The cryo-cooler is another disturbance source that creates a jittering effect on the telescope image, and therefore, we must evaluate its effect once more on the LOS by measuring the jitter magnitude on the azimuth and elevation gimbals. We will use again the model "*Sensitivity_Sim.Mdl*", in folder "… *\Flixan\Examples\Surveillance Satellite React-Wheels\Linear Flex Anal FV*", shown in figure (6.13). We disconnect the stepper-motor disturbance on the Solar Array, and connect the cryo-cooler disturbance source, which is a white noise generator shaped by the disturbance frequency characteristics. This disturbance torque excites the spacecraft bus in all 3 directions by the same amount. We run again the simulation for a while and plot the data using file "pld.m". Figure (6.19) shows the telescope gimbal rates versus angle, LOS jitter, in elevation (blue) and azimuth (green).

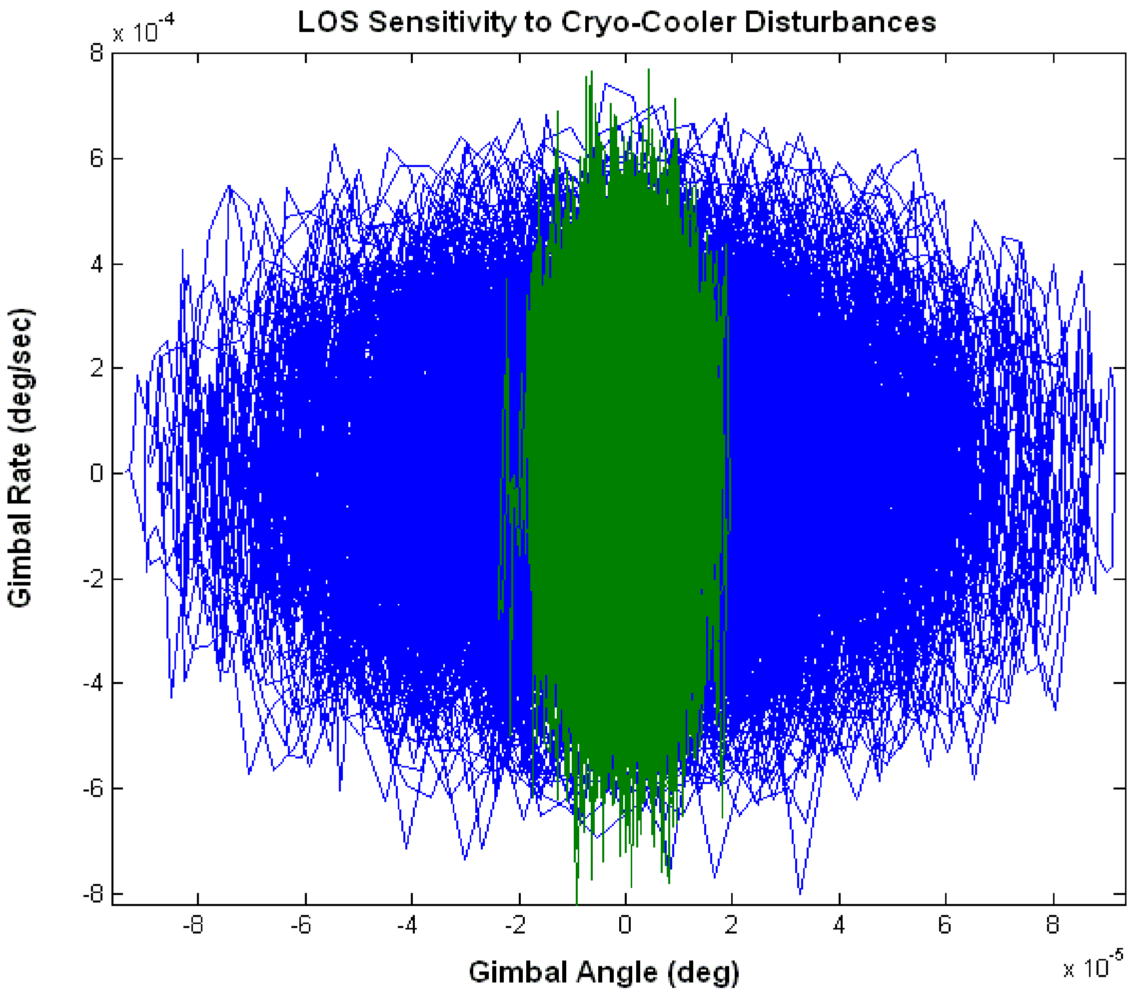

Figure 6.19 Azimuth and Elevation LOS Jitter on the Telescope Gimbals due to the Cryo-Cooler

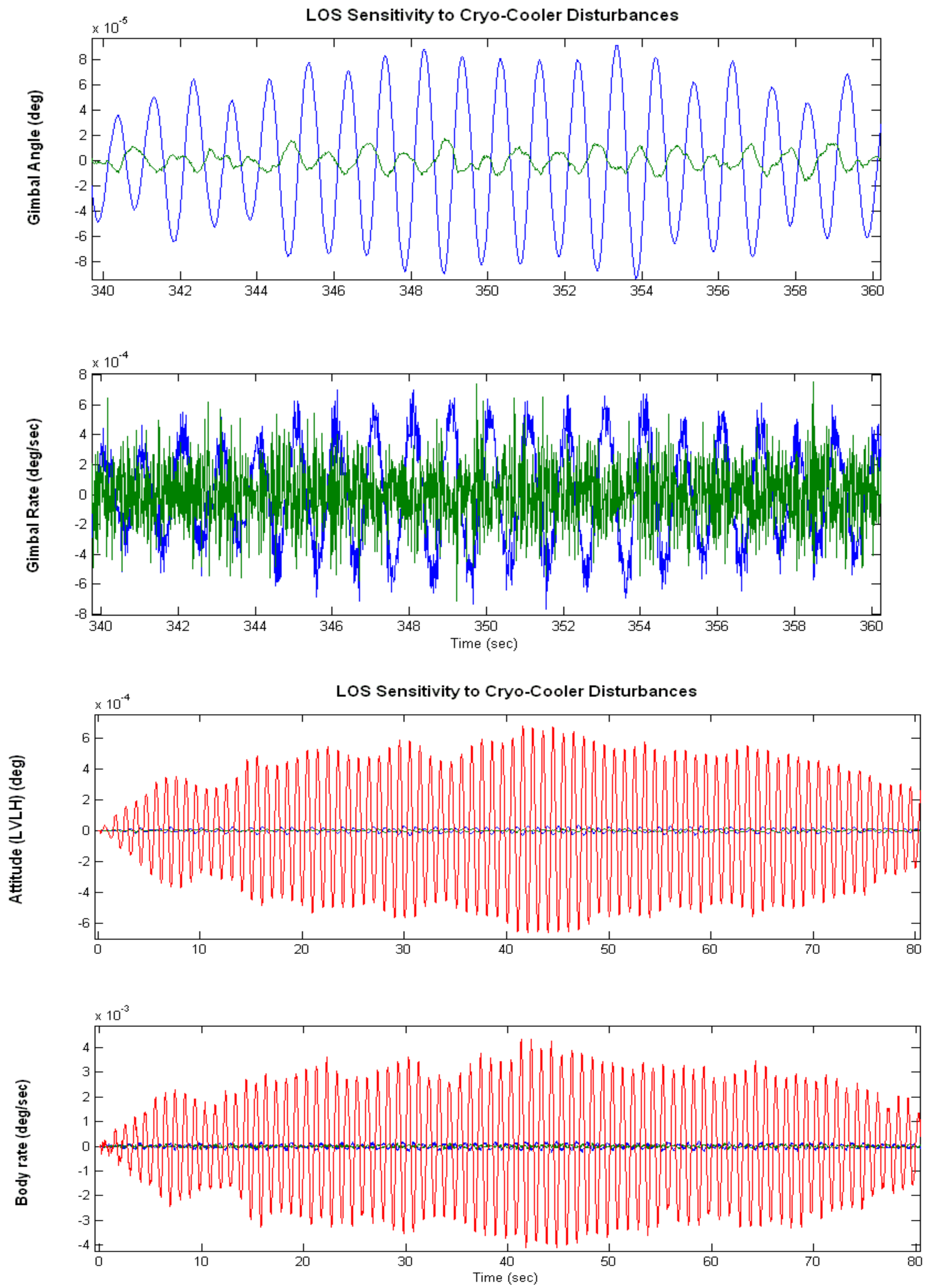

Figure 6.20 Cryo-Cooler effect on the Spacecraft Attitude & Rate. It has a bigger effect in yaw (red)